Carbon and water dynamics during combined heat, drought and elevated atmospheric CO_2 in *Pinus halepensis* seedlings

Zur Erlangung des akademischen Grades eines
DOKTORS DER NATURWISSENSCHAFTEN (Dr. rer. nat.)

von der KIT-Fakultät für
Bauingenieur-, Geo- und Umweltwissenschaften
des Karlsruher Instituts für Technologie (KIT)

genehmigte
DISSERTATION
von

Dipl. Biol. (t.o.) Benjamin Birami
aus Berlin

Karlsruhe, 2021

Tag der mündlichen Prüfung: 28.01.2021

Hauptreferentin: Prof. Dr. Almut Arneth
Korreferentin: Dr. Nadine Ruehr,
Korreferent: Prof. Dr. Jörg-Peter Schnitzler

This document is licensed under a Creative Commons
Attribution-ShareAlike 4.0 International License (CC BY-SA 4.0):
https://creativecommons.org/licenses/by-sa/4.0/deed.en

Acknowledgements

Science is teamwork and this thesis was built upon the friendship and professions of collegues, cooperation partners, supervisors, friends and family. I would like to name especially Yakir Preisler and Dan Yakir and all colleques from Dan Yakir's Lab at the Weizman Institute. Thank you for your warm welcome and support, the inspiring discussions and the food below pines in great company.

I would like to thank Katrin Brauner, who thought it was a good idea for me to do a PhD in Garmisch-Partenkirchen. Arnd Heyer and Simon Stutz from the Plant Biotechnology Lab at University of Stuttgart. Thomas Nägele and Lisa Fürtauer from the Plant Evolutionary Cell Biology Lab at LMU Munich. All friends from the IMK-IFU Garmisch-Partenkirchen, thank you all for your support and the opportunity to work and live in such a pleasant and inspiring environment.

Dear Plant Ecophysiology group: Nadine Ruehr, Andreas Gast, Marielle Gattman, Romy Rehschuh, Selina Schwarz, Daniel Nadal-Sala, Martina Bauerfeind, Andrea Jakab, Ines Bamberger, thank you for your reliability, your help, your honesty and your friendship. You all have grown to my heart in the last five and a half years.

Thank you, Anita Bayer, Thomas Pugh and all other (former) members of the Plant-Atmosphere Interaction group – It was not only all about the food.

Thank you, Marta Kern and Monika Liebl, you both made my life easy at the IMK. Thank you Elija Bleher for your time and for your effort to create a little bit of Campus at the IMK-IFU. Thank you Mechtild Agreiter for your company, the talks and the walks.

Last but not least, my supervisors: Almut Arneth, Rüdiger Grote and Nadine Ruehr: It was a pleasure and an honor to learn from you.

My parents, brother and friends – who embrace my weaknesses and give me strength when I need it.

Contents

Summary:

Forests are key components of Earth's water and carbon cycles. As the predominant plant life form on land, they shape ecosystem functioning and biodiversity and provide key ecosystem services for human well-being. As autotrophic organisms, trees take up atmospheric CO_2 and use it for growth or transport it in form of carbohydrates to their heterotrophic organs, for example to sustain function maintenance of the roots. However, they must face a trade-off, since the uptake of one CO_2 molecule can cost more than 200 water molecules. Trees are able to channel water from the soil through roots, stems and branches to compensate for this loss. Current climate change developments increase the likelihood of extreme weather events such as longer periods of drought, flooding and more frequent heatwaves. Therefore, it is likely that trees may face soon unprecedented climate conditions. The resulting stress intervenes strongly in fundamental plant processes by reducing the availability of soil water and by increasing atmospheric water demand through a rise in temperature.

However, trees are not completely helplessly at the mercy of environmental conditions. They may modify their growth processes to minimize the damage caused by unfavorable environmental conditions to a certain level. Examples of such adaptation are the ability to modify the stomata density and shape so that water loss is limited. The affinity and activity of enzymes can be modified to optimize the stress limited metabolism. The stability and solubility of macromolecules can be improved at low water potential by specific adaptation of hydrophobic exclusion mechanisms using compatible osmolytes. Under conditions of deficiency, carbohydrate reserves (i.e. starch, soluble sugars) can be adapted to enable the plant to survive longer periods of stress. The study of this wide variety of dynamic plant stress responses has led to many advances in plant physiology. Findings on how the physiology of stress -e.g. by heat or drought, affects photosynthesis and growth are currently used for the interpretation of remote sensing data in forest inventory or for crop breeding strategies. They may also be used to parameterize process-based models in order to anticipate forest responses to unprecedented climate conditions.

At the beginning of this work in 2015, the reactions of the forest to extreme events and combined stress conditions were already visible. Apart from short-term laboratory experiments, which provide valuable insights into the responses of individual stressors, and some impressive free-air carbon dioxide enrichment (FACE) experiments, which are only gradually yielding long-term observational data, very little research has focused on the systematic mechanistic response of trees to a combination of stressors (e.g. heatwaves together with drought). Rarely are subsequent

recovery and adaptation processes systematized and how these processes are influenced by elevated CO_2 concentrations (e[CO_2]).

This doctoral thesis is intended to shed light on the less considered multiple stress-CO_2 interactions. As part of a larger international project "Climate feedbacks and benefits of semi-arid forests" (CliFF) the focus is on the drought tolerant conifer *Pinus halepensis* (Miller), also called Aleppo pine. Two separate experiments were conducted to answer the following research questions: 1) How do gas exchange, carbon allocation and regeneration of tree seedlings change after repeated isolated periods of heat or drought or a combination of both (Chapters 2 and 3)? 2.) What is the potential of very high atmospheric [CO_2] to influence heat stress responses and the carbon balance of drought-acclimatized versus well-watered *P. halepensis* seedlings (Chapter 4)?

It has been shown that a combination of heat and drought can increase stress through various interactions. These may lead to increased mortality in the pine seedlings compared to heat stress alone. Strict regulation of a plant's water balance by stomata closure at the expense of evaporative cooling caused the surface temperatures of needles to rise. Similarly, reduced photosynthesis and water availability limited root carbon allocation, which reduced root vitality. Tree mortality occurred with a delay with respect to the immediate stress, indicating that the impact of stress may persist even after it has subsided. Therefore, increases in heatwave temperatures, as predicted for the next decades may have disproportionate and delayed impacts on semi-arid forests. It appears that in regions where trees have evolved to cope with pervasive drought, even a single heatwave exceeding a certain threshold (probably above 47°C needle temperature) can have far-reaching detrimental effects.

Secondly, the dynamics of emissions of biogenic volatile organic compounds (BVOC) from pine seedlings showed clear stress-specific reactions. Decreases in acetone emissions with decreasing soil water content and transpiration were clear indicators of drought. All other measured emitted components reacted exponentially to increasing temperatures during heat stress (maximum 43°C). Monoterpenes and methyl salicylate showed reduced temperature sensitivity during the second heatwave, which was not reflected in a similar decrease of their internal pools. Emissions (methanol, monoterpenes, methyl salicylate and acetaldehyde) differentiated between dying and surviving seedlings days before signs of reduced vitality in water and carbon exchange became visible. These results could mean that the decision whether a seedling dies or not depends on individual early stress physiology and that emission rates within

stress periods are not comparable due to acclimatization. They also give rise to the opportunity to screen the tree`s vulnerability to stress before damage occurs.

Thirdly, the 18-month cultivation of Aleppo pines under e[CO_2] of about 870 ppm had a stimulating effect on tree biomass (+40%), while the seedlings maintained higher water-use efficiency (WUE) during a heatwave of 10 d (25 °C, 30 °C, 35 °C, 38 °C, 40 °C). Drought stress initially enhanced the e[CO_2] effect on the WUE until the stomata completely closed at higher temperatures. Under e[CO_2], net carbon uptake was stimulated, largely due to a reduced respiratory rate. As temperature increased, photosynthesis decreased while respiration peaked between 31-34 °C, resulting in net carbon losses above 30 °C independent of [CO_2]. Increased [CO_2] had only a modest effect on the stress response of the primary metabolome, which differed between roots and needles. This implies first, that the effect of [CO_2] on the physiological responses of trees decreases with stress intensity, such as hot drought, and second that respiration rates adapt to heat stress conditions within days regardless of [CO_2].

In summary, it could be shown that even a highly drought tolerant pine species quickly reaches its limits when exposed to higher maximum temperatures and that drought together with heatwaves disproportionately increase their stress effect. Even effects that are caused by very high CO_2 concentrations are quickly masked by heat-drought stress, although they possibly reduce the individual water consumption of trees along a temperature gradient. Under future conditions with higher frequencies of heatwaves, this will possibly lead to trees becoming net sources of CO_2 more often.

Zusammenfassung:

Wälder sind Schlüsselkomponenten des Wasser- und Kohlenstoffkreislaufs der Erde. Als autotrophe Organismen nehmen Bäume CO_2 auf und nutzen es für ihr Wachstum oder transportieren es in Form von Kohlenhydraten zu ihren heterotrophen Organen, beispielsweise zur Funktionserhaltung der Wurzeln. Sie müssen jedoch einen Kompromiss eingehen, da die Aufnahme eines CO_2-Moleküls mehr als 200 Wassermoleküle kosten kann. Bäume sind in der Lage, Wasser aus dem Boden durch Wurzeln, Stämme und Äste zu leiten, um diesen Verlust auszugleichen. Die aktuellen Entwicklungen des Klimawandels erhöhen die Wahrscheinlichkeit extremer Wetterereignisse wie längere Dürreperioden, Überschwemmungen und häufigere Hitzewellen. Daher ist es wahrscheinlich, dass Bäume schon bald beispiellosen Klimabedingungen ausgesetzt sein könnten. Der daraus resultierende Stress greift stark in

grundlegende Pflanzenprozesse ein, indem er die Verfügbarkeit von Bodenwasser verringert und den atmosphärischen Wasserbedarf durch einen Temperaturanstieg erhöht.

Doch Bäume sind den Umweltbedingungen nicht völlig hilflos ausgeliefert. Sie können ihre Wachstumsprozesse modifizieren, um die durch ungünstige Umweltbedingungen verursachten Schäden auf ein bestimmtes Maß zu minimieren. Beispiele für eine solche Anpassung sind die Fähigkeit, Spaltöffnungsdichte und -form zu modifizieren, sodass der Wasserverlust begrenzt wird. Die Affinität und Aktivität von Enzymen kann verändern werden, um den Stoffwechsel zu optimieren. Die Stabilität und Löslichkeit von Makromolekülen kann bei niedrigem Wasserpotential durch gezielte Anpassung hydrophober Ausschlussmechanismen mit Hilfe kompatibler Osmolyte verbessert werden. Unter Mangelbedingungen können Kohlenhydratreserven (d.h. Stärke, lösliche Zucker) angepasst werden, um der Pflanze zu ermöglichen, längere Stressperioden zu überdauern. Die Untersuchung dieser großen Vielfalt dynamischer pflanzlicher Stressreaktionen hat zu vielen Fortschritten in der Pflanzenphysiologie geführt. Erkenntnisse darüber, wie die Stressphysiologie - z.B. durch Hitze oder Dürre - die Photosynthese und das Wachstum beeinflusst, werden gegenwärtig für die Interpretation von Fernerkundungsdaten bei der Waldinventur oder für Pflanzenzuchtstrategien verwendet. Sie können auch zur Parametrisierung von prozessbasierten Modellen verwendet werden, um die Reaktionen des Waldes auf beispiellose Klimabedingungen vorherzusehen. Zu Beginn dieser Arbeiten im Jahr 2015 waren die Reaktionen des Waldes auf Extremereignisse und kombinierte Stressbedingungen bereits sichtbar. Abgesehen von kurzfristigen Laborexperimenten, die wertvolle Einblicke in die Reaktionen einzelner Stressoren geben, und einigen beeindruckenden Freiluft-Experimenten zur Kohlendioxidanreicherung (FACE), die erst allmählich langfristige Beobachtungsdaten liefern, hat sich nur sehr wenig Forschung auf die systematische mechanistische Reaktion von Bäumen auf eine Kombination von Stressoren (z.B. Hitzewellen zusammen mit Trockenheit) konzentriert. Selten werden nachfolgende Erholungs- und Anpassungsprozesse systematisiert und wie diese Prozesse durch erhöhte CO_2-Konzentrationen (e[CO_2]) beeinflusst werden.

Diese Doktorarbeit soll Licht auf die weniger beachteten multiplen Stress-CO_2-Wechselwirkungen werfen. Als Teil eines größeren internationalen Projekts "Climate feedbacks and benefits of semi-arid forests" (CliFF), liegt der Schwerpunkt auf der trockenheitstoleranten Konifere *Pinus halepensis* (Miller) bzw. Aleppokiefer. Zwei unabhängige Experimente wurden durchgeführt, um die folgenden Forschungsfragen zu klären: 1.) Wie verändern sich Gasaustausch, Kohlenstoffverteilung und Regeneration von Sämlingen nach wiederholten Hitze- oder

Trockenperioden oder einer Kombination aus beiden Stressoren (Kapitel 2 und 3)? 2.) Welches Potenzial hat sehr hohes atmosphärisches [CO_2], um die Hitzestress-Antworten und die Kohlenstoffbilanz von dürreakklimatisierten gegenüber ausreichend versorgten Aleppokiefern-Sämlingen zu beeinflussen (Kapitel 4)?

Es hat sich gezeigt, dass eine Kombination von Hitze und Dürre den Stress für die Sämlinge durch verschiedene Wechselwirkungen verstärken kann. Diese können zu einer erhöhten Sterblichkeit der Sämlinge im Vergleich zu isoliertem Hitzestress führen. Die strenge Regulierung des Wasserhaushalts durch das Schließen der Spaltöffnungen auf Kosten der Verdunstungskühlung, führte zu einem Anstieg der Oberflächentemperaturen der Nadeln. In ähnlicher Weise schränkten die verminderte Photosynthese und die limitierte Wasserverfügbarkeit den Kohlenstofftransport zur Wurzel ein, was deren Vitalität verringerte. Mortalität trat mit einer Verzögerung gegenüber dem unmittelbaren Stress auf, was darauf hindeutet, dass die Auswirkungen von Stress auch nach dessen Abklingen andauern können. Daher kann ein Anstieg der Temperaturen von Hitzewellen, wie er für die nächsten Jahrzehnte vorhergesagt wird, unverhältnismäßige und verzögerte Auswirkungen auf semiaride Wälder haben. Es scheint, dass in Regionen, in denen sich Bäume entwickelt haben die durchdringender Dürre ertragen, selbst eine einzige Hitzewelle die einen bestimmten Schwellenwert (wahrscheinlich über 47°C Nadeltemperatur) überschreitet, weitreichende schädliche Auswirkungen haben kann.

Zweitens zeigte die Dynamik der Emissionen biogener flüchtiger organischer Verbindungen (BVOC) der Pinien Sämlinge deutliche stressspezifische Reaktionen. Verringerungen der Aceton Emissionen mit abnehmendem Bodenwassergehalt und Transpiration waren deutliche Dürreindikatoren. Alle anderen gemessenen emittierten Komponenten reagierten exponentiell auf steigende Temperaturen während des Hitzestresses (maximal 45°C). Monoterpene und Methylsalicylat zeigten während der zweiten Hitzewelle eine verminderte Temperaturempfindlichkeit, die sich nicht in einem ähnlichen Rückgang ihrer internen Sprosspools niederschlug. Emissionen (Methanol, Monoterpene, Methylsalicylat und Acetaldehyd) unterschieden sich zwischen absterbenden und überlebenden Keimlingen, Tage bevor Anzeichen einer verminderten Vitalität im Wasser- und Kohlenstoffaustausch sichtbar wurden. Diese Ergebnisse könnten bedeuten, dass die Entscheidung, ob ein Sämling stirbt oder nicht, von der individuellen frühen Stressphysiologie abhängt und dass die Emissionsraten innerhalb von Stressperioden aufgrund von Akklimatisation nicht vergleichbar sind. Die

Ergebnisse eröffnen auch eine Möglichkeit, Stressanfälligkeit vor einsetzender Schädigung der betroffenen Bäume direkt im Feld zu messen.

Drittens hatte der 18-monatige Anbau von Aleppokiefern unter e[CO_2] von ca. 870 ppm eine stimulierende Wirkung auf die Baumbiomasse (+40%), während die Setzlinge bei einer Hitzewelle von 10 d (25°C, 30°C, 35°C, 38°C, 40°C) eine höhere Wassernutzungseffizienz (WUE) aufrechterhalten konnten. Trockenstress verstärkte zunächst den e[CO_2]-Effekt auf die WUE, bis sich die Spaltöffnungen bei höheren Temperaturen komplett schlossen. Unter e[CO_2] wurde die Netto-Kohlenstoffaufnahme stimuliert, was weitgehend auf eine verminderte Atmungsrate zurückzuführen war. Stieg die Temperatur, nahm die Photosynthese ab, während die Atmung zwischen 31-34 °C ihren Höhepunkt erreichte, was unabhängig von [CO_2] zu Netto-Kohlenstoffverlusten über 30 °C führte. Erhöhtes [CO_2] hatte nur einen bescheidenen Effekt auf die Stressantwort des Primärmetaboloms das sich in Wurzel und Nadel unterschied. Diese Ergebnisse implizieren erstens, dass die Wirkung von [CO_2] auf die physiologischen Reaktionen der Bäume mit der Stress-Intensität, wie z.B. heißer Trockenheit, abnimmt, und zweitens, dass sich die Atmungsraten innerhalb von Tagen unabhängig von [CO_2] an Hitzestress Bedingungen anpassen.

Zusammenfassend konnte gezeigt werden, dass selbst eine ausgesprochen trockentolerante Pinien Art schnell an ihre Grenzen gerät, wenn sie höheren maximal Temperaturen ausgesetzt sind und dass sich Dürre und Hitzewellen disproportional in ihrer Stresswirkung verstärken. Erhöhte CO_2 Konzentrationen können möglicherweise den Individuellen Wasserverbrauch von Bäumen verringern, dieser Effekt wird jedoch selbst unter stark erhöhten Konzentrationen schnell von Trockenstress maskiert. Dies wird möglicherweise dazu führen, dass Bäume auch unter zukünftigen Bedingungen bei einem relativ geringen Temperaturanstieg zu netto Quellen für CO_2 werden.

List of Publications and Contributions:

The content and structure of the included publications were kept in the form of the original publications. 1, 2 and 3 are introduced as chapters at the state post review but previous to journal typesetting. These publications were prepared with the work of co-authors; hence my own contribution is stated:

1. **Birami B., Gattmann M., Heyer AG., Grote R., Arneth A., Ruehr NK. (2018):** Heat waves alter carbon allocation and increase mortality of Aleppo Pine under dry conditions. *Frontiers in Forests and Global Change* **1**: 1285. doi: 10.3389/ffgc.2018.00008.

I contributed by having led the study design and the writing of the publication. I conducted the experiment together with GM and RNK. I performed physical measurements and the chemical analysis and contributed significantly to data analysis.

2. Birami B., Bamberger I., Ghirardo A., Grote R., Arneth A., Gaona-Colmán E., Nadal-Sala D. and Ruehr NK. (2021): Heatwave frequency and seedling death alter stress-specific emissions of volatile organic compounds in Aleppo pine. *Oecologia*. https://doi.org/10.1007/s00442-021-04905-y

I contributed by having led the study design and the writing of the publication. I conducted the experiment together with BI and RNK and contributed significantly to data analysis.

3. **Birami, B., Nägele, T., Gattmann, M., Preisler, Y., Gast, A., Arneth, A. and Ruehr, N.K. (2020)**, Hot drought reduces the effects of elevated CO_2 on tree water-use efficiency and carbon metabolism. *New Phytologist*, 226: 1607-1621. doi:10.1111/nph.16471.

I contributed by having led the study design and the writing of the publication. I conducted the experiment together with GM, GA and RNK and contributed significantly to data analysis. I conducted the physical measurements and the chemical analysis.

In the course of my Doctoral Thesis project, I had the chance to contribute to the following manuscripts as a co-author. These were not introduced as separate chapters, but were used for additional information and interpretation of the Thesis outline.

Trugman, A. T.; Anderegg, L. D.L.; Wolfe, B. T.; Birami, B.; Ruehr, N. K.; Detto, M.; Bartlett, M. K.; Anderegg, W. R.L (2019) Climate and plant trait strategies determine tree carbon allocation to leaves and mediate future forest productivity. *Global Change Biology*

Nadal-Sala, D.; Grote, R.; Birami, B.; Lintunen, Anna; Mammarella, I.; Preisler, Y.; Rotenberg, E.; Salmon, Y.; Tatrinov, F.; Yakir, D.; Ruehr, N.K. (2021) Assessing model performance via the most limiting environmental driver (MLED) in two differently stressed pine stands *Ecological Applications*

Gattmann M, Birami B, Nadal-Sala D, Ruehr NK (2021) Dying by drying: timing of physiological stress thresholds related to tree death is not significantly altered by highly elevated CO_2 in Aleppo pine. *Plant, Cell and Environment*

Acronyms and Abbreviations:

A	carbon assimilation by photosynthesis
Aleppo Pine	*Pinus helepenis* (Miller)
(B)VOC	(biogenic) volatile organic compound
C	Carbon
°C	degrees Celsius
C_a	atmospheric CO_2 concentration
C_i	leaf internal CO_2 concentration
DOY	Day of year
E	evapotranspiration
e[CO_2]	elevated atmospheric CO_2 concentration
a[CO_2]	ambient atmospheric CO_2 concentration, refers to ±400 ppm
FACE	free air carbon dioxide enrichment
G_s	conductance (stomata)
gDW	gramme dryweight
H_2Odd	deionized “double distilled” water
HPLC	High pressure liquid chromatography
k(M)PA	kilo (mega) pascale
µ(m)mol	micro (mili)mole
MPa	mega Pascale
MeSa	Methyl Salicylate
MT	Monoterpene
NSC	non-structural carbon
N	Nitrogen
n	sample count
ppm(t)	parts per million (thousand)
PAR	Photosynthetic active radiation
PTRMS	Protone transfer reaction mass spectrometry
RCP	Representative Concentration Pathways
R	carbon loss through respiration
RH	Relative humidity (air)
SE	standard error of mean
SD	Standard deviation
(R)SWC	(relative) substrate/soil water content
SQT	sesquiterpene
TE	trace elements
TCA	Tri-carbonic acid cycle
VPD	vapor pressure deficit
WUE	water-use efficiency
Ψ	water potential

List of Figures

List of Tables

1 General Introduction

1.1 Forests are challenged by climate change

By means of their mere biomass, forests bear a huge potential to feedback with the atmosphere mitigating or enhancing climate change (Bonan 2008; Kreidenweis et al. 2016; Walker et al. 2020; Zemp et al. 2017). Until today, they act as a central terrestrial carbon sink, which may have re-assimilated about one third of the yearly anthropogenic fossil fuel emissions (Friedlingstein et al. 2019; Keenan and Williams 2018; Le Quéré et al. 2018). Although the potential of forests to remove CO_2 from the atmosphere is immense (Bastin et al. 2019; Doelman et al. 2020; Law et al. 2018; Yosef et al. 2018), the estimate of their actual value as tool for natural carbon storage is critically discussed (Grainger et al. 2019). Concurrent land-use (Arneth et al. 2017; Kreidenweis et al. 2016), relatively short (one to three decades) carbon turnover rates (Pugh et al. 2020) and challenges due to unfavorable climatic conditions may raise uncertainty of the future development of the carbon sink potential.

Atmospheric CO_2 has almost doubled since preindustrial times (before 1900) (Friedli et al. 1986; Yan et al. 2019a). This has led to an increase in average temperatures of 0.75°C–0.99°C (Allen et al. 2018; Folland et al. 2018). An increase in global temperatures in turn increases the likelihood of extreme-weather events (Baker et al. 2018; Seneviratne et al. 2012; Ummenhofer and Meehl 2017) as for example heatwaves (Frank et al. 2015; Giorgi and Lionello 2008; Meehl et al. 2000; Yi et al. 2015). These heatwaves commonly occur in combination with reduced precipitation, which is predicted to result in extraordinary hot drought phases with tremendous implications for forest carbon and water cycling (Breshears et al. 2005; Brodribb et al. 2020; Frank et al. 2015; Isson et al. 2020; Reichstein et al. 2013; Wu et al. 2020).

According to the latest projections of the development of carbon emissions, the most likely climate scenario is an increase in temperature between +3°C (RCP4.5) and +4.5°C (RCP8.5) until the end of the century (Schwalm et al. 2020). The +4.5°C temperature increase refers to an estimated atmospheric CO_2 concentrations between 794 ppm and 1142 ppm (Collins et al. 2013). Even if the world emissions could be limited to keep world warming below 3°C in the next 50 years (Hausfather and Peters 2020), this will result in local temperature peaks that will exceed ambient temperatures by 2 to 5 degrees periodically (Perkins-Kirkpatrick and Gibson 2017; Seneviratne et al. 2012).

If these projections prove to hold true, a dystopic picture might be imagined, as for today a 1°C temperature increase already results in forests suffering from health degradation and widespread

tree mortality (Adams et al. 2010; Allen et al. 2010; Allen et al. 2015; Anderegg et al. 2012; Williams et al. 2013) across boreal (Grandpré et al. 2018; Michaelian et al. 2011; Yi et al. 2013), temperate (Ciais et al. 2005; Neumann et al. 2017; van Mantgem and Stephenson 2007), tropical (Aleixo et al. 2019; Fontes et al. 2018; Johnson et al. 2018; McDowell et al. 2018) and semi-arid regions (Kauwe et al. 2020; Klein et al. 2019; McDowell et al. 2016). Interestingly, these observations may culminate in a trend of largest (e.g. oldest) trees in a system dying first (Trouillier et al. 2019). Another trend can be found in conifers being apparently more vulnerable to droughts and heatwaves than broadleaf trees (McDowell et al. 2016; Wang et al. 2020) because of delayed physiological responses and gradual weakening (DeSoto et al. 2020; Zweifel et al. 2020), which make especially older pines vulnerable to other stressors (Seidl et al. 2017; Stephenson et al. 2019).

Atmospheric CO_2 is the main substrate for photosynthesis, hence, it is influencing the performance and the well-being of trees directly. For instance, higher [CO_2] allow trees to reduce stomatal conductance and to improve water-use efficiency (Ainsworth and Rogers 2007; Wullschleger et al. 2002). This is because CO_2 diffusion inside the photosynthetic apparatus is supported and saturation of ribulose-bisphosphate carboxylase (Rubisco) is enhanced (Bowes 1991; Farquhar et al. 1980). To study the physiological responses of trees to elevated [CO_2], free air carbon dioxide enrichment (FACE) experiments have been conducted from 1990 onward. These experiments revealed striking water saving potentials in elevated [CO_2] environment (Ainsworth and Long 2005; Battipaglia et al. 2013; Kauwe et al. 2013) and on global scale, increase in atmospheric [CO_2] was shown to enhance the proportion of anthropogenic CO_2 re-fixed into forests and other land-ecosystems (Walker et al. 2020). However, this observed fertilization effect of CO_2 was found to be highly dependent on tree age, species and ecosystem equilibrium status (e.g. sink strength) (Calfapietra et al. 2003; Dawes et al. 2010; Jiang et al. 2020; Körner et al. 2005; Körner 2006; Walker et al. 2019). The beneficial effects on biomass gain may also be limited by other parameters like nutrient availability (Fleischer et al. 2019; Körner 2006; Leakey et al. 2009; Walker et al. 2020). Thus, being able to anticipate to what extent the beneficial effects of CO_2 may continue, or even alleviate the negative effects of climate extremes is an urgent, but also challenging topic to study.

Regarding the aspect of increasing demand in renewable energy, forestry, CO_2 mitigation strategies and ecosystem functionality in general, it is crucial to understand the physiological responses of trees to combined stressors and in combination with elevated [CO_2] (e[CO_2]). This

also includes the underlying mechanisms to eventually find a strategy to mitigate negative climate effects.

1.2 Strategies of trees to respond to heat and drought stress

Trees are prone to unfavorable conditions, but they are not defenseless. They have developed a multitude of strategies to cope with stress, mitigating or preventing stress specific damages (Haak et al. 2017; Harfouche et al. 2014; Niinemets 2010; Saijo and Loo 2020; Shaar-Moshe et al. 2019; Teskey et al. 1987). One of the most critical stress situations for trees are exceptional long drought periods, which disrupt trees from their water supply at the soil matrix and threatens them to dry out (Körner 2019).

1.2.1 Drought

The diffusion driven uptake of CO_2 through the leaf stomata causes unavoidable water losses from the water saturated mesophyll to the dryer atmosphere. To replace the transpired water, trees have to extract water from the soil, which is transported in the xylem by means of the cohesion-tension mechanism (Dixon and Joly 1895). This mechanism is driven by capillary forces and adhesive molecule interactions and the water potential difference between the soil and the atmosphere (Jensen et al. 2016). Drought stress affects the water homeostasis and functionality of all tree organs as extraction of water by the roots is strongly limited, let alone under conditions of high vapor pressure deficits (VPD, low saturation vapor pressure of the air). This results in negative water pressures in the xylem, which trees strives to keep in a narrow range via regulation of stomatal aperture (typically between -0.5 and -2 MPa for *P. halepensis* (David-Schwartz et al. 2016; Klein et al. 2011; Oliveras et al. 2003)). If the water potential reaches critical thresholds (species specific, typically between -2 and -3 MPa) the probability increases that water molecules as well as dissolved gases transit into gas phase and are causing embolisms that most likely can only be compensated through growth of new xylem especially in the case of conifers (Brodribb and Cochard 2009; Rehschuh et al. 2020).

If embolism formation cannot be avoided during prolonged drought periods, xylem hydraulic conductance declines and turgidity of cells is lost. Further dehydration can also cause cell lysis (the rupture of the cell membrane from the rigid cell wall) (Hincha et al. 1987; Lang-Pauluzzi 2000). To avoid embolism formation, trees can close the leaf stomata (Brodribb et al. 2017) and decrease non-stomatal transpiration by thickening the leaf cuticle wax layer (Shepherd and Wynne Griffiths 2006). During prolonging drought conditions, the reduction of photosynthetic capacity due to stomatal closure may lead to metabolic imbalance as carbohydrates are being

consumed, which potentially affects the capability of the plant metabolome to sustain stress responses for a long time. (Gentine et al. 2016; Sevanto et al. 2014; Tomé et al. 2014).

The functioning of the tree's metabolism depends on sufficiently amounts of free water. Biochemistry processes of the cells depend on diffusion velocity, which is a function of viscosity (McCall et al. 1959; Schafer and Barfuss 1980) and hence the amount of water solvent. Furthermore, interactions between water molecules and proteins as well as membrane lipids serve for the correct development of lipid micelles and the functional shape of proteins (Chandler 2005; Kauzmann 1959). These interactions (e.g. hydrophobic effect, hydrogen bonds) can be manipulated by adding or removing solutes from the cytoplasm. All organisms, also trees, are using the accumulation of such compatible osmolytes to counter adverse effects of low water potentials (Yancey 2005). As these metabolites are accumulated in high amounts, they have to be non-toxic and used as an alternative carbon source. A collection of metabolites that comprise these conditions are amino acids (e.g. prolin) (Cyr et al. 1990; Verbruggen and Hermans 2008), sugars (e.g. threhalose, polysaccharides) (Hincha et al. 2007; Iordachescu and Imai 2008; Leslie et al. 1995) and alcohols (e.g. cyclitols) (Merchant et al. 2006; Nguyen and Lamant 1988). Furthermore, the synthesis of amino acids and sugars is energetically costly and may help to scavenge a surplus of reduced electron acceptor molecules to prevent the formation of reactive oxygen species during stress (Couée et al. 2006; Kruger and Schaewen 2003; Rizhsky et al. 2004).

1.2.2 Heat

In contrast to the water conserving strategies during drought stress, high temperatures can increase water losses to the atmosphere due to rising vapor pressure deficit (VPD). If enough water is available, trees have been reported to keep stomata open during heatwaves, sustaining high transpiration rates and achieving a substantial cooling effect (Drake et al. 2018; Kauwe et al. 2018; Urban et al. 2017a). However, on molecular levels, high temperatures increase membrane fluidity (Los and Murata 2004) and accelerate enzyme reactions (Daniel and Danson 2013). When temperatures reach a critical threshold (Niinemets 2018; Teskey et al. 1987), membranes can get leaky (Bajji et al. 2001; Saelim and Zwiazek 2000) and lose integrity while proteins denature and become functionless (Daniel et al. 2008).

Especially membrane lipids are targets of reactive oxygen species (Stark 2005) which are produced during heat stress, forming toxic byproducts and messenger molecules that induce stress responses (Mittler et al. 2012). The tolerated temperature range of enzymes can be increased by the expression of small heat shock proteins that act as chaperones and stabilize the

three-dimensional structure of proteins (Al-Whaibi 2011; Hamilton 2001; Richter et al. 2010) and by the accumulation of compatible osmolytes (Hamilton 2001; Jaindl and Popp 2006). The temperature tolerance of membranes can be increased for instance by integrating more saturated fatty acids into the membrane bilayer (Quinn 1988).

Another typical response to high temperatures is the emission of biogenic volatile organic compounds (BVOC) (Joó et al. 2011; Kleist et al. 2012; Loreto and Schnitzler 2010). They are products of the primary- as well as of the secondary metabolism and are thought to play a key role in stress signaling (Kivimäenpää et al. 2020). Some, for instance isoprene, play a role as antioxidants or act membrane stabilizing (Velikova et al. 2011). The response of biogenic volatile organic compounds to temperature is well captured (Grote et al. 2019; Guenther et al. 1993; Harley et al. 2014; Niinemets and Reichstein 2002; Staudt et al. 2017), while their kinetics during multi-stress exposure and repeated stress (e.g. heatwaves together with drought) is less clear (Bamberger et al. 2017; Kleist et al. 2012). Furthermore, changes in emissions that precede mortality are of high interest but not yet well represented for trees and forests. As for grasses, BVOC emissions are known as indicator for drying and degrading biomass (Gouw et al. 1999). A similar knowledge related to trees and forests, as for instance the distinct relationship of temperature gradients to monoterpene emissions (Jardine et al. 2017), might be used as a tool to screen larger areas for severe stress and mortality risk, or for better understanding of air chemistry during and after largescale forest degradation (Geddes et al. 2016).

1.2.3 Heat-drought

High temperatures and low water availability often co-occur under natural conditions during summer drought spells or during extreme heatwaves. The combination of these stressors is especially dangerous for trees (Bertini et al. 2011; Ciais et al. 2005; Schuldt et al. 2020). During a heat wave, drought stress may be amplified as a result of increasing evaporative demand. On the other side, drought induced stomata closure may lead to higher leaf temperatures due to suppressed evaporative cooling (Chaves et al. 2016; Drake et al. 2018; Fontes et al. 2018). Thus, the combinations of heat and drought stress challenges the metabolic stress response of trees and may induce responses that are not found when trees are stressed by only one stressor (Correia et al. 2018). Similar to the trait off between water loss prevention, carbon uptake and cooling capacity (Ruehr et al. 2016), the metabolism may face conflicting strategies (Rizhsky et al. 2004).

From a carbon balance perspective, high temperatures increase the carbon turnover and respiration of the trees (Gauthier et al. 2014; Patterson et al. 2018; Ruehr and Buchmann 2010).

Both, drought and heat, reduce the photosynthetic capacity of the leaves on enzyme activity level (Demirevska-Kepova and Feller 2004; Parry et al. 2002) and also on the level of photosystem efficiency (Dreyer et al. 2001; Duarte et al. 2016; Kitao et al. 2000; Nellaepalli et al. 2014; Tang et al. 2007). Furthermore, a more rapid decrease of solubility of CO_2 (Ku and Edwards 1977a) and the decreasing specificity of Rubisco to CO_2 with increasing temperatures (Jordan and Ogren 1984; Ku and Edwards 1977b). Thus, the fixation of O_2 instead of CO_2 through Rubisco increases with temperature, which additionally lowers carbon yields under stressful conditions. Under conditions, where energy needed for maintenance surpasses carbon fixation rates the carbon balance can become zero or even negative (Ciais et al. 2005; Zhao et al. 2013). If trees manage to adapt their maintenance effort to the new stress conditions (Drake et al. 2019b; Reich et al. 2016), carbon gain and carbon loss may however reach a new equilibrium (Atkin and Tjoelker 2003; Kolb et al. 2013; Larigauderie 1995) allowing the trees to recover (Ruehr et al. 2019).

As introduced in Chapter 1.1, high CO_2 concentrations have the potential to affect not only the carbon supply but also the water balance of trees. This raises the question whether increased atmospheric CO_2 concentrations could support tree growth under drier conditions and whether these positive effects can be maintained at higher temperatures.

1.3 CO_2 and stress mitigation

CO_2 influences plant performance at many physiological interfaces of the tree. Higher CO_2 levels increase photosynthesis and decrease stomatal conductance (Ainsworth and Rogers 2007; Dusenge et al. 2019). Higher photosynthesis rates feedback on carbohydrate levels and other metabolites (Körner et al. 2005; Li et al. 2018). Water balance of the tree is influenced by CO_2 dependent stomata closure, which can reduce water loss through transpiration (Dusenge et al. 2019; Leakey et al. 2009). Both, metabolic changes and better water retention can increase growth rates of trees in e[CO_2] (Bowes 1991; Gamage et al. 2018; Hussain et al. 2001; Klein et al. 2016a; Körner et al. 2005; Major and Mosseler 2019). Some of the mechanisms that explain how CO_2 can change the physiological network of trees and its response to stress are examined below.

1.3.1 Elevated [CO_2] increases leaf internal [CO_2]

Higher atmospheric concentrations (C_a) accelerate diffusion of CO_2 molecules into the stomatal space and the photosynthetic active cells (C_i). High C_i on the other side can reduce stomatal aperture (Dusenge et al. 2019; Engineer et al. 2016; Medlyn et al. 2001), which decreases transpiration (E) and stomatal conductance (g_s). Although a decrease in g_s can increase water-use efficiency (WUE) (Kauwe et al. 2013; Leakey et al. 2009; Wullschleger et al. 2002), which is

especially beneficial under drought conditions, lower evaporative cooling capacity under e[CO_2] can increase leaf temperatures and may be disadvantageous during heatwaves and drought (Bauweraerts et al. 2013; Fauset et al. 2019; Konrad et al. 2020; Peterhansel and Maurino 2011).

Besides the effect on WUE, the maximum rate at which photosynthesis performs is also affected by C_i (Bowes 1991). The central enzyme of the Calvin cycle ribulose-1,5-bisphosphate carboxylase (Rubisco) has not only specificity to CO_2 but also to O_2 (Jordan and Ogren 1984; Ku and Edwards 1977b). Adding O_2 instead of CO_2 to ribulose-1,5-bisphosphate (C5) produces one molecule phosphoglycolate (C2), which is toxic and has to be expensively recycled, and one molecule phosphoglycerate (C3) (instead of two molecules phosphoglycerate C3). Carbon is lost during this process ("photorespiration") and redox-equivalents have to be invested to detoxify byproducts (Peterhansel and Maurino 2011). Thus, saturation of Rubisco activity increases CO_2 fixation efficiency and net photosynthesis (A_{net}). Some studies show, that this effect can even be sustained at higher temperatures (Pan et al. 2018), which would improve plant performance during heat stress. Others show that the nutrients level of the plants plays an important role (Hymus et al. 2001) as protein or chlorophyll may be limiting (Hymus et al. 2002).

1.3.2 Enhanced carbon gain sustains more biomass and affects tree allometry

Plant growth is the main process that causes a positive carbon balance in trees and positively feeds back with both, A_{net} and respiration (R). Higher WUE and higher A_{net} under e[CO_2] usually increases biomass production in trees (Ainsworth and Long 2005; Jiang et al. 2020; Körner 2006). As biomass increases, also R increases, which might accelerate carbon turnover under e[CO_2] (Jiang et al. 2020). Some studies show that under e[CO_2] biomass specific R is downregulated (Drake et al. 1999; Gonzalez-Meler et al. 2004), indicating reduced maintenance costs. The carbon to nitrogen ratio (C:N) typically increases (Cotrufo et al. 1998; Li et al. 2018; Runion et al. 1999) as trees accumulate nonstructural carbon (NSC), phenolic components (Holopainen et al. 2018; Peñuelas and Estiarte 1998) and increase cell wall thickness (Prendin et al. 2017; Richet et al. 2012), which dilutes N on plant level, while proteins are downregulated (Bloom et al. 2002) and nitrate assimilation inhibited (Bloom et al. 2002; Wujeska-Klause et al. 2019). Reduction of R may alleviate maintenance costs during heat and drought stress, while more biomass might counter positive e[CO_2] effects on E and R.

CO_2 not only affects gross biomass production but also allocation of carbon and allometry within the tree (Jiang et al. 2020). Shoot growth and leaf biomass are increased (Ainsworth and Long 2005; Calfapietra et al. 2003; Jiang et al. 2020; Leakey et al. 2009; Trugman et al. 2019) together with fine root mass (Bader et al. 2009; Norby et al. 2004; Pregitzer et al. 1995) and the formation

of root hair (Niu et al. 2011). Especially a spatial distribution change (Duursma et al. 2011; Piñeiro et al. 2020) may have relevance for tree's access to nutrients and water during prolonged drought. Mechanisms behind this pattern are discussed as being higher carbohydrate levels feedback with plant hormones (Geng et al. 2016; Niu et al. 2011). Another trigger for fine root growth may be a higher N demand due to CO_2 fertilization (Norby et al. 2010). Furthermore, cell differentiation and cell division have been shown to be changed by CO_2 directly via HCO_2 responsive proteins (Engineer et al. 2014; Engineer et al. 2016), increasing the rate of cell division (Masle 2000), affecting xylem architecture (Hao et al. 2018; Prendin et al. 2017) and leaf stomata distribution (Higaki et al. 2020; Lawson and Matthews 2020; Woodward and Kelly 1995). At this point the ambivalence of the role of CO_2 in trees becomes apparent, since a higher leaf to sapwood area can hinder short-term acclimatization to heatwaves and drought events (Trugman et al. 2019).

1.3.3 Elevated CO_2 alters the redox state of the metabolome

High atmospheric [CO2] was discussed to reduce stress caused by heat and drought at several metabolic levels (Zinta et al. 2014). These effects are caused by increases in carbon status and relaxations in the metabolic redox state, which are mediators of physiologic stress response (Foyer and Noctor 2011; Noctor et al. 2014; Noctor and Mhamdi 2017). Elevated CO_2 was found to increase base level of carbohydrate derived messenger molecules (Mhamdi and Noctor 2016), for instance salicylic acid, while the reduced amount of reactive oxygen species (ROS) are expected to interfere with stress sensing and signaling reducing the overall stress responsiveness of the plant (AbdElgawad et al. 2016; Cassia et al. 2018). The carbohydrate metabolism as well as photorespiration pathways are crosslinked with the amino acid metabolism (Eisenhut et al. 2017; Peterhansel and Maurino 2011; Wujeska-Klause et al. 2019). Thus, changes in the amino acid composition and the synthesis of compatible osmolytes may be expected and have been found in several studies (Bloom et al. 2002; Dietterich et al. 2015; Geng et al. 2016; Misra and Chen 2015; Noguchi et al. 2015). The consequences of these changes are not fully understood, but they may affect protein synthesis, host-pathogen as well as host-symbiont relationships and last but not least human nutrition.

1.4 Semi-arid forest ecosystems – Pinus halepensis in the Yatir forest in Israel

Semi-arid forest ecosystems are especially vulnerable to decreasing rainfall and increasing extreme heatwaves recurrence (Goldstein et al. 2000; Gonzalez et al. 2012; Liu et al. 2013; Sivakumar et al. 2005). Semi-arid environments are defined by an accentuated seasonality that can be described as a hot (or very cold) dry season when evapotranspiration surpasses the amount of precipitation and a moist season in which precipitation equals, or surpasses

evapotranspiration. In regard to this, (Fischer and Turner 1978) mentioned that growth and assimilation in semi-arid ecosystems is mainly concentrated on the short spring period, when temperatures are favorable and water availability is highest. Although such ecosystems are well adapted to seasonal changes (Arneth et al. 2006; Churkina and Running 1998; Tatarinov et al. 2015), it is highly intuitive to think of future situations of extreme long-lasting drought events and heatwaves that disturb this synchronized system – which could lead to long lasting negative effects on forest resilience and productivity.

In the vast quantity and diversity of semi-arid-regions all over the world, the Yatir forest located in the southeast of Israel, is a unique example of a *Pinus halepensis* (Miller) dominated forest planted at the norther edge of the Negev desert (Fig. 1.1; Flux-Net tower position: IL-Yat, 650 m a.s.l., 31°20'49.2''N, 35°03'07.2''E). It is characterized by an extraordinary small amount of precipitation, on average 200–300 mm per year, concentrated between October and April - following long periods without precipitation during summer and solar irradiation comparable to regions within the Sahara desert, that can reach up to 2000 µmol $m^{-2}s^{-1}$ radiation load (Klein et al. 2016b; Preisler et al. 2019; Rotenberg and Yakir 2010; Tatarinov et al. 2015).

Figure 1.1: Impressions of the Yatir forest plantation (left) and the measurement site inside the forest in reach of the flux tower (right). Pictures are from a site visit in March 2016 during the wet season (own pictures).

Periodically occurring "Hamsin" events, which are characterized by up to seven days of extreme heat, are typically occurring several times during spring and early summer. (Tatarinov et al. 2015) showed that these heatwaves, which often reach up to 35°C resulting in a vapor pressure deficit of up to 6 kPa, occur when productivity is highest and are reducing carbon uptake and canopy conductance. This may cause additional stress on the trees before the onset of the seasonal

summer drought (Stangler et al. 2016; Tatarinov et al. 2015; Thomas et al. 2009). The extreme conditions at the Yatir forest site probably represent the dry edge timberline of *P. halepensis* (Grünzweig et al. 2009), increased tree mortality was found recently in response to extraordinary dry years (Klein et al. 2019; Preisler et al. 2019).

Following questions emerge: Does the Yatir forest has a future in regard to increasing extreme temperatures and even less precipitation than it receives nowadays? Is *P. halepensis* able to profit from higher [CO_2] under these conditions?

1.5 Aims and structure of the thesis

This thesis is part of a collaborative research project that aims to elucidate the “climate feedback and benefits of semi-arid forests (CliFF, YA 274/1-1; SCHM 2736/2-1)” funded by the German Research foundation (DFG) within its German-Israeli Project Cooperation program. The CliFF project has been done in a close collaboration of the Karlsruhe Institute of Technology (KIT) and the Weizmann Institute of Science (WIS). The overall aim of the project is to investigate the impact of semi-arid forests on the Earth's climate from chemical, biological and meteorological perspectives using experimental and modeling approaches.

Within the CliFF project my thesis aims on (1) quantifying the **impact of extreme heatwaves during drought on the physiology of Aleppo pine (*Pinus halepensis*) seedlings** and (2) understanding the role of future **high CO_2 concentrations on plant performance and in altering physiological responses to single and multiple stress**.

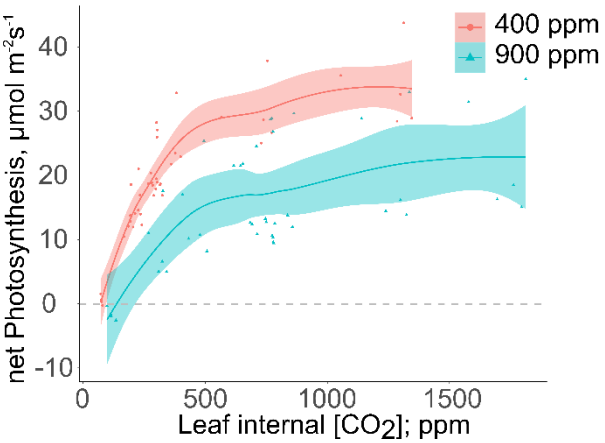

Figure 1.2: A:C_i plot of *P. halepensis* seedlings grown for 9 months at elevated CO_2 (turquoise triangles) and ambient CO_2 (red circles). Ribbons depict 95% confidence interval of R package ggplot2 default loess (locally weighted scatter-plot smother) function fit (colored lines). Data are single measurements of five seedlings per CO_2 treatment.

With this thesis I aim to shed light on how opportunities and limitations of Aleppo pine seedlings might change under future climate conditions. More specific, the perspective range of environmental conditions was set to extreme heat, and moderate soil drought. Soil drought was

introduced to the setup because a characteristic of this semi-arid region is the long precipitation-free period from May to October. The forest site experiences heatwaves ("Hamsin" periods) quite regularly during spring (see (Tatarinov et al. 2015), which have clear consequences for carbon and water cycling. Hence, we designed an experiment that mimicked repeating "Hamsin" events. To assess the response of Aleppo pine to elevated CO_2, we decided to use extremely high CO_2 concentrations following the RCP8.5 scenario for 2100 (Collins et al. 2013; Schwalm et al. 2020). We did so to increase a possible mitigating effect of CO_2 on the trees stress response. This was given because 900 ppm represents a concentration that is near the saturation point of the seedlings photosynthetic systems (Fig. 1.2).

The study has been done in two separately designed experiments. The first experiment was to define stress thresholds that included tree death and post-stress recovery and included measurements of seedlings gas exchange, VOC emissions and metabolites. The second experiment was designed to provide insight into the differences of stress responses of drought-acclimated and sufficiently watered seedlings along a temperature gradient that were grown in either ambient (400 ppm) or strongly elevated CO_2 (900 pm) environments. In this experiment the entire carbon balance of the seedlings could be quantified and alongside an array of primary metabolites measured.

Setup 1: The repeated heatwave approach

The first experiment (2016) was set up to define stress thresholds of tree seedlings (*P. halepensis*, Mill) that were exposed to extreme heat and moderate drought, allowing for seedling recovery as well as mortality under ambient CO_2 conditions (~400 ppm). Environmental drivers where adapted to resemble conditions at a semi-arid *P. halepensis* plantation site in Israel (Yatir forest) during growth conditions for 10 months. Two dry heatwaves were initiated in Mai and June 2016, adding +5 °C to the maximum heatwave temperatures. The recovery and stress limits were assessed on the basis of biogenic volatile organic compound (BVOC) emission via proton transfer reaction mass spectrometry (PTRMS), primary metabolism stress responses and plant-level physiological adaption. These parameters were derived from lab analyses and online gas exchange measurements.

Setup 2: Heatwave responses of Aleppo pine at ambient and elevated [CO_2]

The second experiment (2017) was prepared to decipher the role of high atmospheric [CO_2] on the seedlings' stress response. All seedlings used in this study where grown from seeds either under elevated [CO_2] (~900 ppm) or under ambient [CO_2] (~400 ppm) experiencing the same

environmental conditions regarding radiation, temperature and humidity (soil and air). Half of the cohort was adapted to drought supposedly to result in growth retention and substantial physiological adaption. This threshold was taken from the results of the first setup (2016). All seedlings were exposed to a slow (2d) temperature gradient ramp from 25 °C to 40 °C. Separated net photosynthesis and autotrophic respiration of each seedling was used to calculate tree carbon uptake. Needle tissue as well as root tissue samples were taken to screen the primary metabolome for effects of elevated [CO_2] and drought alongside of a heat gradient. Carbon balance during stress response was derived from simultaneous shoot and root gas exchange measurements and metabolic stress response was analyzed in tissue samples via time-of-flight gas chromatography mass spectrometry (Tof-GCMS).

This led to my working hypotheses: **I) An increase of 5 °C (RCP8.5) in heatwave maxima threatens semi-arid forests** (exemplary study adapting Yatir-forest stand environmental conditions on *P. halepensis* seedlings). **II) Exposition to multiple types of stressors** (heat, drought, and heat-drought) **changes physiological stress response on gas exchange and metabolic levels.** II b) Therefore, it will be possible to assign volatile organic compound signals from the seedlings to either heat or drought and multi-stress scenarios. **III) Increased [CO_2] can improve the growth and water-use efficiency of trees, as temperature increases, higher carbon storage facilitates metabolic acclimation to heat and drought.**

2 Heatwaves alter carbon allocation and increase mortality of Aleppo Pine under dry conditions.

This chapter has been published as: **Birami B., Gattmann M., Heyer AG., Grote R., Arneth A., Ruehr NK. (2018):** Heat waves alter carbon allocation and increase mortality of Aleppo Pine under dry conditions. *Frontiers in Forests and Global Change* **1**: 1285.
doi: 10.3389/ffgc.2018.00008.

Abstract

Climate extremes are likely to occur more frequently in the future, including a combination of heatwaves and drought. The responses of trees to combined stress, as well as post-stress recovery are not fully understood, yet. This study was designed to investigate the responses of semi-arid *Pinus halepensis* seedlings to moderate drought, heat and combined heat-drought stress, as well as post-stress recovery. The seedlings were grown under controlled conditions and exposed to two 4-day-long heatwaves, reaching air temperature maxima of 42 °C and vapor pressure deficit (VPD) of 7 kPa. Day- and nighttime canopy gas exchange was measured and differences in shoot and root allocation of non-structural carbohydrate (NSC) compounds (soluble sugars, starch, cyclitols and carboxylic acids). Fluorescence parameters, nitrate levels, proline content and shoot water potential (ψ) provided additional indicators for stress severity and recovery performance. During the heatwaves, net photosynthesis and stomatal conductance decrease immediately.

This decline was modest under well-watered conditions, with transpiration and dark respiration rates remaining high and despite reductions in root NSC content, trees recovered following heat release. This was not the case in the heat-drought treatment, where stress resulted in mortality and the few surviving seedlings showed stress symptoms, persistent in reduced gas exchange rates and low root NSC content, while leaf nitrate and proline remained elevated three weeks after heat release. Shoot ψ indicated that hydraulic failure was not the reason for mortality in the heat-drought seedlings, but most likely the low transpiration rates, which resulted in needle temperatures >47 °C during heat stress (c. 6 °C above air temperature). In summary, we could demonstrate that heatwaves in combination with moderate drought can either result in mortality or, if the seedlings survive, in delayed recovery. This highlights the potential of an increase in heat wave temperatures to trigger forest decline in semi-arid regions.

2.1 Introduction

Forest dieback related to climate extremes has been observed in most regions of the world (Allen et al. 2010; Anderegg et al. 2012; Anderegg et al. 2015). In particular heatwaves combined with drought, which are increasing in frequency and duration (Meehl and Tebaldi 2004; Schär 2015), could be a major trigger of tree mortality (Allen et al. 2015; Williams et al. 2013), yet our understanding of physiological processes within trees to such extremes is scarce.

Trees tightly regulate stomatal conductance (g_s) to balance water supply and water loss. The close coordination between leaf water potential (ψ) and g_s during drought conditions has been reported manifold (Anderegg et al. 2018; Burghardt and Riederer 2003; Jarvis 1976; Klein and Niu 2014; Ripullone et al. 2007), while the responses of g_s to changes in evaporative demand, particular in combination with high temperatures is less clear. During experimental heat wave conditions, g_s has been found to decline (Drake et al. 2018; Duarte et al. 2016; Ruehr et al. 2016; Tatarinov et al. 2015) or to be not affected (Ameye et al. 2012) or to even increase (Urban et al. 2017a; Urban et al. 2017b). Despite such differences in stomatal responses, most heatwave studies have found transpiration (*E*) to increase under high soil water content. At first, this seems counterintuitive, but can be explained by increases in evaporative demand, which stimulates *E* and cooling of the leaf*,* even though stomata close partially.

Increased *E* causes water-use efficiency (WUE) to sharply decrease, because photosynthesis typically declines at high temperatures (Ameye et al. 2012; Drake et al. 2018; Duarte et al. 2016; Ruehr et al. 2016; Tatarinov et al. 2015; Urban et al. 2017a), which results in a pronounced carbon-water decoupling during heatwaves (Drake et al. 2018). The underlying reasons for the strong decline of photosynthesis under heat stress are manifold and include decreases in g_s (Ruehr et al. 2016), reduced performance of the photosynthetic apparatus (Ameye et al. 2012; Urban et al. 2017a), or a combination of both (Duarte et al. 2016), but also increased photorespiration or photosynthetic inhibition play an important role (Teskey et al. 2015). High temperatures affect key enzymes like Ribulose-bisphosphate-carboxylase directly (Haldimann and Feller 2004), cause inactivation or denaturation of integral proteins and increase membrane leakage as well as cellular lesions (Hays et al. 2001; Hüve et al. 2011; Quinn 1988; van Meer et al. 2008; Watson 2015). Temperature thresholds resulting in permanent photosynthetic and whole-leaf damage are reported to range between 40 °C and 50 °C (Colombo and Timmer 1992; Hüve et al. 2011; Niinemets 2018; O'Sullivan et al. 2017; Rätsep et al. 2018), whereas the exact threshold depends on species, the duration of exposure, water availability and adaptive metabolic responses.

Besides direct tissues damage, temperature increments affect tree C allocation dynamics (Ruehr et al. 2016; Zhao et al. 2013). Because respiration typically increases with temperature, C loss can become larger than C uptake (Zhao et al. 2013) and NSC reserves in trees may deplete. In addition, shoot-to-root allocation patterns are sensitive to stress. While reduced C transport from shoots to roots under drought conditions has been observed (Blessing et al. 2015; Ruehr et al. 2009; Zang et al. 2014), C allocation towards roots can increase under high temperatures (Blessing et al. 2015). However, it remains unclear how such changes in C allocation between C compounds and tissues may affect the stress resilience of trees. For instance, C compounds such as proline or sugar alcohols can prevent protein denaturation at high temperatures (Hamilton 2001; Jaindl and Popp 2006) and maintaining large NSC reserves will be critical to sustain high respiration rates. This indicates a potentially important role of the primary C metabolism in mitigating long-term damages and hence could influence post-stress recovery. It can be speculated that besides actual tissue damage, the amount of C maintained during stress could be a driving force of repair mechanisms (Galiano et al. 2017), but to date not much is known on post-stress C metabolism of trees.

Following stress release, the ability of trees to recover from heatwaves depends on stress severity, which is directly influenced by heat exposure as found for the recovery of photosynthesis (Hüve et al. 2011). If heatwaves are additionally combined with drought, evaporative cooling is diminished and canopy temperature increases (Scherrer et al. 2011). This should then accelerate stress-induced damage and has the potential to further delay post-stress recovery. Semi-arid regions are at particular risk because air temperatures are already high and a few degrees of warming have the potential to quickly surpass critical levels, especially when evaporative cooling is typically low (Liu et al. 2013; Rotenberg and Yakir 2010). In particular the regeneration in semi-arid forests might be jeopardized, because seedlings are most vulnerable to desiccation due to low water storage and rooting depth (limited water supply), while they are growing close to the soil surface, which exposes them to excessively high temperatures (Kolb and Robberecht 1996).

The present study investigates the impacts of high temperatures under well-watered and drought conditions on seedlings of *Pinus halepensis,* originating from one of the driest pine forest plantations in the world, located in the Negev desert (Rotenberg and Yakir 2010). In this region, short heatwaves frequently occur, with instantaneous responses of the forest's carbon and water cycling (Tatarinov et al. 2015). If temperatures are further increasing, as predicted for this region, and precipitation during winter decreases (Giorgi and Lionello 2008; Tabari and Willems 2018), the trees might be pushed beyond their stress tolerance limits and the survival of this unique

forest might be at risk. Thus, to increase understanding of Aleppo pine's responses to extreme heatwaves and the recovery from stress, shoot gas exchange, fluorescence parameters, and some primary metabolites in shoots and roots were determined. In particular the following research questions were adressed: 1) How is shoot gas exchange and water-use efficiency affected during heatwaves with or without drought and do the responses of g_s, photosynthesis and *E* differ with increasing vapor pressure deficit? 2) What are the main drivers of C compound and metabolite dynamics and their allocation between shoots and roots? 3) Are heat and heat-drought stress responses fully reversible post-stress or does mortality occur?

2.2 Material and Methods

2.2.1 Plant cultivation and initial pre-treatment conditions

Pinus halepensis (Miller) seedlings were grown from seeds in a scientific greenhouse facility in Garmisch-Partenkirchen, Germany (732 m a.s.l., 47°28'32.87''N, 11°3'44.03''E). The origin of the seed material is a 50-year-old Aleppo pine plantation in Israel (Yatir forest). Cones of trees were sampled growing in close-proximity to a meteorological station and flux tower (IL-Yat, 650 m a.s.l., 31°20'49.2''N, 35°03'07.2''E). About 2–4 weeks after germination of seedlings in Germany, the seedlings were transferred to 1 L pots each, containing a mixture (2:8) of quartz sand (0.7 mm and 1-2 mm) and vermiculite (ca. 3 mm) with 2 g of slow-release fertilizer (Osmocote® Exact + TE 3-4-month fertilizer 16-9-12+2MgO+TE, Everis International B.V., Heerlen, The Netherlands). Three months before starting the experiment, 7 months-old seedlings were planted in larger pots (2.5 L) containing a mixture of 1:2:1 quartz sand (1-2 mm): quartz sand (Dorsolit 4-6 mm): vermiculite (3 mm) with 6 g of slow-release fertilizer added (Osmocote® Exact +TE 5-6-month fertilizer 15-9-12+2MgO+TE). Potted seedlings were irrigated regularly, starting with 0.1 L per week, which was later adapted to meet increased water demand of the growing seedlings to 0.15 L per week.

Seedlings were grown under average light intensity of 693 ± 324 µmol $m^{-2}s^{-1}$ (supplemented by sodium vapor greenhouse lamps, T-agro 400 W, Philips) and temperatures and humidity adapted to 10-year monthly-averaged day and night air temperature and relative humidity measured at the Yatir forest site (see Supplement, Table S2.1). One month before the start of our experiment, seedlings were gradually acclimated from average daytime temperatures of 18 °C (night: 12 °C) to 25 °C (night: 15 °C). This is close to the 10-year average measured at Yatir forest during May, when the occurrence of short heatwaves is typically observed (Tatarinov et al. 2015).

Seedlings were assigned randomly either to a control, drought, heat or heat-drought treatment with 30 seedlings per group. To maintain ambient air temperature and relative humidity in the

control and drought treatment, while conducting heatwaves in the heat and heat-drought treatment, the seedlings were placed in two adjacent, but individually controllable compartments of the greenhouse facility.

2.2.2 Environmental variables

Air temperature and relative humidity sensors (CS215, Campbell Scientific Inc., Logan, Utah, US, enclosed in aspirated radiation shields type 43502, Young, Traverse City, MI, USA) and photosynthetic active radiation (PAR) (PQS 1, Kipp & Zonen, Delft, The Netherlands) were measured continuously at canopy height in each greenhouse compartment. Carbon dioxide concentration was monitored with a CO_2 probe (GMT 222, Vaisala, Helsinki, Finland). Soil water content was measured automatically in 10 pots per treatment using substrate-specific calibrated probes (10HS, Decagon Devices, Inc., WA, USA). All environmental sensors produced half-hourly data that were recorded with data loggers (CR1000, Campbell Scientific, Inc. USA).

Soil moisture is given as relative soil water content (RSW) as follows:

$$RSW = 100 * \frac{(SWC_{sample} - SWC_{min})}{(SWC_{max} - SWC_{min})} \quad (1)$$

where SWC_{sample} is the actual volumetric soil water content, SWC_{min} is the minimum volumetric soil water content after drying the soil for 48 h at 60 °C. SWC_{max} is the soil water content at maximum water holding capacity, which was about 200 $cm^3\ L^{-1}$ (20 % v/v) for our substrate.

2.2.3 Experimental conditions

Aleppo pine seedlings exposed to heat and heat-drought treatments were subjected to two heatwaves of 4 days each (April 27th – April 30th and May 7th – May 10th, 2016). We simulated heatwaves by a gradual temperature increase over 2 days, reaching a maximum during the following 2 days, according to observations in the Yatir forest (Tatarinov et al. 2015). In order to test how projected further temperature increases of 2 to 6 °C in the Mediterranean region (Seneviratne et al. 2012) might affect survival of tree seedlings, we chose to set 5 °C higher air temperature maxima than have been reported so far (Tatarinov et al. 2015). This resulted in a maximum of 43.1 °C during the first heat wave and 42.4 °C during the second heat wave. Relative humidity (RH) during the heatwaves was kept between 20 and 40 %, which corresponded to a similar air water content as under ambient temperature conditions. This resulted in a pronounced increase of VPD up to 7.5 kPa during the heatwaves (Fig. 2.1A and B), corresponding to observations in the Yatir forest (Tatarinov et al. 2015). In total, extreme air temperatures above 40 °C and VPD > 6 kPa were maintained for 10 hours during the first heat wave and 12 hours

during the second heat wave. Dark-phase (PAR < 10 µmol $m^{-2}s^{-1}$) temperatures reached 33.0 °C during the first- and 32.9 °C during the second heatwave with a total exposure time of 13 hours above 30 °C for each heatwave. Outside light was supplemented by sodium vapor lamps, resulting in an average PAR of 416 ± 105 µmol $m^{-2}s^{-1}$ during the course of the experiment (Fig. 2.1C). Irrigation of the seedlings was adapted to maintain targeted soil water availability. During the initial control conditions and during the recovery at the end of the experiment, seedlings were watered to a RSW of 40-50 % (about 0.15 L three-times per week), which is similar to the average wet season condition of the Yatir forest site (pers. com. Yakir Preisler). One week before the start of the first heat wave, irrigation was withheld in the drought and heat-drought treatment (for four days) until a RSW of about 15 % was reached (Fig. 2.1D). This RSW was maintained by watering with 0.05 L three-times per week. One week after release of the second heat wave, all plants were irrigated to reach similar RSW conditions of 40-50 %.

In order to avoid a possible influence on the seedlings from positioning within the greenhouse the position of the seedlings was altered randomly every two weeks during the initial growth phase. Later, during the experimental phase, after the seedlings were transferred to two separate greenhouse compartments, the seedlings were placed spatially interspersed in a randomized block design. During this phase, seedling position was unchanged because automated shoot cuvettes for gas exchange measurements (see section 2.4) and soil moisture sensors were permanently installed. However, it has been shown that environmental control of our greenhouse facility is exceptionally close (Ruehr et al. 2016). Differences in daily-averaged RH between the greenhouse compartments were below 3 % (ΔPAR < 6 %) when heatwaves were not applied in this experiment. Slightly larger differences in air temperature were detected before the first heat wave (c. 1.0 °C), which could be reduced to 0.2 °C during the remainder of the experiment.

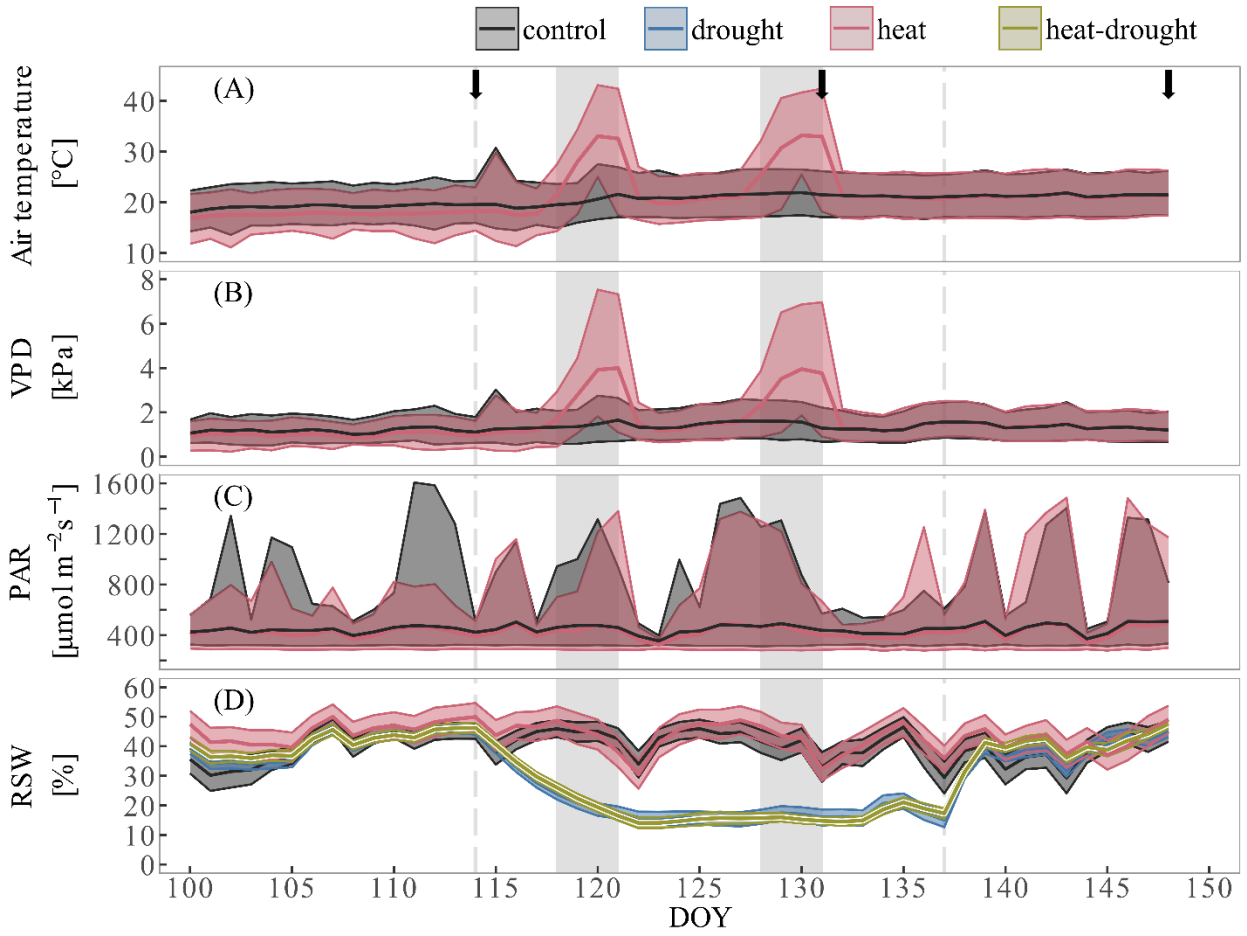

Figure 2.1 Environmental conditions during the course of the experiment. Shown are (A) air temperature, (B) vapor pressure deficit and (C) photosynthetic active radiation. Colored lines depict daily mean values of two sensors at canopy height (control: black, heat: red), shaded area give daily minimum and maximum values. (D) Relative soil water content (rSWC) are treatment averages (n=10) per day. The shaded area is mean ±1 SE. Dotted lines show begin and end of drought phase, grey shaded areas indicate duration of the two heatwaves.

2.2.4 Gas exchange measurements

Net photosynthesis (A_{net}), night respiration (R_{dark}) and light phase transpiration (E_{day}) of *Pinus halepensis* shoots were measured with an automated cuvette system, described previously (Bamberger et al. 2017; Duarte et al. 2016). Highly UV-transmissive acrylic glass tubes (PMMA Saalberg, 30L: 18W) were placed around tree shoots (n = 4 per treatment). The bottom side of each cuvette was sealed by an acrylic glass cap, which could be taken apart for insertion of the seedling. Remaining gaps between tree stem and cap were sealed using plastic putty (Teroson, Düsseldorf, Germany). Each cuvette was supplied with a photodiode for PAR spectrum (G1118, Hamamatsu Photonics, Hamamatsu, Japan) and cross-calibrated with high-precision PAR

sensors (PQS 1, Kipp & Zonen, Delft, the Netherlands). For temperature measurements, each cuvette was equipped with a previously calibrated thermocouple (5SC-TTTI-36-2M, Newport Electronics GmbH, Deckenpfronn, Germany). Air mixing within the cuvettes was maintained by a fan (412 FM, ebm-papst GmbH & Co. KG, Mulfingen, Germany). The cuvettes were measured sequentially for 10 minutes each. After the distal cap had closed automatically, reference air of known CO_2 and H_2O concentration at a rate of 5 L min^{-1} was supplied to the cuvettes. The flow rate was controlled by a digital mass flow controller (F-201CZ–10K, Bronkhorst, Ruurlo, Netherlands). The measurement air (reference) was generated by an oil-free compressor (SLP-07E-S73, Anest Iwata, Yokohama, Japan) with an Ultra Zero Air generator (Ultra Zero Air GT, LNI Schmidlin SA, Geneva, Switzerland). CO_2 and water vapor (nebulizing evaporation pump, LCU Liquid Calibration Unit, Ionicon, Innsbruck, Austria) was supplied at a constant rate to the air stream, resulting in a CO_2 concentration of 438 ± 3 µmol mol^{-1} and a water vapor concentration of 6.5 ± 0.1 mmol mol^{-1} on average during the experiment.

The slight overpressure that was deliberately generated during each measurement prevented outside air from entering the system. The overpressure and relative air tightness of our system resulted in a sample air stream of 1 to 3 L min^{-1}. Concentration changes between reference and sample air (each provided with 0.5 L min^{-1}) were measured using a LI-7000, which was connected to a LI-840 (both LI-COR Inc., Lincoln, NE, USA) for absolute concentration measurements of the reference air stream. The sample cells of the two instruments were all supplied with an air stream of 0.5 L min^{-1} each. The LI-840 and LI-7000 were zero and span calibrated before the start of the experiment and the two measurement cells of the LI-7000 were matched weekly.

As an additional quality check, one cuvette per greenhouse compartment was left empty and allowed detecting any offset between the reference and sample air not caused by plant gas exchange. The concentration differences were small (CO_2: 0.4 [-0.2, 1.2] µmol mol^{-1} in median with lower and upper quartiles; H_2O 0.07 [0.05, 0.12] mmol mol^{-1} with lower and upper quartiles) and were removed by subtraction upon data analysis. After each measurement cycle, the system was flushed with reference air for 1 minute. For flux calculation the last 180 s per measurement were used if the following criterion for stability was met: change in [CO_2] < 0.5 µmol s^{-1} and change in [H_2O] < 0.5 mmol s^{-1}. In total, 94 % of the measurements were used for flux calculations.

Gas exchange rates were calculated following an open chamber approach. In brief, (E_{day}) was derived as follows:

$$E_{day} = \frac{\dot{m}\,\Delta W}{\mathrm{Area}_{leaf}*\left(1-\frac{W_{sample}}{1000}\right)} \quad (2)$$

Where $\dot{m}$ is mass flow [mol s^{-1}] into the cuvettes, ΔW the difference of water vapor in reference- and sample air stream [mol mol^{-1}], W_{sample} the water vapor concentration of the sample air [mol mol^{-1}] and $Area_{leaf}$ [m^2] the half-sided needle area of the shoot.

CO_2 gas exchange fluxes separated into A_{net} and R_{dark} were calculated by:

$$A_{net}\ (R_{dark}) = -\frac{\dot{m}*\Delta CO_2}{\mathrm{Area}_{leaf}} - \frac{CO_{2\,sample}*E}{1000} \quad (3)$$

With ΔCO_2 as the difference in [CO_2] between reference and sample air stream [mol mol^{-1}], $CO_{2sample}$ carbon dioxide concentration of the sample air stream [mol mol^{-1}].

g_s was calculated by:

$$g_s = \frac{E\left(1000-\frac{W_{leaf}+W_{sample}}{2}\right)}{W_{leaf}-W_{sample}} \quad (4)$$

$$W_{leaf} = \frac{e_{sat\,leaf}}{p} * 1000 \quad (5)$$

With stomatal conductance g_s in mol $m^{-2}s^{-1}$, saturated vapor pressure of the leaf with $e_{sat\,leaf} = e_{sat}$ in bar and atmospheric pressure p in kPa. (Duarte et al. 2016) showed that the ventilation generated by the fans in the cuvettes allowed well air mixing and thus boundary layer for the calculation of g_s could be neglected. In order to determine changes in WUE during heat stress, apparent water-use efficiency WUE_a and intrinsic water-use efficiency WUE_i were derived using the following equations:

$$WUE_a = \frac{A_{net}}{E_{day}} \quad (6)$$

$$WUE_i = \frac{A_{net}}{gs} \quad (7)$$

WUE_a is driven by fixation of CO_2 and loss of H_2O at leaf level, which is mostly driven by atmospheric parameters (VPD), concentration differences of CO_2 and H_2O in the air and g_s. Thus, WUEa provides a measure for the water cost of fixed carbon. WUE_i provides a measure for leaf physiological changes when normalized to stomatal response. Thus, WUE_i allows to compare treatments independently of environmental drivers e.g. VPD and is related to the difference between atmospheric [CO_2] and mesophyll [CO_2]. This parameter can provide insight into photosynthetic carbon fixation efficiency (Bonan et al. 2014; Wieser et al. 2018).

2.2.5 Chlorophyll fluorescence

Chlorophyll fluorescence was measured with a portable photosynthesis system (LI-6400XT, LiCor Bioscience, Lincoln, NE, USA) supplemented with a fluorescence head (6400-40 Leaf Chamber Fluorometer, LiCor Bioscience, Lincoln, NE, USA). Chlorophyll fluorescence was measured on 4 seedlings per treatment before the start of the treatments, just one day after the second heat wave had ended and three weeks later during recovery. Measurements were conducted between 9 am and 1 pm at a leaf temperature of 25 °C and reference [CO_2] of 400 µmol mol^{-1}. Needles were clamped into the leaf cuvette fully covering the cuvette area (2 cm^2). Needles were acclimated to actinic light with optimal PAR (1200 µmol $m^{-2}s^{-1}$, pre-determined from light response curves) with a blue light proportion of 10 % for several minutes. As soon as changes in fluorescence intensity (F) ceased to values <5, F was considered stable and the measuring sequence was initiated. First, chlorophyll fluorescence at actinic light (F'_s) was measured as a steady state value, then needles were briefly exposed to a saturating flash of >7000 µmol $m^{-2}s^{-1}$ and maximum fluorescence (F'_m) was measured. This was followed by a fast switch from actinic light to far red radiation. This so-called dark pulse allowed measurement of minimum chlorophyll fluorescence (F'_0). The photochemical parameters effective photosystem II quantum yield (Φ_{PSII}), maximum light adapted quantum yield of the photosystem II (F`v/F`m), coefficients of photochemical fluorescence quenching (qP) and relative electron transfer rate (ETR) were calculated using standard procedures.

2.2.6 Biomass sampling and sample preparation

Entire seedlings were sampled on three occasions during the course of the experiment: pre-stress (April 20th), at the last day of the second heat wave (Mai 10th) and three weeks later, i.e., after recovery (Mai 30th). During each sampling campaign, a minimum of six seedlings per treatment (including dead seedlings as well, see below) were sampled according to a randomized block design. All plant material containing needles above the former cotyledons was assigned as shoot, all plant material below the first roots as root material. Stems were collected but were not used in this study. Additionally, all plant samples were weighted, photographed, and immediately frozen in liquid nitrogen. Time of harvest was between 1 pm and 2 pm. Prior to freezing, water potential measurements of shoots (ψ_{shoot}) were conducted on some seedlings using a pressure chamber (Model, 600 PMS-Instruments, Albany, OR, USA); after a droplet of water appeared at the cut surface, the pressure was slowly released to avoid damage of the tissues. Roots and shoots were ground to fine powder in liquid nitrogen with mortars and pestles. Samples were divided into aliquots and stored at -80 °C for further analysis. Dry weight was assessed gravimetrically by

drying samples for 48 h at 60 °C. In total, 23 control, 22 drought, 28 heat and 28 heat-drought treated seedlings were sampled. For each sampling campaign metabolites were analyzed in root and shoot tissues and averaged per treatment. Results from dead seedlings were treated separately.

2.2.7 Seedling mortality

Stress severity resulted in death of seedlings in the heat and heat-drought treatment. Seedlings were not actively monitored for signs of mortality during the two heatwaves (except for the gas exchange measurements, see Fig. 2.2), but mortality was detected upon two biomass sampling campaigns (stress, recovery). Visual examination showed that the canopy appeared dry and had lost most of their greenness in some likely dead individuals. Because detecting mortality from visual examination might be observer biased, a second criterion based on absolute shoot water content was introduced. In seedlings that looked quite healthy and green, absolute shoot water content was between 58 % and 70 %, while shoot water content in the other seedlings ranged from 8.2 % to 46.7 % (Fig. S2.2). The canopy of these seedlings also appeared (after analyzing the photographs, for example see Fig. S2.1) dry and had lost their greenness. However, we like to highlight that the decline in shoot water content was unlikely the reason of death (e.g., seedlings of the well-watered heat treatment died as well, but ψ_{shoot} did not indicate water stress in the surviving seedlings, see Fig. 2.3), but rather a consequence: after the shoots were permanently damaged and the majority of needles and/or roots no longer functional, water supply ceased and the shoots began to desiccate.

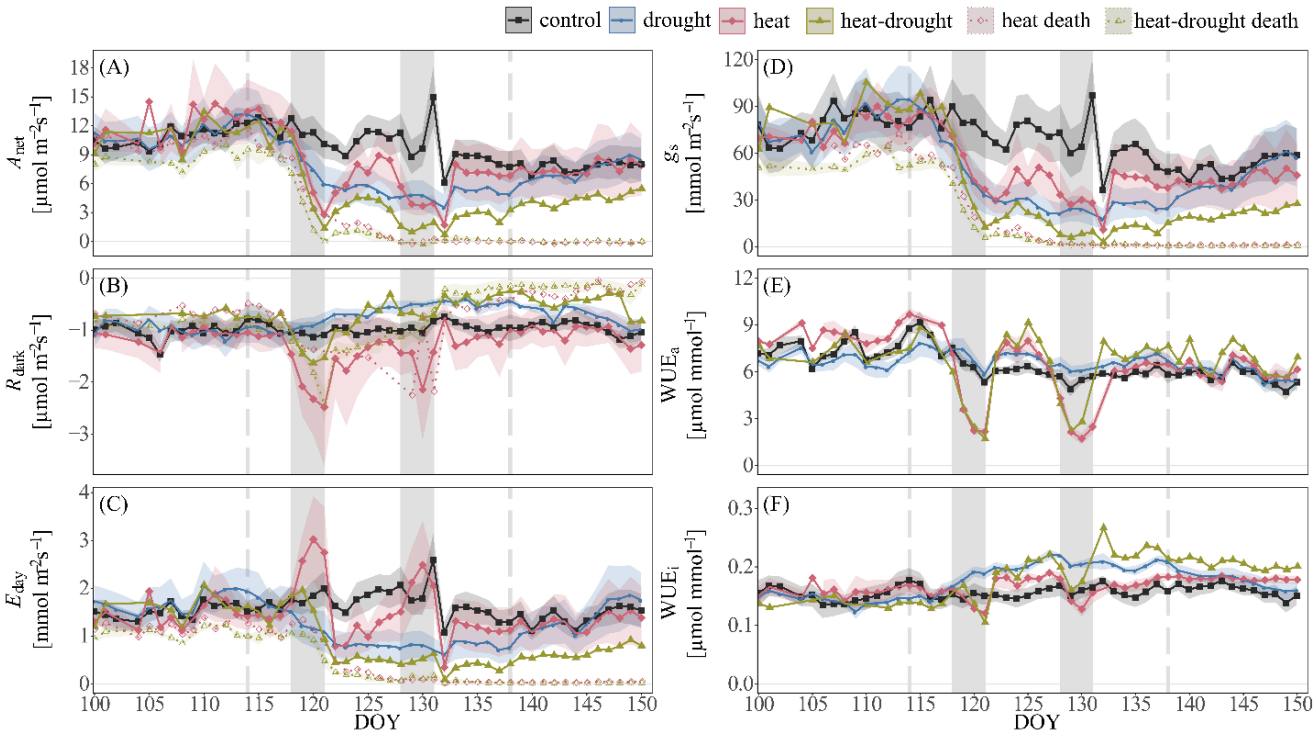

Figure 2.2 Time-series of shoot gas exchange in *Pinus halepensis* seedlings (n=4 per treatment). Shown are daily averages per treatment of (A) net photosynthesis (A_{net}), (B) dark respiration (R_{dark}), (C) transpiration E, (D) stomatal conductance g_s, (E) apparent water-use efficiency (WUE_a) and (F), intrinsic water-use efficiency (WUE_i). Shoot gas exchange of seedlings that died during the course of the experiment in the heat (n=1) and heat-drought treatment (n=3) is indicated by dotted lines. The shaded areas around the mean represent ±1 SE. The two heatwaves are depicted by the light grey areas. The duration of drought is indicated by vertical intermitted lines.

This phenomenon was supported by dendrometer data (Fig. S2.3). Here, stem dehydration indicated by diameter shrinkage of dying seedlings was observed to occur after the heatwaves. Thus, in summary visual examination together with shoot water content data allowed us to separate living and dead seedlings. This step was a necessary prerequisite before analyzing the gas exchange and metabolite data.

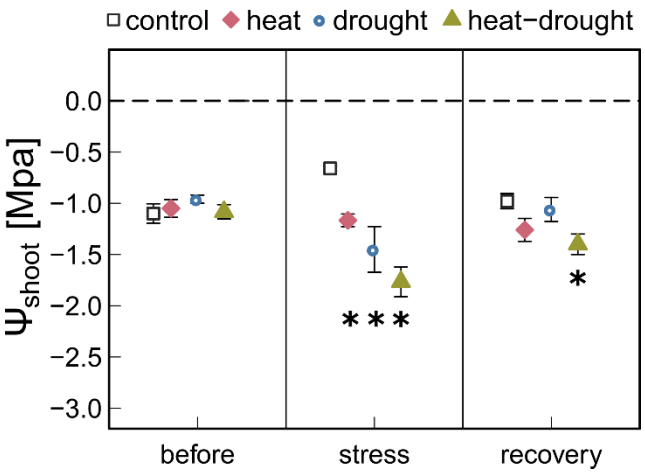

Figure 2.3 Shoot water potential (ψ_{shoot}) in control, drought, heat, heat-drought trees is given before stress (before), after the second heat wave (stress) and 3 weeks after stress (recovery). The error bars are ±1 SE (*n*=6, but heat-drought treatment during stress and recovery *n*=3). Treatment differences from the control are given (*$P \leq 0.05$).

2.2.8 Analysis of Carbohydrates

Analysis of NSC in shoot and root samples was done following the approach reported by (Brauner et al. 2014) based on extraction using boiling ethanol (80%v/v), which was defined as standard method for sugar extraction recently ((Quentin et al. 2015). Extracts were analyzed by HPLC (Dionex DX-500 HPLC system, Thermo Scientific) using pulsed amperometric detection by a gold electrode (Dionex ED Au, Thermo Scientific). Soluble sugar compounds (inositol, pinitol, glucose, fructose, sucrose) were separated by a PA1 column (Dionex CarboPac PA–1, Thermo Scientific). Myo-inositol and D-pinitol were co-eluted by our chromatographic method and therefore are referred to cumulative as cyclitols. Glucose, fructose and sucrose are treated together as soluble NSC because single components responded in the same direction to the treatments applied. Remaining extracts were stored at -20 °C.

Starch extraction was modified according to (Hoch et al. 2003). Remaining pellets from soluble sugar extraction were suspended in 1 ml of deionized water (H_2Odd), heated to 95 °C for 45 minutes and then cooled to 30 °C before 1 ml of amyloglucosidase reagent (10 mM acetate Buffer pH 4.5, 1 mg ml^{-1} amyloglucosidase) was added. Glucose-oxidase reagent was added containing 2 U ml^{-1} horse radish peroxidase, 5 U ml^{-1} glucose oxidase and 0.1 mg ml^{-1} o-Dianisidin. Samples were kept at 30 °C for 2 hours, then the reaction was stopped with 5 N HCL and absorption was measured at 540 nm photometrically (Ultrospec 2000 UV/VIS Spectrophotometer, Pharmacia Biotech).

Analysis of carboxylic acids (malic-, fumaric-, citric acid), extracted into hot water, was done as reported by (Brauner et al. 2014), again using HPLC (Dionex DX-500 HPLC system, Dionex IonPac AS11-HC, Thermo Scientific) coupled to a suppressor (Dionex AERS 500 Carbonate

Electrolytically Regenerated Suppressor, Thermo Scientific) with detection by conductivity (Dionex ED, Thermo Scientific). On the same chromatogram, nitrate, phosphate, sulfate and chloride were detected as well.

2.2.9 Proline

Proline in shoot and root tissues was analyzed following (Rienth et al. 2014). In brief, 25 mg of frozen sample powder was extracted for 10 minutes in 1 ml H_2Odd at 4 °C and centrifuged (13000 rpm for 15 min). 500 µl of supernatant was added to 500 µl of concentrated Formic acid and vortexed for 5 minutes. 500 µl of Ninhydrin reagent was added (3 % Ninhydrin in Dimethylsulfoxide). Samples were heated (100 °C for 15 minutes) and immediately cooled on ice and then centrifuged (at 13000 rpm for 1 min). Absorption of the supernatant was measured at 520 nm (Ultrospec 2000 UV/VIS Spectrophotometer, Pharmacia Biotech).

2.2.10 Needle surface temperature

Needle surface temperature was measured optically by an infrared camera system (PI 450, Optris, Germany) and analyzed using the manufacturer's software. Recordings were taken at the last day of the second heat wave between 1 pm and 4 pm of at least four individuals per treatment. Air temperature during the measurements was used to correct for background radiation. Emissivity of *P. halepensis* needles was set to 0.97 according to (Monod et al. 2009).

2.2.11 Calculation of osmotic pressure potential

Osmotic pressure potential was calculated using the van't Hoff osmotic pressure equation for aqueous mixed electrolyte solvents:

$$\Pi = M*i*R*T \qquad (8)$$

where Π is the osmotic pressure potential Pa (kg m^{-1} s^{-1}), M is the molar fraction of all measured osmotic active components (cumulative) including total C, proline, nitrate, sulfate and phosphate concentrations. R is the ideal gas constant (8.31445 kg m^2 $mol^{-1}K^{-1}s^{-2}$ at standard temperature of 25 °C). The van't Hoff factor i represents the degree of dissociation of each solute component. We calculated with fully dissociated solute components for the case that a salt would dissociate into two ions (eg. $i_{glucose} = 1$, $i_{nitrate} = 2$).

2.2.12 Statistics and Data-analysis

This study focuses on treatment differences from the control and treatment effects on metabolite concentrations, which were analyzed separately per sampling period (pre-stress, stress and recovery) by analysis of variance (ANOVA). Samples that were considered as "dead" have not

been integrated into the analysis. The effect size of treatments compared to the control was calculated as a percent treatment effect (*D*):

$$D = 100 * \frac{(\mathrm{mean_t} - \mathrm{mean_c})}{\mathrm{mean_c}} \quad (9)$$

where $\mathrm{mean_t}$ is the treatment average and $\mathrm{mean_c}$ is the average of the control, the standard error (SE) of the treatment effect (D_{SE}) was calculated as follows:

$$D_{SE} = 100 * \sqrt{\left(\left(\frac{1}{\mathrm{mean_c}}\right) * \mathrm{SE_t}\right)^2 + \left(\left(\frac{\mathrm{mean_t}}{\mathrm{mean_c}^2}\right) * \mathrm{SE_C}\right)^2} \quad (10)$$

with SE_t and SE_c are the SE of treatments or control. Because shoot gas exchange was measured on the same seedlings throughout the experiments, treatment effects were assessed with linear mixed-effects models, which account for the repeated sampling in time design. All data processing and statistical analysis was done using R version 3.2.2 (R Core Team 2015), extended with the "lme4" package (Bates et al. 2015) for linear mixed-effects models.

2.3. Results

2.3.1 Stress intensity and mortality

Heatwaves resulted in pronounced death and caused 5 seedlings (23 %) in the heat treatment and, 15 seedlings (68 %) in the heat-drought treatment to die. The surviving seedlings showed only a moderate reduction in ψ_{shoot} (Fig. 2.3). Thus, it is unlikely that hydraulic failure was a cause of mortality. However, needle temperatures were affected differently by the treatments. While needle temperatures in the control and heat treatment were above ambient air temperatures (control: +3.4 °C, heat: +3.1 °C), needle temperatures in the drought and heat-drought treatment was even higher (drought: +5.2 °C, heat-drought: +5.7 °C; Table 2.1). Thus, the on average 2.6 °C higher shoot temperature under heat combined with drought might have resulted in elevated mortality rates, as needle temperature became excessive (>47 °C). Although the exact time point of mortality was not investigated in each of the seedlings, the continuous gas exchange measurements pointed to the end of the first heat wave (Fig. 2.2 intermitted lines) as daytime gas exchange rates did not recover, but declined even further. A possible death indicator was when shoot R_{dark} reached values close to zero. This appeared to be the case approximately one week after the end of the last heat wave (Fig. 2.2C) and agrees with the continuous diameter measurements (Fig. S2.3). Since the seedlings continued to dry out after death, the shoot water content was below 49 % at biomass sampling two weeks later, which agreed with our death criterion (see Methods section).

Table 2.1: Comparison of needle temperature (T_{needle}) between treatments. Measurements were done using an infrared camera at the end of the second heat wave when air temperature was 40.8–42.1 °C in the heat and heat-drought treatment and 25.1–25.4 °C in the control and drought treatment. Shown are treatment averages, standard error (±1 SE) and temperature difference between needle and air temperature.

Treatment	T_{needle} [°C]	SE	Δ°C (T_{needle} - T_{air})
Control	28.6	0.63 [n=6]	3.4
Drought	30.7	0.33 [n=4]	5.2
Heat	45.3	0.75 [n=6]	3.1
Heat-drought	47.2	0.57 [n=4]	5.7

2.3.2 Shoot gas exchange and chlorophyll fluorescence during stress and recovery

In the surviving seedlings, large differences in shoot gas exchange were observed between the treatments (see Table S2.3 for linear mixed effect model results). While A_{net} and R_{dark} in drought-treated seedlings decreased proportionally (Fig. 2.2A and B), we found contrasting responses under high temperature stress. Most markedly, in both the heat and heat-drought treatment, a sharp decline in A_{net} was contrasted by a pronounced increase in R_{dark} (heat: +101 %, heat-drought: +35 %, $P \leq 0.001$) during the first heat wave. In the surviving heat-drought seedling, the increase in R_{dark} during the first heat wave was not observed during the second heat wave and R_{dark} did not reach control levels through the remainder of the experiment (-49.8 %, $P \leq 0.001$). In contrast, the heat-treated seedlings maintained high R_{dark} rates, and A_{net} recovered instantaneously after the second heatwave had ended.

Canopy transpiration was strongly affected by the two heatwaves and increased markedly in the heat treatment, while water deficit resulted in a reduction of E_{day} in the heat-drought treatment (Fig. 2.2C). In both treatments, the changes in E_{day} were accompanied by decreasing g_s (Fig. 2.2D). Because A_{net} appeared coupled to g_s but uncoupled from E_{day} during heat wave conditions, WUE_a declined sharply while WUE_i remained relatively unchanged, but slightly increased in the surviving heat-drought seedling post-stress ($P \leq 0.001$) (Fig. 2.2E and f).

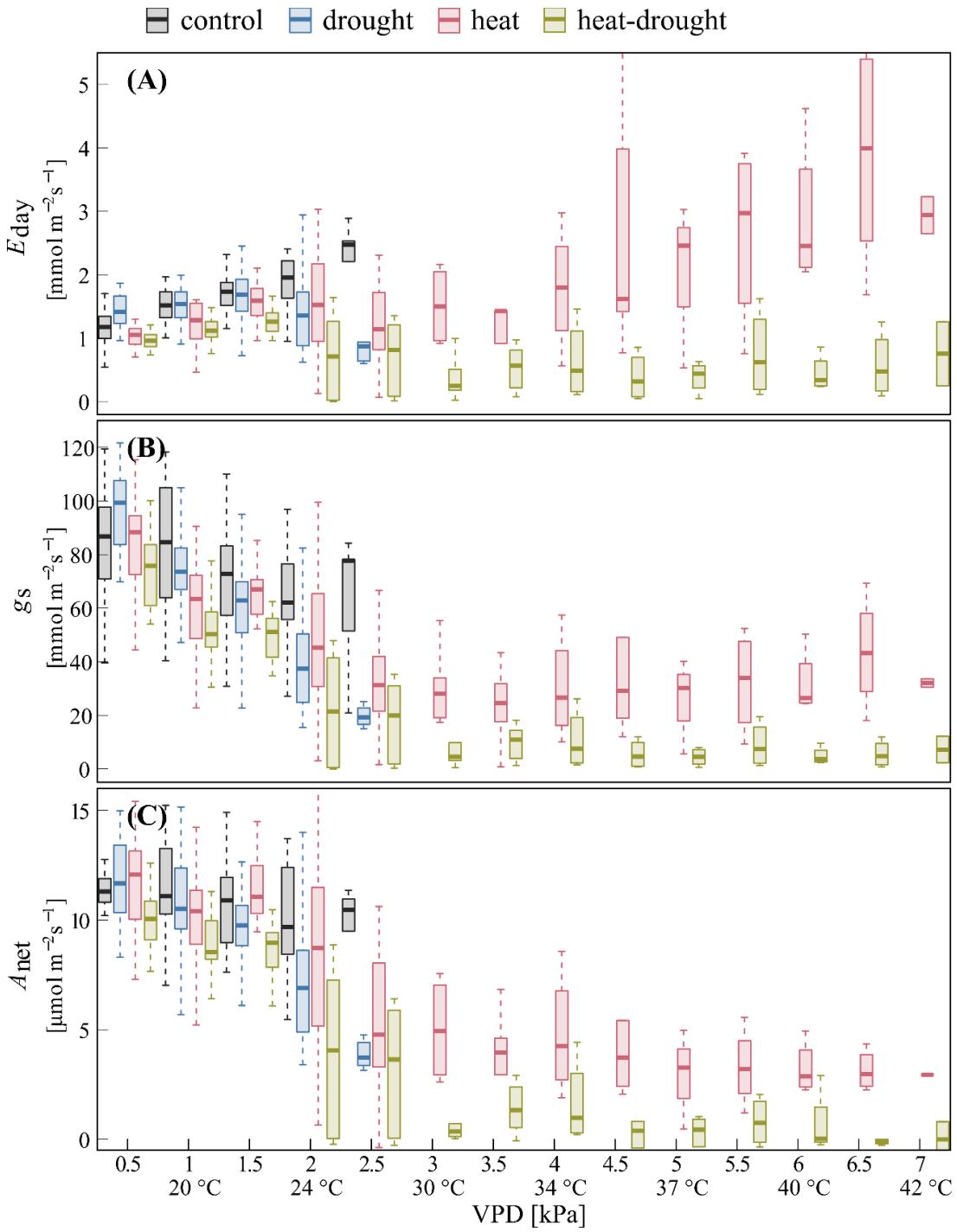

Figure 2.4 Changes in shoot gas exchange in response to VPD for surviving trees. Given are daytime (A) transpiration E_{day}, (B) stomatal conductance g_s and (C) net photosynthesis A_{net} in the control (n=4), drought (n=4), heat (n=3), heat-drought (n=1) treatment during before stress and heat wave conditions. Data are bin-averaged in VPD classes of 0.5 kPa (10 am to 7 pm).

The relationships of shoot gas exchange with VPD (Fig. 2.4) revealed striking differences between drought and well-watered seedlings. In the heat treatment, a decline in g_s was particularly visible during the initial increase in VPD (0.5 to 3 kPa), while g_s remained surprisingly constant at higher VPD. This resulted in increasing E_{day}, while photosynthesis remained constant over a temperature range between 32 °C and 42 °C. In the heat-drought treatment, the decline of g_s indicated stomatal closure at a VPD of about 3.5 kPa, tightly limiting E_{day} and A_{net}.

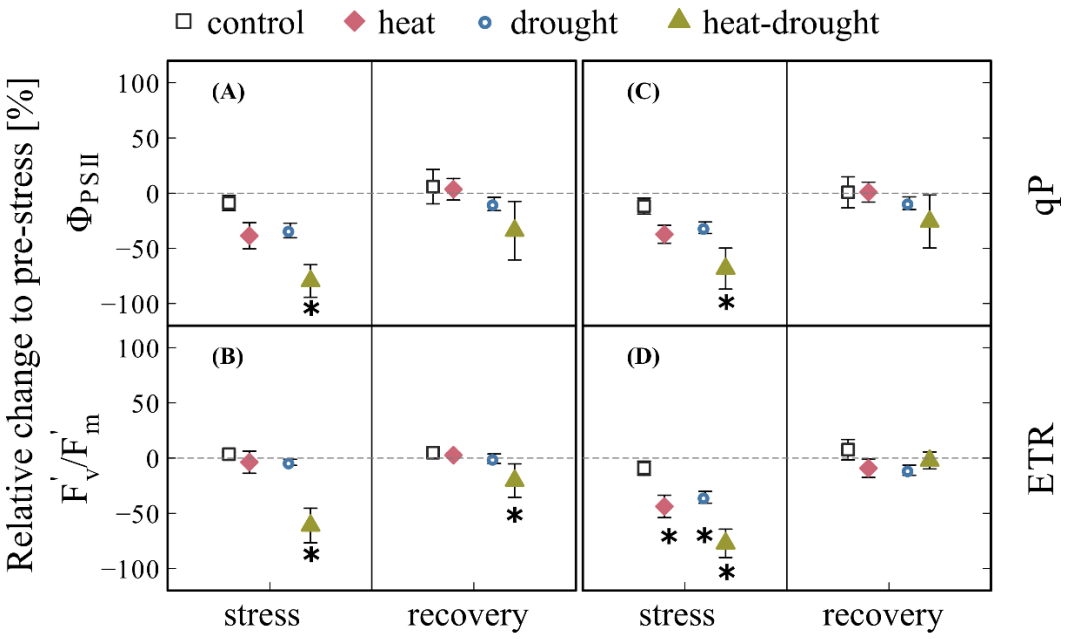

Figure 2.5 Changes in chlorophyll fluorescence parameters during stress and recovery relative to before stress conditions. Parameters shown are: (A) effective photosystem II quantum yield (ΦPSII), (B) maximum quantum yield of the photosystem II (F`v/F`m), (C) coefficients of photochemical fluorescence quenching (qP), (D) relative electron transfer rate (ETR). The error bars are ±1 SE (n=4, but heat-drought treatment during recovery n=3). The intermitted lines provide comparison to before stress conditions. Significant treatment differences from control are given (*P≤0.05).

The impairment of the photosynthetic apparatus under heat-drought stress was clearly visible in all measured chlorophyll fluorescence parameters one day after the last heat wave (Fig. 2.5), where ΦPSII showed the strongest decline with 78 % compared to the control treatment (ANOVA, P≤ 0.001). The parameters also reflected the reduced, but continuing photosynthetic activity in the heat and drought treatment, in which small but not significant reductions were observed. The apparent recovery of all chlorophyll fluorescence parameters in the heat-drought treatment should

be interpreted with caution, because data are reported on the remaining intact needles of three surviving seedlings 20 days following heat release. However, needles of dead seedlings which were measured, did neither assimilate nor respire and had light-adapted fluorescence values of zero (data not shown).

2.3.3 Non-structural carbohydrates

We found no distinct stress responses of NSC concentrations in shoots (Fig. 2.6 A, C, E, G) (slightly reduced starch content in the heat treatment, ANOVA, $P \leq 0.05$), while soluble NSC and starch contents in roots declined in response to heat and heat-drought stress (Fig. 2.6 B and D) (see Table S2.4 for ANOVA results). Heat-drought caused a dramatic depletion of soluble sugars (-97 %, 2.4 µmol gDW^{-1}) and starch (-98 %, 0.8 µmol gDW^{-1}). Carboxylic acids and cyclitols were also significantly affected by heat-drought stress, causing an overall reduction in total C of 83 % compared to the control (ANOVA, $P \leq 0.001$).

During recovery, heat-drought treated seedlings showed a significant increase in carboxylic acids and cyclitols in shoots (Fig. 2.6 E, G) (ANOVA, $P \leq 0.001$). While in the heat and in the heat-drought treatment root soluble NSC and starch increased during recovery close to control values (Fig. 2.6 B, D), in the heat-drought treatment total C remained significantly reduced (-85 %, ANOVA, $P \leq 0.001$). In dying seedlings, NSC contents did not recover (Fig. 2.6) and starch storage in shoots and roots was close to depletion.

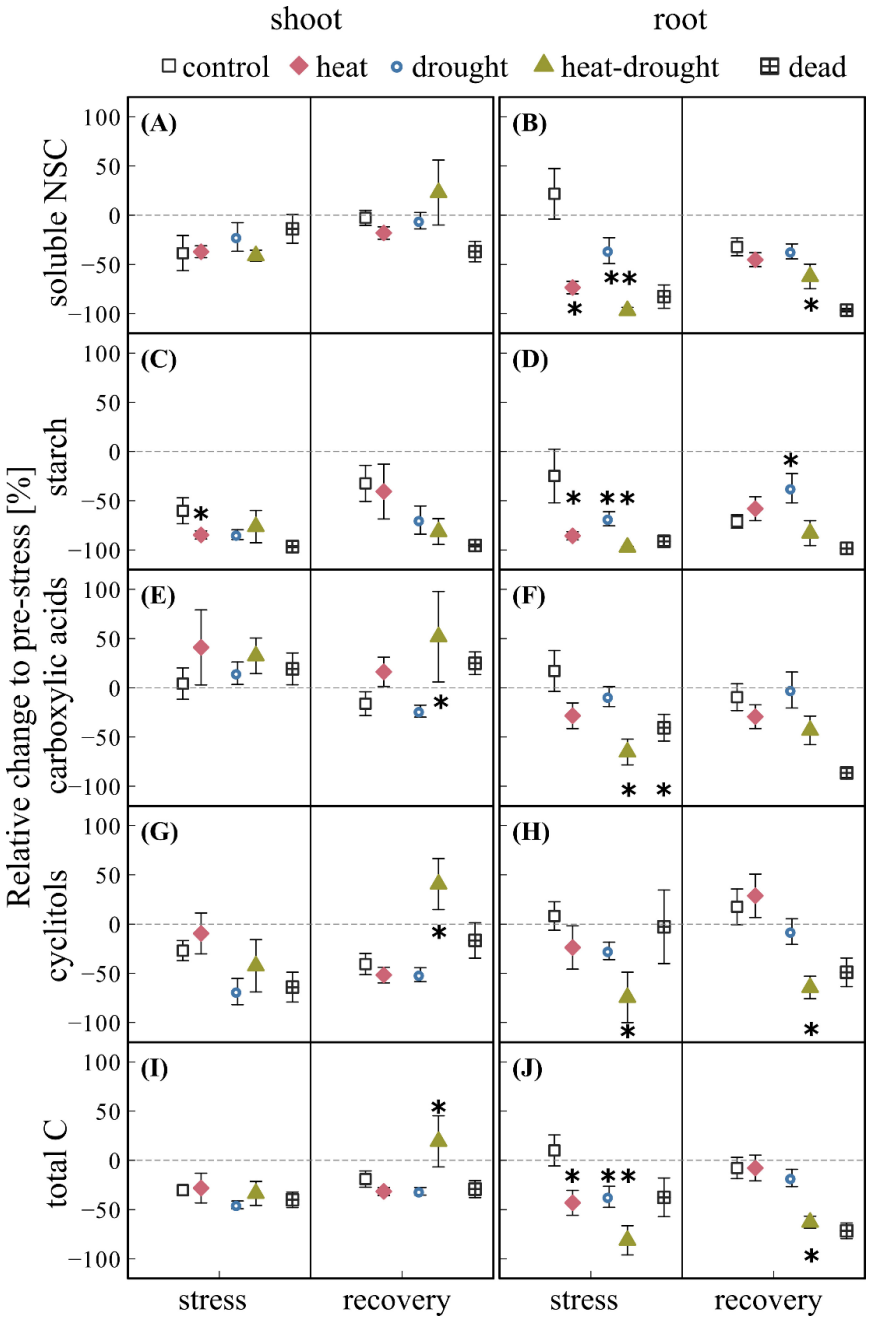

Figure 2.6 Changes in non-structural carbohydrates (NSC) for shoot and root tissues during stress and recovery relative to before stress conditions. Shown are (A, B) soluble NSC (glucose, fructose, sucrose), (C, D) starch (E, F) carboxylic acids (malate, fumarate, citrate), (G, H) cyclitols (myo-inositol, D-pinitol) and (I, J) total carbohydrates (given as C6 equivalents of the shown metabolites) for control, drought, heat, heat-drought and dead seedlings. The error bars are ±1 SE (*n*=6, but heat-drought during stress and recovery *n*=3, dead heat samples *n*=5, dead heat-drought samples *n*=15). The intermitted lines provide comparison to before stress conditions. Significant treatment differences from control are given (*$P \leq 0.05$). See Table S2.2 for absolute concentrations.

2.3.4 Proline, nitrate and osmotic potential

The amino acid proline can act as osmolyte, antioxidative defense and membrane stabilizing molecule (Szabados and Savoure 2010). We found its concentration to increase in shoots of heat and heat-drought treated seedlings during stress and recovery (Fig. 2.7 A, B). Dead seedlings showed accumulation of proline during both sampling campaigns. Proline content in roots was much smaller, and no clear response to the treatments was found.

Shoot nitrate content, proposed here as an indirect measure for N assimilation, was 2 to 4 times higher during stress (ANOVA, $P \leq 0.01$) than prior to stress conditions in heat and heat-drought seedlings. Following recovery, nitrate content in the heat treatment decreased to control levels, while it remained elevated in the heat-drought treatment (ANOVA, $P \leq 0.05$). No obvious effect of the treatments on root nitrate was visible (Fig. 2.7 D). Again, the dead seedlings showed highest concentrations and no decline during recovery.

The osmotic potential (Π) of shoots remained relatively constant in all treatments throughout the experiment. Π in roots showed a tendency to decrease in the drought treatments whereas root NSC declined (Fig. 2.6H). The reason for this was reduced root water content (Table S2.2). A decrease in tissue water content results in more concentrated cytosolic and apoplastic fluids and therefore Π becomes more negative.

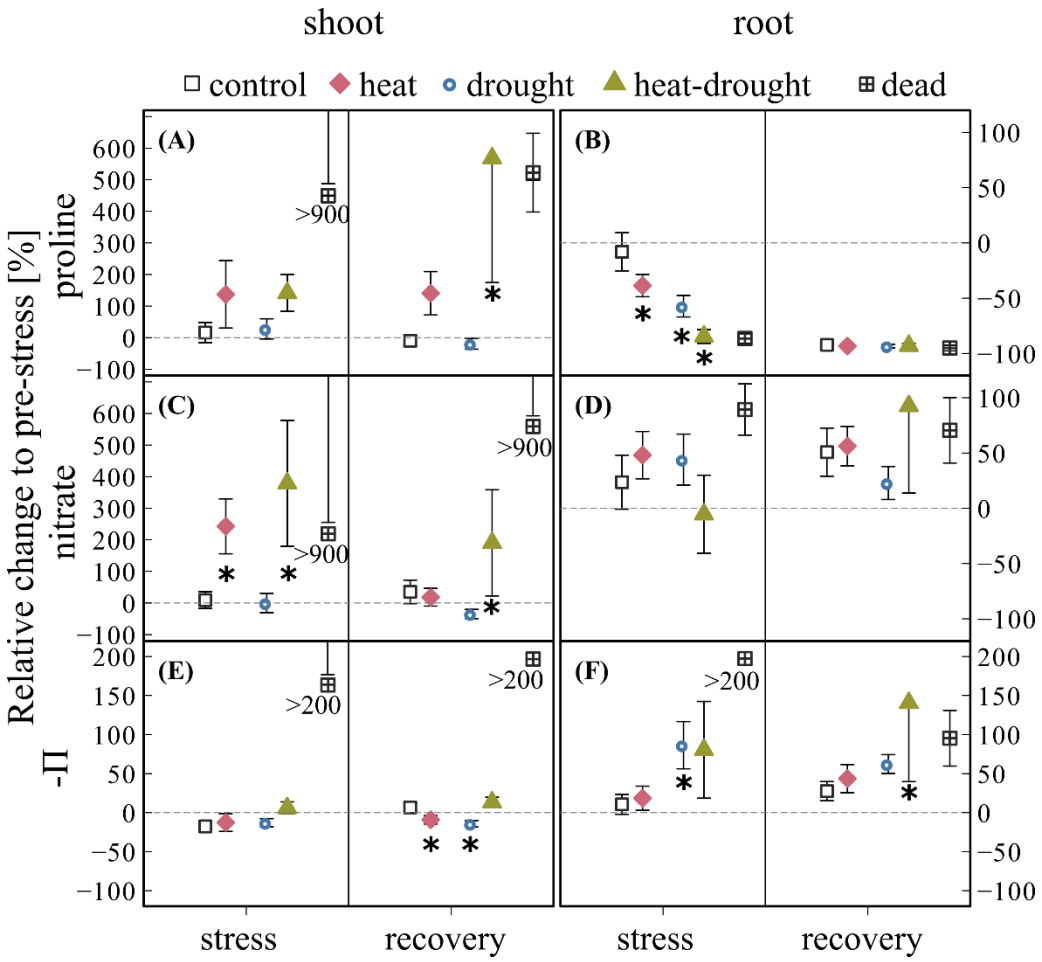

Figure 2.7 Changes in (A, B) proline, (C, D) nitrate concentrations and osmotic potential Π (E, F) in shoots and roots during stress and recovery compared to before stress conditions for control, drought, heat, heat-drought and dead seedlings. Osmotic potential was calculated from measured solutes and tissue water content using the van`t Hoff equation. The error bars are ±1 SE (*n*=6, but heat-drought treatment during stress and recovery *n*=3). The intermitted line provides comparison to before stress conditions. Significant treatment differences from control are given (*P≤0.05). In dead seedlings, when changes exceed axis scaling, the mean value was placed below the SE.

2.4. Discussion

2.4.1 High temperature and mortality

The exact cause of seedling mortality is not clear, but likely relates to the high shoot surface temperatures, which became excessive when transpiration ceased, mainly in the heat-drought treatment. According to the high-resolution dendrometer data measured on a few seedlings (Fig. S2.3), seedlings in the heat-drought treatment most likely died right after the last day of the first heat wave and desiccated rapidly afterwards. In contrast, seedlings in the heat treatment showed strong stem diameter declines (and thus death) only after the second heat wave had ended. Such a delay in stress response might indicate that cellular damage (e.g., in needles, roots and/or cambium cells) accumulates with delay (as has been observed after high temperature stress, e.g. (Hüve et al. 2011) until critical levels are reached beyond which tree functioning cannot longer be maintained. This was also described as indirect damage by Colombo and Timmer (1992). The differences in the time point of mortality between heat and heat-drought treatments might reflect dosage effects of the experienced heat stress.

The reduced transpiration in the heat-drought treatment (c. 0.5 mmol $m^{-2}s^{-1}$) versus the heat treatment (c. 2 mmol $m^{-2}s^{-1}$) at a VPD of 4 kPa and 42 °C air temperature resulted in 2.6 °C higher needle temperatures at the end of the second heatwave (Table 2.1). Such an increase in leaf temperature has also been observed in mature forests when drought-exposed trees were compared to well-watered trees (Scherrer et al. 2011). In regard to the pronounced mortality under heat-drought as observed in our experiment, leaf cooling could have been crucial for survival as leaf temperatures had reached 47 °C, a critical value for tissue damage in conifers (Bigras 2000; Colombo and Timmer 1992). The importance of evaporative cooling at lower VPD was examined recently (Urban et al. 2017a) in *Pinus taeda.* The study showed that seedlings were able to keep stomata open and to maintain high transpiration rates. This resulted in lower leaf heating. According to a field experiment on *Eucalyptus parramattensis* by (Drake et al. 2018), leaf surface heating was reduced by 2.8°C on average because transpiration was maintained at high rates even at temperatures > 43°C.

The ability of the pine seedlings to cool via transpiration was found to fail under the water limiting conditions applied here, which led to excessive surface temperatures when no other cooling mechanism was available. Under field conditions, leaf cooling can originate from transport of sensible heat via high wind speed or convective air flow. Such upward flow conditions and cooling of forest canopy have been shown at the Yatir forest (Eder et al. 2015; Rotenberg and Yakir 2011), where the seed material for this study originates from. However, for seedlings growing

close to the soil surface where wind speed and convective exchange is lower, this cooling mechanisms should be less effective whereas soil surfaces can heat up tremendously (Kolb and Robberecht 1996). The authors found that under such conditions, seedlings with higher stomatal conductance were more likely to survive. This compares well to our findings, where trees with low E_{day} and g_s died, while seedlings that maintained generally higher E_{day} rates survived (Fig. 2.2). In summary, the high temperatures experienced by the seedlings in the heat and heat-drought treatment caused pronounced stress, likely resulting in membrane and protein damage causing higher mortality in trees with lower evaporative cooling capacity.

2.4.2 Stress severity and impairment of N assimilation

The intensity of the heat and heat-drought stress was not only reflected in high mortality rates, but further indicated by highly elevated proline contents (Szabados and Savoure 2010; Verbruggen and Hermans 2008). Proline was not upregulated in response to the applied drought, which was rather mild, as stomata did not close completely and ψ_{shoot} remained well above critical values for xylem embolism formation (Dadshani et al. 2015; David-Schwartz et al. 2016; Delzon et al. 2010; Klein et al. 2011; Oliveras et al. 2003). Therefore, we suggest that proline was of minor importance as osmoprotectant, which is in line with not increased Π of shoots during drought. Proline may also accumulate under salinity stress (Hamilton 2001; Hayat et al. 2012), which seems not relevant in our case, but interestingly a quadratic relationship between shoot chloride content and proline concentrations was found (Fig. S2.4). This might have been caused by increased uptake of chloride by roots at high temperatures ((Turner and Lahav 1985). Proline upregulation under heat stress is reported as beneficial for plants due to its role as protein stabilizer (e.g. complex II of mitochondrial electron transport chain; (Hamilton 2001). Moreover, proline synthesis serves as an efficient NADPH scavenger to regenerate $NADP^+$ (Hayat et al. 2012; Szabados and Savoure 2010; Zhang et al. 2015) and to prevent radical production in the thylakoid electron transfer chain (Kramer et al. 2004). This mechanism might enhance ETR by regenerating electron acceptors, and thus, can reduce oxidative stress. Indeed, we found ETR, calculated from chlorophyll fluorescence measurements, unaffected in the heat treatment, while ETR was strongly reduced in the heat-drought treatment. Thus, the membrane and protein stabilizing ability of proline could not prevent photo inhibition at the time of highest needle temperatures in the heat-drought treatment (>47 °C).

We also found elevated levels of nitrate in shoots of heat and heat-drought stressed Aleppo pines, while nitrate levels in roots did not change, which might indicate heat-induced inactivation of leaf nitrogen assimilation. Decreased nitrate reductase activity has been observed to occur at

temperatures above 40 °C in cereals (Onwueme et al. 1971; Pal et al. 1976), and after heat release, nitrate activity can quickly recover. A fast recovery of N assimilation in Aleppo pine two days after stress release may also be concluded from the drop in leaf nitrate content (see Fig. 2.7), while in the dead seedlings nitrate levels remained highly elevated (> 900 %).

2.4.3 Metabolic responses towards heat-drought stress

The degree of stress and reduction in gas exchange were reflected in root NSC concentrations. In the heat-drought treatment, soluble NSC, starch, carboxylic acids and cyclitols declined to a larger extend than in the heat treatment although root zone temperatures were similar in both treatments (data not shown). Likely, the more pronounced reduction in C uptake in the heat-drought treatment supposedly decreased phloem transport (Ruehr et al. 2009; Sevanto 2014, 2018) , which caused the observed strong depletion of soluble sugars and starch storage in roots. Total NSC levels were close to zero in the roots of the heat-drought seedlings, which may indicate critical C shortage in roots, limiting the otherwise high maintenance respiration in roots at high temperatures (Jarvi and Burton 2018; Tjoelker 2018). This could have potentially affected root functionality and hence contributed to the observed large mortality rates under heat-drought.

Changes in lipids, which can be critical for C supply during stress were not measured. In particular in pine trees, lipids (triglycerides) together with cyclitols are reported to be a large carbon storage pool (Hoch et al. 2003; Piispanen and Saranpaa 2002), and this pool can easily be channeled into the Tri-carboxylic-acid cycle especially during extreme stress (Fischer et al. 2015). This might partly explain the weak responses of carboxylic acids under heat and heat-drought, whereas root NSC was depleted. Furthermore, carboxylic acids together with cyclitols, in sum, did surpass or at least equal the concentration of the typically measured NSC (starch, sucrose, glucose and fructose; Table S2.2), and hence should be considered as important plant carbohydrate pools.

Carboxylic acids exert key functions in the regulatory network of plants. Tri-carboxylic-acid cycle (TCA) intermediates are important for the generation of ATP, and thus key in respiratory processes. Additionally, they can provide carbon skeletons for amino acids and carbohydrates (Fernie et al. 2004). An increase in carboxylic acids during recovery might indicate enhanced investment into provision of carbon skeletons for maintenance and repair mechanisms. For heat-drought treated seedlings this could also mean that carboxylic acids accumulated because R_{dark} was reduced. Similar upregulation of TCA intermediates was recently reported for eucalypts in response to heat and drought (Correia et al. 2018).

While shoot soluble NSC did not decline, shoot R_{dark} was much lower during the second as compared to the first heat wave and during the period of recovery. Presumably, available C for respiration was not limited in the heat-drought treatment at this stage because of actively maintained high sugar levels. This can be concluded from the upregulation of compatible solutes, including cyclitols during recovery. A similar pattern has also been observed in Scots pine where newly assimilated carbohydrates were allocated to cyclitols during recovery from drought (Galiano et al. 2017). Only heat-drought was associated with an increase in cyclitols during recovery, which might be explained by the very high needle temperatures that were found in this treatment. Various enzymes are expected to be protected by cyclitols against heat denaturation (Jaindl and Popp 2006).

Reports on NSC concentrations during drought have often been found to be inconclusive and to differ between species. In all species, hydraulic failure is lethal, but not all drought-induced lethality is connected to NSC depletion (Adams et al. 2017) and NSC concentrations during drought were found to increase, decrease or remain static in a wide range of tree species (Hartmann and Trumbore 2016). Information on isolated heat effects on NSC of tree seedlings is scarce and might depend on heat dosage rather than temperature maxima. It has been postulated that high temperatures lead to an increase in shoot NSC (Sevanto and Dickman 2015). Marias et al. (Marias et al. 2017) has found a similar response, with sugars in shoots increasing, when coffee plants have been exposed to a heat pulse (49°C for 45 min). This is in stark contrast to what we have observed during a longer but less intense heat wave, where NSC in shoots remained relatively constant, while roots NSC declined in the heat and heat-drought treatment. In accordance, a five days heat wave of about 40 °C did also not change NSC concentrations in leaves of *Eucalyptus globulus,* but when drought was added NSC concentrations declined (Correia et al. 2018). To conclude this section, the primary metabolism of Aleppo pine shoots appears to be highly buffered against deviations even under extraordinary stressful conditions. In contrast, the root metabolism decouples from the source supply under mild drought and/or extreme heatwaves and is clearly affected under stress combination. These changes in allocation patterns, especially in response to heat combined with drought, might be a sign of the plants approach to preserve source functionality at the cost of sink integrity.

2.4.4 Photosynthetic inhibition and recovery from acute heat stress

Water availability during heatwaves seems to be a key factor of survival (Bauweraerts et al. 2014; Ruehr et al. 2016), in parts at least related to evaporative cooling capacity (Drake et al. 2018) and the performance of the photosynthetic apparatus, as indicated by leaf fluorescence. While in heat-

drought trees chlorophyll fluorescence parameters (ΦPSII, F`v/F`m, qP and ETR) decreased strongly, the decline was less obvious in the heat treatment one day after the last heat wave had ended. A decline in ΦPSII indicates a saturation of the electron transfer chain, bearing the risk of oxidative stress (Murchie and Lawson 2013). In the investigated Aleppo pine seedlings, other reasons for the reduction of ΦPSII like the capacity of the harvesting complexes, can be neglected because of their pigment`s stability above 60 °C (Rätsep et al. 2018), and because the critical temperatures that causes disaggregation of the light harvesting complex typically lie above 50 °C (Nellaepalli et al. 2014; Tang et al. 2007). ETR, on the other hand, largely depends on thylakoid membrane integrity, which is disturbed at much lower temperatures of about 38 °C (Bukhov et al. 1999; Havaux et al. 1996). Dark adapted maximum operating efficiency Fv/Fm is widely used for the estimation of stress severity (Murchie and Lawson 2013). In this experiment, only F`v/F`m in light adapted state is available for interpretation. This parameter decreases with increasing non-photochemical quenching (Murchie and Lawson 2013), which means the dissipation of excess energy by heat. Together with the hypothesis of a saturated photosystem and reduced ETR, this provides evidence for stress-induced limitations of processes downstream of the photosynthetic apparatus. These processes downstream of the photosynthetic apparatus like enzymatic processes, substrate or thylakoid integrity might have been affected by the heat treatments. Although we did not measure direct photosynthetic damage, there is increasing evidence that thresholds for irreparable/slowly recoverable damage are typically reached at temperatures > 45°C (Hüve et al. 2011), with higher or lower thresholds in tropical or artic regions (O'Sullivan et al. 2017).

The apparent small decline of chlorophyll fluorescence parameters in the heat treatment, measured one day after the last heat wave had ended, may either reflect a relative mild impairment of the photosynthetic apparatus, or indicate a fast recovery of chlorophyll fluorescence parameters one day after the acute stress. Fast recovery responses of photosynthetic parameters after acute heatwaves (when water was not limiting) were also observed in herbaceous plants, as well as in some tree species and typically relate to temperatures < 45°C (Ameye et al. 2012; Guha et al. 2018; Hüve et al. 2011). By contrast, we did not observe complete recovery of ΦPSII in the few surviving heat-drought seedlings, which had been exposed to needle temperatures > 47°C.

2.4.5 Canopy gas exchange affected by high temperatures, atmospheric demand and soil drought

Heat stress, which induces high atmospheric demand has been reported to result in (partial) stomatal closure (Ameye et al. 2012; Bauweraerts et al. 2013; Duarte et al. 2016; Garcia-Forner et al. 2016; Ruehr et al. 2016). In our study, we found that stomata did not fully close in the heat treatment even when extreme vapor pressure deficits of > 6 kPa were reached. Indeed, partial stomatal closure was enough to maintain midday stem WP at moderate levels of -1.2 MPa (measured at the last day of the second heat wave), indicating that the xylem water transport was operating under non-harmful conditions. Under the same atmospheric conditions, but reduced irrigation in the heat-drought treatment, the stress on the hydraulic system of the seedlings was larger (-1.8 MPa) and stomata were almost fully closed to prevent any further drop in ψ_{shoot}, and hence embolism formation. Separating the effects of high temperature and VPD on stomatal responses is challenging. In experiments with temperature rise independent of VPD, g_s could even increase (Urban et al. 2017a; Urban et al. 2017b). A temperature-driven increase in g_s might simply reflect enhanced water loss along with rising temperatures without any further opening of stomata aperture, or could reflect an active cooling mechanism that prevents further closing of stomata. Active leaf cooling seems to be reasonable (Drake et al. 2018; Urban et al. 2017a; Urban et al. 2017b), but the underlying mechanisms have not been detected yet.

A_{net} and E_{day} were uncoupled during the heatwaves, resulting in a strong decline in WUE_a. Both, A_{net} and E_{day} showed slightly different response pattern during the first and the second heat wave with a less pronounced decrease in A_{net} in the former and a less pronounced increase in E_{day} during the latter, which resulted in similar amplitudes of WUE_a decrease in both heatwaves. Even R_{dark} showed this kind of response dampening during the second heat wave, especially in the surviving heat-drought seedling. A similar decline in the amplitudes of gas exchange rates in response to repeated heatwaves were reported in various other tree species (Duarte et al. 2016; Guha et al. 2018) and were linked with cellular damage that decreased heat wave resilience. Thus, trees were able to fully recover following heat release, but under combined heat-drought stress WUE_i remained increased during recovery along with elevated levels of compatible solutes. The increase in WUE_i however, was at the cost of reduced transpiration which resulted in higher needle surface temperatures. In particular, shoot-to-root C allocation patterns changed dramatically under heat-drought stress, which was reflected by an accumulation of compatible solutes (cyclitols) and TCA intermediates (carboxylic acids) in shoots, while non-structural carbohydrates declined dramatically to values close to zero in roots and did hardly recover once stress was released.

2.5 Conclusion

The combination of heat and drought stress affected Aleppo pine seedlings differently than drought or heat alone. This was not restricted to the stress periods *per se*, but became clear post-stress through high mortality rates and delayed recovery of the surviving seedlings. The observed delay in recovery and pronounced mortality in the heat-drought treatment clearly demonstrated that physiological stress responses can continue after environmental stress has been released. Moreover, it showed that a tight regulation of a plant's water balance via stomatal closure at the cost of evaporative cooling can result in excessive needle temperatures under the experimental conditions applied here. The exact cause of death is not clear, but extreme needle temperatures (> 47°C) may have either directly damaged shoot tissues via cell necrosis or may have indirectly affected root vitality via reduced C translocation to roots. In summary, we conclude that increases in heat wave temperatures, as predicted to occur during the next decades, can have disastrous effects in a dry environment. It seems that in semi-arid forests where drought is a common phenomenon, even a single heat wave that surpasses a given threshold (probably above 47 °C needle temperature) may have widely detrimental effects.

2.6 Acknowledgments

This work was supported, in part, by the German Research Foundation through its German-Israeli project cooperation program "Climate feedbacks and benefits of semi-arid forests" (CliFF; grant no. YA 274/1-1 and SCHM 2736/2-1) and by the German Federal Ministry of Education and Research (BMBF), through the Helmholtz Association and its research program ATMO. NKR acknowledges support by the German Research Foundation through its Emmy Noether Program (RU 1657/2-1). BB acknowledges support by GRACE – graduate school for climate and environment financed through the Helmholtz Association. We acknowledge support by Deutsche Forschungsgemeinschaft and Open Access Publishing Fund of Karlsruhe Institute of Technology. The authors would like to thank Andreas Gast for technical support, Ines Bamberger, Sina Rogozinski and Lena Mueller for their help during the experiment, and Simon Stutz, Lisa Wolf and Imke Hörmiller for lab assistance. We want to thank Dan Yakir, Yakir Preisler and Fedor Tatarinov for meteorological data and fruitful discussions.

3 Heatwaves and seedling death alter stress-specific emissions of volatile organic compounds in Aleppo pine.

This chapter has been published as: **Birami B., Bamberger I., Ghirardo A., Grote R., Arneth A., Gaona-Colmán E., Nadal-Sala D. and Ruehr NK.** (2021): Heatwave frequency and seedling death alter stress-specific emissions of volatile organic compounds in Aleppo pine. *Oecologia*. https://doi.org/10.1007/s00442-021-04905-y

Abstract:

Biogenic volatile organic compounds (BVOC) play important roles in plant stress responses and can serve as stress indicators. While the impacts of gradual environmental changes on BVOCs have been studied extensively, insights in emission responses to repeated stress and recovery are widely absent. Therefore, we studied the dynamics of shoot gas exchange and BVOC emissions in *Pinus halepensis* seedlings during an induced moderate drought, two four-day-long heatwaves and the combination of drought and heatwaves. We found clear stress-specific responses of BVOC emissions. Reductions in acetone emissions with declining soil water content and transpiration stood out as a clear drought indicator. All other measured BVOC emissions responded exponentially to rising temperatures during heat stress (maximum of 43°C), but monoterpenes and methyl salicylate showed a reduced temperature sensitivity during the second heatwave. We found that these decreases in monoterpene emissions between heatwaves were not reflected by similar declines of their internal storage pools. Because stress intensity was extremely severe, most of the seedlings in the heat-drought treatment died at the end of the second heatwave (dark respiration ceased). Interestingly, BVOC emissions (methanol, monoterpenes, methyl salicylate and acetaldehyde) differed between dying and surviving seedlings, already well before indications of a reduced vitality became visible in gas exchange dynamics. In summary, we could clearly show that the dynamics of BVOC emissions are sensitive to stress type, stress frequency and stress severity. Moreover, we found indications that stress-induced seedling mortality was preceded by altered methanol, monoterpene and acetaldehyde emission dynamics.

3.1 Introduction:

Climate change is expected to cause not only higher temperatures and a higher variability of precipitation, but also to produce more frequent and more intense extreme events such as heatwaves and drought spells (Baldwin et al. 2019; Kornhuber et al. 2019). This is likely to

intensify forest degradation as has been already observed in many areas world-wide (Anderegg et al. 2019; Brodribb et al. 2020; Hartmann et al. 2018a). In particular the co-occurrences of high temperatures and low water availability seems to damage tree growth and trigger mortality (Choat et al. 2018; Hartmann et al. 2018b; Ruehr et al. 2019; Williams et al. 2013). Nevertheless, the specific mechanisms of this phenomenon are still heavily discussed, since it is unclear how drought and heat effects interact and when stress-induced mortality actually occurs (Hammond et al. 2019; Hartmann et al. 2018b).

At the onset of severe droughts, trees initially react by closing their stomata to prevent excessive water loss, which in turn leads to suboptimal leaf internal carbon dioxide concentrations (C_i) and eventually limits photosynthesis (A_{net}) (Brunner et al. 2015; Gupta et al. 2020). As drought intensifies, the water potential of the conductive xylem can drop below a species-specific critical threshold (Anderegg et al. 2019; Ruehr et al. 2019), followed by embolism impairing water transport. At this point, the probability of drought-induced mortality increases (Hammond et al. 2019) because living tissue becomes dehydrated (Körner 2019). If the stress is not lethal, the organism requires carbon for repair and/or recovery processes, which is why individuals might still die sometime after the stress ceased, if sufficient reserves are not available (Ruehr et al. 2019).

High temperatures have the potential to increase physiological drought stress by increasing the vapor pressure deficit (VPD) of the surrounding air, which then leads to an increase in water loss by transpiration (E) (Panek and Goldstein 2001). Heat stress is amplified by limited water availability because a reduced evaporation limits the possibility for cooling the leaf surface (Ruehr et al. 2016; Williams et al. 2013). High temperatures will first speed up biochemical reactions, reducing the lifetime of proteins and causing imbalances primarily in the energy providing pathways (light assimilation, photosynthesis, respiration) (Niinemets 2018). Apart from higher resource requirements, this response enhances the formation of harmful reactive oxidative species (ROS) (Escandón et al. 2016; Song et al. 2014). Finally, a very high temperature may well lead to direct membrane damages, induce necrosis and eventually tissue senescence (Colombo and Timmer 1992; Daniell et al. 1969; Hüve et al. 2011) and can also lead to mortality (Birami et al. 2018).

Apart from opening stomata to increase evaporative cooling, which increases the risk of dehydration, the production of biogenic volatile organic compounds (BVOC) is another response to cope with abiotic stress (Spinelli et al. 2011). In particular terpenoids such as isoprene, monoterpenes (MT), and sesquiterpenes (SQT) play important roles in detoxifying reactive substances, regardless if these are taken up or formed internally in response to heat or radiation

(Nogués et al. 2015; Vickers et al. 2009). A second protective mechanism is the stabilization of membranes that is established by incorporation of isoprene or MT (Loreto et al. 1998; Mahajan et al. 2019). In addition, it seems that isoprenoids could also act as signaling molecules inducing a network of transcription factors that may play a role for stress tolerance (Harvey and Sharkey 2016).

Under stress conditions, new BVOCs may be emitted, or constitutively emitted BVOCs may increase several-folds above their unstressed rates (Guidolotti et al. 2019; Joó et al. 2011; Yáñez-Serrano et al. 2019). Such stress-induced BVOC emissions can either originate from de novo biosynthesis or are previously formed compounds, which had been stored in specific structures (e.g. MT from resin ducts in coniferous species) (Ghirardo et al. 2010; Turan et al. 2019). Typically damage-released compounds besides isoprene, mono- and sesquiterpenes, are green leaf volatiles, methanol and acetaldehyde as well as methyl salicylate (MeSa) (Guidolotti et al. 2019; Joó et al. 2011).

Thus, with the ongoing rise of temperatures as well as increased frequency and intensity of heatwaves and drought spells, changes in BVOC emissions can be expected. While most volatile emissions have been found to generally increase with temperature (Niinemets et al. 2010), this effect is less clear in response to drought and emissions patterns differ with species and drought intensity. Some authors found that emissions are increased at mild drought stress, while a chronic, prolonged drought decreases emissions (Dani et al. 2015; Eller et al. 2016; Llusià et al. 2016). However, significant amounts of MT emissions were still found in Aleppo pines at very dry conditions where photosynthesis was already dramatically reduced (Seco et al. 2017). So, not only the intensity but also the composition of emissions is likely to change, particular under extreme events, which would influenced vegetation-climate interactions (Harper and Unger 2018; Sporre et al. 2019). BVOCs take part in air chemistry processes and affect regional ozone concentration as well as aerosol abundance, with secondary impacts on cloud formation and radiation balance (Porter and Heald 2019; Zhao et al. 2017). Globally, BVOCs reduce the abundance of radicals in the air and thus increase the longevity of greenhouse gases, i.e. methane (Fuentes et al. 2001; Monson and Holland 2001). Hence, elucidating the variety of BVOC emission responses to different intensity, elongation, and frequency of stress conditions is needed.

Monoterpenes can be found in most conifers, becoming a main compound of resin, stored in large amounts in specialized resin ducts (Celedon and Bohlmann 2019; Turner et al. 2019). Despite representing large storage pools (up to 0.8% of the dry needle matter, (Vanhatalo et al. 2018)), it has been found that in Scots pine 10 - 58% of the emitted MT can still be synthesized de novo

from freshly fixed atmospheric carbon (Ghirardo et al. 2010; Kleist et al. 2012). Similarly, about half of MT measured in Aleppo pine in spring were estimated to be light dependent (Llusià et al. 2016).Apart from specialized storages, MT can be stored non-specifically as glycosylates in micro vesicles, or be integrated in biological membranes (Nagegowda 2010; Yazaki et al. 2017), and even accumulate in epicuticular wax layers (Joensuu et al. 2016). From these unspecific storages, MT can be directly released. Apart from MT, typically stress-induced terpenoids are sesquiterpenes (SQT), which play a role in plant-to-plant signaling in tree defense strategies against insects and pathogens (Joó et al. 2011; Kleist et al. 2012).

In addition to terpenoid emissions, a relatively large amount of BVOCs are oxygenated compounds that originate from various biochemical pathways (Grote et al. 2019). The most abundant in the atmosphere is methanol (Jacob 2005), which is formed mainly during cell wall development and can act as a stress signal transmitter (Dorokhov et al. 2018). Other short-chain volatile organic compounds (VOC) are derived downstream of glycolysis from either pyruvate or acetyl-CoA (Fall 2003; Grote et al. 2019), during anoxic stress conditions (Kelsey et al. 2011; Kreuzwieser et al. 1999), indicating substrate overflow mechanisms (Karl et al. 2002). Thus, acetaldehyde, ethanol and acetone are often produced in roots, phloem or cambial tissues (Kimmerer and Stringer 1988; Rissanen et al. 2020) where they remain dissolved until they reach the leaves via the transpiration stream within the plant (Rissanen et al. 2018). Some of them, especially methanol and acetaldehyde are indicators of high metabolic activity, often found when tissue damage occurs (Fall et al. 1999; Kreuzwieser et al. 1999; Loreto et al. 2006; Portillo-Estrada et al. 2015; Turan et al. 2019).

Dependencies of constitutively emitted BVOCs on temperature have been described extensively (Grote et al. 2014; Guenther et al. 1993; Niinemets et al. 2002), while deficits still exist in representing stress-induced BVOC emissions. Particularly, the emission responses to repeated heat stress under well-watered or drought exposed conditions have not received much attention so far. BVOC emission might be affected by potential acclimation responses and the production of compounds might be limited by decreasing carbon supply (Jud et al. 2016; Vanzo et al. 2015). In case of storage-released terpenoids, the storage capacity might decline and limit emissions during repeated and/or long-term heat stress (Schurgers et al. 2009). Finally, it remains unknown if BVOC emissions of coniferous trees prone to death differ from surviving trees, and hence may provide a death-preceding indicator of mortality.

In order to investigate BVOC responses to heat and combined heat-drought stress, we selected Aleppo pine, a tree species common to the dry and semi-arid regions in the Mediterranean area (Mauri et al. 2016). The seedlings used here originate from the Yatir forest in Israel, an Aleppo

pine plantation at the border to the Negev desert. Based on the literature, we hypothesize that 1) Aleppo pine will change BVOC emissions quantitatively and qualitatively under a combined heat and drought stress and that this response differs from that to only one of these stresses. 2) Emission bouquets differ between first and repeated stress caused by a reduction of storage compounds. 3) If stress induces seedling mortality, the emission is different from those of surviving seedlings.

3.2 Materials and Methods

3.2.1 Plant cultivation

Aleppo pine (*Pinus halepensis*, Miller) seedlings were cultivated from seeds in a controlled greenhouse environment in Garmisch-Partenkirchen, Germany (732 m a.s.l., 47°28’32.87’’N, 11°3’44.03’’E). Seed material originated from five different trees in a 55-year-old Aleppo pine plantation in Israel (Yatir forest, IL-Yat, 650 m a.s.l., 31°20’49.2’’N, 35°03’07.2’’E). The genetic heritage is not clear (Schiller and Atzmon 2009), but due to high levels of heterozygosity, seedling offspring may be referred to as a mixed F1 population (Atzmon et al. 2004; Korol and Schiller 1996). Seedlings (4 weeks old, July 2015) were transplanted to 1 L pots containing mineral substrate (2:8) of quartz sand (0.7 mm and 1-2 mm) and vermiculite (ca. 3 mm) with 2 g of slow-release fertilizer (Osmocote® Exact + TE 3-4 months fertilizer 16-9-12+2MgO+TE, Everis International B.V., Heerlen, The Netherlands). Seven-month-old seedlings (January 2016) were planted in larger pots (2.5 L) containing mineral substrate (1:2:1) of quartz sand (1-2 mm): quartz sand (4-6 mm): vermiculite (3 mm) and 6 g of slow-release fertilizer (Osmocote® Exact +TE 5-6 month fertilizer 15-9-12+2MgO+TE).Air temperature and relative humidity (RH) during cultivation (Table S3.1) were set to mimic the monthly mean of temperature and humidity data of the Yatir forest (averaged over ten years) as described previously (Birami et al. 2018). The position of the seedlings within the greenhouse compartment was iterated randomly in order to avoid any positioning effect (Fig 3.1). Nine-month-old seedlings were divided into four treatments in March 2016: control, heat, drought and heat-drought one month before initiating the heatwave experiment (experiment in April 2016, Fig 3.1). Therefore, 30 seedlings each of the control and drought treatments, as well as the heat and heat-drought treatments were placed into two adjacent environmentally-controlled compartments using a randomized block design (Birami et al. 2018; Ruehr et al. 2016). Substrate-specific calibrated moisture sensors (10HS, Decagon Devices, Inc., WA, USA) have been installed (n=10 per treatment). Per treatment, four seedlings each were equipped with a gas exchange cuvette (n=4 per treatment; see method section 2.3 for

details). Therefore, iteration of the seedlings' placement during the experimental phase was no longer possible.

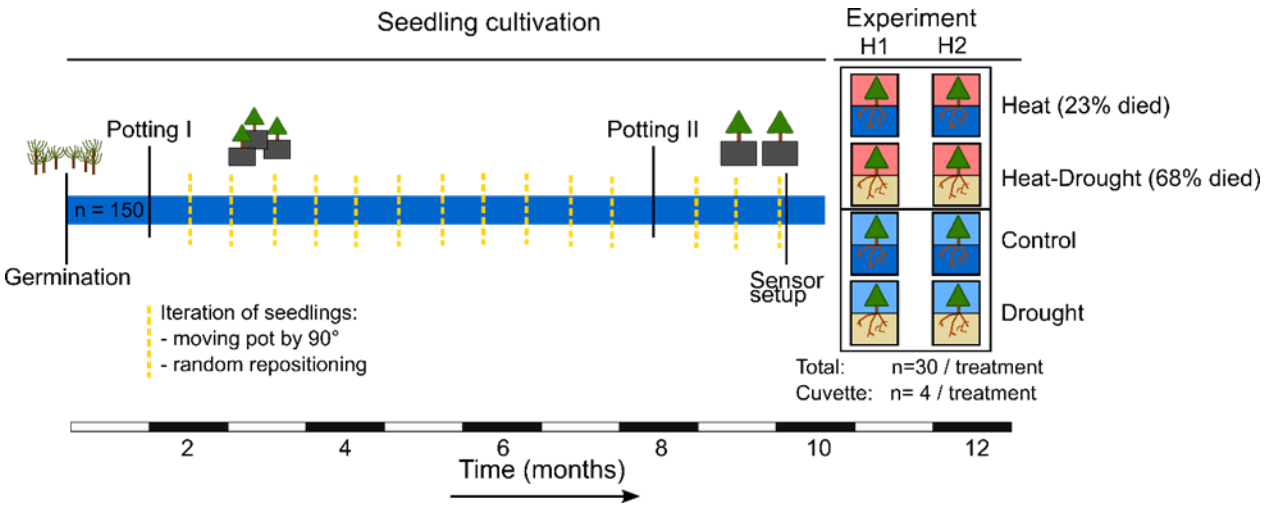

Figure 3.1 Experimental timeline: from Aleppo pine seedling germination until drought was initiated and two heat experiments (each 4 d) were conducted 10 months later. During the cultivation phase all seedlings were grown in one of the climate-controlled greenhouse compartments and positioning among seedlings was regularly iterated. Before the stress experiment was initiated the seedlings were randomly placed in two separate greenhouse compartments to conduct heatwave scenarios. In each treatment, four seedlings were placed in light transmitting gas exchange cuvettes coated with Teflon on the inside. In the heat and heat-drought treatment seedlings died due to overheating during the course of the experiment, mostly during the short recovery phase between heatwave 1 (H1) and heatwave 2 (H2) (see Birami et al. 2018 for details). Note that also seedlings placed in the gas exchange cuvettes died: one seedling in the heat treatment and three seedlings in the heat-drought treatment.

3.2.2 Experimental setup

Seedlings of the heat and heat-drought treatment were exposed to two heatwaves with stepwise increasing temperatures and vapor pressure deficit (VPD) (Fig S3.1). The heatwaves were designed to mimic naturally occurring few day-long heatwaves in the Yatir forest typically occurring during early summer (Tatarinov et al. 2015). In our experiment, each heatwave had a duration of 4 days (April 27th – April 30th and May 7th – May 10th, 2016) and temperature was increased during the first three days. The temperature level of the third day was repeated on the fourth day with a maximum of 42.8 °C during the first heatwave (H1) and 42.2 °C during the second heatwave (H2; see Table 3.1, Fig S3.1).

Table 3.1 Air temperature (T_{Air}) and vapor pressure deficit (VPD) before, during the two heatwaves and after. Averages (±1SD) and minima and maxima are given for each day of the heatwaves and for the periods before, between and after the heatwaves. Note minima occurred during night-time (8h), maxima during day-time (16h).

		T_{Air} [°C]			VPD [kPa]		
		Min	Mean	Max	Min	Mean	Max
	Before	11.1	18.3±2.7	24.8	0.2	1.1±0.4	2.3
Heat-	Day 1	14.4	21.3±3.9	27.1	0.5	1.7±0.7	2.9
wave I	Day 2	17.7	28.2±4.5	33.7	1.1	2.8±1	4.3
	Day 3	25.2	33.5±5	42.8	1.8	4.1±1.7	7.4
	Day 4	17.9	33.5±7	42.2	1.2	4.2±1.9	7.1
	Between	15.7	20.7±3	27	0.6	1.4±0.5	2.6
Heat-	Day1	17.0	26±4.8	32.1	0.9	2.4±1	3.9
wave II	Day2	18.6	31.4±6.5	40.2	1.1	3.7±1.7	6.4
	Day3	25.8	34±5.4	41.5	1.9	4.2±1.7	6.9
	Day4	17.8	33.4±6.7	42.2	0.9	3.9±1.8	6.9
	After	16.7	21.5±2.9	26.5	0.6	1.4±0.5	2.5

The trajectories of two heatwaves differed slightly, with the second heatwave reaching temperatures >40°C already at day two (compared to day three during H1). Note that the seedlings enclosed in cuvettes for BVOC and gas exchange measurements (see section 2.3, Fig S3.2), experienced higher temperatures after the lid of the cuvettes closed automatically (on average 3.8±1 °C at the end of the 10 min measurement cycle; 3-times per day). The average light intensity was 416 ± 105 µmol m^{-2} s^{-1} during day-time and water vapor in the greenhouse compartments and gas exchange cuvettes was kept constant, which resulted in 20-40 % RH and an increase of VPD to a maximum of 7.5 kPa during the heatwaves in the greenhouse compartment, similar to VPD conditions at the Yatir forest during heatwave periods in early summer (Tatarinov et al. 2015). The one-month drought period was initiated (DOY 114) 4 days before the first heatwave (DOY 118-121) and ended (DOY 138) 7 days after the second heatwave (DOY 128-131). Irrigation was reduced to a relative substrate water content (rSWC) of about 15

% in the drought and heat-drought treatment, while it was kept between 40-50 % under well-watered and control conditions (Fig S3.1).

3.2.3 Gas exchange and BVOC emission analyses

A custom-made, open chamber system, which has been previously described (Bamberger et al. 2017; Birami et al. 2018; Duarte et al. 2016), was used to automatically measure gas exchange and BVOC emissions from the shoots of the seedlings as follows. Randomly selected seedlings (*n* = 4 per treatment) were distributed spatially within each greenhouse compartment and their shoots were placed permanently in transparent cuvettes (Fig S3.2a) made from acrylic glass tubes (6.65 L PMMA, Saalberg GmbH, Feldkirchen, Germany). Dismountable acrylic glass caps on the downward-facing side allowed to install the cuvette at the seedlings stem. The inside of the cuvettes had been coated with chemical inert foil FEP (fluorinated ethylene propylene, PTFE Spezialvertrieb, Stuhr, Germany), Small gaps between the stem and the cuvette were sealed with plastic putty (Teroson, Henkel Adhesives, Düsseldorf, Germany) to minimize gas leakage. A fan (412 FM, ebm-papst GmbH & Co. KG, Mulfingen, Germany) guaranteed well-mixing of the air inside the cuvettes. To assess environmental conditions, each cuvette was equipped with a calibrated photo diode (G1118, Hamamatsu Photonics, Hamamatsu, Japan), a calibrated thermocouple (5SC-TTTI-36-2M, Newport Electronics GmbH, Deckenpfronn, Germany).

The 18 cuvettes (*n* = 4 per treatment, *n*=2 for empty background) were measured continuously in an automated sequence as follows. After the distal cap of the cuvette had closed, a constant air stream (5 L F-201CZ-10K, Bronkhorst, Ruurlo, the Netherlands) of clean air with on average 438 ± 3 µmol mol^{-1} [CO_2] and 6.5 ± 0.1 mmol mol^{-1} [H_2O] was supplied for 10 min. Zero air was generated by using an oil-free compressor (SLP-07E-S73, Anest Iwata, Yokohama, Japan) connected to an Ultra Zero Air generator (Ultra Zero Air GT, LNI Schmidlin SA, Geneva, Switzerland). CO_2 was supplied from a gas cylinder and water vapour was added to the air stream via a nebulizing evaporation pump (LCU Liquid Calibration Unit, Ionicon, Innsbruck, Austria). The air supply was channeled through a main tubing made of stainless-steel tubing (3/8-inch Swagelok, Ohio, USA) coated with SilcoNert (Silco Tek GmbH, Bad Homburg, Germany) and gas flow to the cuvettes was controlled by two 2/2-way solenoid valves with a PTFE housing (0121-A-6, 0-FFKM-TE, Bürkert, Ingelfingen, Germany) and PTFE tubing (ScanTube GmbH, Limburg, Germany). The detailed schematic of the measurement system can be found in Bamberger et al. (2017). For background measurements, two empty cuvettes (one each for the control and heat treatment) were measured during each measurement cycle and the recorded data was subtracted from the measurements containing seedlings (Birami et al. 2018).

Differences in [CO_2] and [H_2O] between reference air and measurement air leaving the cuvettes were recorded differentially via a LI-7000 connected to a LI-840 (both LI-COR Inc., Lincoln, NE, USA). Net CO_2 exchange (A_{net}, R_{dark}), transpiration (E) and stomatal conductance (g_s) were calculated as previously described in Birami et al. (2018). BVOC fluxes were measured with a high sensitivity proton-transfer-reaction (quadrupole) mass spectrometer (PTR-(Q)MS, IONICON, Innsbruck, Austria). The PTR-MS was operating at standard conditions with a drift tube pressure of 2.3 mbar and a drift tube voltage of 600 V. More detailed settings of the instrument can be found in Bamberger et al. (2017). Volatile compounds were detected on protonated nominal mass ratios (m z^{-1}) and quantified using a defined VOC mixture (14 components in nitrogen) of standard gas (#24182-650 IONICON, Innsbruck, Austria). PTR-MS calibration was performed at ambient humidity with a liquid calibration unit (LCU, IONICON, Innsbruck, Austria) on a weekly basis using a four-step calibration routine at mole fractions of 7.5, 5, 2.5 and 0 ppb.

Average sensitivity and limit of detection for each compound measured are given in Table 3.2. Since there was no representative for the GLV (e.g. z-3-hexenal) in our standard gas mixture, the sensitivity for $C_6H_{10}O$ on m z^{-1} 99 was estimated to be on average 3.15 ± 0.13 ncps ppb^{-1}, derived from the average sensitivity of xylene and toluene (the compound in the standard mixture being closest to m z^{-1} 99 to consider for the transmission efficiency of the quadrupole mass filter) multiplied by 0.33, its known fractionation patterns (33% on m z^{-1} 99) (Fall et al. 1999). This was corrected for reaction rate coefficient k of z-3-hexenal derived from Cappellin et al. (2012) for a E:N ratio of 120 Td ($k_{toluene}$= 2.08 ;k_{xylene}= 2.27;$k_{z\text{-}3\text{-}hexenal}$= 3.25). The limit of detection for m z^{-1} 99 is hence not given. The sensitivity for $C_8H_8O_3$ m z^{-1}153 (on average 4.96 ± 0.33 ncps ppb^{-1}) was derived from a liquid calibration using a calibration mixture of methyl salicylate (A0366376, CAS: 119-36-8, ACROS Organics, New Jersey, USA) in H_2O (Type 1, MilliQ® Direct8, Merck KGaA, Darmstadt, Germany) (7.8 ppb, 5.2 ppb, 2.6 ppb, 1.3 ppb and 0 ppb). Isoprene could not be distinguished from 2-methyl-3-butene-2-ol (MBO) with our method, hence we did not investigate this compound in detail an address it as “isoprene + MBO”. Ethanol could not be detected in satisfactory quality and was hence not further interpreted (see limit of detection Table 3.2).

To ensure that concentrations of volatiles represented steady state conditions, emissions were calculated from the last 360 sec per 10 minutes measurement (c_{out}, c_0), given that the stability quality criteria was full-filled and backflow from the cuvettes was > 0.3 L min^{-1}. Linear regression data were used to assess stability of the signal using an upper boundary for the regression slope ≤ $3\left(\frac{\sqrt{\langle s\rangle}}{\delta t}\right)$, where $\langle s\rangle$ is the average signal from the analyzer in cps and δt is the length of the time

interval used for averaging in s. Note: the term $\sqrt{\langle s \rangle}$ is given by the Poison-Noise of the analyzer. The fluxes of volatile compounds (E_v in nmol $m^{-2}s^{-1}$) were calculated from the concentration differences of air leaving the cuvette c_{out} and the concentrations leaving an empty chamber c_0 (Niinemets et al. 2011) as follows

$$E_v = (c_{\mathrm{out}} - c_{\mathrm{O}}) \frac{f}{l_{\mathrm{a}}} \quad (1)$$

with the flowrate f in mol s^{-1} to each cuvette and the projected leaf area of the seedlings l_{a} in m^2 (Birami et al. 2018). The projected leaf area was derived from photographs taken during the experiment and estimated through needle color thresholds (Fig S3.2b). The projected area was linearly extrapolated.

Table 3.2 Sensitivity and standard deviation (±1SD) (normalized counts per second per ppb of primary ions H_3O^+ and $H_2OH_3O^+$ within volume, ncps $ppbv^{-1}$) and limit of detection of all measured compounds in the calibration standard averaged over all weekly calibration cycles. For calculation of the apparent fluxes, linear interpolation within two calibration cycles was used, hence the table presents a guideline example for the procedure. BVOC analysed are highlighted with an asterisk. BVOCs not present in the calibration standard (#24182-650 IONICON) are in italic and their respective sensitivities were calculated as described in the methods. Note that m81 was not used in the analyses.

	Mass fragment	Sensitivity	Limit of detection
Compound		ncps $ppbv^{-1}$	ppbv
Methanol *	33	9.55 ± 0.35	0.35 ± 0.05
Acetaldehyde *	45	14.57 ± 0.63	0.11 ± 0.04
Ethanol	47	0.80 ± 0.11	3.52 ± 0.56
Acetone *	59	15.77 ± 1.12	0.06 ± 0.02
Isoprene (MBO's)	69	5.10 ± 0.46	0.09 ± 0.03
Monoterpene fragments	81	5.25 ± 0.76	0.07 ± 0.02
Toluene	93	6.66 ± 0.89	0.08 ± 0.02
Hexenal *	99	3.15 ± 0.13	NaN
O-Xylene	107	6.11 ± 0.98	0.11 ± 0.04
Monoterpene (α-pinene) *	137	1.65 ± 0.37	0.13 ± 0.04
Methyl Salicylate *	153	4.96 ± 0.33	0.08 ± 0.02

3.2.4 Endogenous monoterpene and sesquiterpene measurements

To determine the impacts of two consecutive heatwaves on the pools of endogenous MT and SQT, six additional seedlings per treatment were sampled between 1 pm and 3 pm at the last day of the second heatwave. The lower part of the seedlings' stem was removed and the samples (mainly needles and twigs) were immediately frozen in liquid nitrogen and ground in porcelain mortars to a fine powder and stored at -80 °C until further processing. MT and SQT were analyzed similarly as done before (Ghirardo et al. 2010; Vanhatalo et al. 2018). One mL of hexane (SupraSolv for GCMS, Merck Chemicals GmbH, Germany) containing 859.3 pmol μL^{-1} of δ-2-carene as the internal standard was added as a solvent to 50 mg of the ground and still frozen plant material in 2 mL gas-tight amber glass vials (Merck) and extracted at 4 °C for 3 h in continuous shaking. Samples were incubated overnight at 5 °C, and the supernatant was transferred into a new 2 mL glass vial using a 1 mL gas-tight syringe (Hamilton). Finally, 1 µL per sample was analyzed by thermo-desorption (TD) gas chromatography mass spectrometry (GC-MS) (Ghirardo et al. 2012). The TD-GC-MS was run and GC-MS data were evaluated as reported elsewhere (Ghirardo et al. 2020). Each sample was analyzed in triplicates and medians were taken from technical replicates. Final endogenous MT or SQT content was related to dried plant material, by weighing for each individual sample, a subsample of the freshly ground and frozen plant powder before and after oven drying at 60°C for 48 hours.

3.2.5 Data analyses and statistics

In order to visualize how BVOC emissions vary across treatments, we performed a canonical correspondence analysis (CCA, (TerBraak 1986)) between normalized emission rates, treatment and experimental period. CCA allows to test for the significance of each of the ordination axis, as well as for the influence of factors and cofactors. Monte Carlo permutations (here $n = 1000$) were performed in order to assess if the variability explained by the model is higher than the variability explained by a randomly generated set of variables (Oksanen 2011). BVOC emission rates were daily-averages that were normalized to pre-stress conditions per individual seedling to reduce the effect of biologic variance. Two separated analyses were performed on the surviving seedlings only (excluding m81, m93, m107, see Table 3.2): i) pre-stress vs. first heatwave, and ii) first heatwave vs. second heatwave. CCA analyses was done using the "Vegan" package, V2.5-6 (Oksanen et al. 2013).

Linear mixed effect models (lme, R packages: "lme4", "nlme" and "MuMIn") were used to test for dependencies of BVOC emissions, gas exchange on rSWC or temperature and treatment (fixed effects). Seedling was considered as a random effect. Temporal auto-correlation was accounted

by including a first order Auto-Regressive model in the lme (Box et al. 2016). AICc criteria (Akaike information criterion corrected for a small sample size) was used to select for the most parsimonious model (i.e., best model with as few predictive variables as possible), with a threshold for acceptation of 2, based on (Burnham and Anderson 2004). When the most parsimonious model was identified, a pseudo R^2 was calculated both for the fixed and the combined fixed and random effects and confidence intervals (CI) given (Nakagawa et al. 2013). Normality of the residuals and homoscedasticity were visually inspected.

During the course of the experiment three of the continuous measured seedlings (BVOC, gas exchange) in the heat-drought and one in the heat-treatment died due to overheating (Birami et al. 2018). Hence, treatment-specific analyses of BVOC emissions were done using the surviving seedlings only (heat-drought *n*=1, heat *n*=3, drought *n*=4, control *n*=4). The impact of dying and death on BVOC emissions was analyzed by grouping the heat and heat-drought seedlings into surviving (*n*=4) and dying (n=4). In case to overcome tree-specific differences in absolute emission rates, we normalized the data to a tree-specific median derived from before stress-conditions (110-114 DOY), which was for instance done when analyzing mortality responses. Treatment-averaged absolute emission rates per experimental period can be found in the Supplement (Table S3.4) and are given in Figure 3.4.

3.3 Results

3.3.1 BVOC emission during heatwaves and drought

Because extreme temperatures were reached during the heatwaves, three of the continuously monitored seedlings in the heat-drought, and one in the heat treatment died. Because the dying seedlings experienced different BVOC emissions, we concentrate here on the surviving seedlings first. The emission patterns of the Aleppo pine seedlings in the heat *n*=3 and heat-drought (*n*=1) treatment responded similar to heat stress (Fig 3.2a). High temperatures predominantly increased emissions of MT and methanol compared to pre-stress conditions. Further, we found the emissions of methyl salicylate and hexenal to increase modestly in response to the heatwave. Interestingly, the drought treatment alone did at first not result in a distinct BVOC response (Fig 3.2a), only with progression of the experiment and increasing soil drought (Fig 3.2b).

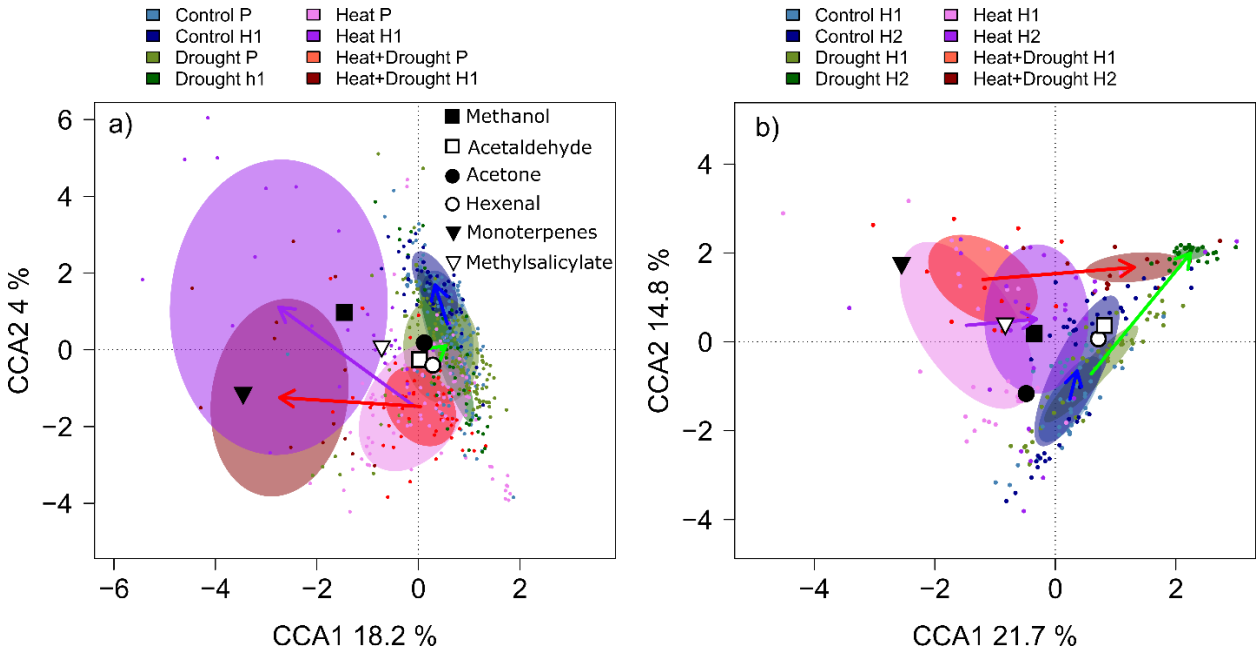

Figure 3.2 a) Pre-stress and treatment-specific stress responses of six selected BVOC emissions of the surviving Aleppo pine seedlings (methanol, acetaldehyde, acetone, hexenal, monoterpenes, methyl salicylate). Shown as a canonical correspondence analysis (CCA; for details see Data analysis and statistics section) to test for different responses of BVOC emissions of control (blue), drought (green), heat (magenta) and heat-drought (red) seedlings for pre-stress (P, lighter color) and first heatwave (H1, darker, corresponding color) conditions. b) Comparison of treatment-specific BVOC emission responses between the first (H1) and the second heatwave (H2). Colored areas depict the 95% confidence interval ellipsoid per treatment and period. Dependencies between the compounds (loadings) and the canonical variates (treatment) are shown for methanol, acetaldehyde, acetone, hexenal, monoterpenes and methyl salicylate. Note that emissions are only given for the surviving seedlings (heat: *n*=3, heat-drought: *n*=1, control: *n*=4, drought: *n*=4).

3.3.2 Sensitivity of acetone emissions to soil water availability

Here we focus on the impact of drought stress on BVOC emissions and found one distinct response. We found acetone to co-vary with soil water content (Fig 3.3) and its emissions to decrease at low water availability (see also Fig 3.2b). We found that a 10 % decrease in rSWC results in a 10 % (5-14 % CI; derived from lme) decrease in acetone emissions compared to well-watered conditions. Furthermore, both g_s and transpiration were included in the lme model, with acetone emissions being better explained by transpiration (pseudo-R^2_{fixed} = 0.39) than by g_s (pseudo-R^2_{fixed} = 0.1). Hence, changes in acetone emission were most likely caused by soil water availability and tree water flux. As we observed that acetone emissions from our potting-medium were negligible (< 3 % of average acetone emission rates from well-watered seedlings; data not

shown), acetone was most likely produced in the root tissues and transported to the shoots via the transpiration stream. No other BVOC showed a clear drought response (Fig 3.2, Table S3.4).

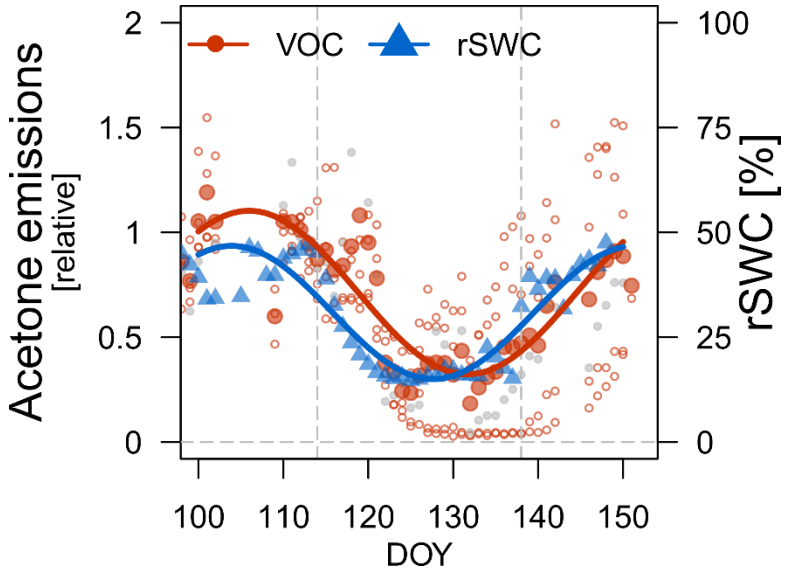

Figure 3.3 Dynamics of daily-averaged relative soil water content (rSWC [%], blue triangles) and acetone emissions during drying and re-wetting shown for the drought (n = 4; open red circles) and heat-drought (n = 1; grey solid circles) treatment. Acetone emissions are given relative to the pre-stress for measurements when PAR ≥ 100 (open filled red circles present daily-averages combining both treatments). Colored lines are added to visualize the overall development and represent a trigonometric best-fit using non-linear regression: α*sin(ω*(x+ϕ))+C with x being DOY and starting parameters (α, ω, ϕ, C).

3.3.3 Impact of repeated heatwaves on gas exchange and BVOC emissions

We investigated the impact of repeating heatwaves on the temperature response of BVOC emissions and gas exchange in the surviving Aleppo pine seedlings (Fig 3.4). A_{net} peaked at about 21.5 °C when VPD had reached 1.8 kPa (increase in temperature exponentially increased VPD following (VPD = exp (0.066(T)-0.85), R^2 = 0.94 of log-transformed function, Fig S3.3b), while g_s decreased to tightly regulate seedling water loss. In contrast, all observed BVOC emissions, except acetone (Fig 3.4h), increased with increasing temperatures exponentially (Figure 3.4c-g). It is notable that although g_s decreased in response to the heatwaves, E (Fig S3.3a) followed an exponential temperature response with slightly lower transpiration rates during the second heatwave.

MT and methanol represented the highest emission rates during heat exposure (Fig 3.4c and d). However, an altered temperature relationship became most obvious for MT and MeSa during the

second heatwave after exposure to the first heatwave. To test for differences in responses of emissions to temperature, separate lme were computed for MT and MeSa for the first- (H1) and the second heatwave (H2). Although the intercepts of the most parsimonious lme did not differ (overlapping 95% CI, implying similar response amplitudes), the response slope to temperature was reduced markedly (MT, H1: 0.26 [0.21-0.31 CI], H2:0.11 [0.08-0.13 CI]; MeSa, H1:0.001 [0.0009-0.0013 CI], H2:0.0006 [0.0004-0.0008 CI]), which shows that the same temperature does not induce the same emission signal during repeated stress. Methanol, hexenal and acetaldehyde did not show a change in heat response between heatwaves. Acetone did not show clear temperature dependencies (Fig 3.4h).

We further studied the endogenous MT pools to test the hypothesis that changes in emission patterns might be a consequence of the depletion of MT storages. Total endogenous MT pools did not decrease in plants exposed to two heatwaves, compared to seedlings grown under control conditions (Fig 3.5a). The same picture emerged when calculating the total MT pool per average seedling (heat: 148±30SE mg, control: 173±40SE mg based on the molar weight of a-pinene of 136.2 g mol^{-1}). This was in contrast to the cumulative MT emissions during the two heatwaves (DOY 114-131) which summed up to 28.1±4.4SE mg (Table S3.2), and would hence account for a 19.7±1.2SE % decrease of the total pool (as derived above). Considering specific compounds, we did not observe a significant impact of heat stress on any of the 14 MT measured (Table S3.2). Notably, the overall content of stress-induced SQT compounds (sum of 14) tended to increase compared to the control seedlings (P = 0.07, TukeyHSD, Fig 3.5b).

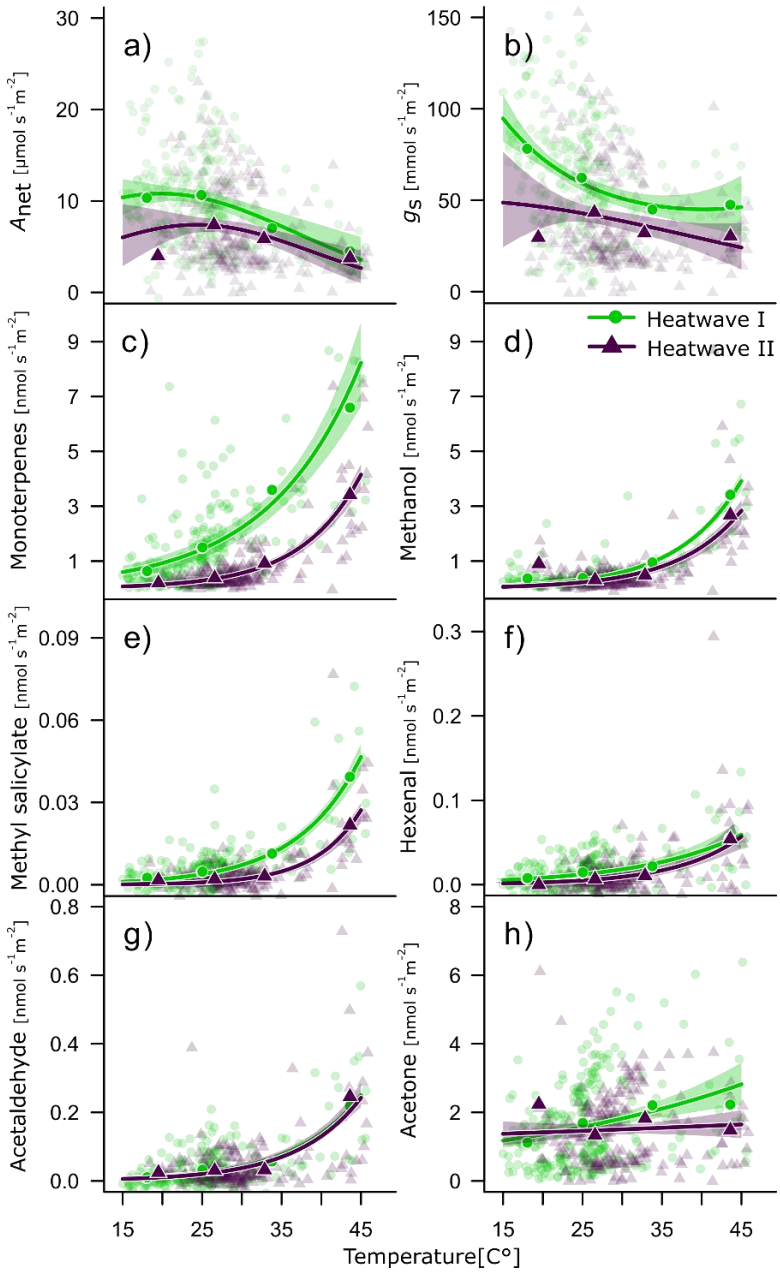

Figure 3.4 Differences in temperature responses of gas exchange and BVOC emissions during the first (filled circles, light green) and second heatwave (triangles, lilac) of the surviving Aleppo pine seedlings in the heat treatment (n=3). Data are given for PAR ≥ 100 µmol $m^{-2}s^{-1}$ including several days before heatwave initiation. a) Temperature (T) responses of photosynthesis (A_{net}) and b) stomatal conductance (g_s,) are shown and the regression lines depict second order exponential functions ($exp(a+b(T)+c(T)^2)$). c) The temperature responses of monoterpenes, d) methanol, e) methyl salicylate, f) hexenal, g) acetaldehyde and h) acetone are depicted by exponential functions (exp(b(T)+c). Shaded areas depict the 95 % confidence intervals of the fitted functions. Note that VPD increased exponentially with temperature: VPD=exp(0.66(T)-0.85) (R^2 = 0.94 of log-transformed function). The transparent data points are single measurements, while the solid symbols are bin-averages (10-50°C by 10°C) and shown for clarity.

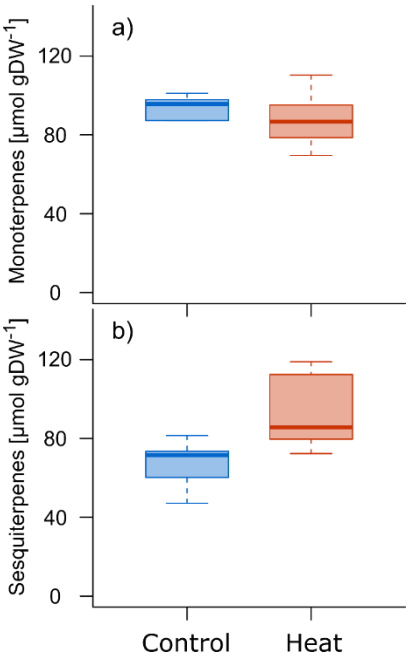

Figure 3.5 Concentrations of a) endogenous monoterpenes and b) sesquiterpenes in green shoots of control and heat-treated Aleppo pine seedlings sampled at the last day of the second heatwave (n = 6 per treatment). The box plots depict the median, lower, and upper quartiles (25^{th}–75^{th} percentiles).

3.3.4 Impacts of tree mortality on BVOC emissions

The stress intensity, in particular in combination of heat stress with drought, resulted in pronounced seedling mortality due to overheating. This overheating was more pronounced in the heat-drought treatment due to the lack of evaporative cooling and needle temperatures of 47°C were reached (Birami et al. 2018). As a consequence, some of the seedlings that were constantly monitored for BVOC emissions died: one in the heat treatment and three in the heat-drought treatment. The first indication for a reduced vitality of the seedlings can be seen in net photosynthesis (A_{net}) and transpiration to reach zero between the two heatwaves (Fig 3.6; horizontal grey bars) (Birami et al. 2018). However, we found clear differences in the emission rates between surviving and dying seedlings already much earlier. We found particularly strong responses in acetaldehyde (Fig 3.6d, TukeyHSD: $P \leq 0.05$) and MT (Fig 3.6b, TukeyHSD: $P \leq 0.05$) emissions, which were much higher during the first heatwave in the later dying compared to the surviving seedlings. Interestingly, these emissions also remained elevated during the first recovery period (between heatwaves). For methanol (Fig 3.6a) and MeSa (Fig 3.6c) emissions we found similar responses, albeit with a shift to increased emissions of the dying seedlings during the second heatwave. A clear indication for the death of the seedlings was the moment when dark respiration ceased (Fig 3.6, black bar represents when shoot respiration reached zero). This was directly after the end of the second heatwave. Further, analysis of shoot water content at the end of the experiment confirmed the differentiation in mortality and surviving seedlings. Surviving seedlings had an absolute shoot water content of 64.2±2 %, while the water content in the dead seedlings averaged at 24.2±13 % (Birami et al. 2018).

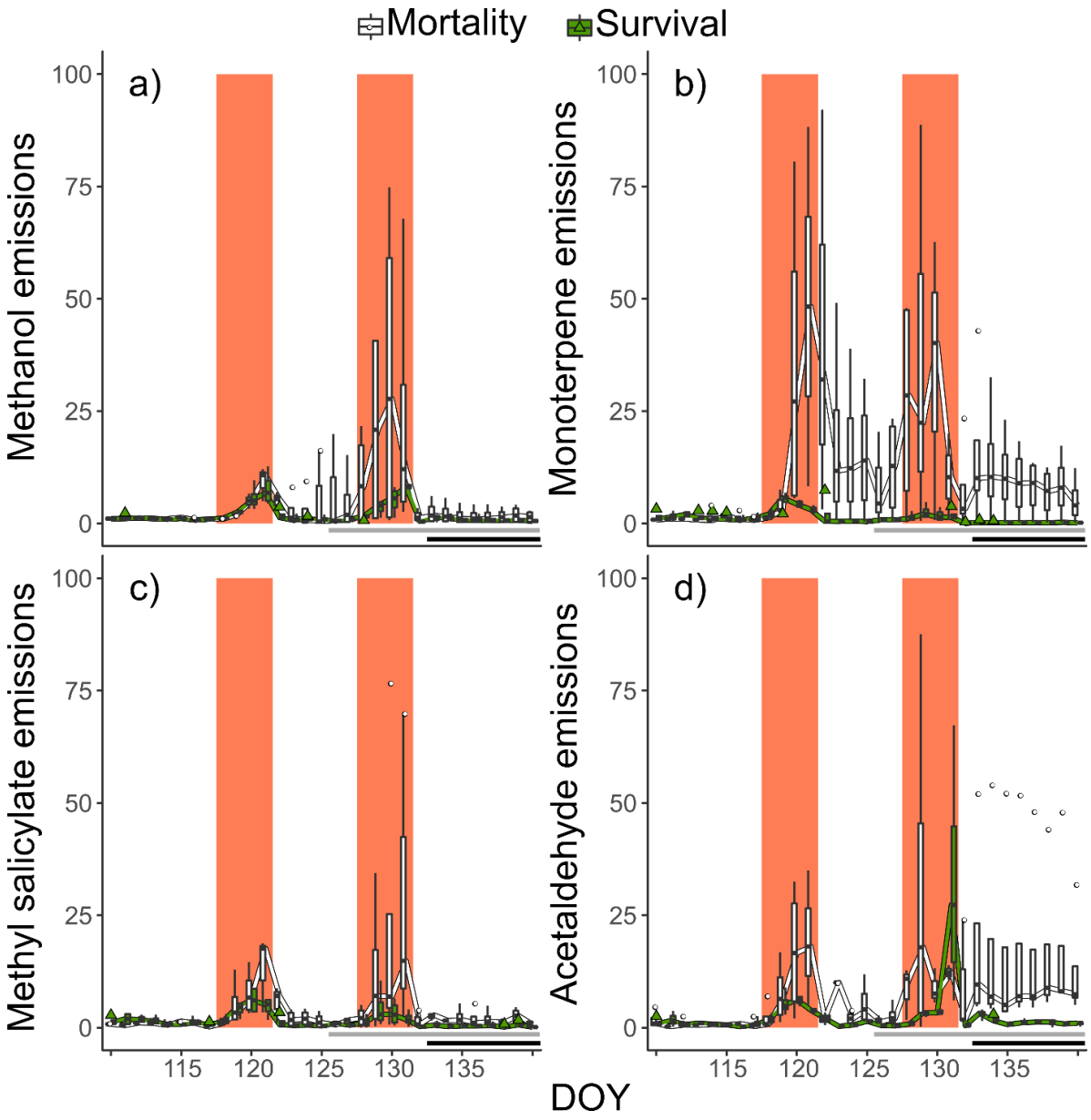

Figure 3.6 Responses of a) methanol, b) methyl salicylate, c) monoterpene and d) acetaldehyde emissions during seedling mortality. The emission data are shown relative to pre-stress derived from daily-averages (for measurements when PAR ≥ 100) per seedling, separated in surviving (green, *n* = 4; including 3 seedlings from the heat and 1 seedling from the heat-drought treatment) and dying (white, *n* = 4; including 1 seedling from the heat and 3 seedlings from the heat-drought treatment). The two heatwaves are highlighted by a solid colored background (DOY 118-121; 128-131). Horizontal grey bars mark the time course on when either daily-averaged transpiration or net photosynthesis or both of the dying seedlings reached zero. The time when dark respiration reached zero and seedlings were clearly dead is indicated by the black horizontal bars. Daily-averaged emission data was derived for measurements of PAR ≥ 100.

3.4 Discussion

Impacts of two consecutive heatwaves on BVOC emissions and gas exchange.

We found a strong stimulation of BVOC emissions during two consecutive heatwaves. Monoterpene, methanol, MeSa, hexenal and acetaldehyde emissions increased exponentially with increasing temperatures. In particular MT emissions showed a sharp increase between 30–43 °C. In contrast, acetone was insensitive to changes in temperature but responded to soil water availability (see below). Monoterpene emissions are known to respond strongly to temperature increase by release from specific storage pools depending on diffusion parameters and volatility (Kleist et al. 2012; Peñuelas and Llusià 1999; Staudt et al. 2017), including leaves and stems (Vanhatalo et al. 2020). On the other hand, MT emissions of pines have been shown to originate to more than 50 % directly from photosynthetic products under stressed conditions (Ghirardo et al. 2010; Taipale et al. 2011). In our experiment, the response of MT emissions of surviving seedlings to temperature was considerable weaker during the second heatwave (emission rates at a specific temperature were about 50 %, and maximum emission tended to be lower than during the first heatwave). With this respect, the results from our study agree well with previous studies on MT and MeSa emissions in Scots pine (Kleist et al. 2012), which reported a down-regulation of emissions during consecutive heatwaves. Such a response may indicate depletion of storages or could point towards metabolic adjustments of volatile biosynthesis.

The MT storage in plants, formed by specialized organs such as resin ducts, is typically large. In our investigations, we have found the monoterpene content to be 1.3 % of dry weight in shoot biomass of Aleppo pine seedlings (Table S3.5), similar to those of dried needle biomass of Scots pine (0.8 %) reported by Vanhatalo et al. (2018). Usually, a depletion of such a large storage is unlikely to happen in short time (few days), as it did not occur in two years old needles after MT emissions of an entire season (Vanhatalo et al. 2018). However, the depletion of MT storages has been proposed as a possible mechanism if plant tissue is exposed to high temperatures over a longer period (days to months) (Schurgers et al. 2009) and are shown to be reduced after 4 years of heat treatment (+3.5 °C) compared to non-treated Douglas fir saplings (Snow et al. 2003). Our measurements showed that the overall MT pools remained unaffected, although the cumulative MT emissions during both heatwaves was expected to deplete approximately 20 % of the total endogenous MT pool of the heat-treated seedlings (Table S3.5). This implies that MT's are de novo produced and directly released during heatwaves. Possibly, de novo MT production was impaired along with photosynthesis during the first heatwave and this caused lower MT emission during the second heatwave, compared to the first one. Although older investigations

could not find a significant contribution of emission from de novo biosynthesis for Aleppo pine (Peñuelas and Llusià 1999), more recent studies indicate that the contribution could be around 50 % (Llusià et al. 2016) and might be as high as 70 % in 3-4 year old trees (Staudt et al. 2017). It has also been shown that MT biosynthesis in general is sensitive to stress which also negatively affects A_{net} - such as drought - (Kleist et al. 2012; Lüpke et al. 2017) since the plastidic intermediate for the terpenoid synthesis is closely connected to photosynthesis (Ghirardo et al. 2014). Another explanation for the observed burst of MT during the heatwaves may be that those emissions originated from MT pools of non-specialized structures such as the lipid phase of cellular compartments and membranes (Joensuu et al. 2016; Nagegowda 2010; Yazaki et al. 2017). Overall their amount is small compared to the pool in specific storage tissue such as resin ducts (Ormeño et al. 2011), but might face less diffusive resistance and can readily enter the gas phase. Following this, intra membrane or cuticular MT are likely to be primarily released during the first heatwave and were not refilled before the second heatwave, contributing to the overall smaller emission rates. Hence, we have no information about the actual compartmentation of the endogenous MT, de novo synthesized MT may have prevented total pool depletion and a delayed refilling of the non-specialized pools may have reduced the emissions during the second heatwave. As reported in poplar, membrane collapse caused by severe heat stress may as well cause such a burst of several BVOC, including MT (Behnke et al. 2013).

Methyl salicylate emissions, which are known to increase under stress in many tree species (Filella et al. 2006; Joó et al. 2011), also showed an altered temperature-response during the second heatwave. While MeSa has been shown to be released under biotic stress, it has also been related to drought (Karl et al. 2008; Scott et al. 2019). As a signal-transmitting metabolite, MeSa is freshly mobilized from precursor molecules (Heil and Ton 2008). The reduced temperature-response of emissions during the second heatwave might thus indicate a suppression of enzymatic activity and might support the hypothesis that, at least, parts of the observed MT burst is caused by de novo production. Suppression of MeSa mobilization from salicylic acid at high temperatures has been previously reported (Shulaev et al. 1997), while in a study on *Arabidopsis thaliana* thermal pre-treatment (38 °C) induced salicylic acid accumulation (non-volatile form of MeSa) that caused thermotolerance of the plants at 47 °C (Clarke et al. 2004).

Overall, we could show that consecutive heatwaves alter the temperature-sensitivity of MT and MeSa emissions and that these changes are not related to any declines of pools in specific structures. Instead, the decrease in responsiveness seems strongly related to a reduced

metabolic activity, possibly due to reduced enzyme production or increased damage of metabolic production chains.

Impact of drought on BVOC emissions

Previously observed responses of BVOC emissions to water availability are inconclusive in the case of Aleppo pine. Some studies report MT emissions to decrease with drought (Blanch et al. 2007; Llusià et al. 2016), while others report increases (Llusià et al. 2008). Overall, the emission response might particularly depend on the severity and duration of drought, increasing at first under mild drought but decreasing with drought progression (Ormeño et al. 2007). In our experiments, we could not observe drought-specific responses of MT emissions, which, however, might be due to a physiological adjustment that reduced MT emissions already under non-stressed conditions. The same response has been shown for mature trees at the same site, which is different to stands under less extreme conditions (Llusià et al. 2016), indicating that the adjustment origins from genetic rather than morphological changes.

On the other hand, we found that reduced acetone emissions were indicative for drought conditions. Acetone represented one of the most abundant volatile compounds emitted. Acetone probably originated from the root tissue and was then transported to the shoots of the seedlings as long as soil water availability is sufficient. This is similar to what has been reported for Aleppo pine stands (Filella et al. 2009) and is also supported by studies demonstrating that the emissions of water soluble short-chained compounds depends on *E* (Rissanen et al. 2018). Acetone is the smallest ketone of the anoxic fermentation chain derived from Acetyl-CoA that is metabolized either from pyruvate or fatty-acid oxidation (Fall 2003; Grote et al. 2019) and is indeed easily water-soluble. It was found to be an indicator for flooding in roots of trees from the Amazonian floodplains (Bracho-Nunez et al. 2012). In temperate and boreal forests, acetone emissions have been generally related to water availability (Janson and Serves 2001; Shao and Wildt 2002). Acetone is thus a likely candidate for an indicator of drought-stress particularly for coniferous forests. This largely supports our first hypothesis that responses of specific BVOC emissions can be directly linked to the type of stress. Where MT emissions were found to be strongly induced by heat stress, acetone emissions were found to decline under drought.

Methanol as an indicator for lethal stress

At the end of the experiment, four of the seedlings constantly monitored for gas exchange and BVOC emission died (heat: n = 1; heat-drought: n = 3). Mortality was more pronounced in the group of heat-drought-stressed seedlings, possibly due to damages from higher leaf temperatures

caused by reduced evaporative cooling (> 47 °C, (Birami et al. 2018)). While the exact time of death is challenging to determine, gas exchange data show that A_{net} and E reached zero between the two heatwaves (Table S3.3) and that shortly afterwards also dark respiration stopped, indicating that shoots became metabolically inactive. We found an increase of methanol emission in dying (but not in surviving) seedlings one day before this occurrence, while otherwise the emission rate was relatively stable as highlighted before (Seco et al. 2015). To the best of our knowledge it is the first time that changes in emission patterns of BVOCs were directly linked to heat-induced mortality.

It has been commonly observed that emission of green leave volatiles and oxygenated VOCs such as methanol increase during heat stress (Kleist et al. 2012). This has been particularly reported under high temperatures and limited water supply (Filella et al. 2009; Jardine et al. 2015). Methanol is produced in considerable amounts during cell wall formation, released by pectin methylesterases (PMEs), allowing to adjust the rigidity of the cell walls. Heat stress (35-65 °C) in turn, was reported to activate apoplastic PMEs (Wu et al. 2018). While methanol is being cleaved from pectine, Ca^{2+} is being released, which passes the cell membrane and starts a cascade of intracellular stress signals (Dorokhov et al. 2018; Wu et al. 2018). Thus, excess in methanol production can be a sign of active growth processes, or be the consequence of the demethylation of several methylated compounds (e.g. DNA, RNA, histones, and other proteins) occurring after cell damage and oxidative stress as it was reviewed by Kim et al. (2015). The co-occurrence of a substantial increase in the emissions of lipoxygenase products such as hexenal (Fig S3.3) with high methanol fluxes (Fig 3.6a), provides a strong indication that methanol emissions were related to cell and membrane damages. Indeed, after membrane disruption, lipoxygenase products are formed when the fatty acid substrates trapped in the cell membrane get in contact with cytosolic enzymes. In turn, the concomitant but stronger methanol emissions might be a reliable indicator of lethal heat dosage (Turan et al. 2019).

Excessive MT and acetaldehyde emissions anticipate higher sensitivity to stress

Monoterpene and acetaldehyde emissions of seedlings that died after the first heatwave were distinct from surviving seedlings, albeit photosynthetic rates were not showing apparent differences between dying and surviving individuals until the first day of stress release (Table S3.3,S3.4 (Birami et al. 2018)). Susceptible seedlings showed a tendency of higher emissions in MeSa, 69 m z-1 (which is an unknown compound that could either be isoprene or MBO, Fig S3.3a), and hexenal (Fig S3.3b).

MeSa and hexenal have been previously depicted as stress sensing and stress signaling molecules (Tawfik et al. 2017; Wu et al. 2018). Acetaldehyde emissions, however, were found to be closely related to stomatal conductance in Aleppo pine (Filella et al. 2009; Seco et al. 2008). This is in contrast to our results, where increasing temperatures decreased stomatal conductance both in surviving and dying seedlings, while acetaldehyde emission rates increased independent of g_s. Increased acetaldehyde production may result from a possible pyruvate substrate overflow mechanism during times of sudden changes in light intensity, when downstream processes of carbohydrate reduction are limited (Karl et al. 2002). Carbohydrate metabolism can also be limited by temperature stress, which is supported by similarities between the metabolic response to anoxia and high temperatures, both inducing anoxic fermentation pathways (Pucciariello et al. 2012) that eventually result in acetaldehyde formation (Kreuzwieser et al. 1999). Formation and production not necessarily results in immediate emission, nonetheless, acetaldehyde is released when terminal cell damage occurs (Behnke et al. 2013; Fall et al. 1999; Loreto et al. 2006; Portillo-Estrada et al. 2015; Turan et al. 2019). Interestingly, also the surviving seedlings showed a higher emission rate of acetaldehyde at the end of the second heatwave, indicating i) that some damages occurred also in the surviving seedlings which might have been fatal in a third heatwave, and ii) that acetaldehyde might be a better sensitivity indicator than MT alone.

Still, it is difficult to explain why the dying seedlings had higher acetaldehyde and MT emissions before and after actual mortality happened (Fig 3.6b and d) although similar observations have been made on different plants or tissues. For example, high emissions of acetaldehyde and other oxygenated VOCs have been reported during the process of grass drying (Gouw et al. 1999). Also, active dehydrogenases that might produce acetaldehyde have been found in dry heartwood (Tohmura et al. 2012) and during industrial drying of pinewood (McDonald et al. 2002). In all cases, it was assumed that acetaldehyde emissions were caused by enzymatic or microbial remnant activity or oxidative decomposition of cellulose i.e., resin components. Regarding the increased MT emissions, it should be considered that the absolute magnitude of emissions from the dying seedlings (55.2±21.7 mg) doubled the cumulative emissions from surviving heat-treated seedlings (28.1±4.4 mg). This would relate to an approximate loss of about 35 % in relation to the stored compounds (Table S3.5), if assume the pool size of an average seedling. Therefore, and because no seedlings died during the same period, it is unlikely that resin ducts have been significantly damaged and were the origin of the MT burst. However, decreased membrane integrity of more sensitive individuals may have facilitated the release of non-specific MT. Furthermore, MT precursors can be formed in the plastidic methylerythritol phosphate pathway (MEP) (Zeidler and Lichtenthaler 2001). As the MEP pathway is promoted under heat and light

stress (Harley et al. 1998), and is well coupled to the abscisic acid sensing network (Asad et al. 2019), increased synthesis of MT by dying seedlings could be explained by a higher stress sensitivity. In summary, we found that the onset of lethal stress induces a distinct BVOC emission composition, which was already detectable about 14 days before mortality actually occurred. This indication of mortality started considerably earlier than any clear trend in gas exchange rates.

Concluding, we found VOC emissions from Aleppo pine seedlings to respond specifically to stress-type and stress-frequency. The reduced temperature sensitivity of monoterpene emissions during a second heatwave was not related to storage depletion in shoot tissues, but likely caused by stress-induced impairment of de novo synthesis and intra-tissue localization. Moreover, we found a distinct response in MT, acetaldehyde emissions to precede seedling mortality with methanol as indicator for lethality under heat and combined heat-drought stress. We did, however, not investigate different ontogenetic stages, which means that a species might acclimate to heatwaves and drought conditions and that emission responses of adult individuals might differ from those of seedlings. In fact, eddy-covariance measurements in different Aleppo pine stands indicate that emissions at the Yatir forest are smaller than at stands with less extreme conditions (Seco et al. 2017), which could be interpreted as a long-term acclimation. Understanding these signals, might help optimizing management for stress mitigation in precision farming or tree planting (Kravitz et al. 2016; Lüttge and Buckeridge 2020), and pave the way to new conceptual modelling frameworks towards characterizing stress severity related to tree mortality.

3.5 Acknowledgements

We would like to thank Marielle Gattmann and Lena Müller for support during the experiment and Baris Weber and Ina Zimmer for technical help during GC-Ms analysis. This study was funded by the German Research Foundation through its German-Israeli project cooperation program (SCHM 2736/2-1 and YA 274/1-1) and by the German Federal Ministry of Education and Research (BMBF), through the Helmholtz Association and its research program ATMO. BB and NKR acknowledge support from the German Research Foundation through its Emmy Noether Program (RU 1657/2-1). We are thankful to all reviewers, who helped to improve this manuscript. This manuscript is to be published as part of a Special Issue honoring Russ Monson. The authors appreciate Russ' contribution to highlighting the CO_2 effects on isoprene emissions, and lively discussions about BVOC emissions modelling.

4 Hot drought reduces the effects of elevated CO_2 on tree water use efficiency and carbon metabolism

This chapter has been published as: **Birami, B., Nägele, T., Gattmann, M., Preisler, Y., Gast, A., Arneth, A. and Ruehr, N.K. (2020)**, Hot drought reduces the effects of elevated CO_2 on tree water-use efficiency and carbon metabolism. New Phytol, 226: 1607-1621. doi:10.1111/nph.16471

Summary

(1) Trees are increasingly exposed to hot droughts due to [CO_2]-induced climate change. However, the direct role of [CO_2] in altering tree physiological responses to drought and heat stress remains ambiguous.

(2) *Pinus halepensis* (Aleppo pine) trees were grown from seed under ambient (421 ppm; a) or elevated (867 ppm; e) [CO_2]. The 1.5-year-old trees, either well-watered or drought-treated during one-month, were transferred to separate gas exchange chambers and temperature gradually increased from 25°C to 40°C over a 10 d period. Continuous whole-tree shoot and root gas exchange measurements were supplemented by primary metabolite analysis.

(3) Elevated [CO_2] reduced tree water loss, reflected in lower stomatal conductance, resulting in a higher water-use-efficiency throughout amplifying heat stress. Net C uptake declined strongly, driven by increases in respiration peaking earlier in the well-watered (31–32°C) than drought (33–34°C) treatments unaffected by growth [CO_2]. Further, drought altered the primary metabolome, while the metabolic response to [CO_2] was subtle and mainly reflected in enhanced root protein stability.

(4) The impact of e[CO_2] on tree stress responses were modest and largely vanished with progressing heat and drought. We therefore conclude that increases in atmospheric [CO_2] cannot counterbalance the impacts of hot drought extremes in Aleppo pine.

4.1 Introduction

Forests are exposed to a rapidly changing climate world-wide and extreme weather events such as heatwaves and drought spells are predicted to increase in frequency and severity as atmospheric [CO_2] is rising (Coumou and Rahmstorf 2012). This has pronounced impacts on forest carbon and water cycling (Williams et al. 2013), particular in already water-limited ecosystems (Choat et al. 2018). Yet, the interacting effects of elevated [CO_2] (e[CO_2]) with extreme environmental conditions such as drought, heat stress and the combination of both, on tree stress resistance are far from clear.

Heatwaves during extended drought periods can be a main cause of forest decline (Anderegg et al. 2012). Hot droughts are particular stressful because evaporative demand is high, while water availability is low and trees need to tightly regulate water loss (Ameye et al. 2012; Birami et al. 2018; Ruehr et al. 2016). This typically induces stomatal closure to maintain the integrity of the water transporting system (Tyree and Zimmermann 2002). Simultaneously carbon (C) assimilation rates decline, while C is needed to support osmoregulation and cellular maintenance (Hartmann and Trumbore 2016; Hsiao 1973; Huang et al. 2012). Therefore, a C imbalance can arise under progressing stress, which triggers a cascade of metabolic adjustments.

A driving force of metabolic activity in plants is respiration (*R*). Typically, about 30–80% of the daily photosynthetic C gain is released back to the atmosphere (Atkin and Tjoelker 2003). During stressful conditions, the amount of respiration to assimilation can change dramatically and trees can become a net source of CO_2. It has been shown that the C loss in trees subjected to higher temperatures and increasing drought is larger and occurs earlier than under cooler conditions. This was due to *R* continuing at relatively high rates while assimilation started to decline earlier in drought-treated trees grown under 35°C compared to 25°C (Zhao et al. 2013). Other work has shown that *R* can strongly increase under rapid warming, even in combination with drought, until rates drop at very high temperatures (Gauthier et al. 2014). In contrast, if trees are exposed to elevated growth temperatures, *R* typically acclimates, nearly offsetting the effect of the warming (Drake et al. 2019a; Reich et al. 2016). Although much research has focused on the temperature relationship of *R*, we have little mechanistic understanding to predict how *R* will respond to day-long heatwaves, let alone in combination with drought and/or changes in [CO_2].

Increasing atmospheric [CO_2] may affect tree stress responses through a variety of plant physiological processes. For instance, e[CO_2] often suppresses photorespiration and dark respiration (Drake et al. 1999; Dusenge et al. 2019), while stimulating C assimilation and productivity under non-stressful conditions (Ainsworth and Long 2005; Ainsworth and Rogers

2007; Ameye et al. 2012; Simón et al. 2018; Zinta et al. 2018). Alongside with increases in C uptake, stomatal conductance (g_s) typically declines (Eamus 1991). This reduction in g_s corresponds with a larger leaf-intercellular [CO_2] concentration (C_i), stimulated photosynthesis and increased plant water-use-efficiency (WUE) – the ratio of C uptake via assimilation per unit water loss from transpiration (Lavergne et al. 2019).

Increases in WUE under e[CO_2] have been observed in many studies (Eamus 1991), particular in water-limiting environments (Wullschleger et al. 2002). However, the combined effects of e[CO_2] stress responses during extreme heat and/or drought stress have rarely been investigated and results remain inconclusive. For instance, e[CO_2] could not mitigate extreme drought stress (withholding water until mortality occurred) in *Pinus radiata* and *Callitris rhomboidea* (Duan et al. 2015) or in *Eucalyptus globullus* when +240 ppm CO_2 was combined with a constant +4°C warming (Duan et al. 2014), while it alleviated extreme heat stress in *Pinus taeda* and *Quercus rubra* (Ameye et al. 2012) and *Larrea tridentata* (Hamerlynck et al. 2000).

A more comprehensive picture on the interacting effects of e[CO_2] on plant stress performance could be gained through a whole tree C perspective – integrating sink and source responses (Dusenge et al. 2019; Ryan and Asao 2019). Moreover, investigating changes in the primary metabolism could allow to identify some of the underlying mechanisms (Mohanta et al. 2017; Xu et al. 2015). For instance, e[CO_2] can increase sugar and starch concentrations, which might buffer plant C losses during drought via enhanced C supply and/or improved osmoregulation (Ainsworth and Long 2005; Ainsworth and Rogers 2007) as well as may reduce oxidative stress (Zinta et al. 2014). However, e[CO_2] may also affect the carbon-to-nitrogen (CN) stoichiometry and N dilution as has been observed, resulting in decreased protein and amino acid concentrations (Johnson and Pregitzer 2007; Poorter et al. 1997). A decrease in protein content may affect assimilation and *R* rates (Drake et al. 1999; Dusenge et al. 2019; Xu et al. 2015), could dampen stress-induced upregulation of amino acids important for osmoregulation (Zinta et al. 2018) and may affect the abundance of heat-shock proteins and therefore plant thermotolerance (Coleman et al. 1991; Huang et al. 2012; Zhang et al. 2018). Hence e[CO_2] can trigger metabolic processes which may directly interact with tree drought and heat stress responses. Yet results remain inconclusive because we miss an integrated understanding of the interactive effects of e[CO_2] and stress on the C balance and primary metabolism of trees.

Here we provide novel insights into the impacts of e[CO_2] on whole-tree, shoot and root stress responses in Aleppo pine saplings originating from a semi-arid forest at the arid timberline (Grünzweig et al. 2009). To elucidate the effects of [CO_2] in combination with drought and heat

stress on physiological responses, we combined measurements of whole-tree C balance, WUE and primary metabolites. More specifically, our hypotheses were: i) e[CO_2] increases photosynthesis which results in a larger net C uptake maintained during heat stress, ii) WUE increases proportionally with atmospheric [CO_2] this increase can be maintained during heat stress but not during hot drought when stomata are closed, and iii) the tree metabolic response to temperature is suppressed under e[CO_2], reflected in a concurrent change in respiratory activity and primary metabolites.

4.2 Material and Methods

4.2.1 Plant material

Pinus halepensis (Miller) saplings were grown from seeds for 18 months under ambient CO_2 (c. 420 ppm) or e[CO_2] (c. 870 ppm, within range of RCP 8.5 for 2100, (Pachauri et al. 2014)) in a scientific glasshouse facility in Garmisch-Partenkirchen, Germany (732 m a.s.l., 47°28'32.87''N, 11°3'44.03''E) with highly UV transmissive glass (70%). The origin of the seed material is a 50-year-old Aleppo pine plantation in Israel (Yatir forest). Cones of trees were sampled growing in close-proximity to a meteorological station and flux tower (IL-Yat, 650 m a.s.l., 31°20'49.2''N, 35°03'07.2''E).

In the following the experimental design of the study is explained in detail from the germination of the seedlings until the 18-month-old saplings were transferred into separate tree gas exchange chambers (see Fig. 4.1). Seeds germinated on vermiculite in two transparent growth chambers either under ambient atmospheric CO_2 (a[CO_2]) or e[CO_2] . About 10 weeks after germination, in July 2016, the seedlings were transferred to pots (5 x 5 x 5 cm, 0.125 l) containing a C-free potting mixture of 1:1:0.5 quartz sand (0.7 mm and 1-2 mm), vermiculite (c. 3 mm) and quartz sand (Dorsolit 4-6 mm) with 1 cm of expanded clay (8-16 mm) as a drainage. Seedlings were fertilized with 2 g of slow-release fertilizer (Osmocote® Exact 3-4M 16-9-12+2MgO+TE, ICL Specialty Fertilizers, The Netherlands) supplemented by liquid fertilizer (Manna® Wuxal Super, Wilhelm Haug Gmbh & Co. KG, Germany).

Placement of the seedlings within the two growth chambers was randomized every second week, and to overcome a possible chamber effect, the CO_2 treatments were iterated in monthly intervals between the chambers (Fig. 4.1). After the saplings were 7-month-old they were placed in two glasshouse compartments referring either to a[CO_2] and e[CO_2] conditions and 10 month old seedlings were individually transferred to larger pots (4.5 l) for a second time. The potting mixture was again a C-free substrate of 1:1:2 vermiculite (3-6 mm), coarse (4-6 mm) and fine quartz sand (2-3 mm) with 1 cm of expanded clay (8-16 mm) as a drainage. 5 g of slow-release fertilizer

(Osmocote® Exact Standard 5-6M 15-9-12+2MgO+TE, ICL Specialty Fertilizers, The Netherlands) was added to the mixture and supplemented by liquid fertilizer, phosphate and magnesium addition once. Incoming light from outside was supplemented with plant growth-lamps (T-agro 400 W, Philips, Hamburg, Germany) and the saplings were irrigated regularly to saturation. A possible effect of the placement within the glasshouse was again overcome by iterating the CO_2 treatments between the two glasshouse bays, four times before the start of the heat stress experiment in September 2017 (Fig. 4.1).

Atmospheric CO_2 differed largely between the glasshouse compartments (421±105 ppm in a[CO_2] and 867±157 ppm in e[CO_2] on average, increase in [CO_2] of 106 % during growth period), while all other growth conditions were kept similar (see Fig. S4.1). Moisture sensors (10HS, Decagon Devices, Inc., WA, USA; calibrate to potting substrate) and an automated drip irrigation system were installed (Rain Bird, Azusa, CA, USA) when seedlings were 15-month-old. The irrigation was adapted to result in a relative substrate water content (RSWC) of 50% (Fig. S4.2) close to the soil water content in the Yatir forest during spring conditions. RSWC was calculated as follows:

$$RSWC = 100* \frac{(SWC_{sample} - SWC_{min})}{(SWC_{max} - SWC_{min})} \quad (1)$$

SWC_{max} in g g^{-1} is the maximum amount of water hold by the substrate (e.g. field capacity). SWC_{min} in g g^{-1} was set to 0 and SWC_{sample} is the measured substrate water content, which was derived from the calibrated moisture sensors.

When seedlings were about 17 months old, half of the seedlings from each CO_2 treatment were randomly selected and assigned to a drought treatment (D). In the drought trees, irrigation was slowly reduced to maintain daily-averaged RSWC at c. 10%, while RSWC in the well-watered trees (W) was maintained at 50%, leading to a pronounced decrease in water potential. Two sets of seedlings from each of the four treatments (a[CO_2]W, e[CO_2]W, a[CO_2]D, e[CO_2]D) were randomly selected 40 d and 50 d after drought had been initiated (Fig. 4.1), transferred to custom-build separate tree gas exchange chambers (see below) and exposed to increasing heat stress (*n*=4 per treatment) for a period of 10 days.

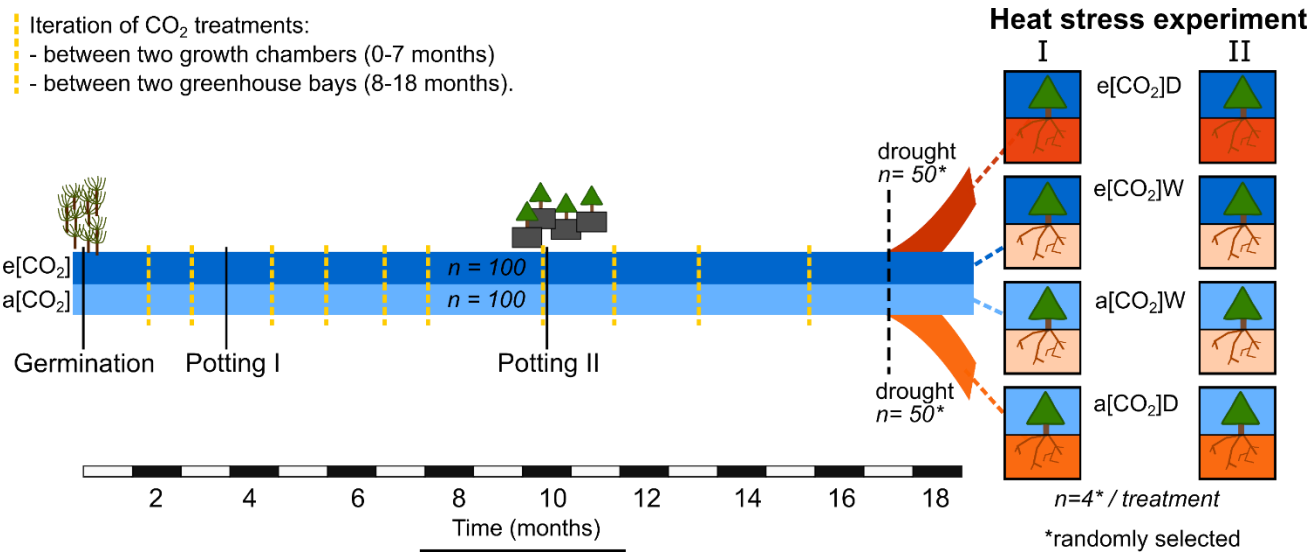

Figure 4.1 Experimental timeline from seedling (*Pinus halepensis*) germination until two heat experiments (each 10 d) were conducted 18 months later. The initiation of the CO_2 (e[CO_2]: dark blue, a[CO_2]: light blue) and drought treatments (orange) is also shown. Seedlings of the four treatments (a[CO_2]W, e[CO_2]W, a[CO_2]D, e[CO_2]D) were randomly selected and transferred to the gas exchange chambers where temperature was step-wise increased (25°C, 30°C, 35°C, 38°C, 40°C) and above- and belowground gas exchange measured. The heat experiment was repeated with a new set of seedlings to increase number of replicates to 8 per treatment. Note that one gas exchange chamber per treatment was left blank to serve as a quality control. The yellow dotted lines depict iteration of the CO_2 treatments between two growth chambers or two glasshouse bays.

4.2.2 Tree gas exchange chambers

4.2.2.1 Chamber system

We developed a tree gas-exchange system with 20 separate chambers divided in an above- and belowground compartment to continuously measure the exchange of H_2O and CO_2. Each of the 20 aboveground compartments were individually temperature-controlled (Fig. 4.2). The aboveground and belowground compartments were separated and gas tightness between the above- and belowground compartment was ensured after enclosing the tree stem. For details on the set-up and constant air supply of the tree gas exchange system see Notes S4.1.

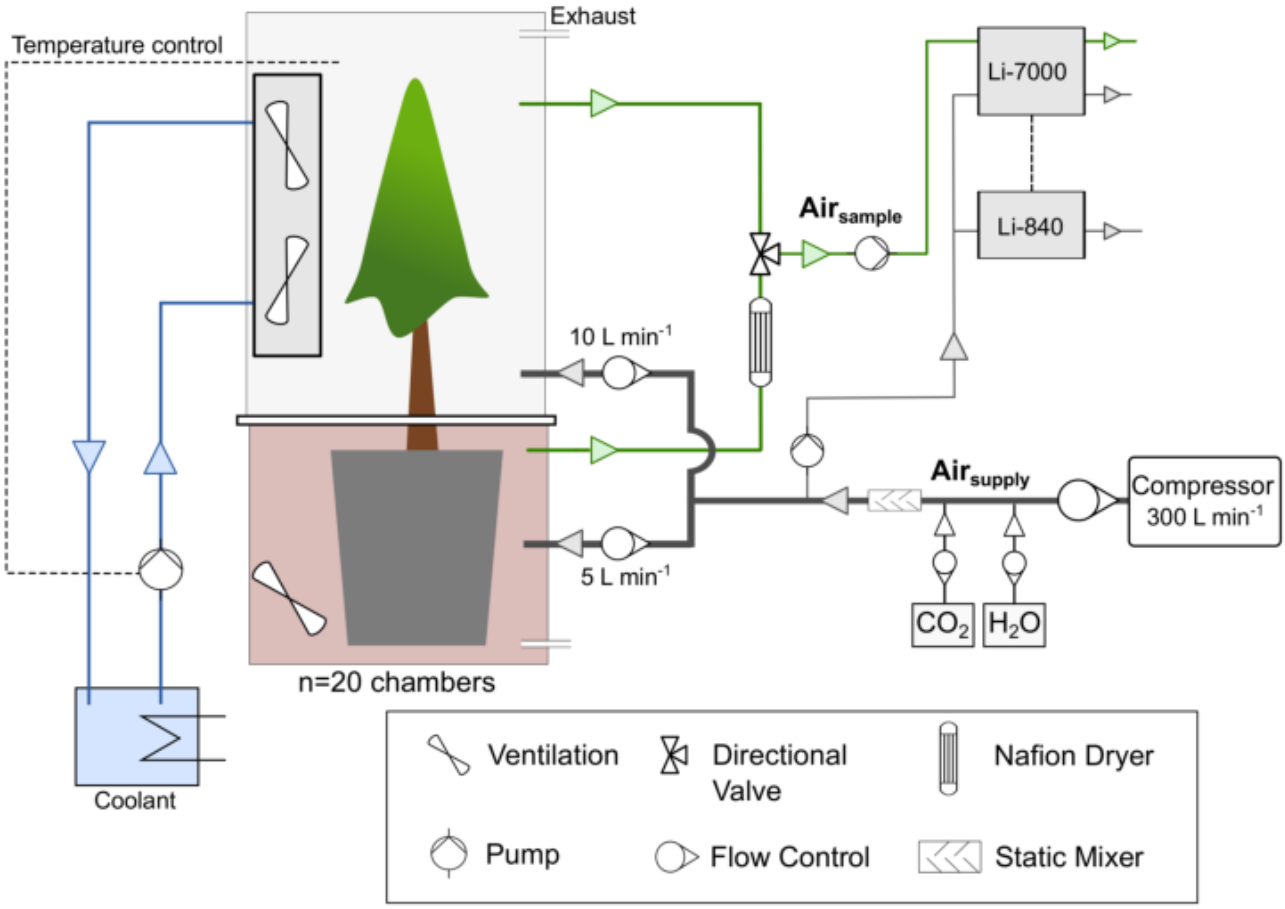

Figure 4.2 Whole tree gas exchange system separated in an above- and belowground compartment, shown exemplary for one chamber (*n*=20 in total). The arrows indicate the direction of flow. The air supply to the chambers is given in black (Air_{supply}) and the sample air is given in green color (Air_{sample}). The Li-840 measured absolute [CO_2] and [H_2O] connected to a Li-7000 to measure differences between Air_{supply} and Air_{sample}. Note that trees (*Pinus halepensis*) were potted in C-free substrate and the belowground CO_2 efflux is therefore interpreted as root respiration.

The chamber system was installed in the glasshouse and outside light was supplemented with plant growth lamps (T-agro 400 W, Philips, Hamburg, Germany). Canopy light conditions inside each chamber were measured automatically with a photodiode (G1118, Hamamatsu Photonics, Hamamatsu, Japan), which had been cross-calibrated with a high-precision PAR sensor (PQS 1, Kipp & Zonen, Delft, the Netherlands). Root-zone conditions were monitored with temperature sensors (TS 107, Campbell Scientific, Inc. USA) and moisture sensors (10HS, Decagon Devices, Pullman, USA). These data were logged half-hourly (CR1000, Campbell Scientific, Inc. USA).

4.2.2.2 Gas exchange measurements

The gas exchange chambers were constantly supplied with an air stream (Air_{supply}) of either 408 ppm or 896 ppm CO_2. Sample air (Air_{sample}) was drawn at a rate of 500 ml min^{-1} and each seedling

was measured once every 80 min using differential gas analysis. We used two gas analyzers, the analyzer measuring absolute [CO_2] and [H_2O] (LI-840, Li-cor, Lincoln, USA) was connected to a differential gas analyzer (Li-7000, Li-cor, Lincoln, USA) quantifying [CO_2] and [H_2O] differences between Air_{supply} and Air_{sample}. The data was logged at 10 s intervals. The gas analyzers have been calibrated following the manufacture's recommendation.

To eliminate any offset between Air_{supply} and Air_{sample} not caused by plant gas exchange, empty aboveground and belowground compartments (n=1 per treatment, four in total) containing C-free potting substrate only, were measured and offsets (on average +0.33±1.2 ppm CO_2 and 0.02±0.05 ppt H_2O in the aboveground compartments) removed accordingly. Differences in CO_2 were slightly larger in the belowground compartments (c. +2 ppm on average) and may refer to some microbial activity in the potting substrate.

Gas exchange fluxes of CO_2 and H_2O were calculated from the concentration differences between Air_{supply} and Air_{sample}. Plant water loss via transpiration (E) [mol s^{-1}] was calculated as

$$E = \frac{\dot{m}\,(W_{sample} - W_{supply})}{(1 - W_{sample})} \qquad (2)$$

where $\dot{m}$ is air mass flow [mol s^{-1}] into the chamber compartment, W_{sample} the water vapor concentration of the Air_{sample} [mol mol^{-1}], W_{supply} the water vapor concentration of the Air_{supply} [mol mol^{-1}].

From daytime E and water vapor concentrations we determined stomatal conductance (g_s) [mol s^{-1}] as follows

$$g_s = \frac{E\left(1000 - \frac{W_{leaf} + W_{sample}}{2}\right)}{W_{leaf} - W_{sample}} \qquad (3)$$

where W_{leaf} [mol mol^{-1}] is derived from the ratio of saturation vapor pressure (kPa) at a given air temperature (°C) and the atmospheric pressure. This approach, which neglects boundary layer conductance, is suitable under well-coupling as confirmed by negligible temperature differences between chamber and tree canopy (<1°C, see Table S4.1).

CO_2 gas exchange [mol s^{-1}], i.e. net photosynthesis (A_{Net}), shoot respiration (R_{shoot}) and root respiration (R_{root}), were calculated as

$$CO_2 \text{ flux} = -\dot{m}(C_{sample} - C_{supply}) - (E\ C_{sample}) \qquad (4)$$

with C_{sample} being the [CO_2] of the Air_{sample} [mol mol^{-1}], C_{supply} the [CO_2] of the Air_{supply} [mol mol^{-1}] and E to correct for dilution through transpiration [mol s^{-1}]. In the case of R_{root} (where sample air was dried) the water vapor dilution term became negative. The daily net C uptake per tree [mg C $tree^{-1}$ day^{-1}] was calculated based on daily-averaged A_{Net} and R as follows

$C_{Net} = A_{Net} - (R_{Shoot} + R_{Root})$ (5)

In order to determine changes in whole tree water-use-efficiency (WUE), apparent WUE_a was derived using the following equation:

$$WUE_a = \frac{A_{net}}{E_{day}} \quad (6)$$

Table 4.1: Needle, shoot, root, total tree biomass, needle area and total soluble C (calculated as carbon equivalents of all measured metabolites) for 1.5-year-old *Pinus halepensis* seedlings are given as treatment averages ±1SE (n = 16 per treatment) at the end of the experiment (post-stress). Significant differences between treatments were derived from ANOVA followed by TukeyHSD and are given in upper-case letters (P<0.05).

Treatment	Needle	Root	Wood	Total
		[g DW]		
a[CO2]W	33.4 ± 1.0 A	51.1 ± 1.4 B	15.4 ± 0.6 A	99.9 ± 2.1 A
e[CO2]W	47.6 ± 1.5 B	66.7 ± 1.9 D	24.5 ± 1.2 B	138.8 ± 2.1 B
a[CO2]D	33.3 ± 1.5 A	43.6 ± 1.2 A	15.8 ± 0.9 A	92.7 ± 2.9 A
e[CO2]D	47.5 ± 1.4 B	60.0 ± 2.2 C	24.2 ± 1.4 B	131.6 ± 4.5 B

Treatment	Needle Area	Soluble C
	[cm^2]	[µmol gDW^{-1}]
a[CO2]W	1296 ± 38 A	1090 ± 209 A
e[CO2]W	1925.3 ± 84 B	847± 79 A
a[CO2]D	1414.6 ± 60 A	2623 ± 454 B
e[CO2]D	2052.5 ± 65 B	2578 ± 349 B

To allow comparison of tissue gas exchange activity between treatments and because root surface area was not available, we calculated gas exchange rates per shoot (i.e., needle and woody tissues) or root dry weight (DW), if not stated otherwise. The percentage share of soluble carbon from tissue biomass was small (<4%, Table S4.2), hence we refrained from taking normalization to soluble C into account. Tree biomass was determined at the end of the experiment and separated into needles, roots and woody tissues before drying at 60°C for 48 h (Table 4.1).

4.2.3 Heat stress experiment

Responses of shoot and root gas exchange with increasing temperature and evaporative demand were assessed continuously using the tree gas exchange system as described in section 2.2 and Notes S4.1.

In brief, randomly selected seedlings were placed into separate gas exchange chambers (*n*=4 per treatment, Fig. 4.1). The chambers containing one tree each were positioned next to each other in a randomized block design. The heat stress experiment was repeated in order to double the numbers of replicates per treatment. Each heat experiment lasted 10 d and after the initial 2 d at 25°C (20°C night-time), temperature was increased stepwise every second day to the following day-time temperatures: 25°C, 35°C, 38°C and 40°C (Fig. 4.3a). We refrained from temperatures above 40°C as tree mortality has been found to strongly increase in Aleppo pine seedlings above this threshold particular in combination with drought (Birami et al. 2018). As during a typical heatwave in the Yatir forest (Tatarinov et al. 2015), vapor pressure deficit (VPD) increased alongside increasing temperature, and this increase was slightly larger in the drought-treated saplings due to low *E* (Fig. 4.3c). Photosynthetic active radiation (PAR) was kept relatively constant between gas exchange chambers and daily-averages were 456±140 µmol $m^{-2}s^{-1}$. To overcome some of the light limitations (saturating PAR for photosynthesis was at 1200 µmol $m^{-2}s^{-1}$) day-time length was set to 16 h, well above the average summer day length in Yatir forest. Irrigation was controlled to maintain the RSWC of well-watered trees at c. 50% and of drought-trees at c. 10% (Fig. 4.3). The irrigation amount did not differ between the [CO_2] treatments (a[CO_2]W and e[CO_2]W: 300 ml d^{-1}; a[CO_2]D and e[CO_2]D: 50 ml d^{-1}) and drought-treated seedlings reached a midday needle water potential (Ψ_{midday}) indicating stomatal closure (Table 4.2, Fig. S4.3).

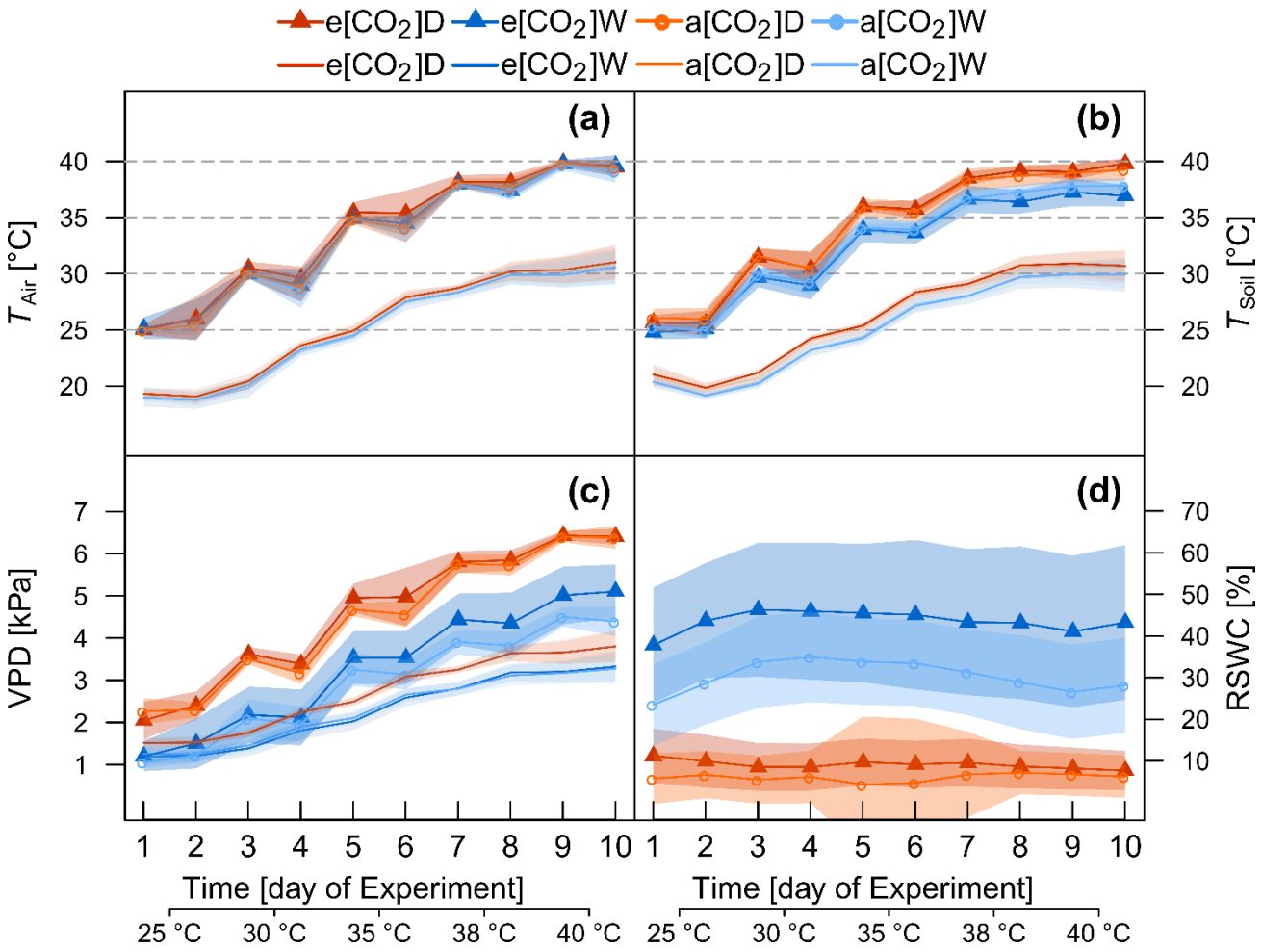

Figure 4.3 Environmental drivers during the heat stress experiment (*Pinus halepensis*) given per treatment. Air temperature (T_{Air}, a), soil temperature (T_{Soil}, b), vapor pressure deficit (VPD, c) and relative substrate water content (RSWC, d) are shown. Data are treatment-averages during daytime (lines including symbols) or nighttime (lines) and the shaded areas are ±1 SD (n=8). Daytime is defined as PAR>100 and nighttime as PAR = 0. Note the temperature difference between day- and nighttime was not constant due to technical limitations but was kept within 7 to 10 °C.

4.2.4 Sample preparation

We sampled needle tissue for analysis of primary metabolites at the last day of the following temperature levels: 25, 35, 38 and 40°C. To avoid disturbance of belowground fluxes, root biomass was only sampled at 25°C (additional set of saplings, not used for the experiments) and at 40°C. Sampling took place in the afternoon between 15–16 h and samples were immediately frozen in liquid nitrogen, stored at -80°C until ground to fine powder in liquid nitrogen before freeze-drying for 72 hours with cooling aggregate at -80°C and sample temperature at -30°C (Alpha 2-4 LSC, Martin Christ Gefriertrocknungsanlagen GmbH, Osterode am Harz, Germany).

The freeze-dried samples were stored in the dark in closed vials at room temperature and analyses of primary metabolites were completed within 2 months (Fürtauer et al. 2019). For details on analysis of primary metabolites via gas chromatography coupled to time-of-flight mass spectrometry (Fürtauer et al. 2016; Weiszmann et al. 2018) and protein content via Bradford assay ((Fürtauer et al. 2018) please see the Notes S4.2.

4.2.5 Statistical data analysis

Data processing, analysis and statistics were carried out using R version 3.5.2 (R Core Team 2018). Gas exchange measurements of each chamber were carefully inspected prior to analyses and day- or nighttime fluxes outside 1.5 times the interquartile range (above the upper quartile and below the lower quartile) per temperature were considered outliers. This removed on average 3.8% of CO_2 and 5.7% of H_2O gas exchange data.

Primary metabolites were scaled to standard deviation before treatment effects in needles and roots at 25°C were visualized by hierarchical clustering (R packages: 'ggplot2' and 'cluster' (Maechler et al. 2018; Wickham 2016)). Further, the overall changes in the primary metabolome depending on tissue, treatment and temperature were analyzed after centering of the scaled data via principal components analysis (PCA).

Treatment effects on biomass, gas exchange rates and metabolites at specific temperature levels were tested using ANOVA and differences between treatments were revealed by *post-hoc* analysis (TukeyHSD). Treatment and Temperature dependencies of gas exchange fluxes and metabolites (fixed effects) were checked by implementing a linear mixed effect model ('lmerTest', (Kuznetsova et al. 2017). In order to account for temporal autocorrelation, tree was accounted as a random factor. Using the reduced sample size AIC criteria (Akaike 1974; Giraud 2015) the most parsimonious model was selected with or without tree as random factor, and the treatment and temperature effect included with and without interaction. We report a pseudo-R^2 (pR^2) for the selected model ('MuMln', (Barton 2019). Homoscedasticity and normality of residuals were checked and if applicable, $\log_e$-transformation applied.

To analyze differences in the temperature relationship of A_{Net} we applied an exponential decay function ($y=e^{-bx}$), in case of respiration (R), we fitted a second-order polynomial function following (Gauthier et al. 2014).

$$R = e^{(a+bT+cT^2)} \qquad (7)$$

The uncertainty of all fitted functions are given as 95% confidence intervals derived from first-order Taylor expansion using the 'propagate' package (Spiess 2018).

4.3 Results

4.3.1 Tree biomass

Differences in above- and belowground biomass were distinct after growing *P. halepensis* seedlings for more than one year under a[CO_2] of 421 ppm or e[CO_2] of 867 ppm (Table 4.1). A doubling of atmospheric [CO_2] increased total tree biomass by 35%. This increase was particularly pronounced in woody tissues (stem and twigs, +47%) and to a lesser extend in needles (+26%). The one-month drought period had no obvious effect on aboveground biomass, but reduced belowground biomass under ambient (-15%) and e[CO_2] (-11%). The amount of non-structural carbohydrates in total biomass varied between 1.5–3.5% and was slightly larger under drought with no clear trend of [CO_2] (Table S4.2).

4.3.2 Tree gas exchange

Impacts of [CO_2] and drought

Elevated [CO_2] affected gas exchange rates expressed per tissue DW (Table 4.2, see also Fig. 4.4). Under well-watered conditions and at ambient temperature (25°C), R was lower in e[CO_2]W compared to a[CO_2]W trees. In addition, e[CO_2] reduced g_s and E, which resulted in an increase of WUE (Table 4.2), while A_{Net} was largely unaffected (Table 4.2). Under drought, the effect of [CO_2] on WUE was pronounced with C_i being increased near stomatal closure allowing for a higher A_{Net} (Table 4.2). The positive effect of e[CO_2] on biomass, C_i and WUE was also reflected in daily net C uptake (i.e. tree C balance) but the degree did depend on water supply. While in the well-watered trees net C uptake tended to double under e[CO_2], drought trees were able to maintain a small C sink if grown under e[CO_2] (Table 4.2).

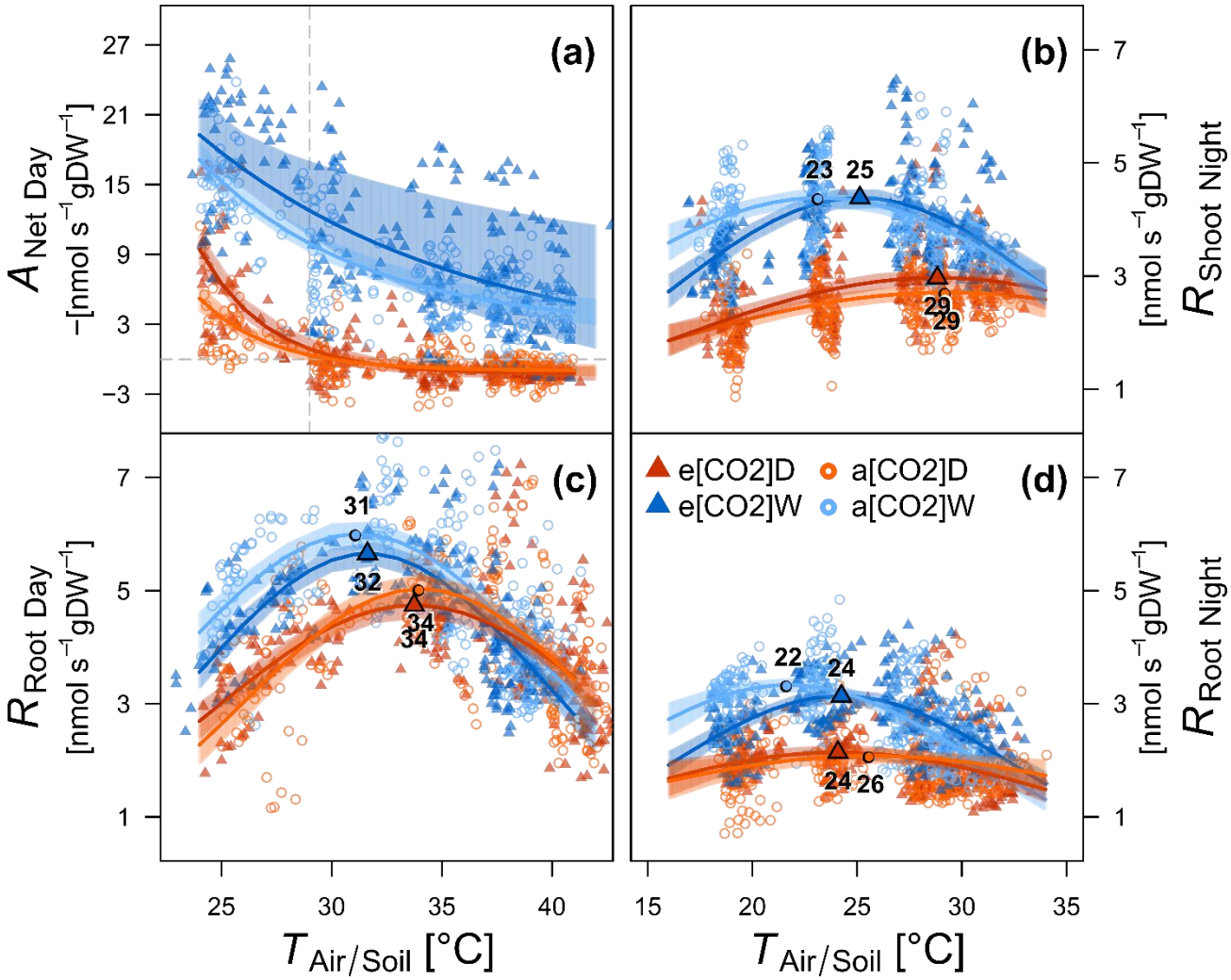

Figure 4.4 Gas exchange dynamics with increasing heat stress under ambient or elevated [CO_2] in drought or well-watered *Pinus halepensis* trees. Shown are hourly-averages per tree and treatment of net photosynthesis (A_{Net}; a), shoot dark respiration R_{Shoot}; b) and day- (10 h to 18 h) or nighttime (23 h to 4 h) root respiration (R_{Root}; c–d). The temperature response of A_{Net} was fitted with an exponential decay function and respiration data fitted to a second-order polynomial function (see Eq. 6). The temperature at the respiratory peak is highlighted. The shaded areas depict the 95% confidence intervals of the fitted functions. Note gas exchange data is expressed per DW shoot or root tissue.

Table 4.2: Gas exchange rates at 25°C expressed per tissue dry weight and tree net C uptake for 1.5-year-old *Pinus halepensis* seedlings are given as treatment averages ±1SE (*n*= 8 per treatment). Tree net C uptake is the sum of photosynthesis (A_{Net}) minus respiration (R). Midday needle water potential ψ_{midday} is given and was measured at the time of tissue sampling for metabolite analysis. Significant differences between treatments were derived from ANOVA followed by TukeyHSD and are given in upper-case letters (*P*<0.05).

Treatment	*E*	g_s	A_{Net}	R_{dark}
	[µmol $s^{-1}g^{-1}$]	[mmol $s^{-1}g^{-1}$]	[nmol $s^{-1}g^{-1}$]	[nmol $s^{-1}g^{-1}$]
a[CO2]W	3.29 ± 0.15 B	0.38±0.04 B	15.3±1.3 B	7.4±0.3 B
e[CO2]W	2.03 ± 0.28 D	0.23±0.07 B	16.5±2.2 B	6±0.2 C
a[CO2]D	0.66 ± 0.17 A	0.08±0.01 A	3.4±1.1 A	3.9±0.4 A
e[CO2]D	0.67 ± 0.16 A	0.04±0.02 A	6.7±1.2 C	4.2±0.3 A

Treatment	C_i	WUE	net C uptake	Needle ψ_{midday}
	[µmol mol^{-1}]	[µmol $mmol^{-1}$]	[mg d^{-1} $tree^{-1}$]	[MPa]
a[CO2]W	263 ± 3 A	4 ± 0.3 A	165.1 ± 29.8 AC	-1.49 ± 0.07 A
e[CO2]W	612 ± 5 C	7.2 ± 0.5 B	379.2 ± 68.8 C	-1.15 ± 0.04 A
a[CO2]D	287 ± 11 A	3.4 ± 0.7 A	-73.2 ± 18.3 B	-2.68 ± 0.3 B
e[CO2]D	482 ± 14 B	9.4 ± 1.3 B	23.2 ± 38.7 AB	-1.83 ± 0.2 A

Heat stress responses altered by [CO_2] and drought

Increasing temperatures affected VPD accordingly (Fig. 4.3c) and we found pronounced responses in gas exchange of the well-watered seedlings. A_{Net} declined with temperature irrespective of the [CO_2] (Fig. 4.4a). This was contrasted by initially increasing C loss via R_{Root} and R_{Shoot} until a respiratory peak has been reached and respiration rates began to decline (Fig. 4.4b-c). This respiratory peak was reached 2–4°C later and at lower rates in the drought-treated saplings. The trees' net C uptake reacted accordingly with a sharp initial decrease, which then leveled-off at increasing heat stress (30–35°C; Fig. 4.5). The effects of e[CO_2] were not distinct

but data showed a tendency of whole-tree net C losses to be observed at slightly higher temperatures under both well-watered and drought conditions.

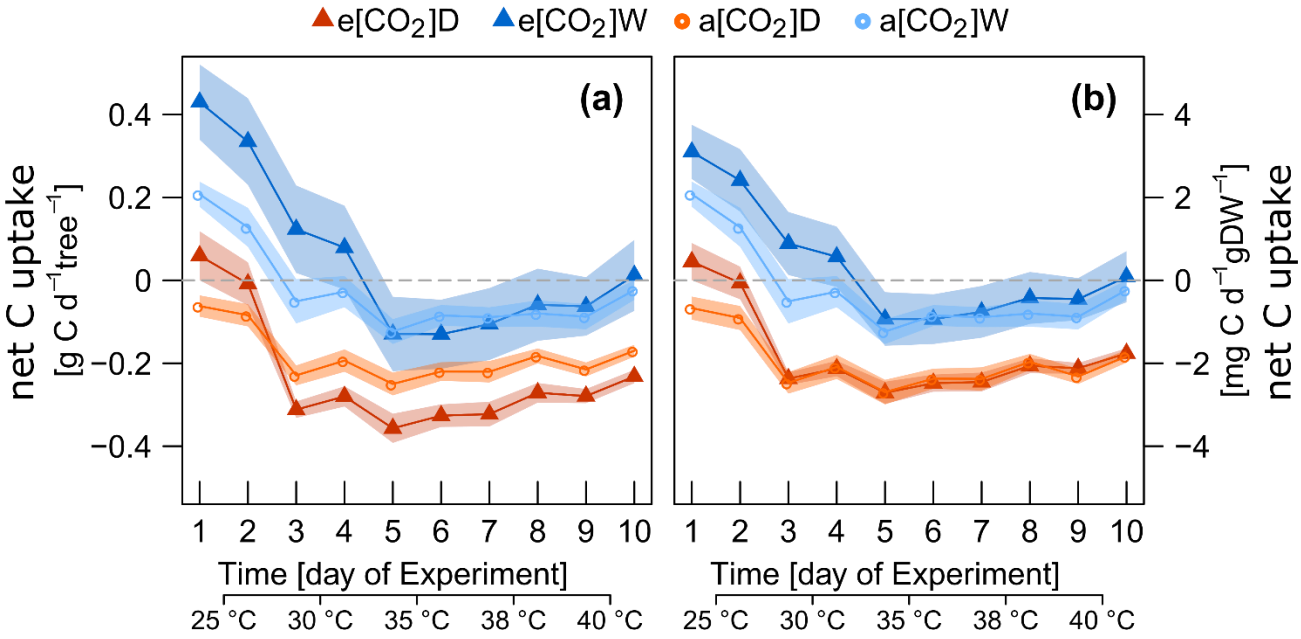

Figure 4.5 Temperature responses of the whole tree carbon balance (i.e., net C uptake) in *Pinus halepensis* seedlings per tree (a) and DW biomass (b). Shown are daily-averages per treatment (a[CO_2]W, e[CO_2]W, a[CO_2]D, e[CO_2]D). Whole tree net C uptake was derived from hourly photosynthesis and respiration data per seedling (Eq. 5). Note that positive numbers reflect a daily net C gain while negative numbers are a net C loss. The shaded areas are ±1 SE (n=8).

A pronounced interaction of e[CO_2] with heat stress became clear in a constantly lower *E* (lme: pR^2=0.89; TukeyHSD, P<0.05) but higher WUE (lme: pR^2=0.81; TukeyHSD, P<0.05) with increasing temperatures under well-watered conditions. This was due to a tight stomatal control in the e[CO_2]W trees (Fig. 4.6a-b, Table S4.3). The picture changed dramatically when heat stress was combined with drought and the water-saving effect of e[CO_2] quickly subsided at temperatures >30°C coinciding with stomatal closure. Interestingly, the C_i:C_a ratio seemed largely unaffected by the [CO_2] and remained almost constant throughout the experiment (Fig. 4.6d, excluding C_i>C_a).

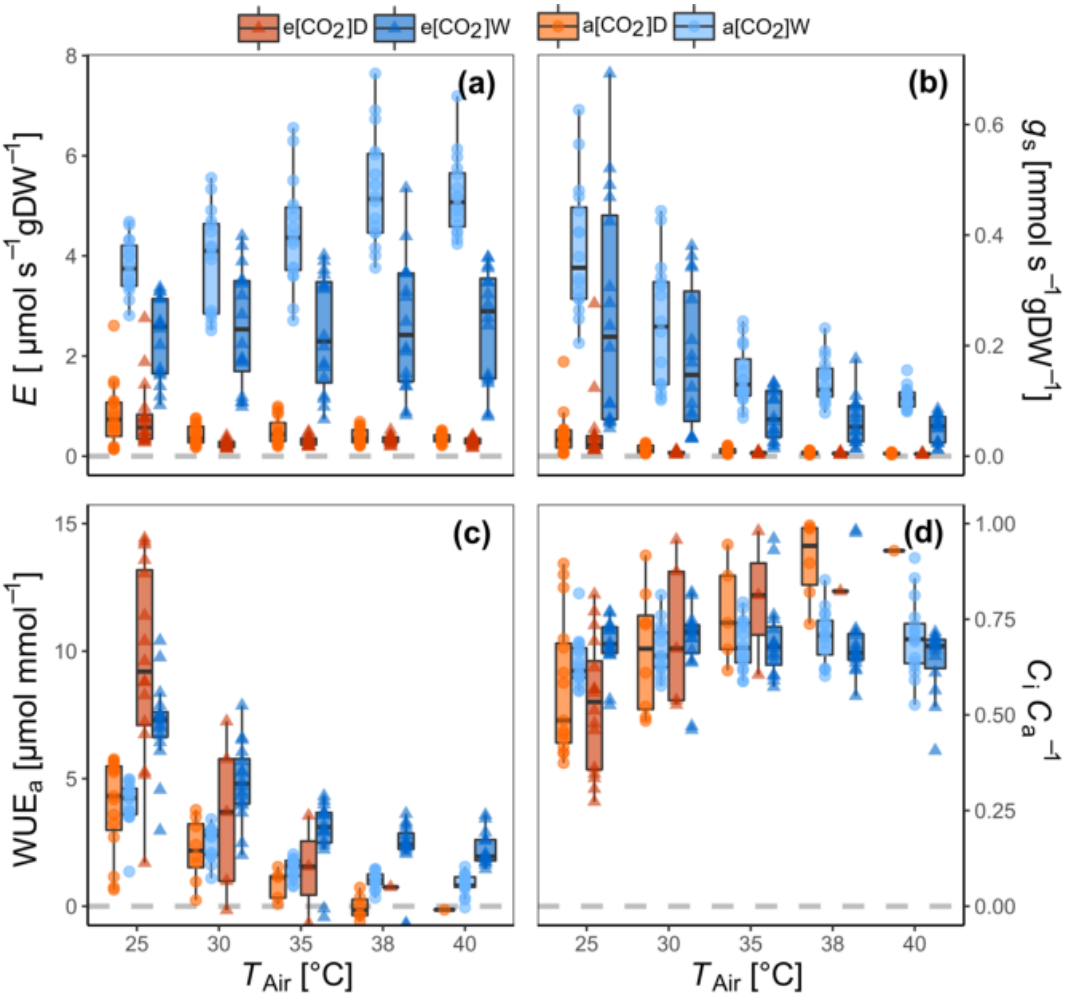

Figure 4.6 Treatment responses of transpiration (*E*; a), stomatal conductance (g_s; b), apparent water use efficiency (WUE_a; c) and the ratio of intercellular to ambient [CO_2] ($C_iC_a^{-1}$; d) with increasing temperature. Data points are daily-averaged values per temperature level and tree (between 10 am and 4 pm). WUE_a and $C_iC_a^{-1}$ are given for $C_i \leq C_a$. The relationships of hourly WUE and g_s with temperature are given in Fig S4.4.

4.3.3 Primary metabolites

Impacts of [CO_2] and drought

The primary metabolism in roots and needles was clearly distinct irrespective of treatment (Fig. 4.7; metabolite profile at 25°C). We found inositol pathway intermediates (e.g., myo-inositol, pinitol), poly-amines and aromatic amino acids to dominate in needle tissues, while monosaccharides, TCA intermediates (e.g. malate) and amino acids of the glutamate and aspartate family were higher concentrated in roots.

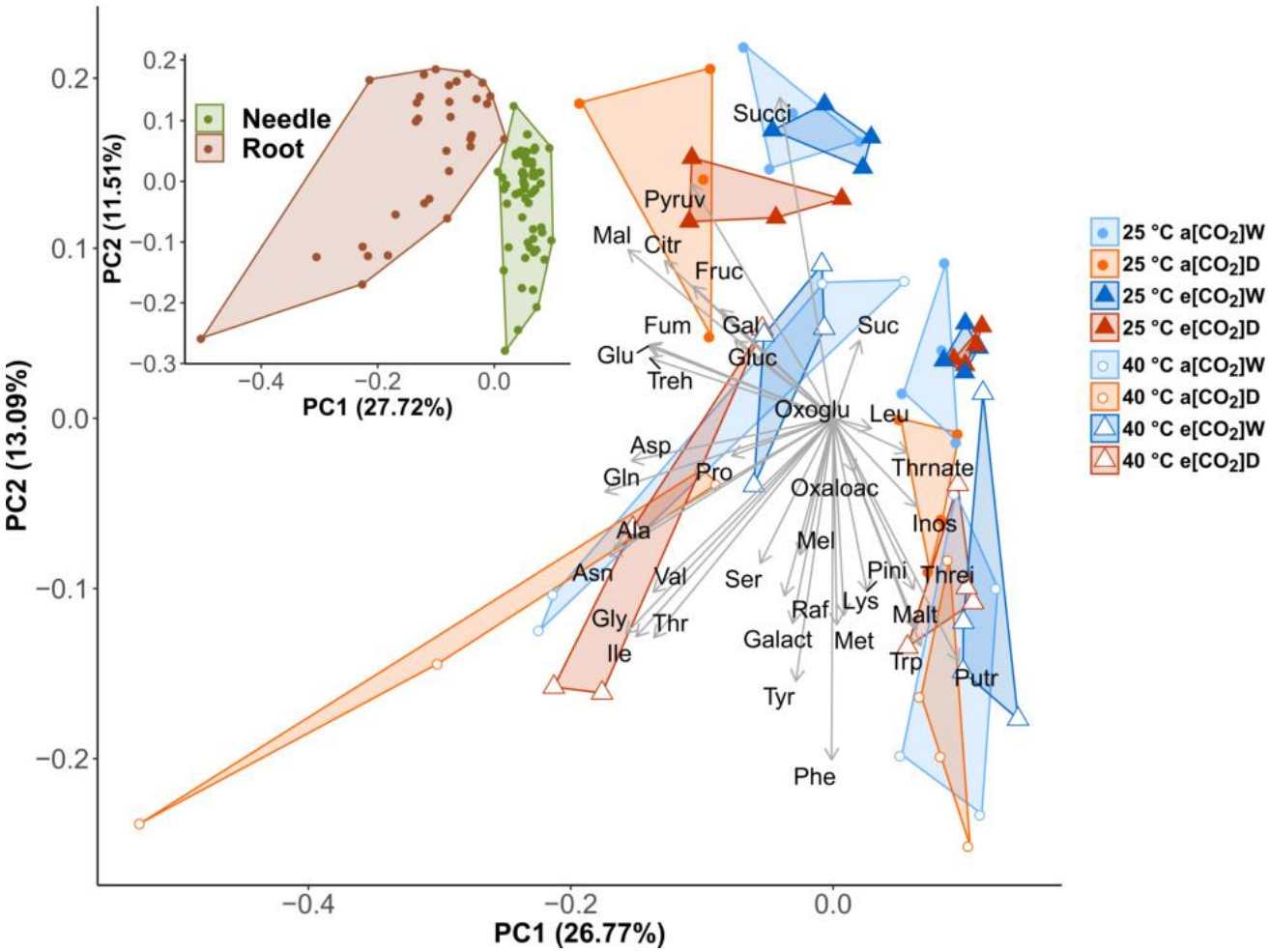

Figure 4.7 Principle component analysis (PCA) of all quantified 38 primary metabolites in shoot and root tissues at 25°C (filled symbols) and at 40°C (open symbols) per treatment. Polygons indicate treatment clustering. The smaller insert visualizes overall changes in root (brown symbols) and needle (green symbols) tissues irrespective of treatment and temperature. Note that all metabolite data was scaled to standard deviation (see Methods). Metabolite abbreviations are: Glucose (Gluc), Fructose (Fruc), Galactose (Gal), Sucrose (Suc), Trehalose (Treh), Maltose (Malt), Melibiose (Mel), Rafinose (Raf), Myo-Inositol (Inos), Pinitol (Pini), Galactinol (Galact), Threitol (Threi), 2-Oxoglutarate (Oxoglu), Oxaloacetate (Oxaloac), Citrate (Citr), Malate (Mal), Succinate (Succi), Fumarate (Fum), Pyruvate (Pyruv), Threonate (Thrnate), Glutamate (Glu), Glutamine (Gln), Aspartate (Asp), Asparagine (Asn), Glycine (Gly), Alanine (Ala), Serine (Ser), Isoleucine (Ile), Leucine (Leu), Valine (Val), Threonine (Thr), Proline (Pro), Lysine (Lys), Methionine (Met), Tyrosine (Tyr), Phenylalanine (Phe), Tryptophane (Trp), Putrescine (Putr).

In addition, we found the metabolic responses to drought larger than the [CO_2] effect as reflected in the clustering (Fig. S4.5). For instance, monosaccharides (lme: pR^2=0.74) and sucrose (lme: pR^2=0.43) were clearly enhanced under drought, accompanied by increased levels of proline in both needles (lme: pR^2=0.47, TukeyHSD, *P*<0.05) and roots (lme: pR^2=0.69, TukeyHSD, *P*<0.05). Further, increased levels of branched-chain amino acids and amino acids of the glutamate and aspartate families were found in drought treatments (e.g. glutamine, needle lme: pR^2=0.59, root lme: pR^2=0.77, TukeyHSD, *P*<0.05). A distinct response of the primary metabolome to e[CO_2] under drought was remarkably absent in roots, while e[CO_2] showed a tendency to mitigate metabolic responses to drought in needle tissues.

Heat stress responses affected by [CO_2] and drought

The temperature increase from 25°C to 40°C affected the primary metabolome in needles and roots differently (Fig. 4.7). A general trend in needle tissues was the decrease of carboxylic acids (lme: pR^2=0.47) and an increase of sugar alcohols (e.g., pinitol, lme: pR^2=0.65 and galactinol, lme: pR^2=0.59), while myo-inositol decreased (lme: pR^2=0.25, TukeyHSD, *P*<0.05). Secondary metabolite precursors such as putrescine (lme: pR^2=0.37,), tyrosine and phenylalanine also increased with temperature (lme: pR^2=0.6-0.84) relatively uniform among treatments. Responses to increasing temperatures became most obvious in the root tissues (Fig. 4.7), where we found amino acids (glutamine, asparagine, alanine, serine, threonine, valine and isoleucine) to accumulate with rising temperatures (lme: pR^2=0.6-0.8). This increase was marked under a[CO_2] in both drought and well-watered trees along with a decline in root protein (lme, pR^2 = 0.38, Fig. 4.8 t). In contrast, needle protein increased above 35°C in all treatments (Fig. 4.8 t) particular under e[CO_2]D (lme: pR^2= 0.23, TukeyHSD, *P*<0.05). In addition, treatment-specific responses to temperature were found in monosaccharides (lme: pR^2=0.74) where drought resulted in an accumulation of monosaccharides in needles (TukeyHSD, *P*<0.05; Fig. 4.8 a-b). In the well-watered treatments, we found monosaccharides to decline in roots (Fig. 4.8 c–d, lme: pR^2= 0.70, TukeyHSD, *P*<0.05). This decline tended to be larger in trees grown under a[CO_2].

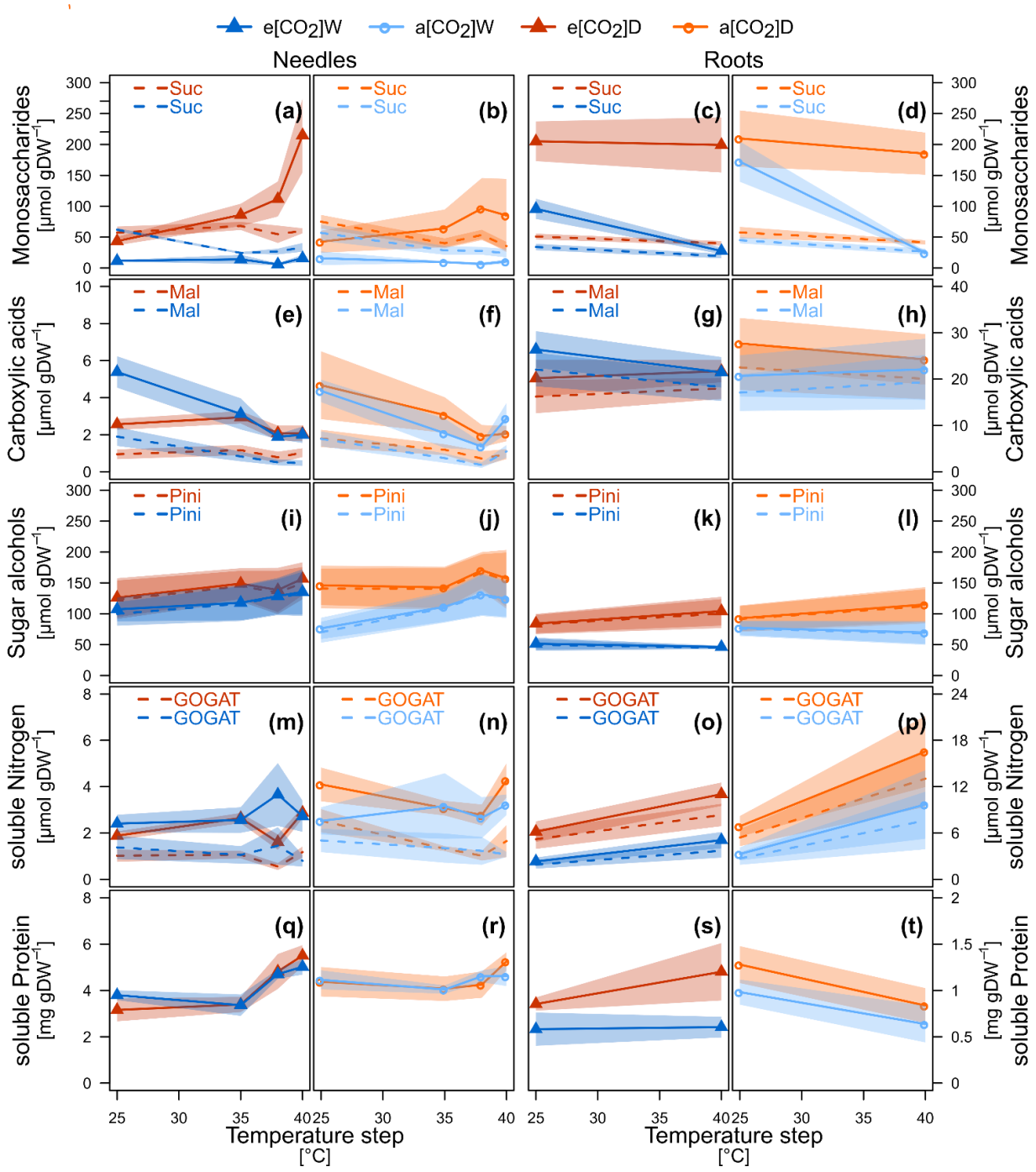

Figure 4.8 Heat stress responses of selected primary metabolites and protein content in leaves and roots. Shown are treatment-averages of sucrose and the sum of monosaccharides (glucose, fructose and galactose; a–d), malate and the sum of carboxylic acids (citrate, malate, fumarate, succinate, oxoglutarate, oxaloacetate; d–g), pinitol and the sum of sugar alcohols (myo-inositol, pinitol, threitol, galactinol; h–k,), glutamate synthase amino acids (GOGAT) and the sum of all measured amino acids including putrescine (l–o) and protein content (p–t). The shaded areas are ±1 SE (n=8).

4.4 Discussion

4.4.1 Tree C balance under e[CO_2]

Aleppo pine trees, grown for 1.5 years under e[CO_2] exhibited a larger biomass than trees grown under a[CO_2]. We cannot exclude limiting effects on growth due to the size of the pots, which were lower than what has been previously recommended (Poorter et al. 2012). Nevertheless, we found clear differences in root biomass, and e[CO_2] to stimulate root growth in agreement with many other studies (for a meta-analysis of FACE studies see (Nie et al. 2013). The observed overall larger biomass of e[CO_2] trees in our study tended to result in a larger net C gain (i.e., net photosynthesis minus respiration; on average +120% per tree). To exclude the CO_2-induced biomass stimulation on these results, we expressed gas exchange rates per tissue DW. Based thereon we did not find e[CO_2] to increase C-fixation rates, as A_{Net} was quite similar between both [CO_2] treatments (Table 4.2) and carboxylation efficiency was unchanged (data not shown). Hence the stimulation of the seedlings' net C gain in the e[CO_2]W treatment was not driven by increased photosynthesis but due to an apparent reduction of R_{Shoot} and R_{Root} under e[CO_2] (-23% on average). It is noteworthy that under drought conditions [CO_2] did not affected respiration rates.

The responses of R to e[CO_2] can be highly variable (Dusenge et al. 2019). Some studies find R to be insensitive to [CO_2] while others find it to either increase or decrease (Ainsworth and Long 2005; Aspinwall et al. 2017; Drake et al. 1999; Dusenge et al. 2019; Gauthier et al. 2014; Gonzalez-Meler et al. 2004; Xu et al. 2015). Our study adds new evidence that e[CO_2] reduces R_{Shoot} or R_{Root} per tissue DW (day- and nighttime) during non-stressful conditions. Correspondingly, we also did not find an upregulation of respiratory substrates such as sugars in response to e[CO_2]. A likely explanation for reduced dark respiration in response to rising [CO_2] may involve lower protein turnover due to N dilution from increases in non-structural carbohydrates or other organic compounds (Xu et al. 2015), yet in our study, the C : N ratio at 25°C derived from the sum of primary metabolites did not differ (Table S4.2). However, we found evidence that e[CO_2] reduced protein content in needle and root tissues at control temperature. Indeed, the CO_2-effect (at 25°C) disappeared when expressing R_{Shoot} per protein content. Because protein turnover is highly energy demanding, a lower protein content of plants under e[CO_2] could reduce the respiratory costs of tissue maintenance (Drake et al. 1999), and may contribute to increased net C uptake under well-watered conditions.

4.4.2 Temperature acclimation of respiration affects tree C balance and is modulated by drought and [CO_2]

The response of *R* to slowly increasing temperatures and VPD did not follow temperature kinetics of a single enzyme, which is exponential in a physiological temperature range (Bond-Lamberty et al. 2004; Michaletz 2018). In contrast, we found *R* to acclimate to several days of heat stress. Moreover, we found that day-time *R* at 40°C was close to the initial rates at 25°C. This is in stark contrast to studies conducting fast temperature curves, which typically find respiratory peaks to occur at much higher temperatures (e.g. (Gauthier et al. 2014). However, an acclimation of leaf *R* to elevated growth temperatures has been reported in many instances (Drake et al. 2019a; Reich et al. 2016) and R_{Shoot} has been shown to decline during consecutive heatwaves (Birami et al. 2018). Likely explanations for the early down-regulation of R_{Shoot} and R_{Root} which we have found in response to heat stress are: i) reduced respiratory demand due to down-regulation of growth and maintenance *R*, ii) adenylate restriction caused by ATP turnover decline and/or iii) reduced C availability (O'Leary et al. 2019). While our study cannot support *R* to be limited by reduced C availability as for instance carboxylic acids did not decrease in root tissues, we can clearly show that Aleppo pine trees are able to regulate respiratory losses to maintain a new equilibrium between C loss and uptake (Fig. 4.4). This was reflected in the whole-tree C balance stabilizing at an almost constant rate between 35°C and 40°C with larger net C loss under drought conditions. An homeostatic linkage between photosynthesis and respiration to temperature has been suggested by a recent synthesis on a large number of studies (Dusenge et al. 2019).

The impacts of e[CO_2] on *R* vanished with increasing heat stress in the well-watered trees and after the respiratory peaks were reached, on average 1–2°C later under e[CO_2], *R* did not differ between the [CO_2] treatments anymore. However, the effect of drought delaying the timing of the respiratory peak was more pronounced. *R* was initially lower under drought until maximum rates were reached about 2–6°C later than in the well-watered trees. The subsequent decline in *R* under drought was less pronounced so that *R* of the drought and well-watered treatments converged. A similar delay of the respiratory peak in response to drought (although at much higher temperatures) has been found during rapid-warming of Eucalypt leaves (Gauthier et al. 2014). In accordance to (Gauthier et al. 2014) we found a declining ratio of A_{Net} to *R* but no indications for C depletion. In summary, this indicated that treatment differences (e.g., drought or [CO_2]) in *R* were distinct at 25°C, but quickly subsided after maximum temperatures were surpassed. The underlying reasons are not clear, but strikingly the trees maintained a new equilibrium between A_{Net} and *R*, and whole-tree net C loss in the well-watered treatments was <0.1% DW d^{-1} and in the drought treatments <0.2% DW d^{-1}, independent of the [CO_2].

4.3 Responses of WUE to elevated [CO_2], heat and drought stress

The apparent lack of a [CO_2] effect on net C uptake under stress was counterbalanced by a very consistent water saving strategy, largely maintained throughout all temperature steps, (Table S3). In the well-watered, e[CO_2] trees, *E* remained constant with increasing VPD and temperature. This was reflected in an improved WUE under e[CO_2], which increased proportional with atmospheric [CO_2] under well-watered conditions. Moreover, this increase in WUE was not only maintained but apparently increased with rising temperatures (25°C: +77%, 30°C: 94%, 35°C: 95%, 40°C: 133% on average) and therefore agrees with our second hypothesis. Several strategies are reported to control WUE in plants (Lavergne et al. 2019) and under rising C_a, three scenarios are typically proposed in which leaves maintain either: constant C_i, constant C_a–C_i, or constant C_i : C_a ((Saurer et al. 2004). A variety of studies have reported constant C_i : C_a as a response to e[CO_2] during drought or other abiotic stresses (Ainsworth and Long 2005; Gimeno et al. 2016; Kauwe et al. 2013). This agrees with our study, where C_i : C_a remained almost constant over the entire experimental temperature gradient in the well-watered seedlings. Constant C_i : C_a could indicate a feedback control on g_s from photosynthetic activity, for instance via temperature-induced downregulation of Rubisco (Crafts-Brandner and Salvucci 2000). We observed similar C_i : C_a patterns in the drought treatments, with a tendency for a larger increase in WUE at 25°C. This water saving effect naturally disappeared when stomata closed almost fully at 30°C. Thus, hot drought quickly diminishes any water saving effect of e[CO_2].

4.4 Plant stress responses affected by elevated [CO_2]

Whole tree gas exchange of H_2O and CO_2 revealed some interacting [CO_2] responses during drought and heat stress, most pronouncedly reflected in increased WUE. However, we found the benefits of e[CO_2] to vanish under more extreme heat or combined heat-drought stress. Recently it has been shown that extreme drought can counterbalance any beneficial [CO_2] effects on C dynamics and water relations (Duan et al. 2013; Duan et al. 2015). In addition, more detrimental effects and larger leaf senescence in trees grown under e[CO_2] compared to a[CO_2] have been found during a hot drought event occurring naturally (Warren et al. 2011). The underlying mechanisms are not yet understood, but excessive leaf-temperature stress under e[CO_2] due to lower g_s (and lower *E*) are thought to be a possible explanation, increasing thermal stress (Bassow et al. 1994; Warren et al. 2011). As the well-mixed conditions inside the tree chambers in our study omitted large differences in surface needle temperatures (Table S4.1), we can excluded additional heating of e[CO_2] trees affecting metabolic stress responses.

Underlying mechanisms for the rather modest effect of [CO_2] on tree stress performance might be reflected in metabolic adjustments in needles and roots. Generally, we found the primary metabolome of roots and shoots to differ, which can be explained by the presence or absence of chemical pathways in specialized tissues like plastids (Li et al. 2016). Elevated [CO_2] tended to mitigate the drought response at 25°C in needle tissues, which fits well to overall water saving strategy (e.g. WUE, see Table 4.2). However, the response to heat stress was distinct but not altered by e[CO_2]. For instance, we found myo-inositol to decline as typical precursor of osmotic active substances like pinitol and galactinol (Nishizawa et al. 2008).

Together with proline these metabolites contribute to thermostability of membranes and proteins (Nishizawa et al. 2008; Zinta et al. 2018). In contrast to needles, root metabolites showed distinct responses to stress, as seen in highly elevated levels of soluble sugars and amino acid increase with heat and drought stress. The apparently larger drought sensitivity of roots was also reflected by a lower root biomass but higher overall metabolite C content compared to the well-watered trees (Table 4.1), indicating that root growth halted during drought and available C was mainly invested into osmoregulation. Possible explanations may involve reduced C transport from source to sink tissues (Brauner et al. 2018; Ruehr et al. 2009) and a larger hydraulic vulnerability of roots (Johnson et al. 2016).

We found some indications for e[CO_2] to potentially mitigate stress-induced metabolic responses, in agreement with others (Zinta et al. 2014; Zinta et al. 2018). In particular, e[CO_2] seemed to lessen the heat-induced changes in monosaccharides and amino acids in roots. Similarly, (Zinta et al. 2018) reported a dampened response of sugars and amino acids to combined heat-drought stress in *Arabidopsis thaliana* grown under e[CO_2]. Hence, the larger increase in amino acid concentrations in roots from trees grown under a[CO_2] in our study could be triggered by protein degradation, which was suggested by a decline in protein content while asparagine accumulated (Brouquisse et al. 1992). Heat stress has been found to decrease root protein content, as protein degradation rates at high temperatures typically exceed protein synthesis (Huang et al. 2012). A larger protein stability is assumed to improve the thermotolerance of plants but may come at a cost of increased maintenance. Interestingly, we found a larger stability of root protein content under e[CO_2] with heat stress, but the average root protein content as well as R_{root} at 40°C did not differ between a[CO_2]W and e[CO_2]W. This may indicate an active downregulation of protein turnover in a[CO_2] trees to reduce the C cost of maintenance respiration. Counterintuitively, we found protein content in needle tissues to increase at temperatures ≥35°C in all treatments. It is noteworthy that e[CO_2] trees, which had a lower protein content at 25°C, exhibited a relatively

larger increase in protein content with heat stress. This increase in soluble protein might be due to an upregulation of heat-shock proteins (Aspinwall et al. 2019) to prevent failure of the photosynthetic apparatus (Escandón et al. 2017) or could be caused by N remobilization for Rubisco, which can explain up to 30% of changes in total protein (Warren and Adams 2001). In summary, we found the stress response of the primary metabolome to be highly tissue-specific and to be largely independent of growth [CO_2] in contrast to our third hypothesis. However, we detected some indications for a slightly enhanced thermotolerance under e[CO_2] reflected in a larger upregulation of needle proteins and improved stability of root proteins, at the expense of lower amino acid accumulation.

4.5 Conclusion

Growing Aleppo pines for 18 months under e[CO_2] of c. 870 ppm had a stimulating effect on tree biomass (+40%), but did not result in larger tree water loss due to reductions in stomatal conductance reflected in a nearly proportional increase in WUE maintained throughout a 10 d heatwave (25°C, 30°C, 35°C, 38°C, 40°C). Drought stress initially amplified the e[CO_2] effect on WUE until stomata closed at higher temperatures. Considering the tree C balance, we found a stimulation of the net C uptake under e[CO_2] largely due to reduced tissue respiration alongside lower protein content. Nevertheless, respiration responded independent of [CO_2] to heat stress with an initial increase followed by a decline above 31–34°C. Photosynthesis decreased simultaneously and the trees started to lose C above 30°C, irrespective of [CO_2]. Elevated [CO_2] had only a modest effect on the stress response of the primary metabolome which differed among tissues. Interactive effects between [CO_2] and heat stress became visible via lower protein degradation in roots under e[CO_2] indicating an improved thermotolerance. In summary, we could show that a doubling of atmospheric [CO_2] has little influence on Aleppo pine seedling responses to heat, drought or hot drought stress. While our study is restricted to physiological responses of seedlings the results have implications for model development, which are two-fold: 1) the effect of atmospheric [CO_2] on tree physiological responses decreases with stress intensity such as hot drought and 2) respiration acclimates to heat stress within days and the relationship with temperature is independent of [CO_2] but altered by drought. In order to more accurately assess mitigating effects of e[CO_2] on drought stress responses of Mediterranean-type forests, e[CO_2] induced changes of whole tree C allocation affecting tree water uptake and water loss need to be considered.

4.6 Acknowledgements

We would like to thank Andrea-Livia Jakab, Lisa Fürtauer and Romy Rehschuh for assistance with the experimental set-up and lab work and Daniel Nadal-Sala for help with statistical analyses. We are also grateful to Dan Yakir and his team members for access to the Yatir research site and fruitful scientific discussions. Further we would like to thank Wolfram Weckwerth and the Department of Molecular Systems Biology (University of Vienna, Austria) who provided us with the expertise and the infrastructure to conduct the metabolome analysis. This work was supported by the German Research Foundation through its German-Israeli project cooperation program (SCHM 2736/2-1 and YA 274/1-1) and by the German Federal Ministry of Education and Research (BMBF), through the Helmholtz Association and its research program ATMO. BB received additional support from the graduate school for climate and environment (GRACE) and NKR acknowledges support from the German Research Foundation through its Emmy Noether Program (RU 1657/2-1).

5 Synthesis

Environmental drivers that shaped ecosystems within climate zones are changing much faster than tree adaption, which works at the timescale of decades and centuries (Walker and Wardle 2014). This is why stress resilience and acclimation to extreme events define the success of tree populations (like *Pinus halepensis*) or determine their displacement by better adapted vegetation (Gonzalez et al. 2010; Higgins et al. 2016; O'Sullivan et al. 2017; Vicente-Serrano et al. 2013). The interplay of negative and positive drivers of plant performance, as reviewed, is not always easy to conclude. This knowledge should equip us with the determination and the proper collateral to evaluate future conditions. This thesis aimed to (1) quantify the **impact of extreme heatwaves during drought on the physiology of *Pinus halepensis* seedlings** and (2) understand the role of future **high CO_2 concentrations on plant performance and in altering physiological responses to single and multiple stress**.

An increase of 5 °C in heatwave maxima threatens *P. halepensis* seedlings in a Yatir forest climate.

Chapter 2 (Setup 2016) successfully showed that a combination of heat and drought synergistically weakens *P. halepensis* seedlings, causing high mortality rates together with delayed recovery of C pools and photosynthesis following stress release. The C balance and storage are directly linked to stress severance as high temperatures reduce source capacity due to downregulated photosynthesis, while drought limits sink strength of the roots due to a disruption of long-distance phloem transport. Furthermore, moderate drought aggravated the water budget of heat stressed trees, rendering evaporative cooling impossible, which accelerated heat damage on leafs. A temperature threshold could be defined (47 °C), at which leaf temperature of the seedlings surpassed the point of recovery. These findings may raise uncertainty to the future of the Yatir forest, if extreme event temperatures raise further without having more water available.

Exposition to multiple types of stressors changes physiological stress response on gas exchange and metabolic levels.

The findings of both Setups 2016 and 2017 support this statement. In Setup 2016, an increase in compatible osmolytes in needle tissue opposed a strong decline in root carbon pools, while single stress exposition to heat resulted in less severe changes in cyclitols and non-structural carbon. While drought led to a dose dependent decline in acetone emissions due to metabolic downregulation, monoterpenes, methanol and methyl-salicylate where strong indicators for heat stress. These findings support the assumption that **it is possible to assign volatile organic**

compound signals (and metabolic adjustments) **from the seedlings to either heat or drought and multi-stress scenarios** Furthermore, the stress response to the second heatwave was less sensible to temperatures, which implies that acclimation to heat is mirrored in the BVOC bouquet. Models that compute such responses should be applied accordingly as the tree's stress history seems to be of immediate importance for BVOC emission. Extremely high monoterpene, methanol and acetaldehyde emissions were found to precede tree mortality. This finding could be important for air chemistry in large forest areas and also for the data interpretation during tree mortality assessment.

The more thorough metabolic analysis in 2017 revealed strong connections between soluble carbon in the needles of heat and drought stressed seedlings, which where even pronounced in an e[CO_2] environment. Here, roots did not show strong effects as one month of drought acclimation increased their basal levels of mono- and disaccharides. However, without drought acclimation, these were quickly consumed with increasing temperatures – which can be compared to the findings in 2016 where roots depleted from soluble carbon when stress was applied short-term. Here, we may have observed the difference between drought acclimation (2017) and sudden drought introduction (2016) during an extreme event. One month of drought acclimation of the metabolome seemed to prime the seedling's roots for better C storage due to reduced activity. Heat, however, had a pronounced effect on the amino acid composition – together with increasing extractable protein in the needles and decreasing protein in the roots. Heat, both in 2016 and 2017 experiments, showed to interfere with the nitrogen metabolism and the nitrogen availability in the tissues and higher [CO_2] does not seem to have large mitigating effects here.

Increased [CO_2] can improve the growth and water-use efficiency of trees, as temperature increases, higher carbon storage facilitates metabolic acclimation to heat and drought.

The thesis results could not prove this hypothesis and even partly rejects it. Elevated [CO_2] showed clear advantages when it came to WUE and stomatal conductance. However, these advantages only translated to an increased C balance, when the seedling were subjected to temperatures below 30 °C. This might conclude in a strict biomass to water equilibrium, which means that a certain amount of biomass needs a minimum of available water, which has to be distributed on tree level. This water threathold is dependent on the basal non-stress stomatal conductance (lower in e[CO_2]). When temperature increases, this increases water demand and an increase in respiratory carbon losses establishes a new carbon equilibrium. This may be supported by recent findings of (Gattmann et al. 2021), where a clear C storage increase under

e[CO_2] opposed no advantages in seedling survival under e[CO_2]. All of the available water was used both by seedlings growing at a[CO_2] and at e[CO_2] due to increased leaf biomass in the latter, resulting in better WUE at leaf level, but no survival advantage due to any water saving.The findings of this thesis ad to the picture of an energy buffered but water limited system in the soil-plant-atmosphere continuum. Mild to moderate drought attenuates growth and reduce productivity of trees. This may be alleviated by higher CO_2 levels, which are able to extend the seedling's growth optima to a certain degree by budgeting the available amount of water and their biomass. However, if drought stress intensifies and interplays with high temperatures the combination of stressors override the positive effects of e[CO_2] on the primary metabolome and gas exchange fluxes.

There are limits to the extent of adaption (phylogenetic development) and acclimation (eco-physiological response) of trees. On the one side, limits may be inherited species specific and may vary largely depending on their genetic setup that restricts geographic distribution (Chevin et al. 2010; Donoghue 2008; Janz et al. 2010; Lancaster and Humphreys 2020; Wang et al. 2018). On the other side, trees are more or less limited by the ability to supply their photosynthetic organs with enough water, to serve for the evaporative demand of the atmosphere. Even plant height is limited by the maximal water potential differences between soil, plant and air (Kanduč et al. 2020; Koch et al. 2004; Niklas and Spatz 2004), which allows water rising up the xylem elements within a tree stem. In this context, e[CO_2] may lead to faster tree growth but not to trees that are more resistant to hydraulic stresses (Duan et al. 2018).

5.1 Contextual Classification of the Results

What can we learn from a greenhouse experiment?

Advantages and limitations of greenhouse experiments: First of all, experiments in a greenhouse facility allow for a tight control of environmental drivers, which is extremely difficult in the field. Upscaling is only possible if different sources and experimental results are considered. In this work, the greenhouse setup allowed a detailed control of abiotic parameters, which are similar (Birami et al. 2018), but never exactly the same as under field conditions (Yatir forest) (Preisler et al. 2019; Tatarinov et al. 2015). Being detached from the natural environment allows for the simulation of different water availability scenarios, as well as for extreme temperature changes. Preparing the e[CO_2] experiments with seedlings which germinated and grew under the higher [CO_2] from start eliminated the CO_2 fertilization effect that was found in free air experiments (FACE) until trees reached a new equilibrium state in the new environment (Körner 2006). Thus, the history of a field experiment individual is often unknown, while individuals used in a

greenhouse share ideally the same. The limitation of highly controlled greenhouse setups is that seedlings can only yield approximations of the physiological capacity of adult trees, while the responses to stress may be faster in seedlings as they can't rely on large carbon and water reserves that larger trees may have, which buffer stressful conditions (Gentine et al. 2016; Grote et al. 2016; Hartmann et al. 2018c). On the one side, lab experiments allow for resolving isolated effect of, for instance, extremely high temperatures on a single individual (e.g. see (Colombo and Timmer 1992)), which can hardly be extracted from a whole ecosystem in the field. On the other side, field experiments are the ideal setup to elucidate the interactions of system components (soil, microbes, and plants) (e.g. see (Jiang et al. 2020) or also (Preisler et al. 2019)).

5.2 Observations and Outlook

The growth effects of [CO_2] on plants have been recognized since the early 1900 (Blackman 1905) and were further discussed in the context of “Liebig`s law of the minimum” (Browne 1942; Norby et al. 1986), meaning that the most limiting nutrient may constrain plant growth no matter how much of other essential parameters are supplied. About a century and more than +100 ppm [CO_2] later, a global leaf area increase due to increasing atmospheric CO_2 being framed in the context of “world greening” (Donohue et al. 2013), which describes the increase of satellite sensed green biomass cover derived from visual index (VI) satellite observations. These observations were traced back to CO_2 fertilization effects (Donohue et al. 2013; Zhu et al. 2016) but are critically discussed (Keenan et al. 2020) as large fractions are caused by massive human management (Chen et al. 2019) or by the increase of vegetation periods in cold regions due to warming (Xu et al. 2013; Zhu et al. 2016). Uncertainties arise in vegetation parameterization and methodology (Smith et al. 2019; Walther et al. 2016; Yan et al. 2019b) especially in dry environments were effects variation of CO_2 are thought to be strongest (Smith et al. 2019).

However, findings supporting the hypothesis that the fertilizing CO_2 effect has reached its maximum are accumulating (Peñuelas et al. 2017), as other environmental drivers like too high temperatures and low water availability emerge limiting. Stress physiology of plants is complex and characterized by concurrent networks that may explain the non-uniform response of plants to CO_2. The stress physiology of plants growing under elevated [CO_2] only begins to be revealed and is not yet fully implemented in vegetation models (Albrich et al. 2020), though would improve the correct interpretation of large scale observations. Hence natural conditions seldom resemble optimum conditions and plants are constantly exposed to pathogens and other elicitors, the findings of this thesis have to be interpreted as CO_2 effects on vegetation should not be overestimated and are further constrained by stress severity. Thus, aside from CO_2 and water limitations, maximum heat dosage could be most limiting for long-term tree performance.

6 References

AbdElgawad H, Zinta G, Beemster GTS, Janssens IA, Asard H (2016) Future Climate CO_2 Levels Mitigate Stress Impact on Plants: Increased Defense or Decreased Challenge? Front Plant Sci 7:556. https://doi.org/10.3389/fpls.2016.00556

Adams HD, Macalady AK, Breshears DD, Allen CD, Stephenson NL, Saleska SR, Huxman TE, McDowell NG (2010) Climate-Induced Tree Mortality: Earth System Consequences. Eos Trans. AGU 91:153. https://doi.org/10.1029/2010EO170003

Adams HD, Zeppel MJB, Anderegg WRL, Hartmann H, Landhäusser SM, Tissue DT, Huxman TE, Hudson PJ, Franz TE, Allen CD, Anderegg LDL, Barron-Gafford GA, Beerling DJ, Breshears DD, Brodribb TJ, Bugmann H, Cobb RC, Collins AD, Dickman LT, Duan H, Ewers BE, Galiano L, Galvez DA, Garcia-Forner N, Gaylord ML, Germino MJ, Gessler A, Hacke UG, Hakamada R, Hector A, Jenkins MW, Kane JM, Kolb TE, Law DJ, Lewis JD, Limousin J-M, Love DM, Macalady AK, Martínez-Vilalta J, Mencuccini M, Mitchell PJ, Muss JD, O'Brien MJ, O'Grady AP, Pangle RE, Pinkard EA, Piper FI, Plaut JA, Pockman WT, Quirk J, Reinhardt K, Ripullone F, Ryan MG, Sala A, Sevanto S, Sperry JS, Vargas R, Vennetier M, Way DA, Xu C, Yepez EA, McDowell NG (2017) A multi-species synthesis of physiological mechanisms in drought-induced tree mortality. Nat Ecol Evol 1:1285–1291. https://doi.org/10.1038/s41559-017-0248-x

Ainsworth EA, Long SP (2005) What have we learned from 15 years of free-air CO_2 enrichment (FACE)? A meta-analytic review of the responses of photosynthesis, canopy properties and plant production to rising CO_2. New Phytol 165:351–371. https://doi.org/10.1111/j.1469-8137.2004.01224.x

Ainsworth EA, Rogers A (2007) The response of photosynthesis and stomatal conductance to rising CO_2: mechanisms and environmental interactions. Plant Cell Environ 30:258–270. https://doi.org/10.1111/j.1365-3040.2007.01641.x

Akaike H (1974) A new look at the statistical model identification. IEEE Trans. Automat. Contr. 19:716–723. https://doi.org/10.1109/TAC.1974.1100705

Albrich K, Rammer W, Turner MG, Ratajczak Z, Braziunas KH, Hansen WD, Seidl R, Hickler T (2020) Simulating forest resilience: A review. Global Ecol Biogeogr 22:1. https://doi.org/10.1111/geb.13197

Aleixo I, Norris D, Hemerik L, Barbosa A, Prata E, Costa F, Poorter L (2019) Amazonian rainforest tree mortality driven by climate and functional traits. Nat. Clim. Chang. 9:384–388. https://doi.org/10.1038/s41558-019-0458-0

Allen CD, Macalady AK, Chenchouni H, Bachelet D, McDowell NG, Vennetier M, Kitzberger T, Rigling A, Breshears DD, Hogg EH, Gonzalez P, Fensham R, Zhang Z, Castro J, Demidova N, Lim J-H, Allard G, Running SW, Semerci A, Cobb N (2010) A global overview of drought and heat-induced tree mortality reveals emerging climate change risks for forests. Forest Ecology and Management 259:660–684. https://doi.org/10.1016/j.foreco.2009.09.001

Allen CD, Breshears DD, McDowell NG (2015) On underestimation of global vulnerability to tree mortality and forest die-off from hotter drought in the Anthropocene. Ecosphere 6:art129. https://doi.org/10.1890/ES15-00203.1

Allen MR, O.P. Dube, W. Solecki, F. Aragón-Durand, W. Cramer, S. Humphreys, M. Kainuma, J. Kala, N. Mahowald, Y. Mulugetta, R. Perez, M. Wairiu, and K. Zickfeld (2018) Framing and Context. In: Global Warming of 1.5ºC. An IPCC Special Report on the impacts of global warming of 1.5ºC above pre-industrial levels and related global greenhouse gas emission

pathways, in the context of strengthening the global response to the threat of climate change, sustainable development, and efforts to eradicate poverty [Masson-Delmotte, V., P. Zhai, H.-O. Portner, D. Roberts, J. Skea, P.R. Shukla, A. Pirani, W. Moufouma-Okia, C. Péan, R. Pidcock, S. Connors, J.B.R. Matthews, Y. Chen, X. Zhou, M.I. Gomis, E. Lonnoy, T. Maycock, M. Tignor and T. Waterfield (eds.)]. World Meteorological Organization, Geneva, Switzerland, 49–91.

Al-Whaibi MH (2011) Plant heat-shock proteins: A mini review. Journal of King Saud University - Science 23:139–150. https://doi.org/10.1016/j.jksus.2010.06.022

Ameye M, Wertin TM, Bauweraerts I, McGuire MA, Teskey RO, Steppe K (2012) The effect of induced heat waves on *Pinus taeda* and *Quercus rubra* seedlings in ambient and elevated CO_2 atmospheres. New Phytol 196:448–461. https://doi.org/10.1111/j.1469-8137.2012.04267.x

Anderegg WRL, Kane JM, Anderegg LDL (2012) Consequences of widespread tree mortality triggered by drought and temperature stress. Nature Climate change 3:30–36. https://doi.org/10.1038/nclimate1635

Anderegg WRL, Hicke JA, Fisher RA, Allen CD, Aukema J, Bentz B, Hood S, Lichstein JW, Macalady AK, McDowell NG, Pan Y, Raffa K, Sala A, Shaw JD, Stephenson NL, Tague C, Zeppel M (2015) Tree mortality from drought, insects, and their interactions in a changing climate. New Phytol 208:674–683. https://doi.org/10.1111/nph.13477

Anderegg WRL, Wolf A, Arango-Velez A, Choat B, Chmura DJ, Jansen S, Kolb T, Li S, Meinzer FC, Pita P, Resco de Dios V, Sperry JS, Wolfe BT, Pacala S (2018) Woody plants optimise stomatal behaviour relative to hydraulic risk. Ecol Lett 21:968–977. https://doi.org/10.1111/ele.12962

Anderegg WRL, Anderegg LDL, Kerr KL, Trugman AT (2019) Widespread drought-induced tree mortality at dry range edges indicates that climate stress exceeds species' compensating mechanisms. Global Change Biology 25:3793–3802. https://doi.org/10.1111/gcb.14771

Arneth A, Veenendaal EM, Best C, Timmermans W, Kolle O, Montagnani L, Shibistova O (2006) Water use strategies and ecosystem-atmosphere exchange of CO_2 in two highly seasonal environments. Biogeosciences Discuss. 3:345–382. https://doi.org/10.5194/bgd-3-345-2006

Arneth A, Sitch S, Pongratz J, Stocker BD, Ciais P, Poulter B, Bayer AD, Bondeau A, Calle L, Chini LP, Gasser T, Fader M, Friedlingstein P, Kato E, Li W, Lindeskog M, Nabel, J. E. M. S., Pugh TAM, Robertson E, Viovy N, Yue C, Zaehle S (2017) Historical carbon dioxide emissions caused by land-use changes are possibly larger than assumed. Nature Geosci 10:79–84. https://doi.org/10.1038/ngeo2882

Asad MAU, Zakari SA, Zhao Q, Zhou L, Ye Y, Cheng F (2019) Abiotic Stresses Intervene with ABA Signaling to Induce Destructive Metabolic Pathways Leading to Death: Premature Leaf Senescence in Plants. Int J Mol Sci 20. https://doi.org/10.3390/ijms20020256

Aspinwall MJ, Jacob VK, Blackman CJ, Smith RA, Tjoelker MG, Tissue DT (2017) The temperature response of leaf dark respiration in 15 provenances of *Eucalyptus grandis* grown in ambient and elevated CO_2. Functional Plant Biol. 44:1075. https://doi.org/10.1071/FP17110

Aspinwall MJ, Pfautsch S, Tjoelker MG, Vårhammar A, Possell M, Drake JE, Reich PB, Tissue DT, Atkin OK, Rymer PD, Dennison S, van Sluyter SC (2019) Range size and growth temperature influence Eucalyptus species responses to an experimental heatwave. Global Change Biology. https://doi.org/10.1111/gcb.14590

Atkin O, Tjoelker MG (2003) Thermal acclimation and the dynamic response of plant respiration to temperature. Trends Plant Sci 8:343–351. https://doi.org/10.1016/S1360-1385(03)00136-5

Atzmon N, Moshe Y, Schiller G (2004) Ecophysiological response to severe drought in *Pinus halepensis* Mill. trees of two provenances. Plant Ecology 171:15–22. https://doi.org/10.1023/B:VEGE.0000029371.44518.38

Bader M, Hiltbrunner E, Körner C (2009) Fine root responses of mature deciduous forest trees to free air carbon dioxide enrichment (FACE). Functional Ecology 23:913–921. https://doi.org/10.1111/j.1365-2435.2009.01574.x

Bajji M, Kinet J-MaL, Stanley* (2001) The use of the electrolyte leakage method for assessing cell membrane stability as a water stress tolerance test in durum wheat. Plant Growth Regul 00:1–10

Baker HS, Millar RJ, Karoly DJ, Beyerle U, Guillod BP, Mitchell D, Shiogama H, Sparrow S, Woollings T, Allen MR (2018) Higher CO_2 concentrations increase extreme event risk in a 1.5 °C world. Nature Clim Change 8:604–608. https://doi.org/10.1038/s41558-018-0190-1

Baldwin JW, Dessy JB, Vecchi GA, Oppenheimer M (2019) Temporally Compound Heat Wave Events and Global Warming: An Emerging Hazard. Earth's Future 7:411–427. https://doi.org/10.1029/2018EF000989

Bamberger I, Ruehr NK, Schmitt M, Gast A, Wohlfahrt G, Arneth A (2017) Isoprene emission and photosynthesis during heatwaves and drought in black locust. Biogeosciences 14:3649–3667. https://doi.org/10.5194/bg-14-3649-2017

Barton K (2019) MuMIn: Multi-Model Inference: R package. [WWW document] <URL:https://CRAN.R-project.org/package=MuMIn>.

Bassow SL, McConnaughay KDM, Bazzaz FA (1994) The Response of Temperate Tree Seedlings Grown in Elevated CO_2 to Extreme Temperature Events. Ecological Applications 4:593–603. https://doi.org/10.2307/1941960

Bastin J-F, Finegold Y, Garcia C, Mollicone D, Rezende M, Routh D, Zohner CM, Crowther TW (2019) The global tree restoration potential. Science 365:76–79. https://doi.org/10.1126/science.aax0848

Bates D, Mächler M, Bolker B, Walker S (2015) Fitting Linear Mixed-Effects Models Using lme4. J. Stat. Soft. 67. https://doi.org/10.18637/jss.v067.i01

Battipaglia G, Saurer M, Cherubini P, CALFAPIETRA C, McCarthy HR, Norby RJ, Francesca Cotrufo M (2013) Elevated CO_2 increases tree-level intrinsic water use efficiency: insights from carbon and oxygen isotope analyses in tree rings across three forest FACE sites. New Phytol 197:544–554. https://doi.org/10.1111/nph.12044

Bauweraerts I, Wertin TM, Ameye M, McGuire MA, Teskey RO, Steppe K (2013) The effect of heat waves, elevated [CO_2] and low soil water availability on northern red oak (*Quercus rubra* L.) seedlings. Global Change Biology 19:517–528. https://doi.org/10.1111/gcb.12044

Bauweraerts I, Ameye M, Wertin TM, McGuire MA, Teskey RO, Steppe K (2014) Water availability is the decisive factor for the growth of two tree species in the occurrence of consecutive heat waves. Agricultural and Forest Meteorology 189-190:19–29. https://doi.org/10.1016/j.agrformet.2014.01.001

Behnke K, Ghirardo A, Janz D, Kanawati B, Esperschütz J, Zimmer I, Schmitt-Kopplin P, Niinemets Ü, Polle A, Schnitzler JP, Rosenkranz M (2013) Isoprene function in two contrasting poplars under salt and sunflecks. Tree Physiol 33:562–578. https://doi.org/10.1093/treephys/tpt018

Bertini G, Amoriello T, Fabbio G, Piovosi M (2011) Forest growth and climate change: Evidences from the ICP-Forests intensive monitoring in Italy. iForest 4:262–267. https://doi.org/10.3832/ifor0596-004

Bigras FJ (2000) Selection of white spruce families in the context of climate change: Heat tolerance. Tree Physiol 20:1227–1234. https://doi.org/10.1093/treephys/20.18.1227

Birami B, Gattmann M, Heyer AG, Grote R, Arneth A, Ruehr NK (2018) Heat Waves Alter Carbon Allocation and Increase Mortality of Aleppo Pine Under Dry Conditions. Front. For. Glob. Change 1:1285. https://doi.org/10.3389/ffgc.2018.00008

Blackman FF (1905) Optima and Limiting Factors. Annals of Botany os-19:281–296. https://doi.org/10.1093/oxfordjournals.aob.a089000

Blanch J-S, Peñuelas J, Llusià J (2007) Sensitivity of terpene emissions to drought and fertilization in terpene-storing *Pinus halepensis* and non-storing *Quercus ilex*. Physiol Plant 131:211–225. https://doi.org/10.1111/j.1399-3054.2007.00944.x

Blessing CH, Werner RA, Siegwolf R, Buchmann N (2015) Allocation dynamics of recently fixed carbon in beech saplings in response to increased temperatures and drought. Tree Physiol 35:585–598. https://doi.org/10.1093/treephys/tpv024

Bloom AJ, Smart DR, Nguyen DT, Searles PS (2002) Nitrogen assimilation and growth of wheat under elevated carbon dioxide. Proc Natl Acad Sci U S A 99:1730–1735. https://doi.org/10.1073/pnas.022627299

Bonan GB (2008) Forests and climate change: forcings, feedbacks, and the climate benefits of forests. Science 320:1444–1449. https://doi.org/10.1126/science.1155121

Bonan GB, Williams M, Fisher RA, Oleson KW (2014) Modeling stomatal conductance in the earth system: Linking leaf water-use efficiency and water transport along the soil–plant–atmosphere continuum. Geosci. Model Dev. 7:2193–2222. https://doi.org/10.5194/gmd-7-2193-2014

Bond-Lamberty B, Wang C, Gower ST (2004) Contribution of root respiration to soil surface CO_2 flux in a boreal black spruce chronosequence. Tree Physiol 24:1387–1395. https://doi.org/10.1093/treephys/24.12.1387

Bowes G (1991) Growth at elevated CO_2: Photosynthetic responses mediated through Rubisco. Plant Cell Environ 14:795–806. https://doi.org/10.1111/j.1365-3040.1991.tb01443.x

Box GEP, Jenkins GM, Reinsel GC, Ljung GM (2016) Time series analysis: Forecasting and control, Fifth edition. Wiley Series in Probability and Statistics. John Wiley & Sons Inc, Hoboken, New Jersey

Bracho-Nunez A, Knothe NM, Costa WR, Maria Astrid LR, Kleiss B, Rottenberger S, Piedade MTF, Kesselmeier J (2012) Root anoxia effects on physiology and emissions of volatile organic compounds (VOC) under short- and long-term inundation of trees from Amazonian floodplains. Springerplus 1:9. https://doi.org/10.1186/2193-1801-1-9

Brauner K, Hormiller I, Nagele T, Heyer AG (2014) Exaggerated root respiration accounts for growth retardation in a starchless mutant of Arabidopsis thaliana. Plant J 79:82–91. https://doi.org/10.1111/tpj.12555

Brauner K, Birami B, Brauner HA, Heyer AG (2018) Diurnal periodicity of assimilate transport shapes resource allocation and whole-plant carbon balance. Plant J 94:776–789. https://doi.org/10.1111/tpj.13898

Breshears DD, Cobb NS, Rich PM, Price KP, Allen CD, Balice RG, Romme WH, Kastens JH, Floyd ML, Belnap J, Anderson JJ, Myers OB, Meyer CW (2005) Regional vegetation die-off in response to global-change-type drought. Proc Natl Acad Sci U S A 102:15144–15148. https://doi.org/10.1073/pnas.0505734102

Brodribb TJ, Cochard H (2009) Hydraulic failure defines the recovery and point of death in water-stressed conifers. Plant Physiol 149:575–584. https://doi.org/10.1104/pp.108.129783

Brodribb TJ, Am McAdam S, Carins Murphy MR (2017) Xylem and stomata, coordinated through time and space. Plant Cell Environ 40:872–880. https://doi.org/10.1111/pce.12817

Brodribb TJ, Powers J, Cochard H, Choat B (2020) Hanging by a thread? Forests and drought. Science 368:261–266. https://doi.org/10.1126/science.aat7631

Brouquisse R, James F, Pradet A, Raymond P (1992) Asparagine metabolism and nitrogen distribution during protein degradation in sugar-starved maize root tips. Planta 188:384–395. https://doi.org/10.1007/BF00192806

Browne CA (1942) Liebig and the law of the minimum. FA Moulton, ed, Liebig and After Liebig. A Century of Progressin Agricultural Chemistry. American Association for the Advancement of Science, Washington, DC:pp 71–82

Brunner I, Herzog C, Dawes MA, Arend M, Sperisen C (2015) How tree roots respond to drought. Front Plant Sci 6:547. https://doi.org/10.3389/fpls.2015.00547

Bukhov NG, Wiese C, Neimanis S, Heber U (1999) Heat sensitivity of chloroplasts and leaves: Leakage of protons from thylakoids and reversible activation of cyclic electron transport. Photosynthesis Research 59:81–93. https://doi.org/10.1023/A:1006149317411

Burghardt M, Riederer M (2003) Ecophysiological relevance of cuticular transpiration of deciduous and evergreen plants in relation to stomatal closure and leaf water potential. J Exp Bot 54:1941–1949. https://doi.org/10.1093/jxb/erg195

Burnham KP, Anderson DR (2004) Model Selection and Multimodel Inference. Springer New York, New York, NY

Calfapietra C, Gielen B, Galema ANJ, Lukac M, Angelis P de, Moscatelli MC, Ceulemans R, Scarascia-Mugnozza G (2003) Free-air CO_2 enrichment (FACE) enhances biomass production in a short-rotation poplar plantation. Tree Physiol 23:805–814. https://doi.org/10.1093/treephys/23.12.805

Cappellin L, Karl T, Probst M, Ismailova O, Winkler PM, Soukoulis C, Aprea E, Märk TD, Gasperi F, Biasioli F (2012) On quantitative determination of volatile organic compound concentrations using proton transfer reaction time-of-flight mass spectrometry. Environ Sci Technol 46:2283–2290. https://doi.org/10.1021/es203985t

Cassia R, Nocioni M, Correa-Aragunde N, Lamattina L (2018) Climate Change and the Impact of Greenhouse Gasses: CO2 and NO, Friends and Foes of Plant Oxidative Stress. Front Plant Sci 9:273. https://doi.org/10.3389/fpls.2018.00273

Celedon JM, Bohlmann J (2019) Oleoresin defenses in conifers: chemical diversity, terpene synthases and limitations of oleoresin defense under climate change. New Phytol 224:1444–1463. https://doi.org/10.1111/nph.15984

Chandler D (2005) Interfaces and the driving force of hydrophobic assembly. Nature 437:640–647. https://doi.org/10.1038/nature04162

Chaves MM, Costa JM, Zarrouk O, Pinheiro C, Lopes CM, Pereira JS (2016) Controlling stomatal aperture in semi-arid regions-The dilemma of saving water or being cool? Plant Sci 251:54–64. https://doi.org/10.1016/j.plantsci.2016.06.015

Chen C, Park T, Wang X, Piao S, Xu B, Chaturvedi RK, Fuchs R, Brovkin V, Ciais P, Fensholt R, Tømmervik H, Bala G, Zhu Z, Nemani RR, Myneni RB (2019) China and India lead in greening of the world through land-use management. Nat Sustain 2:122–129. https://doi.org/10.1038/s41893-019-0220-7

Chevin L-M, Lande R, Mace GM (2010) Adaptation, plasticity, and extinction in a changing environment: towards a predictive theory. PLoS Biol 8:e1000357. https://doi.org/10.1371/journal.pbio.1000357

Choat B, Brodribb TJ, Brodersen CR, Duursma RA, López R, Medlyn BE (2018) Triggers of tree mortality under drought. Nature 558:531–539. https://doi.org/10.1038/s41586-018-0240-x

Churkina G, Running SW (1998) Contrasting Climatic Controls on the Estimated Productivity of Global Terrestrial Biomes. Ecosystems 1:206–215. https://doi.org/10.1007/s100219900016

Ciais P, Reichstein M, Viovy N, Granier A, Ogée J, Allard V, Aubinet M, Buchmann N, Bernhofer C, Carrara A, Chevallier F, Noblet N de, Friend AD, Friedlingstein P, Grünwald T, Heinesch B, Keronen P, Knohl A, Krinner G, Loustau D, Manca G, Matteucci G, Miglietta F, Ourcival JM, Papale D, Pilegaard K, Rambal S, Seufert G, Soussana JF, Sanz MJ, Schulze ED, Vesala T, Valentini R (2005) Europe-wide reduction in primary productivity caused by the heat and drought in 2003. Nature 437:529–533. https://doi.org/10.1038/nature03972

Clarke SM, Mur LAJ, Wood JE, Scott IM (2004) Salicylic acid dependent signaling promotes basal thermotolerance but is not essential for acquired thermotolerance in Arabidopsis thaliana. Plant J 38:432–447. https://doi.org/10.1111/j.1365-313X.2004.02054.x

Coleman JS, Rochefort L, Bazzaz FA, Woodward FI (1991) Atmospheric CO_2, plant nitrogen status and the susceptibility of plants to an acute increase in temperature. Plant Cell Environ 14:667–674. https://doi.org/10.1111/j.1365-3040.1991.tb01539.x

Collins M, Knutti R, Arblaster J, Dufresne J-L, Fichefet T, Friedlingstein P, Gao X, Gutowski W, Johns T, Krinner G, Shongwe M, Tebaldi C, Weaver A, Wehner M (2013) Long-term Climate Change: Projections, Commitments and Irreversibility. Climate Change 2013: The Physical Science Basis. Contribution of Working Group I to the Fifth Assessment Report of the Intergovernmental Panel on Climate Change [Stocker, T.F., D. Qin, G.-K. Plattner, M. Tignor, S.K. Allen, J. Boschung, A. Nauels, Y. Xia, V. Bex and P.M. Midgley (eds.)]. Cambridge University Press, Cambridge, United Kingdom and New York, NY, USA.

Colombo SJ, Timmer VR (1992) Limits of tolerance to high temperatures causing direct and indirect damage to black spruce. Tree Physiol 11:95–104. https://doi.org/10.1093/treephys/11.1.95

Correia B, Hancock RD, Amaral J, Gomez-Cadenas A, Valledor L, Pinto G (2018) Combined drought and heat activates protective responses in *Eucalyptus globulus* that are not activated when subjected to drought or heat stress alone. Front. Plant Sci. 9:233. https://doi.org/10.3389/fpls.2018.00819

Cotrufo MF, Ineson P, Scott A (1998) Elevated CO_2 reduces the nitrogen concentration of plant tissues. Global Change Biol 4:43–54. https://doi.org/10.1046/j.1365-2486.1998.00101.x

Couée I, Sulmon C, Gouesbet G, El Amrani A (2006) Involvement of soluble sugars in reactive oxygen species balance and responses to oxidative stress in plants. J Exp Bot 57:449–459. https://doi.org/10.1093/jxb/erj027

Coumou D, Rahmstorf S (2012) A decade of weather extremes. Nature Climate change. https://doi.org/10.1038/nclimate1452

Crafts-Brandner SJ, Salvucci ME (2000) Rubisco activase constrains the photosynthetic potential of leaves at high temperature and CO_2. Proc Natl Acad Sci U S A 97:13430–13435. https://doi.org/10.1073/pnas.230451497

Cyr DR, Buxton GF, Webb DP, Dumbroff EB (1990) Accumulation of free amino acids in the shoots and roots of three northern conifers during drought. Tree Physiol 6:293–303. https://doi.org/10.1093/treephys/6.3.293

Dadshani S, Kurakin A, Amanov S, Hein B, Rongen H, Cranstone S, Blievernicht U, Menzel E, Léon J, Klein N, Ballvora A (2015) Non-invasive assessment of leaf water status using a dual-mode microwave resonator. Plant Methods 11:8. https://doi.org/10.1186/s13007-015-0054-x

Dani KGS, Jamie IM, Prentice IC, Atwell BJ (2015) Species-specific photorespiratory rate, drought tolerance and isoprene emission rate in plants. Plant Signal Behav 10:e990830. https://doi.org/10.4161/15592324.2014.990830

Daniel RM, Danson MJ (2013) Temperature and the catalytic activity of enzymes: a fresh understanding. FEBS Letters 587:2738–2743. https://doi.org/10.1016/j.febslet.2013.06.027

Daniel RM, Danson MJ, Eisenthal R, Lee CK, Peterson ME (2008) The effect of temperature on enzyme activity: new insights and their implications. Extremophiles : life under extreme conditions 12:51–59. https://doi.org/10.1007/s00792-007-0089-7

Daniell JW, Chappell WE, Couch HB (1969) Effect of Sublethal and Lethal Temperature on Plant Cells. Plant Physiol 44:1684–1689. https://doi.org/10.1104/pp.44.12.1684

David-Schwartz R, Paudel I, Mizrachi M, Delzon S, Cochard H, Lukyanov V, Badel E, Capdeville G, Shklar G, Cohen S (2016) Indirect evidence for genetic differentiation in vulnerability to embolism in *Pinus halepensis*. Front Plant Sci 7:768. https://doi.org/10.3389/fpls.2016.00768

Dawes MA, Hättenschwiler S, Bebi P, Hagedorn F, Handa IT, Körner C, Rixen C (2010) Species-specific tree growth responses to 9 years of CO_2 enrichment at the alpine treeline. Journal of Ecology 21:no-no. https://doi.org/10.1111/j.1365-2745.2010.01764.x

Delzon S, Douthe C, Sala A, Cochard H (2010) Mechanism of water-stress induced cavitation in conifers: bordered pit structure and function support the hypothesis of seal capillary-seeding. Plant Cell Environ 33:2101–2111. https://doi.org/10.1111/j.1365-3040.2010.02208.x

Demirevska-Kepova K, Feller U (2004) Heat sensitivity of Rubisco, Rubisco activase and Rubisco binding protein in higher plants. Acta Physiol Plant 26:103–114. https://doi.org/10.1007/s11738-004-0050-7

DeSoto L, Cailleret M, Sterck F, Jansen S, Kramer K, Robert EMR, Aakala T, Amoroso MM, Bigler C, Camarero JJ, Čufar K, Gea-Izquierdo G, Gillner S, Haavik LJ, Hereş A-M, Kane JM, Kharuk VI, Kitzberger T, Klein T, Levanič T, Linares JC, Mäkinen H, Oberhuber W, Papadopoulos A, Rohner B, Sangüesa-Barreda G, Stojanovic DB, Suárez ML, Villalba R, Martínez-Vilalta J (2020) Low growth resilience to drought is related to future mortality risk in trees. Nat Commun 11:545. https://doi.org/10.1038/s41467-020-14300-5

Dietterich LH, Zanobetti A, Kloog I, Huybers P, Leakey ADB, Bloom AJ, Carlisle E, Fernando N, Fitzgerald G, Hasegawa T, Holbrook NM, Nelson RL, Norton R, Ottman MJ, Raboy V, Sakai H, Sartor KA, Schwartz J, Seneweera S, Usui Y, Yoshinaga S, Myers SS (2015) Impacts of elevated atmospheric CO_2 on nutrient content of important food crops. Sci Data 2:150036. https://doi.org/10.1038/sdata.2015.36

Dixon HH, Joly J (1895) On the ascent of sap. Phil. Trans. R. Soc. Lond. B 186:563–576. https://doi.org/10.1098/rstb.1895.0012

Doelman JC, Stehfest E, van Vuuren DP, Tabeau A, Hof AF, Braakhekke MC, Gernaat, David E H J, van den Berg M, van Zeist W-J, Daioglou V, van Meijl H, Lucas PL (2020) Afforestation for climate change mitigation: Potentials, risks and trade-offs. Global Change Biology 26:1576–1591. https://doi.org/10.1111/gcb.14887

Donoghue MJ (2008) Colloquium paper: a phylogenetic perspective on the distribution of plant diversity. Proc Natl Acad Sci U S A 105 Suppl 1:11549–11555. https://doi.org/10.1073/pnas.0801962105

Donohue RJ, Roderick ML, McVicar TR, Farquhar GD (2013) Impact of CO_2 fertilization on maximum foliage cover across the globe's warm, arid environments. Geophys. Res. Lett. 40:3031–3035. https://doi.org/10.1002/grl.50563

Dorokhov YL, Sheshukova EV, Komarova TV (2018) Methanol in Plant Life. Front Plant Sci 9:1623. https://doi.org/10.3389/fpls.2018.01623

Drake JE, Tjoelker MG, Vårhammar A, Medlyn BE, Reich PB, Leigh A, Pfautsch S, Blackman CJ, López R, Aspinwall MJ, Crous KY, Duursma RA, Kumarathunge D, Kauwe MG de, Jiang M, Nicotra AB, Tissue DT, Choat B, Atkin OK, Barton CVM (2018) Trees tolerate an extreme heatwave via sustained transpirational cooling and increased leaf thermal tolerance. Global Change Biology 24:2390–2402. https://doi.org/10.1111/gcb.14037

Drake JE, Furze ME, Tjoelker MG, Carrillo Y, Barton CVM, Pendall E (2019a) Climate warming and tree carbon use efficiency in a whole-tree 13 CO_2 tracer study. New Phytol 222:1313–1324. https://doi.org/10.1111/nph.15721

Drake JE, Tjoelker MG, Aspinwall MJ, Reich PB, Pfautsch S, Barton CVM (2019b) The partitioning of gross primary production for young Eucalyptus tereticornis trees under experimental warming and altered water availability. New Phytol 222:1298–1312. https://doi.org/10.1111/nph.15629

Drake BG, Azcon-Bieto J, Berry J, Bunce J, Dijkstra P, Farrar J, Gifford RM, Gonzalez-Meler MA, Koch G, Lambers H, Siedow J, Wullschleger S (1999) Does elevated atmospheric CO_2 concentration inhibit mitochondrial respiration in green plants? Plant Cell Environ 22:649–657. https://doi.org/10.1046/j.1365-3040.1999.00438.x

Dreyer E, Le Roux X, Montpied P, Daudet FA, Masson F (2001) Temperature response of leaf photosynthetic capacity in seedlings from seven temperate tree species. Tree Physiol 21:223–232. https://doi.org/10.1093/treephys/21.4.223

Duan H, Amthor JS, Duursma RA, O'Grady AP, Choat B, Tissue DT (2013) Carbon dynamics of eucalypt seedlings exposed to progressive drought in elevated CO_2 and elevated temperature. Tree Physiol 33:779–792. https://doi.org/10.1093/treephys/tpt061

Duan H, Duursma RA, Huang G, Smith RA, Choat B, O'Grady AP, Tissue DT (2014) Elevated CO_2 does not ameliorate the negative effects of elevated temperature on drought-induced mortality in *Eucalyptus radiata* seedlings. Plant Cell Environ 37:1598–1613. https://doi.org/10.1111/pce.12260

Duan H, O'Grady AP, Duursma RA, Choat B, Huang G, Smith RA, Jiang Y, Tissue DT (2015) Drought responses of two gymnosperm species with contrasting stomatal regulation strategies under elevated CO_2 and temperature. Tree Physiol 35:756–770. https://doi.org/10.1093/treephys/tpv047

Duan H, Chaszar B, Lewis JD, Smith RA, Huxman TE, Tissue DT (2018) CO_2 and temperature effects on morphological and physiological traits affecting risk of drought-induced mortality. Tree Physiol 38:1138–1151. https://doi.org/10.1093/treephys/tpy037

Duarte AG, Katata G, Hoshika Y, Hossain M, Kreuzwieser J, Arneth A, Ruehr NK (2016) Immediate and potential long-term effects of consecutive heat waves on the photosynthetic performance and water balance in Douglas-fir. J Plant Physiol 205:57–66. https://doi.org/10.1016/j.jplph.2016.08.012

Dusenge ME, Duarte AG, Way DA (2019) Plant carbon metabolism and climate change: elevated CO_2 and temperature impacts on photosynthesis, photorespiration and respiration. New Phytol 221:32–49. https://doi.org/10.1111/nph.15283

Duursma RA, Barton CVM, Eamus D, Medlyn BE, Ellsworth DS, Forster MA, Tissue DT, Linder S, McMurtrie RE (2011) Rooting depth explains CO_2 x drought interaction in Eucalyptus saligna. Tree Physiol 31:922–931. https://doi.org/10.1093/treephys/tpr030

Eamus D (1991) The interaction of rising CO_2 and temperatures with water use efficiency. Plant Cell Environ 14:843–852. https://doi.org/10.1111/j.1365-3040.1991.tb01447.x

Eder F, Roo F de, Rotenberg E, Yakir D, Schmid HP, Mauder M (2015) Secondary circulations at a solitary forest surrounded by semi-arid shrubland and their impact on eddy-covariance measurements. Agricultural and Forest Meteorology 211-212:115–127. https://doi.org/10.1016/j.agrformet.2015.06.001

Eisenhut M, Bräutigam A, Timm S, Florian A, Tohge T, Fernie AR, Bauwe H, Weber APM (2017) Photorespiration Is Crucial for Dynamic Response of Photosynthetic Metabolism and Stomatal Movement to Altered CO_2 Availability. Mol Plant 10:47–61. https://doi.org/10.1016/j.molp.2016.09.011

Eller ASD, Young LL, Trowbridge AM, Monson RK (2016) Differential controls by climate and physiology over the emission rates of biogenic volatile organic compounds from mature trees in a semi-arid pine forest. Oecologia 180:345–358. https://doi.org/10.1007/s00442-015-3474-4

Engineer CB, Ghassemian M, Anderson JC, Peck SC, Hu H, Schroeder JI (2014) Carbonic anhydrases, EPF2 and a novel protease mediate CO_2 control of stomatal development. Nature 513:246–250. https://doi.org/10.1038/nature13452

Engineer CB, Hashimoto-Sugimoto M, Negi J, Israelsson-Nordström M, Azoulay-Shemer T, Rappel W-J, Iba K, Schroeder JI (2016) CO_2 Sensing and CO_2 Regulation of Stomatal Conductance: Advances and Open Questions. Trends Plant Sci 21:16–30. https://doi.org/10.1016/j.tplants.2015.08.014

Escandón M, Cañal MJ, Pascual J, Pinto G, Correia B, Amaral J, Meijón M (2016) Integrated physiological and hormonal profile of heat-induced thermotolerance in *Pinus radiata*. Tree Physiol 36:63–77. https://doi.org/10.1093/treephys/tpv127

Escandón M, Valledor L, Pascual J, Pinto G, Cañal MJ, Meijón M (2017) System-wide analysis of short-term response to high temperature in *Pinus radiata*. J Exp Bot 68:3629–3641. https://doi.org/10.1093/jxb/erx198

Fall R (2003) Abundant oxygenates in the atmosphere: a biochemical perspective. Chem Rev 103:4941–4952. https://doi.org/10.1021/cr0206521

Fall R, Karl T, Hansel A, Jordan A, Lindinger W (1999) Volatile organic compounds emitted after leaf wounding: On-line analysis by proton-transfer-reaction mass spectrometry. J. Geophys. Res. 104:15963–15974. https://doi.org/10.1029/1999JD900144

Farquhar GD, Caemmerer S von, Berry JA (1980) A biochemical model of photosynthetic CO_2 assimilation in leaves of C 3 species. Planta 149:78–90. https://doi.org/10.1007/BF00386231

Fauset S, Oliveira L, Buckeridge MS, Foyer CH, Galbraith D, Tiwari R, Gloor M (2019) Contrasting responses of stomatal conductance and photosynthetic capacity to warming and elevated CO_2 in the tropical tree species *Alchornea glandulosa* under heatwave conditions. Environmental and Experimental Botany 158:28–39. https://doi.org/10.1016/j.envexpbot.2018.10.030

Fernie AR, Carrari F, Sweetlove LJ (2004) Respiratory metabolism: glycolysis, the TCA cycle and mitochondrial electron transport. Current Opinion in Plant Biology 7:254–261. https://doi.org/10.1016/j.pbi.2004.03.007

Filella I, Peñuelas J, Llusià J (2006) Dynamics of the enhanced emissions of monoterpenes and methyl salicylate, and decreased uptake of formaldehyde, by *Quercus ilex* leaves after application of jasmonic acid. New Phytol 169:135–144. https://doi.org/10.1111/j.1469-8137.2005.01570.x

Filella I, Penuelas J, Seco R (2009) Short-chained oxygenated VOC emissions in *Pinus halepensis* in response to changes in water availability. Acta Physiol Plant 31:311–318. https://doi.org/10.1007/s11738-008-0235-6

Fischer S, Hanf S, Frosch T, Gleixner G, Popp J, Trumbore S, Hartmann H (2015) *Pinus sylvestris* switches respiration substrates under shading but not during drought. New Phytol 207:542–550. https://doi.org/10.1111/nph.13452

Fischer RA, Turner NC (1978) Plant Productivity in the Arid and Semiarid Zones. Annu. Rev. Plant. Physiol. 29:277–317. https://doi.org/10.1146/annurev.pp.29.060178.001425

Fleischer K, Rammig A, Kauwe MG de, Walker AP, Domingues TF, Fuchslueger L, Garcia S, Goll DS, Grandis A, Jiang M, Haverd V, Hofhansl F, Holm JA, Kruijt B, Leung F, Medlyn BE, Mercado LM, Norby RJ, Pak B, Randow C von, Quesada CA, Schaap KJ, Valverde-Barrantes OJ, Wang Y-P, Yang X, Zaehle S, Zhu Q, Lapola DM (2019) Amazon forest response to CO_2 fertilization dependent on plant phosphorus acquisition. Nat. Geosci. 12:736–741. https://doi.org/10.1038/s41561-019-0404-9

Folland CK, Boucher O, Colman A, Parker DE (2018) Causes of irregularities in trends of global mean surface temperature since the late 19th century. Sci Adv 4:eaao5297. https://doi.org/10.1126/sciadv.aao5297

Fontes CG, Dawson TE, Jardine K, McDowell N, Gimenez BO, Anderegg L, Negrón-Juárez R, Higuchi N, Fine PVA, Araújo AC, Chambers JQ (2018) Dry and hot: the hydraulic consequences of a climate change-type drought for Amazonian trees. Philos Trans R Soc Lond , B, Biol Sci 373. https://doi.org/10.1098/rstb.2018.0209

Foyer CH, Noctor G (2011) Ascorbate and glutathione: the heart of the redox hub. Plant Physiol 155:2–18. https://doi.org/10.1104/pp.110.167569

Frank D, Reichstein M, Bahn M, Thonicke K, Frank D, Mahecha MD, Smith P, van der Velde M, Vicca S, Babst F, Beer C, Buchmann N, Canadell JG, Ciais P, Cramer W, Ibrom A, Miglietta F, Poulter B, Rammig A, Seneviratne SI, Walz A, Wattenbach M, Zavala MA, Zscheischler J (2015) Effects of climate extremes on the terrestrial carbon cycle: concepts, processes and potential future impacts. Global Change Biology 21:2861–2880. https://doi.org/10.1111/gcb.12916

Friedli H, Lötscher H, Oeschger H, Siegenthaler U, Stauffer B (1986) Ice core record of the 13C/12C ratio of atmospheric CO_2 in the past two centuries. Nature 324:237–238. https://doi.org/10.1038/324237a0

Friedlingstein P, Jones MW, O'Sullivan M, Andrew RM, Hauck J, Peters GP, Peters W, Pongratz J, Sitch S, Le Quéré C, Bakker DCE, Canadell JG, Ciais P, Jackson RB, Anthoni P, Barbero L, Bastos A, Bastrikov V, Becker M, Bopp L, Buitenhuis E, Chandra N, Chevallier F, Chini LP, Currie KI, Feely RA, Gehlen M, Gilfillan D, Gkritzalis T, Goll DS, Gruber N, Gutekunst S, Harris I, Haverd V, Houghton RA, Hurtt G, Ilyina T, Jain AK, Joetzjer E, Kaplan JO, Kato E, Klein Goldewijk K, Korsbakken JI, Landschützer P, Lauvset SK, Lefèvre N, Lenton A, Lienert S, Lombardozzi D, Marland G, McGuire PC, Melton JR, Metzl N, Munro DR, Nabel, Julia E. M. S., Nakaoka S-i, Neill C, Omar AM, Ono T, Peregon

A, Pierrot D, Poulter B, Rehder G, Resplandy L, Robertson E, Rödenbeck C, Séférian R, Schwinger J, Smith N, Tans PP, Tian H, Tilbrook B, Tubiello FN, van der Werf, Guido R., Wiltshire AJ, Zaehle S (2019) Global Carbon Budget 2019. Earth Syst. Sci. Data 11:1783–1838. https://doi.org/10.5194/essd-11-1783-2019

Fuentes J, Hayden B, Garstang M, Lerdau M, Fitzjarrald D, Baldocchi D, Monson R, Lamb B, Geron C (2001) New Directions: VOCs and biosphere–atmosphere feedbacks. Atmospheric Environment 35:189–191. https://doi.org/10.1016/S1352-2310(00)00365-4

Fürtauer L, Weckwerth W, Nägele T (2016) A Benchtop Fractionation Procedure for Subcellular Analysis of the Plant Metabolome. Front Plant Sci 7:1912. https://doi.org/10.3389/fpls.2016.01912

Fürtauer L, Pschenitschnigg A, Scharkosi H, Weckwerth W, Nägele T (2018) Combined multivariate analysis and machine learning reveals a predictive module of metabolic stress response in Arabidopsis thaliana. Mol Omics 14:437–449. https://doi.org/10.1039/c8mo00095f

Fürtauer L, Küstner L, Weckwerth W, Heyer AG, Nägele T (2019) Resolving subcellular plant metabolism. Plant J 100:438–455. https://doi.org/10.1111/tpj.14472

Galiano L, Timofeeva G, Saurer M, Siegwolf R, Martínez-Vilalta J, Hommel R, Gessler A (2017) The fate of recently fixed carbon after drought release: towards unravelling C storage regulation in *Tilia platyphyllos* and *Pinus sylvestris*. Plant Cell Environ. https://doi.org/10.1111/pce.12972

Gamage D, Thompson M, Sutherland M, Hirotsu N, Makino A, Seneweera S (2018) New insights into the cellular mechanisms of plant growth at elevated atmospheric carbon dioxide concentrations. Plant Cell Environ 41:1233–1246. https://doi.org/10.1111/pce.13206

Garcia-Forner N, Adams HD, Sevanto S, Collins AD, Dickman LT, Hudson PJ, Zeppel MJB, Jenkins MW, Powers H, Martínez-Vilalta J, McDowell NG (2016) Responses of two semiarid conifer tree species to reduced precipitation and warming reveal new perspectives for stomatal regulation. Plant Cell Environ 39:38–49. https://doi.org/10.1111/pce.12588

Gattmann M, Birami B, Nadal-Sala D, Ruehr NK (2021) Dying by drying: timing of physiological stress thresholds related to tree death is not significantly altered by highly elevated CO_2 in Aleppo pine. Plant Cell Environ. 44:356–370. https://doi.org/10.1111/pce.13937

Gauthier PPG, Crous KY, Ayub G, Duan H, Weerasinghe LK, Ellsworth DS, Tjoelker MG, Evans JR, Tissue DT, Atkin OK (2014) Drought increases heat tolerance of leaf respiration in *Eucalyptus globulus* saplings grown under both ambient and elevated atmospheric CO_2 and temperature. J Exp Bot 65:6471–6485. https://doi.org/10.1093/jxb/eru367

Geddes JA, Heald CL, Silva SJ, Martin RV (2016) Land cover change impacts on atmospheric chemistry: Simulating projected large-scale tree mortality in the United States. Atmos. Chem. Phys. 16:2323–2340. https://doi.org/10.5194/acp-16-2323-2016

Geng S, Misra BB, Armas E de, Huhman DV, Alborn HT, Sumner LW, Chen S (2016) Jasmonate-mediated stomatal closure under elevated CO_2 revealed by time-resolved metabolomics. Plant J 88:947–962. https://doi.org/10.1111/tpj.13296

Gentine P, Guérin M, Uriarte M, McDowell NG, Pockman WT (2016) An allometry-based model of the survival strategies of hydraulic failure and carbon starvation. Ecohydrol. 9:529–546. https://doi.org/10.1002/eco.1654

Ghirardo A, Koch K, Taipale R, Zimmer I, Schnitzler J-P, Rinne J (2010) Determination of de novo and pool emissions of terpenes from four common boreal/alpine trees by $13CO_2$ labelling and PTR-MS analysis. Plant Cell Environ 33:781–792. https://doi.org/10.1111/j.1365-3040.2009.02104.x

Ghirardo A, Heller W, Fladung M, Schnitzler J-P, Schroeder H (2012) Function of defensive volatiles in pedunculate oak (*Quercus robur*) is tricked by the moth *Tortrix viridana*. Plant Cell Environ 35:2192–2207. https://doi.org/10.1111/j.1365-3040.2012.02545.x

Ghirardo A, Wright LP, Bi Z, Rosenkranz M, Pulido P, Rodríguez-Concepción M, Niinemets Ü, Brüggemann N, Gershenzon J, Schnitzler J-P (2014) Metabolic flux analysis of plastidic isoprenoid biosynthesis in poplar leaves emitting and nonemitting isoprene. Plant Physiol 165:37–51. https://doi.org/10.1104/pp.114.236018

Ghirardo A, Lindstein F, Koch K, Buegger F, Schloter M, Albert A, Michelsen A, Winkler JB, Schnitzler J-P, Rinnan R (2020) Origin of volatile organic compound emissions from subarctic tundra under global warming. Global Change Biology 26:1908–1925. https://doi.org/10.1111/gcb.14935

Gimeno TE, Crous KY, Cooke J, O'Grady AP, Ósvaldsson A, Medlyn BE, Ellsworth DS, Whitehead D (2016) Conserved stomatal behaviour under elevated CO_2 and varying water availability in a mature woodland. Funct Ecol 30:700–709. https://doi.org/10.1111/1365-2435.12532

Giorgi F, Lionello P (2008) Climate change projections for the Mediterranean region. Global and Planetary Change 63:90–104. https://doi.org/10.1016/j.gloplacha.2007.09.005

Giraud C (2015) Introduction to high-dimensional statistics. A Chapman & Hall book, vol 139. CRC Press, Boca Raton

Goldstein AH, Hultman NE, Fracheboud JM, Bauer MR, Panek JA, Xu M, Qi Y, Guenther AB, Baugh W (2000) Effects of climate variability on the carbon dioxide, water, and sensible heat fluxes above a ponderosa pine plantation in the Sierra Nevada (CA). Agricultural and Forest Meteorology 101:113–129. https://doi.org/10.1016/S0168-1923(99)00168-9

Gonzalez P, Neilson RP, Lenihan JM, Drapek RJ (2010) Global patterns in the vulnerability of ecosystems to vegetation shifts due to climate change. Global Ecology and Biogeography 19:755–768. https://doi.org/10.1111/j.1466-8238.2010.00558.x

Gonzalez P, Tucker CJ, Sy H (2012) Tree density and species decline in the African Sahel attributable to climate. Journal of Arid Environments 78:55–64. https://doi.org/10.1016/j.jaridenv.2011.11.001

Gonzalez-Meler MA, Taneva L, Trueman RJ (2004) Plant respiration and elevated atmospheric CO_2 concentration: cellular responses and global significance. Annals of Botany 94:647–656. https://doi.org/10.1093/aob/mch189

Gouw JA de, Howard CJ, Custer TG, Fall R (1999) Emissions of volatile organic compounds from cut grass and clover are enhanced during the drying process. Geophys. Res. Lett. 26:811–814. https://doi.org/10.1029/1999GL900076

Grainger A, Iverson LR, Marland GH, Prasad A (2019) Comment on "The global tree restoration potential". Science 366. https://doi.org/10.1126/science.aay8334

Grandpré L de, Kneeshaw DD, Perigon S, Boucher D, Marchand M, Pureswaran D, Girardin MP, Chen H (2018) Adverse climatic periods precede and amplify defoliator-induced tree mortality in eastern boreal North America. J Ecol 107:452–467. https://doi.org/10.1111/1365-2745.13012

Grote R, Morfopoulos C, Niinemets Ü, Sun Z, Keenan TF, Pacifico F, Butler T (2014) A fully integrated isoprenoid emissions model coupling emissions to photosynthetic characteristics. Plant Cell Environ 37:1965–1980. https://doi.org/10.1111/pce.12326

Grote R, Gessler A, Hommel R, Poschenrieder W, Priesack E (2016) Importance of tree height and social position for drought-related stress on tree growth and mortality. Trees 30:1467–1482. https://doi.org/10.1007/s00468-016-1446-x

Grote R, Sharma M, Ghirardo A, Schnitzler J-P (2019) A New Modeling Approach for Estimating Abiotic and Biotic Stress-Induced de novo Emissions of Biogenic Volatile Organic Compounds From Plants. Front. For. Glob. Change 2:224. https://doi.org/10.3389/ffgc.2019.00026

Grünzweig JM, Hemming D, Maseyk K, Lin T, Rotenberg E, Raz-Yaseef N, Falloon PD, Yakir D (2009) Water limitation to soil CO_2 efflux in a pine forest at the semiarid “timberline”. J. Geophys. Res. 114. https://doi.org/10.1029/2008JG000874

Guenther AB, Zimmerman PR, Harley PC, Monson RK, Fall R (1993) Isoprene and monoterpene emission rate variability: Model evaluations and sensitivity analyses. J. Geophys. Res. 98:12609. https://doi.org/10.1029/93JD00527

Guha A, Han J, Cummings C, McLennan DA, Warren JM (2018) Differential ecophysiological responses and resilience to heat wave events in four co-occurring temperate tree species. Environ. Res. Lett. 13:65008. https://doi.org/10.1088/1748-9326/aabcd8

Guidolotti G, Pallozzi E, Gavrichkova O, Scartazza A, Mattioni M, Loreto F, Calfapietra C (2019) Emission of constitutive isoprene, induced monoterpenes, and other volatiles under high temperatures in Eucalyptus camaldulensis: A 13 C labelling study. Plant Cell Environ 42:1929–1938. https://doi.org/10.1111/pce.13521

Gupta A, Rico-Medina A, Caño-Delgado AI (2020) The physiology of plant responses to drought. Science 368:266–269. https://doi.org/10.1126/science.aaz7614

Haak DC, Fukao T, Grene R, Hua Z, Ivanov R, Perrella G, Li S (2017) Multilevel Regulation of Abiotic Stress Responses in Plants. Front Plant Sci 8:1564. https://doi.org/10.3389/fpls.2017.01564

Haldimann P, Feller U (2004) Inhibition of photosynthesis by high temperature in oak (*Quercus pubescens* L.) leaves grown under natural conditions closely correlates with a reversible heat-dependent reduction of the activation state of ribulose-1,5-bisphosphate carboxylase/oxygenase. Plant Cell Environ 27:1169–1183. https://doi.org/10.1111/j.1365-3040.2004.01222.x

Hamerlynck EP, Huxman TE, Loik ME, Smith SD (2000) Effects of extreme high temperature, drought and elevated CO_2 on photosynthesis of the Mojave Desert evergreen shrub, Larrea tridentata. Plant Ecology 148:183–193. https://doi.org/10.1023/A:1009896111405

Hamilton EW (2001) Mitochondrial adaptations to NaCl. Complex I is protected by anti-oxidants and small heat shock proteins, whereas Complex II is protected by proline and betaine. Plant Physiol 126:1266–1274. https://doi.org/10.1104/pp.126.3.1266

Hammond WM, Yu K, Wilson LA, Will RE, Anderegg WRL, Adams HD (2019) Dead or dying? Quantifying the point of no return from hydraulic failure in drought-induced tree mortality. New Phytol 223:1834–1843. https://doi.org/10.1111/nph.15922

Hao G-Y, Holbrook NM, Zwieniecki MA, Gutschick VP, BassiriRad H (2018) Coordinated responses of plant hydraulic architecture with the reduction of stomatal conductance under elevated CO_2 concentration. Tree Physiol 38:1041–1052. https://doi.org/10.1093/treephys/tpy001

Harfouche A, Meilan R, Altman A (2014) Molecular and physiological responses to abiotic stress in forest trees and their relevance to tree improvement. Tree Physiol 34:1181–1198. https://doi.org/10.1093/treephys/tpu012

Harley P, Fridd-Stroud V, Greenberg J, Guenther A, Vasconcellos P (1998) Emission of 2-methyl-3-buten-2-ol by pines: A potentially large natural source of reactive carbon to the atmosphere. J. Geophys. Res. 103:25479–25486. https://doi.org/10.1029/98JD00820

Harley P, Eller A, Guenther A, Monson RK (2014) Observations and models of emissions of volatile terpenoid compounds from needles of ponderosa pine trees growing in situ: control by light, temperature and stomatal conductance. Oecologia 176:35–55. https://doi.org/10.1007/s00442-014-3008-5

Harper KL, Unger N (2018) Global climate forcing driven by altered BVOC fluxes from 1990 to 2010 land cover change in maritime Southeast Asia. Atmos. Chem. Phys. 18:16931–16952. https://doi.org/10.5194/acp-18-16931-2018

Hartmann H, Trumbore S (2016) Understanding the roles of nonstructural carbohydrates in forest trees - from what we can measure to what we want to know. New Phytol 211:386–403. https://doi.org/10.1111/nph.13955

Hartmann H, Schuldt B, Sanders TGM, Macinnis-Ng C, Boehmer HJ, Allen CD, Bolte A, Crowther TW, Hansen MC, Medlyn BE, Ruehr NK, Anderegg WRL (2018a) Monitoring global tree mortality patterns and trends. Report from the VW symposium 'Crossing scales and disciplines to identify global trends of tree mortality as indicators of forest health'. New Phytol 217:984–987. https://doi.org/10.1111/nph.14988

Hartmann H, Moura CF, Anderegg WRL, Ruehr NK, Salmon Y, Allen CD, Arndt SK, Breshears DD, Davi H, Galbraith D, Ruthrof KX, Wunder J, Adams HD, Bloemen J, Cailleret M, Cobb RC, Gessler A, Grams TEE, Jansen S, Kautz M, Lloret F, O'Brien M (2018b) Research frontiers for improving our understanding of drought-induced tree and forest mortality. New Phytol 218:15–28. https://doi.org/10.1111/nph.15048

Hartmann H, Adams HD, Hammond WM, Hoch G, Landhäusser SM, Wiley E, Zaehle S (2018c) Identifying differences in carbohydrate dynamics of seedlings and mature trees to improve carbon allocation in models for trees and forests. Environmental and Experimental Botany. https://doi.org/10.1016/j.envexpbot.2018.03.011

Harvey CM, Sharkey TD (2016) Exogenous isoprene modulates gene expression in unstressed *Arabidopsis thaliana* plants. Plant Cell Environ 39:1251–1263. https://doi.org/10.1111/pce.12660

Hausfather Z, Peters GP (2020) Emissions – the 'business as usual' story is misleading. Nature 577:618–620. https://doi.org/10.1038/d41586-020-00177-3

Havaux M, Tardy, F. Ravenel, J., Chanu, D. and Parot, P. (1996) Thylakoid membrane stability to heat stress studied by flash spectroscopic measurements of the electrochromic shift in intact potato leaves: influence of the xanthophyll content. Plant Cell Environ 19:1359–1368. https://doi.org/10.1111/j.1365-3040.1996.tb00014.x

Hayat S, Hayat Q, Alyemeni MN, Wani AS, Pichtel J, Ahmad A (2012) Role of proline under changing environments: a review. Plant Signal Behav 7:1456–1466. https://doi.org/10.4161/psb.21949

Hays LM, Crowe JH, Wolkers W, Rudenko S (2001) Factors affecting leakage of trapped solutes from phospholipid vesicles during thermotropic phase transitions. Cryobiology 42:88–102. https://doi.org/10.1006/cryo.2001.2307

Heil M, Ton J (2008) Long-distance signalling in plant defence. Trends Plant Sci 13:264–272. https://doi.org/10.1016/j.tplants.2008.03.005

Higaki T, Akita K, Hasezawa S (2020) Elevated CO_2 promotes satellite stomata production in young cotyledons of *Arabidopsis thaliana*. Genes Cells 25:475–482. https://doi.org/10.1111/gtc.12773

Higgins SI, Buitenwerf R, Moncrieff GR (2016) Defining functional biomes and monitoring their change globally. Global Change Biology 22:3583–3593. https://doi.org/10.1111/gcb.13367

Hincha DK, Höfner R, Schwab KB, Heber U, Schmitt JM (1987) Membrane rupture is the common cause of damage to chloroplast membranes in leaves injured by freezing or excessive wilting. Plant Physiol 83:251–253

Hincha DK, Livingston DP, Premakumar R, Zuther E, Obel N, Cacela C, Heyer AG (2007) Fructans from oat and rye: composition and effects on membrane stability during drying. Biochim Biophys Acta 1768:1611–1619. https://doi.org/10.1016/j.bbamem.2007.03.011

Hoch G, Richter A, Körner C (2003) Non-structural carbon compounds in temperate forest trees. Plant Cell Environ 26:1067–1081. https://doi.org/10.1046/j.0016-8025.2003.01032.x

Holopainen JK, Virjamo V, Ghimire RP, Blande JD, Julkunen-Tiitto R, Kivimäenpää M (2018) Climate Change Effects on Secondary Compounds of Forest Trees in the Northern Hemisphere. Front Plant Sci 9:1445. https://doi.org/10.3389/fpls.2018.01445

Hsiao TC (1973) Plant Responses to Water Stress. Annu. Rev. Plant. Physiol. 24:519–570. https://doi.org/10.1146/annurev.pp.24.060173.002511

Huang B, Rachmilevitch S, Xu J (2012) Root carbon and protein metabolism associated with heat tolerance. J Exp Bot 63:3455–3465. https://doi.org/10.1093/jxb/ers003

Hussain M, Kubiske ME, Connor KF (2001) Germination of CO_2-enriched *Pinus taeda* L. seeds and subsequent seedling growth responses to CO_2 enrichment. Funct Ecology 15:344–350. https://doi.org/10.1046/j.1365-2435.2001.00521.x

Hüve K, Bichele I, Rasulov B, Niinemets U (2011) When it is too hot for photosynthesis: heat-induced instability of photosynthesis in relation to respiratory burst, cell permeability changes and H_2O_2 formation. Plant Cell Environ 34:113–126. https://doi.org/10.1111/j.1365-3040.2010.02229.x

Hymus GJ, Baker NR, Long SP (2001) Growth in Elevated CO $_2$ Can Both Increase and Decrease Photochemistry and Photoinhibition of Photosynthesis in a Predictable Manner. *Dactylis glomerata* Grown in Two Levels of Nitrogen Nutrition. Plant Physiol. 127:1204–1211. https://doi.org/10.1104/pp.010248

Hymus GJ, Snead TG, Johnson DP, Hungate BA, Drake BG (2002) Acclimation of photosynthesis and respiration to elevated atmospheric CO_2 in two Scrub Oaks. Global Change Biol 8:317–328. https://doi.org/10.1046/j.1354-1013.2001.00472.x

Iordachescu M, Imai R (2008) Trehalose biosynthesis in response to abiotic stresses. J Integr Plant Biol 50:1223–1229. https://doi.org/10.1111/j.1744-7909.2008.00736.x

Isson TT, Planavsky NJ, Coogan LA, Stewart EM, Ague JJ, Bolton EW, Zhang S, McKenzie NR, Kump LR (2020) Evolution of the Global Carbon Cycle and Climate Regulation on Earth. Global Biogeochem. Cycles 34:45. https://doi.org/10.1029/2018GB006061

Jacob DJ (2005) Global budget of methanol: Constraints from atmospheric observations. J. Geophys. Res. 110:955. https://doi.org/10.1029/2004JD005172

Jaindl M, Popp M (2006) Cyclitols protect glutamine synthetase and malate dehydrogenase against heat induced deactivation and thermal denaturation. Biochem Biophys Res Commun 345:761–765. https://doi.org/10.1016/j.bbrc.2006.04.144

Janson R, Serves C de (2001) Acetone and monoterpene emissions from the boreal forest in northern Europe. Atmospheric Environment 35:4629–4637. https://doi.org/10.1016/S1352-2310(01)00160-1

Janz D, Behnke K, Schnitzler J-P, Kanawati B, Schmitt-Kopplin P, Polle A (2010) Pathway analysis of the transcriptome and metabolome of salt sensitive and tolerant poplar species reveals evolutionary adaption of stress tolerance mechanisms. BMC Plant Biol 10:150. https://doi.org/10.1186/1471-2229-10-150

Jardine KJ, Chambers JQ, Holm J, Jardine AB, Fontes CG, Zorzanelli RF, Meyers KT, Souza VF de, Garcia S, Gimenez BO, Piva, Luani R de O, Higuchi N, Artaxo P, Martin S, Manzi AO (2015) Green Leaf Volatile Emissions during High Temperature and Drought Stress in a Central Amazon Rainforest. Plants (Basel) 4:678–690. https://doi.org/10.3390/plants4030678

Jardine KJ, Jardine AB, Holm JA, Lombardozzi DL, Negron-Juarez RI, Martin ST, Beller HR, Gimenez BO, Higuchi N, Chambers JQ (2017) Monoterpene 'thermometer' of tropical forest-atmosphere response to climate warming. Plant Cell Environ 40:441–452. https://doi.org/10.1111/pce.12879

Jarvi MP, Burton AJ (2018) Adenylate control contributes to thermal acclimation of sugar maple fine-root respiration in experimentally warmed soil. Plant Cell Environ 41:504–516. https://doi.org/10.1111/pce.13098

Jarvis PG (1976) The interpretation of the variations in leaf water potential and stomatal conductance found in canopies in the field. Philosophical Transactions of the Royal Society B: Biological Sciences 273:593–610. https://doi.org/10.1098/rstb.1976.0035

Jensen KH, Berg-Sørensen K, Bruus H, Holbrook NM, Liesche J, Schulz A, Zwieniecki MA, Bohr T (2016) Sap flow and sugar transport in plants. Rev. Mod. Phys. 88:320. https://doi.org/10.1103/RevModPhys.88.035007

Jiang M, Medlyn BE, Drake JE, Duursma RA, Anderson IC, Barton CVM, Boer MM, Carrillo Y, Castañeda-Gómez L, Collins L, Crous KY, Kauwe MG de, Dos Santos BM, Emmerson KM, Facey SL, Gherlenda AN, Gimeno TE, Hasegawa S, Johnson SN, Känneste A, Macdonald CA, Mahmud K, Moore BD, Nazaries L, Neilson EHJ, Nielsen UN, Niinemets Ü, Noh NJ, Ochoa-Hueso R, Pathare VS, Pendall E, Pihlblad J, Piñeiro J, Powell JR, Power SA, Reich PB, Renchon AA, Riegler M, Rinnan R, Rymer PD, Salomón RL, Singh BK, Smith B, Tjoelker MG, Walker JKM, Wujeska-Klause A, Yang J, Zaehle S, Ellsworth DS (2020) The fate of carbon in a mature forest under carbon dioxide enrichment. Nature 580:227–231. https://doi.org/10.1038/s41586-020-2128-9

Joensuu J, Altimir N, Hakola H, Rostás M, Raivonen M, Vestenius M, Aaltonen H, Riederer M, Bäck J (2016) Role of needle surface waxes in dynamic exchange of mono- and sesquiterpenes. Atmos. Chem. Phys. 16:7813–7823. https://doi.org/10.5194/acp-16-7813-2016

Johnson DJ, Needham J, Xu C, Massoud EC, Davies SJ, Anderson-Teixeira KJ, Bunyavejchewin S, Chambers JQ, Chang-Yang C-H, Chiang J-M, Chuyong GB, Condit R, Cordell S, Fletcher C, Giardina CP, Giambelluca TW, Gunatilleke N, Gunatilleke S, Hsieh C-F, Hubbell S, Inman-Narahari F, Kassim AR, Katabuchi M, Kenfack D, Litton CM, Lum S, Mohamad M, Nasardin M, Ong PS, Ostertag R, Sack L, Swenson NG, Sun IF, Tan S, Thomas DW, Thompson J, Umaña MN, Uriarte M, Valencia R, Yap S, Zimmerman J, McDowell NG, McMahon SM (2018) Climate sensitive size-dependent survival in tropical trees. Nat Ecol Evol 2:1436–1442. https://doi.org/10.1038/s41559-018-0626-z

Johnson RM, Pregitzer KS (2007) Concentration of sugars, phenolic acids, and amino acids in forest soils exposed to elevated atmospheric CO_2 and O3. Soil Biology and Biochemistry 39:3159–3166. https://doi.org/10.1016/j.soilbio.2007.07.010

Johnson DM, Wortemann R, McCulloh KA, Jordan-Meille L, Ward E, Warren JM, Palmroth S, Domec J-C (2016) A test of the hydraulic vulnerability segmentation hypothesis in angiosperm and conifer tree species. Tree Physiol 36:983–993. https://doi.org/10.1093/treephys/tpw031

Joó É, Dewulf J, Amelynck C, Schoon N, Pokorska O, Šimpraga M, Steppe K, Aubinet M, van Langenhove H (2011) Constitutive versus heat and biotic stress induced BVOC emissions in *Pseudotsuga menziesii*. Atmospheric Environment 45:3655–3662. https://doi.org/10.1016/j.atmosenv.2011.04.048

Jordan DB, Ogren WL (1984) The CO_2/O_2 specificity of ribulose 1,5-bisphosphate carboxylase/oxygenase: Dependence on ribulosebisphosphate concentration, pH and temperature. Planta 161:308–313. https://doi.org/10.1007/BF00398720

Jud W, Vanzo E, Li Z, Ghirardo A, Zimmer I, Sharkey TD, Hansel A, Schnitzler J-P (2016) Effects of heat and drought stress on post-illumination bursts of volatile organic compounds in isoprene-emitting and non-emitting poplar. Plant Cell Environ 39:1204–1215. https://doi.org/10.1111/pce.12643

Kanduč M, Schneck E, Loche P, Jansen S, Schenk HJ, Netz RR (2020) Cavitation in lipid bilayers poses strict negative pressure stability limit in biological liquids. Proc Natl Acad Sci U S A 117:10733–10739. https://doi.org/10.1073/pnas.1917195117

Karl T, Curtis AJ, Rosenstiel TN, Monson RK, Fall R (2002) Transient releases of acetaldehyde from tree leaves - products of a pyruvate overflow mechanism? Plant Cell Environ 25:1121–1131. https://doi.org/10.1046/j.1365-3040.2002.00889.x

Karl T, Guenther A, Turnipseed A, Patton EG, Jardine K (2008) Chemical sensing of plant stress at the ecosystem scale. Biogeosciences 5:1287–1294. https://doi.org/10.5194/bg-5-1287-2008

Kauwe MG de, Medlyn BE, Zaehle S, Walker AP, Dietze MC, Hickler T, Jain AK, Luo Y, Parton WJ, Prentice IC, Smith B, Thornton PE, Wang S, Wang Y-P, Wårlind D, Weng E, Crous KY, Ellsworth DS, Hanson PJ, Seok Kim H, Warren JM, Oren R, Norby RJ (2013) Forest water use and water use efficiency at elevated CO_2: A model-data intercomparison at two contrasting temperate forest FACE sites. Global Change Biology 19:1759–1779. https://doi.org/10.1111/gcb.12164

Kauwe MG de, Medlyn BE, Pitman AJ, Drake JE, Ukkola A, Griebal A, Pendall E, Prober S, Roderick M (2018) Examining the evidence for sustained transpiration during heat extremes. Biogeosciences Discuss.:1–17. https://doi.org/10.5194/bg-2018-399

Kauwe MG de, Medlyn BE, Ukkola AM, Mu M, Sabot MEB, Pitman AJ, Meir P, Cernusak L, Rifai SW, Choat B, Tissue DT, Blackman CJ, Li X, Roderick M, Briggs PR (2020) Identifying areas at risk of drought-induced tree mortality across South-Eastern Australia. Global Change Biology. https://doi.org/10.1111/gcb.15215

Kauzmann W (1959) Some Factors in the Interpretation of Protein Denaturation. In: Advances in Protein Chemistry Volume 14, vol 14. Elsevier, pp 1–63

Keenan TF, Williams CA (2018) The Terrestrial Carbon Sink. Annu. Rev. Environ. Resour. 43:219–243. https://doi.org/10.1146/annurev-environ-102017-030204

Keenan TF, Luo X, Zhang Y, Zhou S (2020) Ecosystem aridity and atmospheric CO_2. Science 368:251–252. https://doi.org/10.1126/science.abb5449

Kelsey RG, Joseph G, McWilliams MG (2011) Ethanol synthesis by anoxic root segments from five cedar species relates to their habitat attributes but not their known differences in vulnerability to Phytophthora lateralis root disease. Can. J. For. Res. 41:1202–1211. https://doi.org/10.1139/X11-043

Kim J-M, Sasaki T, Ueda M, Sako K, Seki M (2015) Chromatin changes in response to drought, salinity, heat, and cold stresses in plants. Front Plant Sci 6:114. https://doi.org/10.3389/fpls.2015.00114

Kimmerer TW, Stringer MA (1988) Alcohol dehydrogenase and ethanol in the stems of trees: Evidence for anaerobic metabolism in the vascular cambium. Plant Physiol 87:693–697. https://doi.org/10.1104/pp.87.3.693

Kitao M, Lei TT, Koike T, Tobita H, Maruyama Y, Matsumoto Y, Ang L-H (2000) Temperature response and photoinhibition investigated by chlorophyll fluorescence measurements for four distinct species of dipterocarp trees. Physiol Plant 109:284–290. https://doi.org/10.1034/j.1399-3054.2000.100309.x

Kivimäenpää M, Babalola AB, Joutsensaari J, Holopainen JK (2020) Methyl Salicylate and Sesquiterpene Emissions Are Indicative for Aphid Infestation on Scots Pine. Forests 11:573. https://doi.org/10.3390/f11050573

Klein T, Niu S (2014) The variability of stomatal sensitivity to leaf water potential across tree species indicates a continuum between isohydric and anisohydric behaviours. Funct Ecol 28:1313–1320. https://doi.org/10.1111/1365-2435.12289

Klein T, Cohen S, Yakir D (2011) Hydraulic adjustments underlying drought resistance of *Pinus halepensis*. Tree Physiol 31:637–648. https://doi.org/10.1093/treephys/tpr047

Klein T, Bader MK, Leuzinger S, Mildner M, Schleppi P, Siegwolf RT, Körner C, Lines E (2016a) Growth and carbon relations of mature *Picea abies* trees under 5 years of free-air CO_2 enrichment. J Ecol 104:1720–1733. https://doi.org/10.1111/1365-2745.12621

Klein T, Rotenberg E, Tatarinov F, Yakir D (2016b) Association between sap flow-derived and eddy covariance-derived measurements of forest canopy CO_2 uptake. New Phytol 209:436–446. https://doi.org/10.1111/nph.13597

Klein T, Cahanovitc R, Sprintsin M, Herr N, Schiller G (2019) A nation-wide analysis of tree mortality under climate change: Forest loss and its causes in Israel 1948–2017. Forest Ecology and Management 432:840–849. https://doi.org/10.1016/j.foreco.2018.10.020

Kleist E, Mentel TF, Andres S, Bohne A, Folkers A, Kiendler-Scharr A, Rudich Y, Springer M, Tillmann R, Wildt J (2012) Irreversible impacts of heat on the emissions of monoterpenes, sesquiterpenes, phenolic BVOC and green leaf volatiles from several tree species. Biogeosciences 9:5111–5123. https://doi.org/10.5194/bg-9-5111-2012

Koch GW, Sillett SC, Jennings GM, Davis SD (2004) The limits to tree height. Nature 428:851–854. https://doi.org/10.1038/nature02417

Kolb T, Dore S, Montes-Helu M (2013) Extreme late-summer drought causes neutral annual carbon balance in southwestern ponderosa pine forests and grasslands. Environ. Res. Lett. 8:15015. https://doi.org/10.1088/1748-9326/8/1/015015

Kolb PF, Robberecht R (1996) High temperature and drought stress effects on survival of *Pinus ponderosa* seedlings. Tree Physiol 16:665–672. https://doi.org/10.1093/treephys/16.8.665

Konrad W, Katul G, Roth-Nebelsick A (2020) Leaf temperature and its dependence on atmospheric CO_2 and leaf size. Geological Journal 30:258. https://doi.org/10.1002/gj.3757

Körner C (2006) Plant CO_2 responses: an issue of definition, time and resource supply. New Phytol 172:393–411. https://doi.org/10.1111/j.1469-8137.2006.01886.x

Körner C (2019) No need for pipes when the well is dry-a comment on hydraulic failure in trees. Tree Physiol 39:695–700. https://doi.org/10.1093/treephys/tpz030

Körner C, Asshoff R, Bignucolo O, Hättenschwiler S, Keel SG, Peláez-Riedl S, Pepin S, Siegwolf RTW, Zotz G (2005) Carbon flux and growth in mature deciduous forest trees exposed to elevated CO_2. Science 309:1360–1362. https://doi.org/10.1126/science.1113977

Kornhuber K, Osprey S, Coumou D, Petri S, Petoukhov V, Rahmstorf S, Gray L (2019) Extreme weather events in early summer 2018 connected by a recurrent hemispheric wave-7 pattern. Environ. Res. Lett. 14:54002. https://doi.org/10.1088/1748-9326/ab13bf

Korol L, Schiller G (1996) Relations between native Israeli and Jordanian Aleppo pine (*Pinus halepensis* Mill.) based on Allozyme analysis: A Note. Forest Genetics 3:197–202

Kramer DM, Avenson TJ, Edwards GE (2004) Dynamic flexibility in the light reactions of photosynthesis governed by both electron and proton transfer reactions. Trends Plant Sci 9:349–357. https://doi.org/10.1016/j.tplants.2004.05.001

Kravitz B, Guenther AB, Gu L, Karl T, Kaser L, Pallardy SG, Peñuelas J, Potosnak MJ, Seco R (2016) A new paradigm of quantifying ecosystem stress through chemical signatures. Ecosphere 7:23. https://doi.org/10.1002/ecs2.1559

Kreidenweis U, Humpenöder F, Stevanović M, Bodirsky BL, Kriegler E, Lotze-Campen H, Popp A (2016) Afforestation to mitigate climate change: Impacts on food prices under consideration of albedo effects. Environ. Res. Lett. 11:85001. https://doi.org/10.1088/1748-9326/11/8/085001

Kreuzwieser J, Scheerer U, Rennenberg H (1999) Metabolic origin of acetaldehyde emitted by poplar (*Populus tremula* x *P. alba*) trees. J Exp Bot 50:757–765. https://doi.org/10.1093/jxb/50.335.757

Kruger NJ, Schaewen A von (2003) The oxidative pentose phosphate pathway: Structure and organisation. Current Opinion in Plant Biology 6:236–246. https://doi.org/10.1016/S1369-5266(03)00039-6

Ku SB, Edwards GE (1977a) Oxygen Inhibition of Photosynthesis: I. Temperature Dependence and Relation to O_2/CO_2 Solubility Ratio. Plant Physiol 59:986–990. https://doi.org/10.1104/pp.59.5.986

Ku SB, Edwards GE (1977b) Oxygen Inhibition of Photosynthesis: II. Kinetic Characteristics as Affected by Temperature. Plant Physiol 59:991–999. https://doi.org/10.1104/pp.59.5.991

Kuznetsova A, Brockhoff PB, Christensen RHB (2017) lmerTest Package: Tests in Linear Mixed Effects Models. Journal of statistical Software, 82 (13), 1-26. URL:http://doi.org/10.18637/jss.v082.i13

Lancaster LT, Humphreys AM (2020) Global variation in the thermal tolerances of plants. Proc Natl Acad Sci USA 117:13580–13587. https://doi.org/10.1073/pnas.1918162117

Lang-Pauluzzi I (2000) The behaviour of the plasma membrane during plasmolysis: a study by UV microscopy. J Microsc 198:188–198

Larigauderie A (1995) Acclimation of Leaf Dark Respiration to Temperature in Alpine and Lowland Plant Species. Annals of Botany 76:245–252. https://doi.org/10.1006/anbo.1995.1093

Lavergne A, Graven H, Kauwe MG de, Keenan TF, Medlyn BE, Prentice IC (2019) Observed and modelled historical trends in the water-use efficiency of plants and ecosystems. Global Change Biology 25:2242–2257. https://doi.org/10.1111/gcb.14634

Law BE, Hudiburg TW, Berner LT, Kent JJ, Buotte PC, Harmon ME (2018) Land use strategies to mitigate climate change in carbon dense temperate forests. Proc Natl Acad Sci U S A 115:3663–3668. https://doi.org/10.1073/pnas.1720064115

Lawson T, Matthews J (2020) Guard Cell Metabolism and Stomatal Function. Annu Rev Plant Biol 71:273–302. https://doi.org/10.1146/annurev-arplant-050718-100251

Le Quéré C, Andrew RM, Friedlingstein P, Sitch S, Hauck J, Pongratz J, Pickers PA, Korsbakken JI, Peters GP, Canadell JG, Arneth A, Arora VK, Barbero L, Bastos A, Bopp L, Chevallier F, Chini LP, Ciais P, Doney SC, Gkritzalis T, Goll DS, Harris I, Haverd V,

Hoffman FM, Hoppema M, Houghton RA, Hurtt G, Ilyina T, Jain AK, Johannessen T, Jones CD, Kato E, Keeling RF, Goldewijk KK, Landschützer P, Lefèvre N, Lienert S, Liu Z, Lombardozzi D, Metzl N, Munro DR, Nabel, Julia E. M. S., Nakaoka S-i, Neill C, Olsen A, Ono T, Patra P, Peregon A, Peters W, Peylin P, Pfeil B, Pierrot D, Poulter B, Rehder G, Resplandy L, Robertson E, Rocher M, Rödenbeck C, Schuster U, Schwinger J, Séférian R, Skjelvan I, Steinhoff T, Sutton A, Tans PP, Tian H, Tilbrook B, Tubiello FN, van der Laan-Luijkx, Ingrid T., van der Werf, Guido R., Viovy N, Walker AP, Wiltshire AJ, Wright R, Zaehle S, Zheng B (2018) Global Carbon Budget 2018. Earth Syst. Sci. Data 10:2141–2194. https://doi.org/10.5194/essd-10-2141-2018

Leakey ADB, Ainsworth EA, Bernacchi CJ, Rogers A, Long SP, Ort DR (2009) Elevated CO_2 effects on plant carbon, nitrogen, and water relations: six important lessons from FACE. J Exp Bot 60:2859–2876. https://doi.org/10.1093/jxb/erp096

Leslie SB, Israeli E, Leighthart B, Crowe JH, Crowe LM (1995) Trehalose and Sucrose Protect Both Membranes and Proteins in Intact Bacteria during Drying. APPLIED AND ENVIRONMENTAL MICROBIOLOGY, 61:3592–3597

Li D, Heiling S, Baldwin IT, Gaquerel E (2016) Illuminating a plant's tissue-specific metabolic diversity using computational metabolomics and information theory. Proc Natl Acad Sci U S A 113:E7610-E7618. https://doi.org/10.1073/pnas.1610218113

Li W, Hartmann H, Adams HD, Zhang H, Jin C, Zhao C, Guan D, Wang A, Yuan F, Wu J (2018) The sweet side of global change-dynamic responses of non-structural carbohydrates to drought, elevated CO_2 and nitrogen fertilization in tree species. Tree Physiol. https://doi.org/10.1093/treephys/tpy059

Liu H, Williams PA, Allen CD, Guo D, Wu X, Anenkhonov OA, Liang E, Sandanov DV, Yin Y, Qi Z, Badmaeva NK (2013) Rapid warming accelerates tree growth decline in semi-arid forests of Inner Asia. Global Change Biology 19:2500–2510. https://doi.org/10.1111/gcb.12217

Llusià J, Peñuelas J, Alessio GA, Estiarte M (2008) Contrasting Species-Specific, Compound-Specific, Seasonal, and Interannual Responses of Foliar Isoprenoid Emissions to Experimental Drought in a Mediterranean Shrubland. International Journal of Plant Sciences 169:637–645. https://doi.org/10.1086/533603

Llusià J, Roahtyn S, Yakir D, Rotenberg E, Seco R, Guenther A, Peñuelas J (2016) Photosynthesis, stomatal conductance and terpene emission response to water availability in dry and mesic Mediterranean forests. Trees 30:749–759. https://doi.org/10.1007/s00468-015-1317-x

Loreto F, Forster A, Durr M, Csiky O, Seufert G (1998) On the monoterpene emission under heat stress and on the increased thermotolerance of leaves of *Quercus ilex* L. fumigated with selected monoterpenes. Plant Cell Environ 21:101–107. https://doi.org/10.1046/j.1365-3040.1998.00268.x

Loreto F, Schnitzler J-P (2010) Abiotic stresses and induced BVOCs. Trends Plant Sci 15:154–166. https://doi.org/10.1016/j.tplants.2009.12.006

Loreto F, Barta C, Brilli F, Nogues I (2006) On the induction of volatile organic compound emissions by plants as consequence of wounding or fluctuations of light and temperature. Plant Cell Environ 29:1820–1828. https://doi.org/10.1111/j.1365-3040.2006.01561.x

Los DA, Murata N (2004) Membrane fluidity and its roles in the perception of environmental signals. Biochim Biophys Acta 1666:142–157. https://doi.org/10.1016/j.bbamem.2004.08.002

Lüpke M, Leuchner M, Steinbrecher R, Menzel A (2017) Quantification of monoterpene emission sources of a conifer species in response to experimental drought. AoB Plants 9:plx045. https://doi.org/10.1093/aobpla/plx045

Lüttge U, Buckeridge M (2020) Trees: Structure and function and the challenges of urbanization. Trees 26:751. https://doi.org/10.1007/s00468-020-01964-1

Maechler M, Rousseeuw P, Struyf A, Hubert, M., Hornik K. (2018) cluster: Cluster Analysis Basic and Extensions

Mahajan P, Singh HP, Kaur S, Batish DR, Kohli RK (2019) β-Pinene moderates Cr(VI) phytotoxicity by quenching reactive oxygen species and altering antioxidant machinery in maize. Environ Sci Pollut Res Int 26:456–463. https://doi.org/10.1007/s11356-018-3562-1

Major JE, Mosseler A (2019) Interactive effects of CO_2 and soil water treatments on growth and biomass allocation in pines and spruces. Forest Ecology and Management 442:21–33. https://doi.org/10.1016/j.foreco.2019.03.056

Marias DE, Meinzer FC, Still C (2017) Impacts of leaf age and heat stress duration on photosynthetic gas exchange and foliar nonstructural carbohydrates in *Coffea arabica*. Ecol Evol 7:1297–1310. https://doi.org/10.1002/ece3.2681

Masle J (2000) The effects of elevated $CO(_2)$ concentrations on cell division rates, growth patterns, and blade anatomy in young wheat plants are modulated by factors related to leaf position, vernalization, and genotype. Plant Physiol 122:1399–1415. https://doi.org/10.1104/pp.122.4.1399

Mauri A, Di Leo M, Rigo D de, Caudullo G (2016) *Pinus halepensis* and *Pinus brutia* in Europe: distribution, habitat, usage and threats. In: San-Miguel-Ayanz, J., de Rigo, D., Caudullo, G., Houston Durrant, T., Mauri, A. (Eds.), European Atlas of Forest Tree Species. Publ. Off. EU, Luxembourg, pp. e0166b8+

McCall DW, Douglass DC, Anderson EW (1959) Diffusion in Liquids. The Journal of Chemical Physics 31:1555–1557. https://doi.org/10.1063/1.1730651

McDonald AG, Dare PH, Gifford JS, Steward D, Riley S (2002) Assessment of air emissions from industrial kiln drying of *Pinus radiata* wood. Holz als Roh- und Werkstoff 60:181–190. https://doi.org/10.1007/s00107–002-0293-1

McDowell N, Allen CD, Anderson-Teixeira K, Brando P, Brienen R, Chambers J, Christoffersen B, Davies S, Doughty C, Duque A, Espirito-Santo F, Fisher R, Fontes CG, Galbraith D, Goodsman D, Grossiord C, Hartmann H, Holm J, Johnson DJ, Kassim AR, Keller M, Koven C, Kueppers L, Kumagai T, Malhi Y, McMahon SM, Mencuccini M, Meir P, Moorcroft P, Muller-Landau HC, Phillips OL, Powell T, Sierra CA, Sperry J, Warren J, Xu C, Xu X (2018) Drivers and mechanisms of tree mortality in moist tropical forests. New Phytol 219:851–869. https://doi.org/10.1111/nph.15027

McDowell NG, Williams AP, Xu C, Pockman WT, Dickman LT, Sevanto S, Pangle R, Limousin J, Plaut J, Mackay DS, Ogee J, Domec JC, Allen CD, Fisher RA, Jiang X, Muss JD, Breshears DD, Rauscher SA, Koven C (2016) Multi-scale predictions of massive conifer mortality due to chronic temperature rise. Nature Clim Change 6:295–300. https://doi.org/10.1038/nclimate2873

Medlyn BE, Barton CVM, Broadmeadow MSJ, Ceulemans R, Angelis P de, Forstreuter M, Freeman M, Jackson SB, Kellomäki S, Laitat E, Rey A, Roberntz P, Sigurdsson BD, Strassemeyer J, Wang K, Curtis PS, Jarvis PG (2001) Stomatal conductance of forest species after long-term exposure to elevated CO_2 concentration: A synthesis. New Phytologist 149:247–264. https://doi.org/10.1046/j.1469-8137.2001.00028.x

Meehl GA, Tebaldi C (2004) More intense, more frequent, and longer lasting heat waves in the 21st century. Science 305:994–997. https://doi.org/10.1126/science.1098704

Meehl GA, Zwiers F, Evans J, Knutson T, Mearns L, Whetton P (2000) Trends in Extreme Weather and Climate Events: Issues Related to Modeling Extremes in Projections of Future Climate Change *. Bull. Amer. Meteor. Soc. 81:427–436. https://doi.org/10.1175/1520-0477(2000)081<0427:TIEWAC>2.3.CO;2

Merchant A, Tausz M, Arndt SK, Adams MA (2006) Cyclitols and carbohydrates in leaves and roots of 13 Eucalyptus species suggest contrasting physiological responses to water deficit. Plant Cell Environ 29:2017–2029. https://doi.org/10.1111/j.1365-3040.2006.01577.x

Mhamdi A, Noctor G (2016) High CO2 Primes Plant Biotic Stress Defences through Redox-Linked Pathways. Plant Physiol 172:929–942. https://doi.org/10.1104/pp.16.01129

Michaelian M, Hogg EH, Hall RJ, Arsenault E (2011) Massive mortality of aspen following severe drought along the southern edge of the Canadian boreal forest. Global Change Biology 17:2084–2094. https://doi.org/10.1111/j.1365-2486.2010.02357.x

Michaletz ST (2018) Evaluating the kinetic basis of plant growth from organs to ecosystems. New Phytol 219:37–44. https://doi.org/10.1111/nph.15015

Misra BB, Chen S (2015) Advances in understanding CO_2 responsive plant metabolomes in the era of climate change. Metabolomics 11:1478–1491. https://doi.org/10.1007/s11306-015-0825-4

Mittler R, Finka A, Goloubinoff P (2012) How do plants feel the heat? Trends in Biochemical Sciences 37:118–125. https://doi.org/10.1016/j.tibs.2011.11.007

Mohanta TK, Bashir T, Hashem A, Abd Allah EF (2017) Systems biology approach in plant abiotic stresses. Plant Physiol Biochem 121:58–73. https://doi.org/10.1016/j.plaphy.2017.10.019

Monod B, Collin A, Parent G, Boulet P (2009) Infrared radiative properties of vegetation involved in forest fires. Fire Safety Journal 44:88–95. https://doi.org/10.1016/j.firesaf.2008.03.009

Monson RK, Holland EA (2001) Biospheric Trace Gas Fluxes and Their Control Over Tropospheric Chemistry. Annu. Rev. Ecol. Syst. 32:547–576. https://doi.org/10.1146/annurev.ecolsys.32.081501.114136

Murchie EH, Lawson T (2013) Chlorophyll fluorescence analysis: a guide to good practice and understanding some new applications. J Exp Bot 64:3983–3998. https://doi.org/10.1093/jxb/ert208

Nagegowda DA (2010) Plant volatile terpenoid metabolism: biosynthetic genes, transcriptional regulation and subcellular compartmentation. FEBS Letters 584:2965–2973. https://doi.org/10.1016/j.febslet.2010.05.045

Nakagawa S, Schielzeth H, O'Hara RB (2013) A general and simple method for obtaining R2 from generalized linear mixed-effects models. Methods Ecol Evol 4:133–142. https://doi.org/10.1111/j.2041-210x.2012.00261.x

Nellaepalli S, Zsiros O, Tóth T, Yadavalli V, Garab G, Subramanyam R, Kovács L (2014) Heat- and light-induced detachment of the light harvesting complex from isolated photosystem I supercomplexes. J Photochem Photobiol B, Biol 137:13–20. https://doi.org/10.1016/j.jphotobiol.2014.04.026

Neumann M, Mues V, Moreno A, Hasenauer H, Seidl R (2017) Climate variability drives recent tree mortality in Europe. Global Change Biology 23:4788–4797. https://doi.org/10.1111/gcb.13724

Nguyen A, Lamant A (1988) Pinitol and myo-inositol accumulation in water-stressed seedlings of maritime pine. Phytochemistry 27:3423–3427. https://doi.org/10.1016/0031-9422(88)80742-8

Nie M, Lu M, Bell J, Raut S, Pendall E (2013) Altered root traits due to elevated CO_2: A meta-analysis. Global Ecology and Biogeography 22:1095–1105. https://doi.org/10.1111/geb.12062

Niinemets Ü, Reichstein M (2002) A model analysis of the effects of nonspecific monoterpenoid storage in leaf tissues on emission kinetics and composition in Mediterranean sclerophyllous Quercus species. Global Biogeochem. Cycles 16:57-1-57-26. https://doi.org/10.1029/2002GB001927

Niinemets U, Seufert G, Steinbrecher R, Tenhunen JD (2002) A model coupling foliar monoterpene emissions to leaf photosynthetic characteristics in Mediterranean evergreen Quercus species. New Phytol 153:257–275. https://doi.org/10.1046/j.0028-646X.2001.00324.x

Niinemets Ü (2010) Responses of forest trees to single and multiple environmental stresses from seedlings to mature plants: Past stress history, stress interactions, tolerance and acclimation. Forest Ecology and Management 260:1623–1639. https://doi.org/10.1016/j.foreco.2010.07.054

Niinemets Ü, Monson RK, Arneth A, Ciccioli P, Kesselmeier J, Kuhn U, Noe SM, Peñuelas J, Staudt M (2010) The leaf-level emission factor of volatile isoprenoids: Caveats, model algorithms, response shapes and scaling. Biogeosciences 7:1809–1832. https://doi.org/10.5194/bg-7-1809-2010

Niinemets Ü, Kuhn U, Harley PC, Staudt M, Arneth A, Cescatti A, Ciccioli P, Copolovici L, Geron C, Guenther A, Kesselmeier J, Lerdau MT, Monson RK, Peñuelas J (2011) Estimations of isoprenoid emission capacity from enclosure studies: Measurements, data processing, quality and standardized measurement protocols. Biogeosciences 8:2209–2246. https://doi.org/10.5194/bg-8-2209-2011

Niinemets Ü (2018) When leaves go over the thermal edge. Plant Cell Environ 41:1247–1250. https://doi.org/10.1111/pce.13184

Niklas KJ, Spatz H-C (2004) Growth and hydraulic (not mechanical) constraints govern the scaling of tree height and mass. Proc Natl Acad Sci U S A 101:15661–15663. https://doi.org/10.1073/pnas.0405857101

Nishizawa A, Yabuta Y, Shigeoka S (2008) Galactinol and raffinose constitute a novel function to protect plants from oxidative damage. Plant Physiol 147:1251–1263. https://doi.org/10.1104/pp.108.122465

Niu YF, Jin GL, Chai RS, Wang H, Zhang YS (2011) Responses of root hair development to elevated CO_2. Plant Signal Behav 6:1414–1417. https://doi.org/10.4161/psb.6.9.17302

Noctor G, Mhamdi A (2017) Climate Change, CO_2, and Defense: The Metabolic, Redox, and Signaling Perspectives. Trends Plant Sci 22:857–870. https://doi.org/10.1016/j.tplants.2017.07.007

Noctor G, Mhamdi A, Foyer CH (2014) The roles of reactive oxygen metabolism in drought: not so cut and dried. Plant Physiol 164:1636–1648. https://doi.org/10.1104/pp.113.233478

Noguchi K, Watanabe CK, Terashima I (2015) Effects of Elevated Atmospheric CO_2 on Primary Metabolite Levels in *Arabidopsis thaliana* Col-0 Leaves: An Examination of Metabolome Data. Plant Cell Physiol 56:2069–2078. https://doi.org/10.1093/pcp/pcv125

Nogués I, Medori M, Calfapietra C (2015) Limitations of monoterpene emissions and their antioxidant role in Cistus sp. under mild and severe treatments of drought and warming.

Environmental and Experimental Botany 119:76–86. https://doi.org/10.1016/j.envexpbot.2015.06.001

Norby RJ, O'Neill EG, Luxmoore RJ (1986) Effects of Atmospheric $CO(_2)$ Enrichment on the Growth and Mineral Nutrition of *Quercus alba* Seedlings in Nutrient-Poor Soil. Plant Physiol 82:83–89. https://doi.org/10.1104/pp.82.1.83

Norby RJ, Ledford J, Reilly CD, Miller NE, O'Neill EG (2004) Fine-root production dominates response of a deciduous forest to atmospheric CO_2 enrichment. Proc Natl Acad Sci U S A 101:9689–9693. https://doi.org/10.1073/pnas.0403491101

Norby RJ, Warren JM, Iversen CM, Medlyn BE, McMurtrie RE (2010) CO_2 enhancement of forest productivity constrained by limited nitrogen availability. Proc Natl Acad Sci U S A 107:19368–19373. https://doi.org/10.1073/pnas.1006463107

Oksanen J (2011) Multivariate analysis of ecological communities in R: vegan tutorial. R package version 1(7):1–43

Oksanen J, Blanchet FG, Friendly M, Kindt R, Legendre P, McGlinn D, Minchin PR, O'Hara RB, Simpson GL, Solymos P, tevens MHH, Szoecs E, Wagner Helene (2013) Package 'vegan': Community ecology package. version, 2(5-6):1–295

O'Leary BM, Asao S, Millar AH, Atkin OK (2019) Core principles which explain variation in respiration across biological scales. New Phytol 222:670–686. https://doi.org/10.1111/nph.15576

Oliveras I, Martínez-Vilalta J, Jimenez-Ortiz T, José Lledó M, Escarré A, Piñol J (2003) Hydraulic properties of *Pinus halepensis*, *Pinus pinea* and T*etraclinis articulata* in a dune ecosystem of Eastern Spain. Plant Ecology 169:131–141. https://doi.org/10.1023/A:1026223516580

Onwueme IC, Laude HM, Huffaker RC (1971) Nitrate reductase activity in relation to heat stress in barley seedlings. Crop Science 11:195–200. https://doi.org/10.2135/cropsci1971.0011183X001100020009x

Ormeño E, Mévy JP, Vila B, Bousquet-Mélou A, Greff S, Bonin G, Fernandez C (2007) Water deficit stress induces different monoterpene and sesquiterpene emission changes in Mediterranean species. Relationship between terpene emissions and plant water potential. Chemosphere 67:276–284. https://doi.org/10.1016/j.chemosphere.2006.10.029

Ormeño E, Goldstein A, Niinemets Ü (2011) Extracting and trapping biogenic volatile organic compounds stored in plant species. TrAC Trends in Analytical Chemistry 30:978–989. https://doi.org/10.1016/j.trac.2011.04.006

O'Sullivan OS, Heskel MA, Reich PB, Tjoelker MG, Weerasinghe LK, Penillard A, Zhu L, Egerton JJG, Bloomfield KJ, Creek D, Bahar NHA, Griffin KL, Hurry V, Meir P, Turnbull MH, Atkin OK (2017) Thermal limits of leaf metabolism across biomes. Glob Change Biol 23:209–223. https://doi.org/10.1111/gcb.13477

Pachauri R, Meyer L, Barros V, Broome J, Cramer W, Crist R, Church, JR., Clarke L, Dahe DQ, Dasqupta P((2014) IPCC: Climate Change 2014. Synthesis Report. Contribution of Working Groups I, II and III to the Fifth Assessment Report of the Intergovernmental Panel on Climate Change Geneva, Switzerland: IPCC

Pal UR, Johnson RR, Hageman RH (1976) Nitrate reductase activity in heat (drought) tolerant and intolerant maize genotypes. Crop Science 16:775–779. https://doi.org/10.2135/cropsci1976.0011183X001600060009x

Pan C, Ahammed GJ, Li X, Shi K (2018) Elevated CO2 Improves Photosynthesis Under High Temperature by Attenuating the Functional Limitations to Energy Fluxes, Electron Transport

and Redox Homeostasis in Tomato Leaves. Front Plant Sci 9:1739. https://doi.org/10.3389/fpls.2018.01739

Panek JA, Goldstein AH (2001) Response of stomatal conductance to drought in ponderosa pine: Implications for carbon and ozone uptake. Tree Physiol 21:337–344. https://doi.org/10.1093/treephys/21.5.337

Parry MAJ, Andralojc PJ, Khan S, Lea PJ, Keys AJ (2002) Rubisco activity: effects of drought stress: Effects of Drought Stress. Annals of Botany 89 Spec No:833–839. https://doi.org/10.1093/aob/mcf103

Patterson AE, Arkebauer R, Quallo C, Heskel MA, Li X, Boelman N, Griffin KL (2018) Temperature response of respiration and respiratory quotients of 16 co-occurring temperate tree species. Tree Physiol. https://doi.org/10.1093/treephys/tpx176

Peñuelas J, Estiarte M (1998) Can elevated CO2 affect secondary metabolism and ecosystem function? Trends in Ecology & Evolution 13:20–24. https://doi.org/10.1016/S0169-5347(97)01235-4

Peñuelas J, Llusià J (1999) Short-term responses of terpene emission rates to experimental changes of PFD in *Pinus halepensis* and *Quercus ilex* in summer field conditions. Environmental and Experimental Botany 42:61–68. https://doi.org/10.1016/S0098-8472(99)00018-0

Peñuelas J, Ciais P, Canadell JG, Janssens IA, Fernández-Martínez M, Carnicer J, Obersteiner M, Piao S, Vautard R, Sardans J (2017) Shifting from a fertilization-dominated to a warming-dominated period. Nat Ecol Evol 1:1438–1445. https://doi.org/10.1038/s41559-017-0274-8

Perkins-Kirkpatrick SE, Gibson PB (2017) Changes in regional heatwave characteristics as a function of increasing global temperature. Sci Rep 7:12256. https://doi.org/10.1038/s41598-017-12520-2

Peterhansel C, Maurino VG (2011) Photorespiration redesigned. Plant Physiol 155:49–55. https://doi.org/10.1104/pp.110.165019

Piispanen R, Saranpaa P (2002) Neutral lipids and phospholipids in Scots pine (*Pinus sylvestris*) sapwood and heartwood. Tree Physiol 22:661–666. https://doi.org/10.1093/treephys/22.9.661

Piñeiro J, Ochoa-Hueso R, Drake J, Tjoelker MG, Power SA (2020) Water availability drives fine root dynamics in a Eucalyptus woodland under elevated atmospheric CO_2 concentration. Funct Ecol. https://doi.org/10.1111/1365-2435.13660

Poorter H, van Berkel Y, Baxter R, Den Hertog J, Dijkstra P, Gifford RM, Griffin KL, Roumet C, ROY J, Wong SC (1997) The effect of elevated CO_2 on the chemical composition and construction costs of leaves of 27 C3 species. Plant Cell Environ 20:472–482. https://doi.org/10.1046/j.1365-3040.1997.d01-84.x

Poorter H, B Hler J, van Dusschoten D, Climent J, Postma JA (2012) Pot size matters: a meta-analysis of the effects of rooting volume on plant growth. Funct Plant Biol 39:839–850. https://doi.org/10.1071/FP12049

Porter WC, Heald CL (2019) The mechanisms and meteorological drivers of the summertime ozone–temperature relationship. Atmos. Chem. Phys. 19:13367–13381. https://doi.org/10.5194/acp-19-13367-2019

Portillo-Estrada M, Kazantsev T, Talts E, Tosens T, Niinemets Ü (2015) Emission Timetable and Quantitative Patterns of Wound-Induced Volatiles Across Different Leaf Damage Treatments in Aspen (*Populus Tremula*). J Chem Ecol 41:1105–1117. https://doi.org/10.1007/s10886-015-0646-y

Pregitzer KS, Zak DR, Curtis PS, Kubiske ME, Teeri JA, Vogel CS (1995) Atmospheric CO_2, soil nitrogen and turnover of fine roots. New Phytol 129:579–585. https://doi.org/10.1111/j.1469-8137.1995.tb03025.x

Preisler Y, Tatarinov F, Grünzweig JM, Bert D, Ogée J, Wingate L, Rotenberg E, Rohatyn S, Her N, Moshe I, Klein T, Yakir D, Sala A (2019) Mortality versus survival in drought-affected Aleppo pine forest depends on the extent of rock cover and soil stoniness. Funct Ecol 33:901–912. https://doi.org/10.1111/1365-2435.13302

Prendin AL, Petit G, Fonti P, Rixen C, Dawes MA, Arx G, Larjavaara M (2017) Axial xylem architecture of *Larix decidua* exposed to CO_2 enrichment and soil warming at the tree line. Funct Ecol 32:273–287. https://doi.org/10.1111/1365-2435.12986

Pucciariello C, Banti V, Perata P (2012) ROS signaling as common element in low oxygen and heat stresses. Plant Physiol Biochem 59:3–10. https://doi.org/10.1016/j.plaphy.2012.02.016

Pugh TAM, Rademacher T, Shafer SL, Steinkamp J, Barichivich J, Beckage B, Haverd V, Harper A, Heinke J, Nishina K, Rammig A, Sato H, Arneth A, Hantson S, Hickler T, Kautz M, Quesada B, Smith B, Thonicke K (2020) Understanding the uncertainty in global forest carbon turnover. Biogeosciences 17:3961–3989. https://doi.org/10.5194/bg-17-3961-2020

Quentin AG, Pinkard EA, Ryan MG, Tissue DT, Baggett LS, Adams HD, Maillard P, Marchand J, Landhäusser SM, Lacointe A, Gibon Y, Anderegg WRL, Asao S, Atkin OK, Bonhomme M, Claye C, Chow PS, Clément-Vidal A, Davies NW, Dickman LT, Dumbur R, Ellsworth DS, Falk K, Galiano L, Grünzweig JM, Hartmann H, Hoch G, Hood S, Jones JE, Koike T, Kuhlmann I, Lloret F, Maestro M, Mansfield SD, Martínez-Vilalta J, Maucourt M, McDowell NG, Moing A, Muller B, Nebauer SG, Niinemets Ü, Palacio S, Piper F, Raveh E, Richter A, Rolland G, Rosas T, Saint Joanis B, Sala A, Smith RA, Sterck F, Stinziano JR, Tobias M, Unda F, Watanabe M, Way DA, Weerasinghe LK, Wild B, Wiley E, Woodruff DR (2015) Non-structural carbohydrates in woody plants compared among laboratories. Tree Physiol 35:1146–1165. https://doi.org/10.1093/treephys/tpv073

Quinn PJ (1988) Effects of temperature on cell membranes. Symp Soc Exp Biol 42:237–258

R Core Team (2015) R: A language and environment for statistical computing. R Foundation for Statistical Computing, Vienna, Austria. URL https://www.R-project.org/

R Core Team (2018) R: A Language and Environment for Statistical Computing. R Foundation for Statistical Computing, Vienna, Austria. URL https://www.R-project.org/

Rätsep M, Muru R, Freiberg A (2018) High temperature limit of photosynthetic excitons. Nat Commun 9:99. https://doi.org/10.1038/s41467-017-02544-7

Rehschuh R, Cecilia A, Zuber M, Faragó T, Baumbach T, Hartmann H, Jansen S, Mayr S, Ruehr NK (2020) Drought-induced xylem embolism limits the recovery of leaf gas exchange in Scots pine. Plant Physiol. https://doi.org/10.1104/pp.20.00407

Reich PB, Sendall KM, Stefanski A, Wei X, Rich RL, Montgomery RA (2016) Boreal and temperate trees show strong acclimation of respiration to warming. Nature 531:633–636. https://doi.org/10.1038/nature17142

Reichstein M, Bahn M, Ciais P, Frank D, Mahecha MD, Seneviratne SI, Zscheischler J, Beer C, Buchmann N, Frank DC, Papale D, Rammig A, Smith P, Thonicke K, van der Velde M, Vicca S, Walz A, Wattenbach M (2013) Climate extremes and the carbon cycle. Nature 500:287–295. https://doi.org/10.1038/nature12350

Richet N, Afif D, Tozo K, Pollet B, Maillard P, Huber F, Priault P, Banvoy J, Gross P, Dizengremel P, Lapierre C, Perré P, Cabané M (2012) Elevated CO_2 and/or ozone modify lignification in the wood of poplars (*Populus tremula* x *alba*). J Exp Bot 63:4291–4301. https://doi.org/10.1093/jxb/ers118

Richter K, Haslbeck M, Buchner J (2010) The heat shock response: life on the verge of death. Mol Cell 40:253–266. https://doi.org/10.1016/j.molcel.2010.10.006

Rienth M, Romieu C, Gregan R, Walsh C, Torregrosa L, Kelly MT (2014) Validation and application of an improved method for the rapid determination of proline in grape berries. J Agric Food Chem 62:3384–3389. https://doi.org/10.1021/jf404627n

Ripullone F, Guerrieri MR, Nole' A, Magnani F, Borghetti M (2007) Stomatal conductance and leaf water potential responses to hydraulic conductance variation in *Pinus pinaster* seedlings. Trees 21:371–378. https://doi.org/10.1007/s00468-007-0130-6

Rissanen K, Hölttä T, Bäck J (2018) Transpiration directly regulates the emissions of water-soluble short-chained OVOCs. Plant Cell Environ 41:2288–2298. https://doi.org/10.1111/pce.13318

Rissanen K, Vanhatalo A, Salmon Y, Bäck J, Hölttä T (2020) Stem emissions of monoterpenes, acetaldehyde and methanol from Scots pine (*Pinus sylvestris* L.) affected by tree-water relations and cambial growth. Plant Cell Environ. https://doi.org/10.1111/pce.13778

Rizhsky L, Liang H, Shuman J, Shulaev V, Davletova S, Mittler R (2004) When defense pathways collide. The response of Arabidopsis to a combination of drought and heat stress. Plant Physiol 134:1683–1696. https://doi.org/10.1104/pp.103.033431

Rotenberg E, Yakir D (2010) Contribution of semi-arid forests to the climate system. Science 327:451–454. https://doi.org/10.1126/science.1179998

Rotenberg E, Yakir D (2011) Distinct patterns of changes in surface energy budget associated with forestation in the semiarid region. Global Change Biology 17:1536–1548. https://doi.org/10.1111/j.1365-2486.2010.02320.x

Ruehr NK, Buchmann N (2010) Soil respiration fluxes in a temperate mixed forest: seasonality and temperature sensitivities differ among microbial and root-rhizosphere respiration. Tree Physiol 30:165–176. https://doi.org/10.1093/treephys/tpp106

Ruehr NK, Offermann CA, Gessler A, Winkler JB, Ferrio JP, Buchmann N, Barnard RL (2009) Drought effects on allocation of recent carbon: from beech leaves to soil CO_2 efflux. New Phytol 184:950–961. https://doi.org/10.1111/j.1469-8137.2009.03044.x

Ruehr NK, Gast A, Weber C, Daub B, Arneth A (2016) Water availability as dominant control of heat stress responses in two contrasting tree species. Tree Physiol 36:164–178. https://doi.org/10.1093/treephys/tpv102

Ruehr NK, Grote R, Mayr S, Arneth A (2019) Beyond the extreme: Recovery of carbon and water relations in woody plants following heat and drought stress. Tree Physiol. https://doi.org/10.1093/treephys/tpz032

Runion GB, Entry JA, Prior SA, Mitchell RJ, Rogers HH (1999) Tissue chemistry and carbon allocation in seedlings of *Pinus palustris* subjected to elevated atmospheric $CO(_2)$ and water stress. Tree Physiol 19:329–335. https://doi.org/10.1093/treephys/19.4-5.329

Ryan MG, Asao S (2019) Clues for our missing respiration model. New Phytol 222:1167–1170. https://doi.org/10.1111/nph.15805

Saelim S, Zwiazek JJ (2000) Preservation of Thermal Stability of Cell Membranes and Gas Exchange in High Temperature Acclimated Xylia xylocarpa Seedlings. J Plant Physiol 156:380–385. https://doi.org/10.1016/S0176-1617(00)80077-2

Saijo Y, Loo EP-I (2020) Plant immunity in signal integration between biotic and abiotic stress responses. New Phytol 225:87–104. https://doi.org/10.1111/nph.15989

Saurer M, Siegwolf RTW, Schweingruber FH (2004) Carbon isotope discrimination indicates improving water-use efficiency of trees in northern Eurasia over the last 100 years. Global Change Biol 10:2109–2120. https://doi.org/10.1111/j.1365-2486.2004.00869.x

Schafer JA, Barfuss DW (1980) Mechanisms of transmembrane transport in isolated cells and their experimental study. Pharmacology & Therapeutics 10:223–260. https://doi.org/10.1016/0163-7258(80)90082-0

Schär C (2015) Climate extremes: The worst heat waves to come. Nature Climate change. https://doi.org/10.1038/nclimate2864

Scherrer D, Bader MK-F, Körner C (2011) Drought-sensitivity ranking of deciduous tree species based on thermal imaging of forest canopies. Agricultural and Forest Meteorology 151:1632–1640. https://doi.org/10.1016/j.agrformet.2011.06.019

Schiller G, Atzmon N (2009) Performance of Aleppo pine (*Pinus halepensis*) provenances grown at the edge of the Negev desert: A review. Journal of Arid Environments 73:1051–1057. https://doi.org/10.1016/j.jaridenv.2009.06.003

Schuldt B, Buras A, Arend M, Vitasse Y, Beierkuhnlein C, Damm A, Gharun M, Grams TE, Hauck M, Hajek P, Hartmann H, Hiltbrunner E, Hoch G, Holloway-Phillips M, Körner C, Larysch E, Lübbe T, Nelson DB, Rammig A, Rigling A, Rose L, Ruehr NK, Schumann K, Weiser F, Werner C, Wohlgemuth T, Zang CS, Kahmen A (2020) A first assessment of the impact of the extreme 2018 summer drought on Central European forests. Basic and Applied Ecology 45:86–103. https://doi.org/10.1016/j.baae.2020.04.003

Schurgers G, Arneth A, Holzinger R, Goldstein AH (2009) Process-based modelling of biogenic monoterpene emissions combining production and release from storage. Atmos. Chem. Phys. 9:3409–3423. https://doi.org/10.5194/acp-9-3409-2009

Schwalm CR, Glendon S, Duffy PB (2020) RCP8.5 tracks cumulative CO_2 emissions. Proc Natl Acad Sci USA 117:19656–19657. https://doi.org/10.1073/pnas.2007117117

Scott ER, Li X, Kfoury N, Morimoto J, Han W-Y, Ahmed S, Cash SB, Griffin TS, Stepp JR, Robbat A, Orians CM (2019) Interactive effects of drought severity and simulated herbivory on tea (*Camellia sinensis*) volatile and non-volatile metabolites. Environmental and Experimental Botany 157:283–292. https://doi.org/10.1016/j.envexpbot.2018.10.025

Seco R, Peñuelas J, Filella I (2008) Formaldehyde emission and uptake by Mediterranean trees *Quercus ilex* and *Pinus halepensis*. Atmospheric Environment 42:7907–7914. https://doi.org/10.1016/j.atmosenv.2008.07.006

Seco R, Karl T, Guenther A, Hosman KP, Pallardy SG, Gu L, Geron C, Harley P, Kim S (2015) Ecosystem-scale volatile organic compound fluxes during an extreme drought in a broadleaf temperate forest of the Missouri Ozarks (central USA). Global Change Biology 21:3657–3674. https://doi.org/10.1111/gcb.12980

Seco R, Karl T, Turnipseed A, Greenberg J, Guenther A, Llusià J, Peñuelas J, Dicken U, Rotenberg E, Kim S, Yakir D (2017) Springtime ecosystem-scale monoterpene fluxes from Mediterranean pine forests across a precipitation gradient. Agricultural and Forest Meteorology 237-238:150–159. https://doi.org/10.1016/j.agrformet.2017.02.007

Seidl R, Thom D, Kautz M, Martin-Benito D, Peltoniemi M, Vacchiano G, Wild J, Ascoli D, Petr M, Honkaniemi J, Lexer MJ, Trotsiuk V, Mairota P, Svoboda M, Fabrika M, Nagel TA, Reyer CPO (2017) Forest disturbances under climate change. Nat Clim Chang 7:395–402. https://doi.org/10.1038/nclimate3303

Seneviratne SI, N. Nicholls, D. Easterling, C.M. Goodess, S. Kanae, J. Kossin, Y. Luo, J. Marengo, K. McInnes, M. Rahimi, M. Reichstein, A. Sorteberg, C. Vera, and X. Zhang (2012) Changes in climate extremes and their impacts on the natural physical environment. Managing the Risks of Extreme Events and Disasters to Advance Climate Change Adaptation

Sevanto S (2014) Phloem transport and drought. J Exp Bot 65:1751–1759. https://doi.org/10.1093/jxb/ert467

Sevanto S (2018) Drought impacts on phloem transport. Current Opinion in Plant Biology 43:76–81. https://doi.org/10.1016/j.pbi.2018.01.002

Sevanto S, Dickman LT (2015) Where does the carbon go?--Plant carbon allocation under climate change. Tree Physiol 35:581–584. https://doi.org/10.1093/treephys/tpv059

Sevanto S, McDowell NG, Dickman LT, Pangle R, Pockman WT (2014) How do trees die? A test of the hydraulic failure and carbon starvation hypotheses. Plant Cell Environ 37:153–161. https://doi.org/10.1111/pce.12141

Shaar-Moshe L, Hayouka R, Roessner U, Peleg Z (2019) Phenotypic and metabolic plasticity shapes life-history strategies under combinations of abiotic stresses. Plant Direct 3:e00113. https://doi.org/10.1002/pld3.113

Shao M, Wildt J (2002) Quantification of acetone emission from pine plants. Sci China Ser B 45:532. https://doi.org/10.1360/02yb9070

Shepherd T, Wynne Griffiths D (2006) The effects of stress on plant cuticular waxes. New Phytol 171:469–499. https://doi.org/10.1111/j.1469-8137.2006.01826.x

Shulaev V, Silverman P, Raskin I (1997) Airborne signalling by methyl salicylate in plant pathogen resistance. Nature 385:718–721. https://doi.org/10.1038/385718a0

Simón BF de, Cadahía E, Aranda I (2018) Metabolic response to elevated CO_2 levels in *Pinus pinaster* Aiton needles in an ontogenetic and genotypic-dependent way. Plant Physiol Biochem 132:202–212. https://doi.org/10.1016/j.plaphy.2018.09.006

Sivakumar MVK, Das HP, Brunini O (2005) Impacts of Present and Future Climate Variability and Change on Agriculture and Forestry in the Arid and Semi-Arid Tropics. Climatic Change 70:31–72. https://doi.org/10.1007/s10584-005-5937-9

Smith WK, Dannenberg MP, Yan D, Herrmann S, Barnes ML, Barron-Gafford GA, Biederman JA, Ferrenberg S, Fox AM, Hudson A, Knowles JF, MacBean N, Moore DJ, Nagler PL, Reed SC, Rutherford WA, Scott RL, Wang X, Yang J (2019) Remote sensing of dryland ecosystem structure and function: Progress, challenges, and opportunities. Remote Sensing of Environment 233:111401. https://doi.org/10.1016/j.rse.2019.111401

Snow MD, Bard RR, Olszyk DM, Minster LM, Hager AN, Tingey DT (2003) Monoterpene levels in needles of Douglas fir exposed to elevated CO_2 and temperature. Physiol Plant 117:352–358. https://doi.org/10.1034/j.1399-3054.2003.00035.x

Song Y, Chen Q, Ci D, Shao X, Zhang D (2014) Effects of high temperature on photosynthesis and related gene expression in poplar. BMC Plant Biol 14:111. https://doi.org/10.1186/1471-2229-14-111

Spiess AN (2018) propagate: Propagation of Uncertainty. https://CRAN.R-project.org/package=propagate

Spinelli F, Cellini A, Marchetti L, Mudigere K, Piovene C (2011) Emission and Function of Volatile Organic Compounds in Response to Abiotic Stress. In: Shanker A (ed) Abiotic Stress in Plants - Mechanisms and Adaptations. InTech, pp 1–29

Sporre MK, Blichner SM, Karset IHH, Makkonen R, Berntsen TK (2019) BVOC–aerosol–climate feedbacks investigated using NorESM. Atmos. Chem. Phys. 19:4763–4782. https://doi.org/10.5194/acp-19-4763-2019

Stangler DF, Hamann A, Kahle H-P, Spiecker H (2016) A heat wave during leaf expansion severely reduces productivity and modifies seasonal growth patterns in a northern hardwood forest. Tree Physiol. https://doi.org/10.1093/treephys/tpw094

Stark G (2005) Functional Consequences of Oxidative Membrane Damage. J Membrane Biol 205:1–16. https://doi.org/10.1007/s00232-005-0753-8

Staudt M, Bourgeois I, Al Halabi R, Song W, Williams J (2017) New insights into the parametrization of temperature and light responses of mono - and sesquiterpene emissions from Aleppo pine and rosemary. Atmospheric Environment 152:212–221. https://doi.org/10.1016/j.atmosenv.2016.12.033

Stephenson NL, Das AJ, Ampersee NJ, Bulaon BM, Yee JL, Edwards D (2019) Which trees die during drought?: The key role of insect host-tree selection. J Ecol 107:2383–2401. https://doi.org/10.1111/1365-2745.13176

Szabados L, Savoure A (2010) Proline: a multifunctional amino acid. Trends Plant Sci 15:89–97. https://doi.org/10.1016/j.tplants.2009.11.009

Tabari H, Willems P (2018) Seasonally varying footprint of climate change on precipitation in the Middle East. Sci Rep 8:4435. https://doi.org/10.1038/s41598-018-22795-8

Taipale R, Kajos MK, Patokoski J, Rantala P, Ruuskanen TM, Rinne J (2011) Role of de novo biosynthesis in ecosystem scale monoterpene emissions from a boreal Scots pine forest. Biogeosciences 8:2247–2255. https://doi.org/10.5194/bg-8-2247-2011

Tang Y, Wen X, Lu Q, Yang Z, Cheng Z, Lu C (2007) Heat stress induces an aggregation of the light-harvesting complex of photosystem II in spinach plants. Plant Physiol 143:629–638. https://doi.org/10.1104/pp.106.090712

Tatarinov F, Rotenberg E, Maseyk K, Ogée J, Klein T, Yakir D (2015) Resilience to seasonal heat wave episodes in a Mediterranean pine forest. New Phytol:n/a-n/a. https://doi.org/10.1111/nph.13791

Tawfik MM, Yamato KT, Kohchi T, Koeduka T, Matsui K (2017) n-Hexanal and (Z)-3-hexenal are generated from arachidonic acid and linolenic acid by a lipoxygenase in *Marchantia polymorpha* L. Biosci Biotechnol Biochem 81:1148–1155. https://doi.org/10.1080/09168451.2017.1285688

TerBraak CJF (1986) Canonical Correspondence Analysis: A New Eigenvector Technique for Multivariate Direct Gradient Analysis. Ecology 67:1167–1179. https://doi.org/10.2307/1938672

Teskey RO, Bongarten BC, Cregg BM, Dougherty PM, Hennessey TC (1987) Physiology and genetics of tree growth response to moisture and temperature stress: An examination of the characteristics of loblolly pine (*Pinus taeda* L.). Tree Physiol 3:41–61. https://doi.org/10.1093/treephys/3.1.41

Teskey RO, Wertin T, Bauweraerts I, Ameye M, McGuire MA, Steppe K (2015) Responses of tree species to heat waves and extreme heat events. Plant Cell Environ 38:1699–1712. https://doi.org/10.1111/pce.12417

Thomas CK, Law BE, Irvine J, Martin JG, Pettijohn JC, Davis KJ (2009) Seasonal hydrology explains interannual and seasonal variation in carbon and water exchange in a semiarid mature ponderosa pine forest in central Oregon. J. Geophys. Res. 114. https://doi.org/10.1029/2009JG001010

Tjoelker MG (2018) The role of thermal acclimation of plant respiration under climate warming: Putting the brakes on a runaway train? Plant Cell Environ 41:501–503. https://doi.org/10.1111/pce.13126

Tohmura S-i, Ishikawa A, Miyamoto K, Inoue A (2012) Acetaldehyde emission from wood induced by the addition of ethanol. J Wood Sci 58:57–63. https://doi.org/10.1007/s10086-011-1215-9

Tomé F, Nägele T, Adamo M, Garg A, Marco-Llorca C, Nukarinen E, Pedrotti L, Peviani A, Simeunovic A, Tatkiewicz A, Tomar M, Gamm M (2014) The low energy signaling network. Front Plant Sci 5:353. https://doi.org/10.3389/fpls.2014.00353

Trouillier M, van der Maaten-Theunissen M, Scharnweber T, Würth D, Burger A, Schnittler M, Wilmking M (2019) Size matters—a comparison of three methods to assess age- and size-dependent climate sensitivity of trees. Trees 33:183–192. https://doi.org/10.1007/s00468-018-1767-z

Trugman AT, Anderegg LDL, Wolfe BT, Birami B, Ruehr NK, Detto M, Bartlett MK, Anderegg WRL (2019) Climate and plant trait strategies determine tree carbon allocation to leaves and mediate future forest productivity. Global Change Biology. https://doi.org/10.1111/gcb.14680

Turan S, Kask K, Kanagendran A, Li S, Anni R, Talts E, Rasulov B, Kännaste A, Niinemets Ü (2019) Lethal heat stress-dependent volatile emissions from tobacco leaves: what happens beyond the thermal edge? J Exp Bot 70:5017–5030. https://doi.org/10.1093/jxb/erz255

Turner DW, Lahav E (1985) Temperature influences nutrient absorption and uptake rates of bananas grown in controlled environments. Scientia Horticulturae 26:311–322. https://doi.org/10.1016/0304-4238(85)90015-9

Turner GW, Parrish AN, Zager JJ, Fischedick JT, Lange BM (2019) Assessment of flux through oleoresin biosynthesis in epithelial cells of loblolly pine resin ducts. J Exp Bot 70:217–230. https://doi.org/10.1093/jxb/ery338

Tyree MT, Zimmermann MH (2002) Hydraulic Architecture of Whole Plants and Plant Performance. In: Timell TE, Tyree MT, Zimmermann MH (eds) Xylem Structure and the Ascent of Sap. Springer Berlin Heidelberg, Berlin, Heidelberg, pp 175–214

Ummenhofer CC, Meehl GA (2017) Extreme weather and climate events with ecological relevance: a review. Philos Trans R Soc Lond , B, Biol Sci 372. https://doi.org/10.1098/rstb.2016.0135

Urban J, Ingwers MW, McGuire MA, Teskey RO (2017a) Increase in leaf temperature opens stomata and decouples net photosynthesis from stomatal conductance in *Pinus taeda* and *Populus deltoides x nigra*. J Exp Bot 68:1757–1767. https://doi.org/10.1093/jxb/erx052

Urban J, Ingwers M, McGuire MA, Teskey RO (2017b) Stomatal conductance increases with rising temperature. Plant Signal Behav 12:e1356534. https://doi.org/10.1080/15592324.2017.1356534

van Mantgem PJ, Stephenson NL (2007) Apparent climatically induced increase of tree mortality rates in a temperate forest. Ecol Letters 10:909–916. https://doi.org/10.1111/j.1461-0248.2007.01080.x

van Meer G, Voelker DR, Feigenson GW (2008) Membrane lipids: where they are and how they behave. Nat Rev Mol Cell Biol 9:112–124. https://doi.org/10.1038/nrm2330

Vanhatalo A, Ghirardo A, Juurola E, Schnitzler J-P, Zimmer I, Hellén H, Hakola H, Bäck J (2018) Long-term dynamics of monoterpene synthase activities, monoterpene storage pools and emissions in boreal Scots pine. Biogeosciences 15:5047–5060. https://doi.org/10.5194/bg-15-5047-2018

Vanhatalo A, Aalto J, Chan T, Hölttä T, Kolari P, Rissanen K, Kabiri K, Hellén H, Bäck J (2020) Scots Pine Stems as Dynamic Sources of Monoterpene and Methanol Emissions. Front. For. Glob. Change 2:1331. https://doi.org/10.3389/ffgc.2019.00095

Vanzo E, Jud W, Li Z, Albert A, Domagalska MA, Ghirardo A, Niederbacher B, Frenzel J, Beemster GTS, Asard H, Rennenberg H, Sharkey TD, Hansel A, Schnitzler J-P (2015)

Facing the Future: Effects of Short-Term Climate Extremes on Isoprene-Emitting and Nonemitting Poplar. Plant Physiol 169:560–575. https://doi.org/10.1104/pp.15.00871

Velikova V, Várkonyi Z, Szabó M, Maslenkova L, Nogues I, Kovács L, Peeva V, Busheva M, Garab G, Sharkey TD, Loreto F (2011) Increased thermostability of thylakoid membranes in isoprene-emitting leaves probed with three biophysical techniques. Plant Physiol 157:905–916. https://doi.org/10.1104/pp.111.182519

Verbruggen N, Hermans C (2008) Proline accumulation in plants: a review. Amino Acids 35:753–759. https://doi.org/10.1007/s00726-008-0061-6

Vicente-Serrano SM, Gouveia C, Camarero JJ, Beguería S, Trigo R, López-Moreno JI, Azorín-Molina C, Pasho E, Lorenzo-Lacruz J, Revuelto J, Morán-Tejeda E, Sanchez-Lorenzo A (2013) Response of vegetation to drought time-scales across global land biomes. Proc Natl Acad Sci U S A 110:52–57. https://doi.org/10.1073/pnas.1207068110

Vickers CE, Gershenzon J, Lerdau MT, Loreto F (2009) A unified mechanism of action for volatile isoprenoids in plant abiotic stress. Nat Chem Biol 5:283–291. https://doi.org/10.1038/nchembio.158

Walker AP, Kauwe MG de, Medlyn BE, Zaehle S, Iversen CM, Asao S, Guenet B, Harper A, Hickler T, Hungate BA, Jain AK, Luo Y, Lu X, Lu M, Luus K, Megonigal JP, Oren R, Ryan E, Shu S, Talhelm A, Wang Y-P, Warren JM, Werner C, Xia J, Yang B, Zak DR, Norby RJ (2019) Decadal biomass increment in early secondary succession woody ecosystems is increased by CO_2 enrichment. Nat Commun 10:454. https://doi.org/10.1038/s41467-019-08348-1

Walker AP, Kauwe MG de, Bastos A, Belmecheri S, Georgiou K, Keeling R, McMahon SM, Medlyn BE, Moore DJP, Norby RJ, Zaehle S, Anderson-Teixeira KJ, Battipaglia G, Brienen RJW, Cabugao KG, Cailleret M, Campbell E, Canadell J, Ciais P, Craig ME, Ellsworth D, Farquhar G, Fatichi S, Fisher JB, Frank D, Graven H, Gu L, Haverd V, Heilman K, Heimann M, Hungate BA, Iversen CM, Joos F, Jiang M, Keenan TF, Knauer J, Körner C, Leshyk VO, Leuzinger S, Liu Y, MacBean N, Malhi Y, McVicar T, Penuelas J, Pongratz J, Powell AS, Riutta T, Sabot MEB, Schleucher J, Sitch S, Smith WK, Sulman B, Taylor B, Terrer C, Torn MS, Treseder K, Trugman AT, Trumbore SE, van Mantgem PJ, Voelker SL, Whelan ME, Zuidema PA (2020) Integrating the evidence for a terrestrial carbon sink caused by increasing atmospheric CO_2. New Phytol. https://doi.org/10.1111/nph.16866

Walker LR, Wardle DA (2014) Plant succession as an integrator of contrasting ecological time scales. Trends in Ecology & Evolution 29:504–510. https://doi.org/10.1016/j.tree.2014.07.002

Walther S, Voigt M, Thum T, Gonsamo A, Zhang Y, Köhler P, Jung M, Varlagin A, Guanter L (2016) Satellite chlorophyll fluorescence measurements reveal large-scale decoupling of photosynthesis and greenness dynamics in boreal evergreen forests. Global Change Biology 22:2979–2996. https://doi.org/10.1111/gcb.13200

Wang J, Ding J, Tan B, Robinson KM, Michelson IH, Johansson A, Nystedt B, Scofield DG, Nilsson O, Jansson S, Street NR, Ingvarsson PK (2018) A major locus controls local adaptation and adaptive life history variation in a perennial plant. Genome Biol 19:72. https://doi.org/10.1186/s13059-018-1444-y

Wang W, English NB, Grossiord C, Gessler A, Das AJ, Stephenson NL, Baisan CH, Allen CD, McDowell NG (2020) Mortality predispositions of conifers across Western USA. New Phytol. https://doi.org/10.1111/nph.16864

Warren JM, Norby RJ, Wullschleger SD (2011) Elevated CO_2 enhances leaf senescence during extreme drought in a temperate forest. Tree Physiol 31:117–130. https://doi.org/10.1093/treephys/tpr002

Warren CR, Adams MA (2001) Distribution of N, Rubisco and photosynthesis in *Pinus pinaster* and acclimation to light. Plant Cell Environ 24:597–609. https://doi.org/10.1046/j.1365-3040.2001.00711.x

Watson H (2015) Biological membranes. Essays Biochem 59:43–69. https://doi.org/10.1042/bse0590043

Weiszmann J, Fürtauer L, Weckwerth W, Nägele T (2018) Vacuolar sucrose cleavage prevents limitation of cytosolic carbohydrate metabolism and stabilizes photosynthesis under abiotic stress. FEBS J 285:4082–4098. https://doi.org/10.1111/febs.14656

Wickham H (2016) ggplot2: Elegant Graphics for Data Analysis. Springer-Verlag New York. http://ggplot2.org

Wieser G, Oberhuber W, Waldboth B, Gruber A, Matyssek R, Siegwolf RT, Grams TE (2018) Long-term trends in leaf level gas exchange mirror tree-ring derived intrinsic water-use efficiency of *Pinus cembra* at treeline during the last century. Agricultural and Forest Meteorology 248:251–258. https://doi.org/10.1016/j.agrformet.2017.09.023

Williams PA, Allen CD, Macalady AK, Griffin D, Woodhouse CA, Meko DM, Swetnam TW, Rauscher SA, Seager R, Grissino-Mayer HD, Dean JS, Cook ER, Gangodagamage C, Cai M, McDowell NG (2013) Temperature as a potent driver of regional forest drought stress and tree mortality. Nature Climate change 3:292–297. https://doi.org/10.1038/nclimate1693

Woodward FI, Kelly CK (1995) The influence of CO_2 concentration on stomatal density. New Phytol 131:311–327. https://doi.org/10.1111/j.1469-8137.1995.tb03067.x

Wu H-C, Bulgakov VP, Jinn T-L (2018) Pectin Methylesterases: Cell Wall Remodeling Proteins Are Required for Plant Response to Heat Stress. Front Plant Sci 9:1612. https://doi.org/10.3389/fpls.2018.01612

Wu D, Piao S, Zhu D, Wang X, Ciais P, Bastos A, Xu X, Xu W (2020) Accelerated terrestrial ecosystem carbon turnover and its drivers. Global Change Biology. https://doi.org/10.1111/gcb.15224

Wujeska-Klause A, Crous KY, Ghannoum O, Ellsworth DS (2019) Lower photorespiration in elevated CO_2 reduces leaf N concentrations in mature Eucalyptus trees in the field. Global Change Biology. https://doi.org/10.1111/gcb.14555

Wullschleger SD, Tschaplinski TJ, Norby RJ (2002) Plant water relations at elevated CO_2 - implications for water-limited environments. Plant Cell Environ 25:319–331. https://doi.org/10.1046/j.1365-3040.2002.00796.x

Xu L, Myneni RB, Chapin III FS, Callaghan TV, Pinzon JE, Tucker CJ, Zhu Z, Bi J, Ciais P, Tømmervik H, Euskirchen ES, Forbes BC, Piao SL, Anderson BT, Ganguly S, Nemani RR, Goetz SJ, Beck PSA, Bunn AG, Cao C, Stroeve JC (2013) Temperature and vegetation seasonality diminishment over northern lands. Nature Clim Change 3:581–586. https://doi.org/10.1038/nclimate1836

Xu Z, Jiang Y, Zhou G (2015) Response and adaptation of photosynthesis, respiration, and antioxidant systems to elevated CO_2 with environmental stress in plants. Front Plant Sci 6:701. https://doi.org/10.3389/fpls.2015.00701

Yan Y, Bender ML, Brook EJ, Clifford HM, Kemeny PC, Kurbatov AV, Mackay S, Mayewski PA, Ng J, Severinghaus JP, Higgins JA (2019a) Two-million-year-old snapshots of atmospheric gases from Antarctic ice. Nature 574:663–666. https://doi.org/10.1038/s41586-019-1692-3

Yan D, Scott RL, Moore D, Biederman JA, Smith WK (2019b) Understanding the relationship between vegetation greenness and productivity across dryland ecosystems through the integration of PhenoCam, satellite, and eddy covariance data. Remote Sensing of Environment 223:50–62. https://doi.org/10.1016/j.rse.2018.12.029

Yancey PH (2005) Organic osmolytes as compatible, metabolic and counteracting cytoprotectants in high osmolarity and other stresses. J Exp Biol 208:2819–2830. https://doi.org/10.1242/jeb.01730

Yáñez-Serrano AM, Mahlau L, Fasbender L, Byron J, Williams J, Kreuzwieser J, Werner C (2019) Heat stress increases the use of cytosolic pyruvate for isoprene biosynthesis. J Exp Bot 70:5827–5838. https://doi.org/10.1093/jxb/erz353

Yazaki K, Arimura G-I, Ohnishi T (2017) 'Hidden' Terpenoids in Plants: Their Biosynthesis, Localization and Ecological Roles. Plant Cell Physiol 58:1615–1621. https://doi.org/10.1093/pcp/pcx123

Yi Y, Kimball JS, Jones LA, Reichle RH, Nemani R, Margolis HA (2013) Recent climate and fire disturbance impacts on boreal and arctic ecosystem productivity estimated using a satellite-based terrestrial carbon flux model. J. Geophys. Res. Biogeosci. 118:606–622. https://doi.org/10.1002/jgrg.20053

Yi C, Pendall E, Ciais P (2015) Focus on extreme events and the carbon cycle. Environ. Res. Lett. 10:70201. https://doi.org/10.1088/1748-9326/10/7/070201

Yosef G, Walko R, Avisar R, Tatarinov F, Rotenberg E, Yakir D (2018) Large-scale semi-arid afforestation can enhance precipitation and carbon sequestration potential. Sci Rep 8:996. https://doi.org/10.1038/s41598-018-19265-6

Zang U, Goisser M, Häberle K-H, Matyssek R, Matzner E, Borken W (2014) Effects of drought stress on photosynthesis, rhizosphere respiration, and fine-root characteristics of beech saplings: A rhizotron field study. Z. Pflanzenernähr. Bodenk. 177:168–177. https://doi.org/10.1002/jpln.201300196

Zeidler J, Lichtenthaler HK (2001) Biosynthesis of 2-methyl-3-buten-2-ol emitted from needles of *Pinus ponderosa* via the non-mevalonate DOXP/MEP pathway of isoprenoid formation. Planta 213:323–326. https://doi.org/10.1007/s004250100562

Zemp DC, Schleussner C-F, Barbosa HMJ, Hirota M, Montade V, Sampaio G, Staal A, Wang-Erlandsson L, Rammig A (2017) Self-amplified Amazon forest loss due to vegetation-atmosphere feedbacks. Nat Commun 8:1786. https://doi.org/10.1038/ncomms14681

Zhang L, Alfano JR, Becker DF (2015) Proline metabolism increases katG expression and oxidative stress resistance in *Escherichia coli*. J Bacteriol 197:431–440. https://doi.org/10.1128/JB.02282-14

Zhang X, Högy P, Wu X, Schmid I, Wang X, Schulze WX, Jiang D, Fangmeier A (2018) Physiological and Proteomic Evidence for the Interactive Effects of Post-Anthesis Heat Stress and Elevated CO_2 on Wheat. Proteomics 18:e1800262. https://doi.org/10.1002/pmic.201800262

Zhao J, Hartmann H, Trumbore S, Ziegler W, Zhang Y (2013) High temperature causes negative whole-plant carbon balance under mild drought. New Phytol 200:330–339. https://doi.org/10.1111/nph.12400

Zhao DF, Buchholz A, Tillmann R, Kleist E, Wu C, Rubach F, Kiendler-Scharr A, Rudich Y, Wildt J, Mentel TF (2017) Environmental conditions regulate the impact of plants on cloud formation. Nat Commun 8:14067. https://doi.org/10.1038/ncomms14067

Zhu Z, Piao S, Myneni RB, Huang M, Zeng Z, Canadell JG, Ciais P, Sitch S, Friedlingstein P, Arneth A, Cao C, Cheng L, Kato E, Koven C, Li Y, Lian X, Liu Y, Liu R, Mao J, Pan Y, Peng

S, Peñuelas J, Poulter B, Pugh TAM, Stocker BD, Viovy N, Wang X, Wang Y, Xiao Z, Yang H, Zaehle S, Zeng N (2016) Greening of the Earth and its drivers. Nature Clim Change 6:791–795. https://doi.org/10.1038/nclimate3004

Zinta G, AbdElgawad H, Domagalska MA, Vergauwen L, Knapen D, Nijs I, Janssens IA, Beemster GTS, Asard H (2014) Physiological, biochemical, and genome-wide transcriptional analysis reveals that elevated CO_2 mitigates the impact of combined heat wave and drought stress in *Arabidopsis thaliana* at multiple organizational levels. Global Change Biology 20:3670–3685. https://doi.org/10.1111/gcb.12626

Zinta G, AbdElgawad H, Peshev D, Weedon JT, van den Ende W, Nijs I, Janssens IA, Beemster GTS, Asard H (2018) Dynamics of metabolic responses to periods of combined heat and drought in Arabidopsis thaliana under ambient and elevated atmospheric CO_2. J Exp Bot 69:2159–2170. https://doi.org/10.1093/jxb/ery055

Zweifel R, Etzold S, Sterck F, Gessler A, Anfodillo T, Mencuccini M, Arx G von, Lazzarin M, Haeni M, Feichtinger L, Meusburger K, Knuesel S, Walthert L, Salmon Y, Bose AK, Schoenbeck L, Hug C, Girardi N de, Giuggiola A, Schaub M, Rigling A (2020) Determinants of legacy effects in pine trees - implications from an irrigation-stop experiment. New Phytol 227:1081–1096. https://doi.org/10.1111/nph.16582

Table S2.1: Greenhouse facility plan for the temperature control by temperature steps of 3 hours for the light phase and 6 hours for the dark phase. Values of each temperature step are derived from field measurements at the Yatir forest measurement site (Israel, monthly mean over 10 years 2004 – 2014).

T [°C] hour of day	Jan	Feb	Mar	Apr	Mai	Jun	Jul	Aug	Sep	Oct	Nov	Dec
0-6	8.9	10.1	11.6	14	16.3	18.9	18.7	19.4	18.2	16.4	13	10
6-9	8.5	10	11.9	15.1	18.8	21.6	20.4	20.6	19.1	17	13.1	9.8
9-12	11.6	13.3	15.7	18.7	22.5	25.7	24.6	25.2	23.7	21.4	17.2	13.2
12-15	13.7	15.4	18.1	21.3	25.1	28.7	27.8	28.6	26.7	23.9	19.1	15.1
15-18	12.6	14.5	17.1	20.3	23.8	27.4	26.7	27.2	24.9	21.8	17.3	13.5
18-20	10.5	12.1	14.1	17.2	20.4	23.9	23.3	23.6	21.4	18.9	14.9	11.5
20-0	9.7	10.9	12.5	15.2	18	20.9	20.5	21.1	19.5	17.5	13.9	10.7

Table S2.2**:** Averages (upper table) and Standard error of mean (lower table) of all analyzed metabolites and parameters except of gas exchange measurement data. Values of metabolites are in µmol gDW^{-1}, Water potential (WP) is in MPa. Needle water content (NW) and root water content (RW) are in [g%]. Status depicts a numerical value for living (1) and dead (0) seedlings. "Part" depicts shoots (N) and roots (R).

Treatment	Harvest	Part	Status	NW	RW	Glucose	Fructose	Sucrose	Cyclitols	Citrate	Malate	Fumarate	Nitrate	Sulfate	Phosphate	Proline	Starch	sNSC	CS	totalC	WP	PhiPSII	FvFm	qP	qN	ETR	-Π
C	I	N	1	65.2	68.0	29.5	24.9	118.8	346.4	64.4	33.1	29.4	1.3	31.9	35.6	15.1	77.5	292.0	106.1	874.8	-1.1	0.21	0.45	0.46	49.09	112.38	1.73
C	II	N	1	66.1	66.8	15.4	14.6	72.7	285.7	69.5	44.8	27.7	1.7	37.9	38.3	15.4	33.5	175.5	117.9	647.6	-0.66	0.18	0.46	0.40	1.86	98.01	1.45
C	III	N	1	63.5	61.9	42.4	40.0	97.7	232.3	50.6	36.0	30.3	2.1	27.1	35.3	11.9	56.9	277.9	94.8	752.4	-0.98	0.21	0.47	0.46	1.84	116.10	1.88
C	I	R	1	65.2	68.0	5.1	4.9	31.1	187.8	33.3	11.9	18.3	92.5	65.8	33.6	38.1	30.0	72.3	53.4	347.7	NA	NA	NA	NA	NA	NA	0.88
C	II	R	1	66.1	66.8	6.9	4.9	39.4	155.8	30.3	14.4	13.4	105.6	61.4	29.9	26.4	20.3	90.6	48.8	318.6	NA	NA	NA	NA	NA	NA	0.88
C	III	R	1	63.1	64.2	5.9	4.1	20.2	169.4	24.6	10.2	9.5	128.8	75.9	29.6	2.2	7.8	50.4	37.7	267.1	NA	NA	NA	NA	NA	NA	1.01
CD	I	N	1	65.5	67.3	33.3	27.4	109.5	400.4	67.2	37.0	32.6	1.1	39.7	33.0	12.0	83.1	279.8	113.6	949.7	-0.96	0.19	0.45	0.42	1.82	99.72	1.72
CD	II	N	1	63.8	53.5	42.9	28.9	75.3	123.0	74.6	52.8	29.8	1.6	46.4	52.5	17.0	13.1	222.4	129.7	508.6	-1.45	0.13	0.43	0.31	1.72	69.63	1.54
CD	III	N	1	63.6	56.9	32.8	29.6	103.6	189.8	47.0	27.6	31.3	1.0	33.6	29.1	10.7	25.6	269.7	86.2	636.8	-1.06	0.18	0.44	0.42	1.78	96.05	1.51
CD	I	R	1	65.5	67.3	6.3	6.4	34.1	173.9	25.3	12.1	15.9	93.9	56.2	28.7	31.9	32.7	81.0	44.0	334.0	NA	NA	NA	NA	NA	NA	0.86
CD	II	R	1	63.8	53.5	5.5	3.1	19.5	104.9	24.7	11.9	7.9	123.1	77.6	35.7	12.3	8.5	47.6	38.0	182.3	NA	NA	NA	NA	NA	NA	1.48
CD	III	R	1	63.9	54.6	7.1	5.1	17.4	133.1	28.8	11.1	6.8	105.0	66.7	25.4	1.9	16.9	47.0	40.8	237.8	NA	NA	NA	NA	NA	NA	1.29
H	III	N	0	28.8	58.0	55.1	49.8	24.7	315.2	78.4	69.4	34.4	31.9	81.5	75.2	95.0	5.8	154.3	147.6	626.4	NA	NA	NA	NA	NA	NA	12.43
H	III	R	0	28.8	58.0	2.2	1.6	0.1	69.8	2.6	1.9	1.4	159.8	48.7	8.7	2.3	0.4	4.1	4.8	79.0	NA	NA	NA	NA	NA	NA	1.15
H	I	N	1	65.8	67.3	39.2	24.3	113.5	449.6	65.4	40.8	29.0	1.2	21.0	35.2	12.4	105.6	290.5	112.0	1021.6	-1.05	0.19	0.43	0.44	1.77	102.47	1.80
H	II	N	1	64.9	61.7	39.9	31.5	54.1	354.1	95.5	67.0	29.0	5.3	55.6	41.7	31.4	12.8	179.6	159.5	667.3	-1.17	0.12	0.43	0.29	1.80	60.65	1.54
H	III	N	1	63.4	61.9	24.4	22.6	93.5	188.8	75.0	43.2	41.4	1.8	39.9	36.9	31.9	50.0	234.0	131.4	635.6	-1.26	0.21	0.46	0.46	1.78	98.00	1.60
H	I	R	1	65.8	67.3	7.6	6.9	38.8	124.7	24.0	11.6	17.3	96.7	58.9	25.3	24.7	28.6	92.0	43.2	291.0	NA	NA	NA	NA	NA	NA	0.80
H	II	R	1	64.9	61.7	1.8	2.3	7.9	109.7	19.5	6.8	8.8	126.6	58.0	22.5	17.6	3.9	19.7	29.9	164.6	NA	NA	NA	NA	NA	NA	0.94
H	III	R	1	63.4	61.9	4.5	3.6	16.3	185.5	20.6	8.1	5.1	133.6	74.1	23.5	1.9	11.3	40.7	29.4	267.0	NA	NA	NA	NA	NA	NA	1.14
HD	II	N	0	36.3	24.8	46.6	30.0	84.7	140.5	89.8	44.0	23.4	16.3	78.5	51.9	119.6	2.8	246.1	134.8	556.7	NA	NA	NA	NA	NA	NA	5.94
HD	III	N	0	13.6	43.0	49.1	44.4	52.6	334.2	87.6	52.8	22.4	8.0	41.5	54.0	75.7	2.7	198.6	137.7	679.6	NA	NA	NA	NA	NA	NA	25.40
HD	II	R	0	36.3	24.8	4.8	2.2	3.0	140.1	16.4	7.0	5.6	161.8	72.4	27.2	3.9	2.4	12.9	24.8	180.7	NA	NA	NA	NA	NA	NA	5.85
HD	III	R	0	13.6	43.0	1.0	0.3	0.2	75.5	3.6	1.8	1.9	138.0	66.1	15.2	0.9	0.5	1.8	6.1	83.8	NA	NA	NA	NA	NA	NA	1.78
HD	I	N	1	63.4	62.0	64.9	31.1	92.1	370.0	72.9	45.3	26.4	2.5	28.6	33.3	13.5	70.7	280.2	120.7	871.0	-1.08	0.22	0.44	0.50	1.80	116.71	1.81
HD	II	N	1	61.8	34.1	29.5	22.0	58.4	225.5	100.1	50.7	23.7	7.4	40.1	39.3	32.0	19.9	168.3	149.7	617.0	-1.77	0.04	0.17	0.14	1.30	24.66	1.87
HD	III	N	1	62.4	47.8	65.6	68.1	108.9	550.5	100.9	60.4	45.9	4.5	24.0	52.3	88.6	15.6	351.4	171.7	1108.3	-1.40	0.13	0.35	0.34	1.77	105.54	2.00
HD	I	R	1	63.4	62.0	4.8	4.9	21.3	90.1	15.7	5.3	10.5	59.0	35.4	18.1	20.3	16.6	52.3	26.2	186.0	NA	NA	NA	NA	NA	NA	0.64
HD	II	R	1	61.8	34.1	0.5	0.4	0.7	36.7	10.3	3.2	3.0	80.9	28.3	18.7	4.4	0.8	2.4	14.5	54.4	NA	NA	NA	NA	NA	NA	1.43
HD	III	R	1	62.4	47.8	4.4	3.6	10.0	51.3	17.5	5.4	3.9	164.6	81.3	21.5	2.0	4.6	28.1	23.7	107.7	NA	NA	NA	NA	NA	NA	1.91

Treatment	Harvest	Part	Status	NW	RW	Glucose	Fructose	Sucrose	Cyclitols	Citrate	Malate	Fumarate	Nitrate	Sulfate	Phosphate	Proline	Starch	sNSC	CS	totalC	WP	PhiPSII	FvFm	qP	qN	ETR	-Π
C	I	N	1	0.7	2.2	4.8	4.9	7.2	70.2	6.9	2.6	3.8	0.3	6.2	2.1	3.5	17.4	17.0	10.3	83.8	0.1	0.0	0.0	0.0	47.3	11.8	0.08
C	II	N	1	0.7	1.9	3.5	5.0	21.4	35.1	13.3	5.0	1.4	0.3	8.3	2.9	3.7	10.0	50.0	16.7	40.7	0.0	0.0	0.0	0.0	0.0	5.9	0.07
C	III	N	1	0.8	2.5	7.0	6.8	4.8	39.2	8.9	4.9	2.6	0.5	3.8	4.5	1.9	13.1	14.7	12.5	70.9	0.1	0.0	0.0	0.1	0.0	9.0	0.07
C	I	R	1	0.7	2.2	0.5	1.0	2.9	34.3	8.0	2.4	2.3	17.5	13.3	4.0	14.9	9.5	7.0	10.9	43.9	NA	NA	NA	NA	NA	NA	0.07
C	II	R	1	0.7	1.9	2.7	2.2	6.9	14.0	5.2	4.5	1.1	18.9	12.6	4.4	3.5	6.8	17.9	7.5	37.8	NA	NA	NA	NA	NA	NA	0.09
C	III	R	1	0.7	1.5	1.0	0.6	2.1	19.9	2.8	2.1	1.5	15.1	10.9	2.6	0.2	1.5	5.6	4.5	23.0	NA	NA	NA	NA	NA	NA	0.08
CD	I	N	1	0.6	1.9	6.9	6.7	12.8	60.7	9.6	3.6	2.5	0.2	8.1	3.6	2.7	26.1	21.2	12.3	86.5	0.0	0.0	0.0	0.0	0.0	1.9	0.11
CD	II	N	1	0.8	1.6	13.9	9.1	9.0	51.3	9.3	4.6	2.2	0.4	9.0	8.1	3.7	3.7	39.5	10.5	30.7	0.2	0.0	0.0	0.0	0.0	5.1	0.08
CD	III	N	1	0.4	2.0	4.4	2.8	10.5	24.5	3.2	2.8	1.7	0.2	3.3	1.0	1.8	11.5	18.0	4.8	25.9	0.1	0.0	0.0	0.0	0.0	3.4	0.05
CD	I	R	1	0.6	1.9	1.2	1.5	3.9	23.4	2.8	2.6	2.1	13.0	8.3	3.9	2.9	9.8	10.5	4.9	44.8	NA	NA	NA	NA	NA	NA	0.07
CD	II	R	1	0.8	1.6	1.8	1.1	4.1	7.2	1.9	1.1	0.9	16.8	11.7	4.3	2.2	1.5	9.2	2.4	27.4	NA	NA	NA	NA	NA	NA	0.23
CD	III	R	1	0.5	2.0	0.9	0.5	1.6	13.3	4.9	2.0	1.1	9.3	5.7	2.7	0.4	3.2	4.5	6.7	16.9	NA	NA	NA	NA	NA	NA	0.07
H	III	N	0	6.4	4.3	17.6	25.1	6.1	60.6	13.2	9.8	7.3	10.9	19.8	12.7	19.2	1.2	52.3	22.9	26.6	NA	NA	NA	NA	NA	NA	3.11
H	III	R	0	6.4	4.3	1.5	1.6	0.1	40.1	2.4	1.6	0.4	31.6	7.3	2.1	2.0	0.0	3.3	3.7	46.8	NA	NA	NA	NA	NA	NA	0.53
H	I	N	1	0.3	2.0	4.5	2.8	8.6	47.4	9.2	4.6	0.7	0.2	6.5	4.7	2.4	29.2	20.7	12.0	67.6	0.1	0.0	0.0	0.0	0.0	6.0	0.08
H	II	N	1	1.0	2.8	8.6	4.6	2.5	77.7	22.5	23.9	6.4	1.1	8.1	9.9	13.6	2.9	13.8	42.1	137.6	0.1	0.0	0.0	0.0	0.1	10.7	0.19
H	III	N	1	0.6	1.5	4.1	1.1	5.9	28.5	10.4	6.2	2.0	0.3	2.8	1.8	8.2	22.4	12.0	15.0	27.2	0.1	0.0	0.0	0.0	0.1	8.2	0.08
H	I	R	1	0.3	2.0	1.4	1.1	4.9	22.2	2.2	2.0	4.1	13.0	9.5	2.5	2.4	3.9	11.4	5.5	38.2	NA	NA	NA	NA	NA	NA	0.06
H	II	R	1	1.0	2.8	0.3	0.5	1.9	29.7	3.7	2.8	1.5	14.9	11.0	2.4	1.7	1.0	4.5	4.7	34.4	NA	NA	NA	NA	NA	NA	0.11
H	III	R	1	0.6	1.5	0.7	0.6	1.7	25.8	3.2	1.7	1.0	10.3	5.8	2.4	0.2	2.9	4.4	4.2	31.4	NA	NA	NA	NA	NA	NA	0.13
HD	II	N	0	2.1	3.1	8.3	3.7	20.1	58.6	11.7	7.1	2.3	10.5	20.4	10.0	38.8	0.6	38.8	16.5	69.5	NA	NA	NA	NA	NA	NA	1.15
HD	III	N	0	2.6	1.8	14.0	12.7	7.1	110.7	7.1	6.5	2.1	3.1	10.7	6.4	17.2	1.4	31.3	10.4	131.0	NA	NA	NA	NA	NA	NA	4.70
HD	II	R	0	2.1	3.1	3.0	1.3	2.3	51.9	3.5	3.3	0.4	14.4	15.2	2.3	1.1	1.2	8.8	5.2	55.1	NA	NA	NA	NA	NA	NA	1.05
HD	III	R	0	2.6	1.8	0.1	0.1	0.2	22.7	1.6	0.7	0.4	30.7	10.4	0.7	0.4	0.1	0.4	2.3	24.8	NA	NA	NA	NA	NA	NA	0.31
HD	I	N	1	0.7	2.4	29.3	8.9	20.1	26.9	15.5	7.1	1.8	0.7	7.0	3.3	5.1	25.8	62.2	19.1	50.6	0.1	0.0	0.0	0.0	0.0	8.5	0.21
HD	II	N	1	0.6	3.0	4.2	4.6	9.4	102.8	15.5	6.8	2.1	2.9	3.9	3.9	6.6	13.5	12.5	18.5	110.4	0.1	0.0	0.1	0.1	0.1	13.8	0.12
HD	III	N	1	1.0	3.3	32.8	32.8	16.1	94.4	36.9	15.5	7.3	2.5	11.0	26.6	51.0	10.8	91.9	51.0	237.8	0.1	0.1	0.1	0.1	0.1	7.3	0.09
HD	I	R	1	0.7	2.4	0.8	1.0	3.6	19.2	1.5	1.2	2.3	10.6	6.1	2.8	2.0	4.7	8.6	3.2	33.2	NA	NA	NA	NA	NA	NA	0.08
HD	II	R	1	0.6	3.0	0.5	0.4	0.7	36.7	4.1	1.4	1.0	29.4	16.4	6.6	1.7	0.2	2.4	5.3	42.8	NA	NA	NA	NA	NA	NA	0.49
HD	III	R	1	1.0	3.3	1.1	0.8	4.8	15.6	4.8	1.3	0.3	65.9	17.6	1.2	0.5	3.4	9.0	5.7	15.6	NA	NA	NA	NA	NA	NA	0.80

Table S2.3: Linear mixed effect model output that tested for interaction of the treatment group (drought, heat, heat-drought) and the experimental time-period (before stress, heat wave 1, heat release 1, heat wave 2, heat release 2, wet recovery) against the control. Experimental time-periods are equivalent to the visually highlighted experimental condition in Fig. 1 (main text). Chamber identity and day of year were assigned to random effects. Significance codes are depicted as follows: p ≤ 0 '***' 0.001 '**' 0.01 '*' 0.05 '.' 0.1 ' ' 1. Non-significant differences are marked with "n.s.".

	Assimilation [A_{net}]			
	value	SE	t-statistics	significance
(Intercept)	11.95	1.01	11.85	***
drought	1.34	1.88	0.71	n.s.
heat	-0.03	1.49	-0.02	n.s.
heat-drought	-1.66	1.88	-0.89	n.s.
heat wave 1	0.81	0.99	0.82	n.s.
heat release 1	-0.28	0.90	-0.31	n.s.
heat wave 2	1.06	0.99	1.07	n.s.
heat release 2	-2.29	0.81	-2.82	**
wet recovery	-2.55	0.82	-3.13	**
drought:heat wave 1	-7.98	1.05	-7.59	***
heat:heat wave 1	-5.26	0.85	-6.19	***
heat-drought:heat wave 1	-5.63	1.10	-5.14	***
drought:heat release 1	-9.75	1.06	-9.17	***
heat :heat release 1	-3.60	0.85	-4.24	***
heat-drought:heat release 1	-6.04	1.07	-5.66	***
drought:heat wave 2	-11.38	1.05	-10.86	***
heat:heat wave 2	-8.02	0.85	-9.41	***
heat-drought:heat wave 2	-9.48	1.15	-8.27	***
drought:heat release 2	-8.59	0.91	-9.40	***
heat:heat release 2	-1.39	0.74	-1.89	.
heat-drought:heat release 2	-5.40	0.95	-5.67	***
drought:wet recovery	-6.97	0.94	-7.44	***
heat:wet recovery	0.23	0.73	0.32	n.s.
heat-drought:wet recovery	-3.67	0.93	-3.96	***

	Respiration [R_{night}]			
	value	SE	t-statistics	significance
(Intercept)	-0.95	0.18	-5.34	***
drought	-0.03	0.25	-0.10	n.s.
heat	0.07	0.27	0.28	n.s.
heat-drought	1.53	0.40	3.84	**
heat wave 1	-0.12	0.17	-0.70	n.s.
heat release 1	-0.05	0.15	-0.33	n.s.
heat wave 2	-0.01	0.17	-0.07	n.s.
heat release 2	0.04	0.14	0.32	n.s.
wet recovery	0.00	0.11	0.01	n.s.
drought:heat wave 1	0.18	0.23	0.80	n.s.
heat:heat wave 1	-1.11	0.25	-4.46	***
heat-drought:heat wave 1	-1.91	0.36	-5.32	***
drought:heat release 1	0.37	0.21	1.75	.
heat :heat release 1	-0.56	0.23	-2.44	*
heat-drought:heat release 1	-1.16	0.34	-3.40	***
drought:heat wave 2	0.69	0.23	3.00	**
heat:heat wave 2	-0.79	0.25	-3.19	**
heat-drought:heat wave 2	-1.26	0.35	-3.63	***
drought:heat release 2	0.46	0.19	2.46	*
heat:heat release 2	-0.28	0.20	-1.37	n.s.
heat-drought:heat release 2	-0.98	0.29	-3.44	***
drought:wet recovery	0.28	0.15	1.81	.
heat:wet recovery	-0.18	0.17	-1.09	n.s.
heat-drought:wet recovery	-1.02	0.24	-4.22	***

	Transpiration [E_{day}]			
	value	SE	t-statistics	significance
(Intercept)	1.71	0.21	8.10	***
drought	0.22	0.41	0.53	n.s.
heat	-0.33	0.33	-1.00	n.s.
heat-drought	-0.29	0.41	-0.71	n.s.
heat wave 1	0.35	0.14	2.54	*
heat release 1	0.27	0.13	2.08	*
heat wave 2	0.67	0.14	4.83	***
heat release 2	-0.06	0.12	-0.51	n.s.
wet recovery	0.01	0.12	0.07	n.s.
drought:heat wave 1	-1.57	0.20	-8.02	***
heat:heat wave 1	0.91	0.16	5.71	***
heat-drought:heat wave 1	-0.27	0.20	-1.31	n.s.
drought:heat release 1	-1.81	0.20	-9.10	***
heat :heat release 1	-0.44	0.16	-2.81	**
heat-drought:heat release 1	-1.19	0.20	-5.99	***
drought:heat wave 2	-2.21	0.20	-11.31	***
heat:heat wave 2	0.09	0.16	0.59	n.s.
heat-drought:heat wave 2	-1.52	0.21	-7.09	***
drought:heat release 2	-1.57	0.17	-9.20	***
heat:heat release 2	0.00	0.14	0.00	n.s.
heat-drought:heat release 2	-1.01	0.18	-5.69	***
drought:wet recovery	-1.40	0.17	-7.99	***
heat:wet recovery	0.27	0.14	2.01	*
heat-drought:wet recovery	-0.78	0.17	-4.53	***

	Stomatal conductance [g_s]			
	value	SE	t-statistics	significance
(Intercept)	10.92	2.30	4.75	***
drought	4.88	3.23	1.51	n.s.
heat	0.82	3.49	0.23	n.s.
heat-drought	8.58	5.11	1.68	n.s.
heat wave 1	1.27	1.51	0.84	n.s.
heat release 1	1.41	1.36	1.03	n.s.
heat wave 2	-2.01	1.51	-1.33	n.s.
heat release 2	-1.17	1.23	-0.95	n.s.
wet recovery	-1.33	1.01	-1.31	n.s.
drought:heat wave 1	-7.62	2.01	-3.79	***
heat:heat wave 1	-0.85	2.18	-0.39	n.s.
heat-drought:heat wave 1	-13.70	3.15	-4.35	***
drought:heat release 1	-10.89	1.83	-5.94	***
heat :heat release 1	-1.96	1.99	-0.98	n.s.
heat-drought:heat release 1	-16.79	2.98	-5.63	***
drought:heat wave 2	-8.15	2.01	-4.06	***
heat:heat wave 2	-2.88	2.18	-1.32	n.s.
heat-drought:heat wave 2	-15.78	3.05	-5.18	***
drought:heat release 2	-8.62	1.64	-5.27	***
heat:heat release 2	1.35	1.76	0.76	n.s.
heat-drought:heat release 2	-14.77	2.50	-5.92	***
drought:wet recovery	-4.59	1.34	-3.42	***
heat:wet recovery	-2.56	1.46	-1.75	.
heat-drought:wet recovery	-14.83	2.11	-7.02	***

	Intrinsic water-use-efficiency [WUE_i]			
	value	SE	t-statistics	significance
(Intercept)	-0.14	0.01	-19.12	***
drought	0.01	0.01	0.52	n.s.
heat	-0.02	0.01	-1.53	n.s.
heat-drought	0.02	0.01	1.13	n.s.
heat wave 1	0.01	0.01	1.25	n.s.
heat release 1	0.00	0.01	0.41	n.s.
heat wave 2	0.00	0.01	-0.52	n.s.
heat release 2	-0.01	0.01	-0.83	n.s.
wet recovery	0.00	0.01	-0.67	n.s.
drought:heat wave 1	-0.08	0.01	-5.55	***
heat:heat wave 1	0.03	0.01	2.71	**
heat-drought:heat wave 1	-0.02	0.02	-1.43	n.s.
drought:heat release 1	-0.09	0.01	-6.23	***
heat :heat release 1	-0.02	0.01	-2.03	*
heat-drought:heat release 1	-0.07	0.01	-4.96	***
drought:heat wave 2	-0.08	0.01	-5.58	***
heat:heat wave 2	0.03	0.01	2.10	*
heat-drought:heat wave 2	-0.05	0.02	-3.40	***
drought:heat release 2	-0.08	0.01	-6.24	***
heat:heat release 2	0.00	0.01	0.02	n.s.
heat-drought:heat release 2	-0.04	0.01	-2.76	**
drought:wet recovery	-0.07	0.01	-5.42	***
heat:wet recovery	-0.01	0.01	-1.34	n.s.
heat-drought:wet recovery	-0.07	0.01	-5.55	***

Table S2.4: Results of Analysis of Variance Analysis (ANOVA) for metabolites and chlorophyll fluorescence parameters. Analysis was done to reveal differences between the treatments and the control within a sampling period (post-stress, recovery). Significance is given with: 0 '***' 0.001 '**' 0.01 '*' and n.s (not significant).

	Estimate	Std. Error	t value	Pr(<|t|)	Significance
Part: Needles		Period: Stress		Metabolite: sNSC	
Intercept	175.487	34.769	5.047	7.16e-05	***
Drought	46.922	51.179	0.917	0.371	n.s.
Heat	4.083	49.171	0.083	0.935	n.s.
Heat-Drought	-7.219	63.480	-0.114	0.911	n.s.
				Metabolite: Starch	
Intercept	33.513	7.050	4.754	0.000107	***
Drought	-20.404	10.377	-1.966	0.062639	n.s.
Heat	-20.714	9.654	-2.146	0.043738	*
Heat-Drought	-13.572	11.691	-1.161	0.258720	n.s.
				Metabolite: CS	
Intercept	117.86	28.35	4.157	0.000446	***
Drought	11.87	41.73	0.284	0.778904	n.s.
Heat	41.60	38.82	1.072	0.296076	n.s.
Heat-Drought	31.86	47.02	0.678	0.505419	n.s.
				Metabolite: Cyclitols	
Intercept	285.74	60.42	4.729	0.000128	***
Drought	-162.77	88.93	-1.830	0.082167	n.s.
Heat	68.34	85.45	0.800	0.433203	n.s.
Heat-Drought	-60.27	100.19	-0.602	0.554264	n.s.
				Metabolite: totalC	
Intercept	647.57	93.79	6.904	1.05e-06	***
Drought	-138.96	138.06	-1.006	0.326	n.s.
Heat	19.71	128.43	0.153	0.880	n.s.
Heat-Drought	-30.56	171.25	-0.178	0.860	n.s.
				Metabolite: Nitrate	
Intercept	1.6923	1.0855	1.559	0.13394	n.s.
Drought	-0.1414	1.5978	-0.088	0.93033	n.s.
Heat	3.6216	1.4864	2.436	0.02382	*
Heat-Drought	5.7304	1.8001	3.183	0.00447	**
				Metabolite: Proline	
Intercept	15.397	8.969	1.717	0.101	n.s.
Drought	1.572	13.203	0.119	0.906	n.s.
Heat	16.048	12.282	1.307	0.205	n.s.
Heat-Drought	16.648	14.874	1.119	0.276	n.s.
				Parameter: WP	
Intercept	-0.6600	0.1478	-4.466	0.000390	***
Drought	-0.7900	0.2001	-3.948	0.001151	**
Heat	-0.5067	0.2001	-2.532	0.022186	*
Heat-Drought	-1.1067	0.2413	-4.586	0.000304	***
				Parameter: qP	
Intercept	0.40319	0.04961	8.128	3.2e-06	***
Drought	-0.08941	0.07015	-1.275	0.22660	n.s.
Heat	-0.11655	0.07015	-1.661	0.12253	n.s.
Heat-Drought	-0.25835	0.07015	-3.683	0.00313	**
				Parameter: ETR	
Intercept	98.010	9.913	9.887	1.07e-07	***
Drought	-28.384	13.299	-2.134	0.050986	*
Heat	-37.362	13.299	-2.809	0.013921	*
Heat-Drought	-73.353	14.018	-5.233	0.000127	***
				Parameter: PhiPSII	
Intercept	0.18484	0.02091	8.840	1.33e-06	***

Drought	-0.05043	0.02957	-1.705	0.1138	n.s.
Heat	-0.06021	0.02957	-2.036	0.0644	n.s.
Heat-Drought	-0.14334	0.02957	-4.847	0.0004	***
				Parameter: Fv`/Fm`	
Intercept	0.45935	0.04173	11.008	1.26e-07	***
Drought	-0.03290	0.05901	-0.558	0.587414	n.s.
Heat	-0.03210	0.05901	-0.544	0.596490	n.s.
Heat-Drought	-0.28669	0.05901	-4.858	0.000393	***
				Parameter: -Π	
Intercept	1.45354	0.12355	11.765	1.36e-09	***
Drought	0.08364	0.17472	0.479	0.6383	n.s.
Heat	0.08677	0.17472	0.497	0.6258	n.s.
Heat-Drought	0.41590	0.21399	1.944	0.0687	n.s

Part: Needles		Period: Post-Stress		Metabolite: sNSC	
Intercept	277.863	22.147	12.546	1.55e-12	***
Drought	-8.204	29.713	-0.276	0.7847	n.s.
Heat	-43.866	30.438	-1.441	0.1615	n.s.
Heat-Drought	73.586	42.408	1.735	0.0946	n.s.
				Metabolite: Starch	
Intercept	56.949	15.135	3.763	0.000791	***
Drought	-31.380	21.404	-1.466	0.153760	n.s.
Heat	-6.979	21.990	-0.317	0.753326	n.s.
Heat-Drought	-41.303	31.506	-1.311	0.200519	n.s.
				Metabolite: CS	
Intercept	94.782	13.090	7.241	6.99e-08	***
Drought	-8.544	18.513	-0.462	0.64799	n.s.
Heat	36.582	19.020	1.923	0.06466	n.s.
Heat-Drought	76.944	27.250	2.824	0.00865	**
				Metabolite: Cyclitols	
Intercept	232.31	33.00	7.041	1.17e-07	***
Drought	-42.49	46.66	-0.911	0.370	n.s.
Heat	-43.55	47.94	-0.908	0.371	n.s.
Heat-Drought	318.21	68.69	4.633	7.57e-05	***
				Metabolite: totalC	
Intercept	752.42	59.40	12.666	1.25e-12	***
Drought	-115.61	79.70	-1.451	0.1589	n.s.
Heat	-116.82	81.64	-1.431	0.1644	n.s.
Heat-Drought	355.85	113.75	3.128	0.0043	**
				Metabolite: Nitrate	
Intercept	2.0951	0.5173	4.050	0.000388	***
Drought	-1.0836	0.7131	-1.520	0.140219	n.s.
Heat	-0.2633	0.7316	-0.360	0.721739	n.s.
Heat-Drought	2.4061	1.0346	2.326	0.027802	*
				Metabolite: Proline	
Intercept	11.950	8.673	1.378	0.179191	n.s.
Drought	-1.244	12.266	-0.101	0.919970	n.s.
Heat	19.962	12.602	1.584	0.124418	n.s.
Heat-Drought	76.689	18.055	4.248	0.000216	***
				Parameter: WP	
Intercept	-0.9800	0.1002	-9.785	2.31e-07	***
Drought	-0.0800	0.1416	-0.565	0.5818	n.s.
Heat	-0.2800	0.1416	-1.977	0.0697	n.s.
Heat-Drought	-0.4200	0.1874	-2.242	0.0431	*
				Parameter: qP	
Intercept	0.460310	0.0567840	8.106	5.76e-06	***
Drought	-0.04475	0.08030	-0.557	0.588	n.s.
Heat	0.000849	0.0803047	0.011	0.992	n.s.
Heat-Drought	-0.12076	0.0867390	-1.392	0.191	n.s.
				Parameter: ETR	

Intercept	116.097	7.807	14.872	1.27e-12	***
Drought	-20.049	11.491	-1.745	0.0957	n.s.
Heat	-18.102	10.409	-1.739	0.0967	n.s.
Heat-Drought	-10.557	14.253	-0.741	0.4671	n.s.
				Parameter: PhiPSII	
Intercept	0.214833	0.027599	7.784	8.47e-06	***
Drought	-0.03192	0.039031	-0.818	0.4308	n.s.
Heat	-0.00485	0.039031	-0.124	0.9033	n.s.
Heat-Drought	-0.08084	0.042159	-1.918	0.0815	n.s.
				Parameter: Fv`/Fm`	
Intercept	0.46536	0.02735	17.014	3.01e-09	***
Drought	-0.02417	0.03868	-0.625	0.5448	n.s.
Heat	-0.01024	0.03868	-0.265	0.7960	n.s.
Heat-Drought	-0.11225	0.04178	-2.687	0.0212	*
				Parameter: -Π	
Intercept	1.88320	0.08254	22.817	3.44e-14	***
Drought	-0.36916	0.09920	-3.722	0.0017	**
Heat	-0.2804	0.10655	-2.632	0.0175	*
Heat-Drought	0.11664	0.14296	0.816	0.4258	n.s.

Part: Roots		Period: Stress		Metabolite: sNSC	
Intercept	90.57	10.82	8.371	3.95e-08	***
Drought	-42.95	15.93	-2.697	0.013497	*
Heat	-70.83	14.82	-4.781	0.000101	***
Heat-Drought	-88.22	17.94	-4.917	7.30e-05	***
				Metabolite: Starch	
Intercept	20.279	3.752	5.404	2.32e-05	***
Drought	-11.739	5.523	-2.125	0.04559	*
Heat	-16.415	5.138	-3.195	0.00436	**
Heat-Drought	-19.526	6.223	-3.138	0.00497	**
				Metabolite: CS	
Intercept	48.838	5.293	9.228	7.77e-09	***
Drought	-10.878	7.791	-1.396	0.177230	n.s.
Heat	-18.978	7.247	-2.619	0.016049	*
Heat-Drought	-34.346	8.777	-3.913	0.000799	***
				Metabolite: Cyclitols	
Intercept	155.83	23.14	6.735	1.49e-06	***
Drought	-50.98	35.84	-1.422	0.17034	n.s.
Heat	-46.12	31.68	-1.456	0.16100	n.s.
Heat-Drought	-119.14	38.37	-3.105	0.00558	**
				Metabolite: totalC	
Intercept	318.64	34.07	9.353	6.17e-09	***
Drought	-136.36	50.15	-2.719	0.012857	*
Heat	-154.02	46.65	-3.301	0.003398	**
Heat-Drought	-264.20	56.50	-4.676	0.000129	***
				Metabolite: Nitrate	
Intercept	105.64	17.76	5.948	6.65e-06	***
Drought	17.50	26.14	0.669	0.511	n.s.
Heat	20.95	24.32	0.861	0.399	n.s.
Heat-Drought	-24.75	29.45	-0.840	0.410	n.s.
				Metabolite: Proline	
Intercept	26.419	2.392	11.047	3.30e-10	***
Drought	-14.141	3.520	-4.017	0.000624	***
Heat	-8.785	3.275	-2.683	0.013938	*
Heat-Drought	-22.010	3.966	-5.550	1.66e-05	***
				Parameter: -Π	
Intercept	0.87905	0.19369	4.539	0.000179	***
Drought	0.60329	0.28510	2.116	0.046454	*
Heat	0.06231	0.26522	0.235	0.816521	n.s.
Heat-Drought	0.55576	0.32119	1.730	0.098250	n.s.

Part: Roots		Period: Post-Stress		Metabolite: sNSC	
Intercept	50.441	4.848	10.405	3.98e-11	***
Drought	-3.414	6.856	-0.498	0.6224	n.s.
Heat	-9.716	7.044	-1.379	0.1787	n.s.
Heat-Drought	-22.330	10.091	-2.213	0.0352	*
				Metabolite: Starch	
Intercept	7.809	2.537	3.078	0.00463	**
Drought	9.101	3.588	2.536	0.01706	*
Heat	3.496	3.687	0.948	0.35110	n.s.
Heat-Drought	-3.208	5.282	-0.607	0.54855	n.s.
				Metabolite: CS	
Intercept	37.737	5.133	7.352	5.25e-08	***
Drought	3.021	7.259	0.416	0.680	n.s.
Heat	-8.290	7.458	-1.112	0.276	n.s.
Heat-Drought	-14.062	10.684	-1.316	0.19	n.s.
				Metabolite: Cyclitols	
Intercept	169.36	18.97	8.930	1.1e-09	***
Drought	-36.30	26.82	-1.353	0.18678	n.s.
Heat	16.12	27.56	0.585	0.56327	n.s.
Heat-Drought	-118.10	39.48	-2.991	0.00574	**
				Metabolite: totalC	
Intercept	267.1153	22.7984	11.716	2.61e-12	***
Drought	-29.3553	32.2418	-0.910	0.37034	n.s.
Heat	-0.1547	33.1253	-0.005	0.99631	n.s.
Heat-Drought	-159.462	47.4586	-3.360	0.00226	**
				Metabolite: Nitrate	
Intercept	128.835	14.895	8.650	2.14e-09	***
Drought	-23.8135	21.064	-1.130	0.268	n.s.
Heat	4.743	21.641	0.219	0.828	n.s.
Heat-Drought	35.778	31.005	1.154	0.258	n.s.
				Metabolite: Proline	
Intercept	2.2307	0.2844	7.843	1.53e-08	***
Drought	-0.3072	0.4022	-0.764	0.451	n.s.
Heat	-0.3189	0.4132	-0.772	0.447	n.s.
Heat-Drought	-0.2175	0.5921	-0.367	0.716	n.s.
				Parameter: -Π	
Intercept	1.0134	0.1486	6.821	2.07e-07	***
Drought	0.2765	0.2101	1.316	0.199	n.s.
Heat	0.1277	0.2159	0.591	0.559	n.s.
Heat-Drought	0.9002	0.3093	2.911	0.007	**

Table S2.5: Results of multiple comparison test (Tukey HSD) calculated from ANOVA tables that yielded significant treatment effects. Listed below are the extracted adjusted $p \leq 0.05$ for all groups within a “Harvest”. “Part” depicts plant organ (Shoot = N, Root =R), “Harvest” depicts period (II = post-stress, III = recovery).

Treatment	Part	Harvest	Metabolite	p adj
HD-C	N	II	Nitrate	0.0214659
HD-CD	N	II	Nitrate	0.0222330
CD-C	N	II	WP	0.0056924
HD-C	N	II	WP	0.0015601
HD-C	N	II	qP	0.0143740
H-C	N	II	ETR	0.0596938
HD-C	N	II	ETR	0.0006491
HD-CD	N	II	ETR	0.0206220
HD-C	N	II	PhiPSII	0.0019557
HD-CD	N	II	PhiPSII	0.0370529
HD-C	N	II	Fv`/Fm’	0.0019203
HD-CD	N	II	Fv`/Fm’	0.0049181
HD-H	N	II	Fv`/Fm’	0.0048043
H-C	R	II	sNSC	0.0005420
HD-C	R	II	sNSC	0.0003950
H-C	R	II	Starch	0.0209324
HD-C	R	II	Starch	0.0237123
HD-C	R	II	CS	0.0041108
HD-C	R	II	Cyclitols	0.0263386
CD-C	R	II	totalC	0.0575419
H-C	R	II	totalC	0.0165367
HD-C	R	II	totalC	0.0006926
CD-C	R	II	Proline	0.0032292
HD-C	R	II	Proline	0.0000913
HD-H	R	II	Proline	0.0128814
HD-H	N	III	sNSC	0.0429869
HD-C	N	III	CS	0.0406311
HD-CD	N	III	CS	0.0196521
HD-C	N	III	Cyclitols	0.0004180
HD-CD	N	III	Cyclitols	0.0000787
HD-H	N	III	Cyclitols	0.0000903
HD-C	N	III	totalC	0.0210000

HD-CD	N	III	totalC	0.0012667
HD-H	N	III	totalC	0.0014140
HD-CD	N	III	Nitrate	0.0102790
HD-C	N	III	Proline	0.0011698
HD-CD	N	III	Proline	0.0009742
HD-H	N	III	Proline	0.0213430
HD-CD	N	III	-П	0.0076173
HD-H	N	III	-П	0.0407579
HD-C	R	III	Cyclitols	0.0277008
HD-H	R	III	Cyclitols	0.0115458
HD-C	R	III	totalC	0.0114547
HD-CD	R	III	totalC	0.0487846
HD-H	R	III	totalC	0.0128068
HD-C	R	III	-П	0.0333670

M

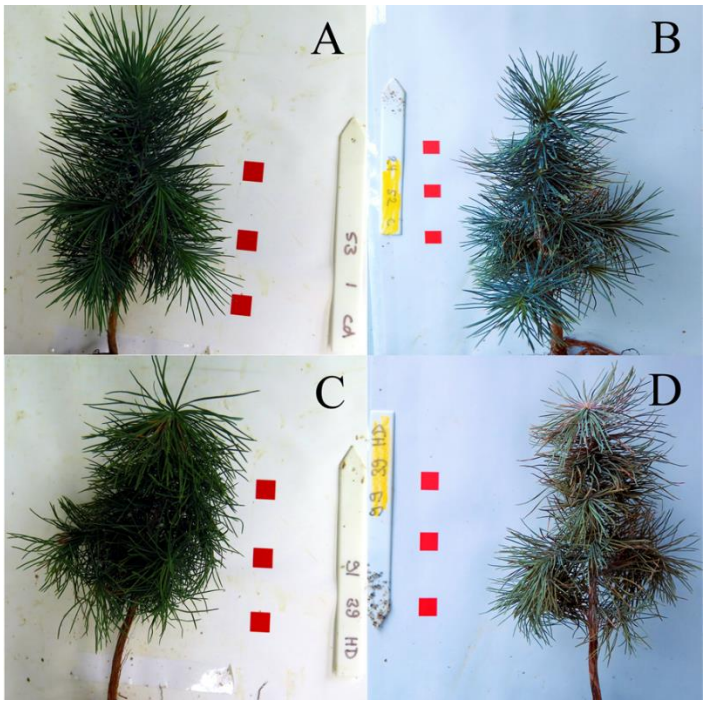

Figure S2.1: Visual verification of living (A, B) and dead (C, D) seedlings. Pictures where taken during the harvesting periods (pre-stress, stress and recovery). Due to unfavorable light conditions we applied automated white correction and automated color correction.

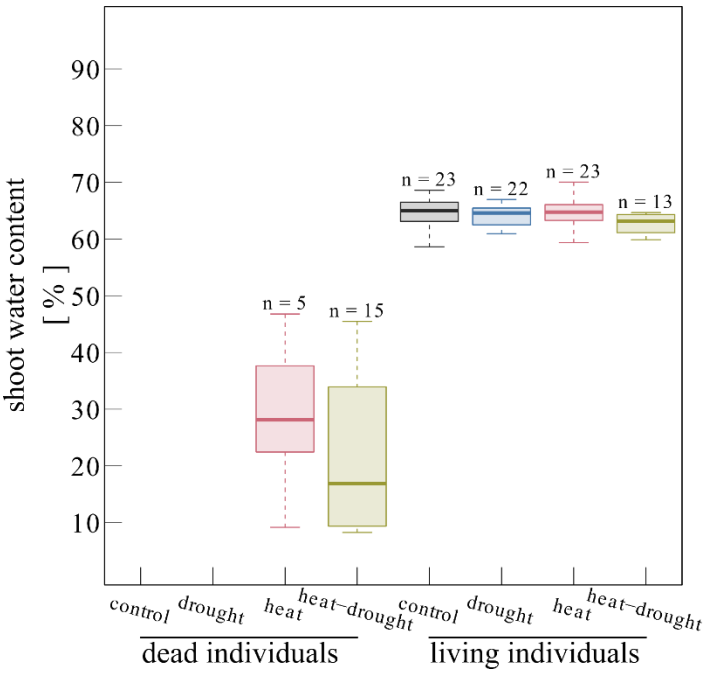

Figure S2.2: Percent of shoot water content depicted per treatment. Water content is given as percentage of fresh weight (FW). Seedlings were considered dead if the shoot water content declined below 55%.

N

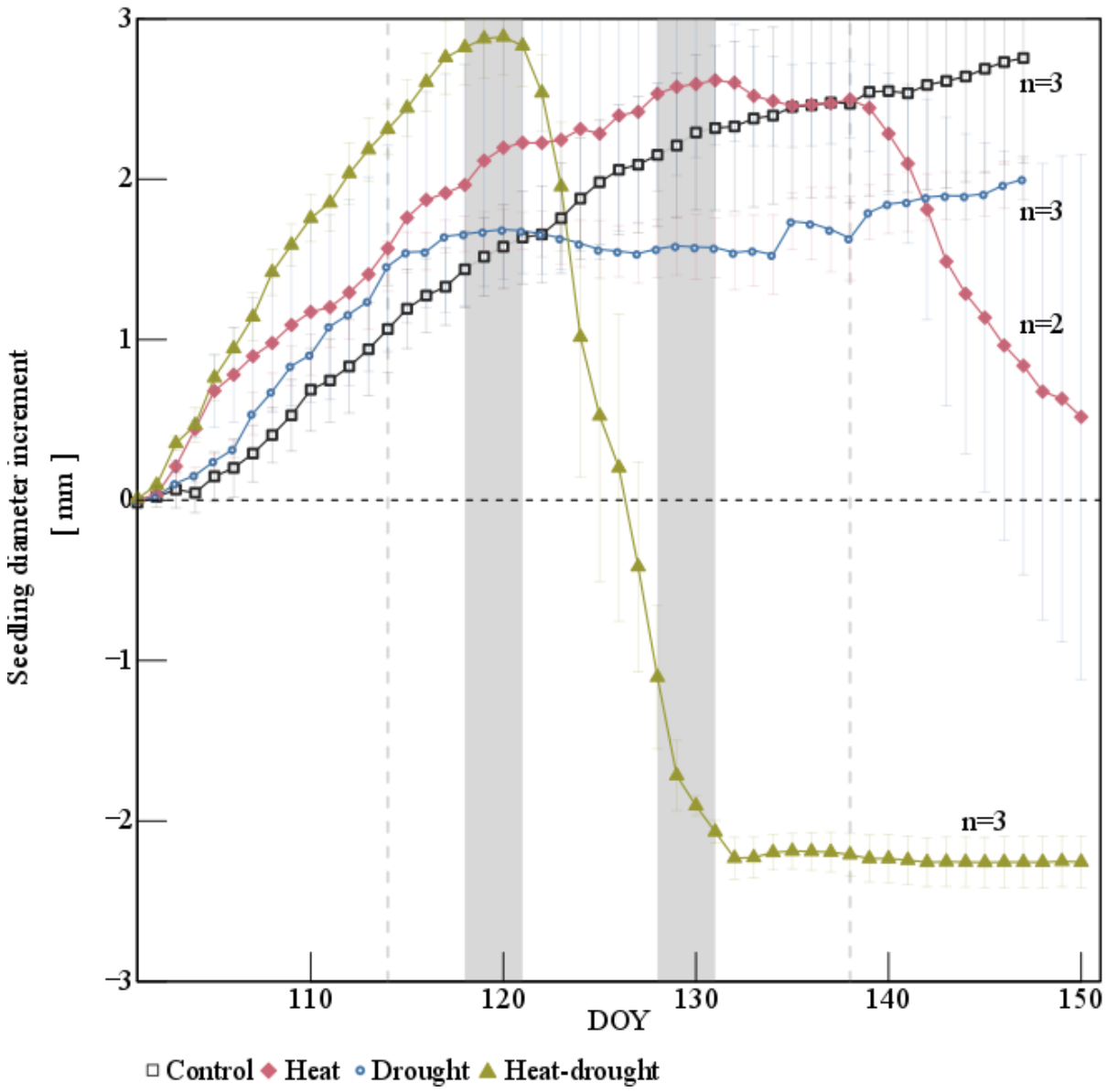

Figure S2.3: Stem diameter increment increase of *Pinus halepensis* seedlings subjected to either control (black hollow squares), drought (blue hollow circles), heat (red squares) or heat-drought (green triangle). The two heat waves are depicted by the grey areas. The drought phase is indicated by grey vertical dotted lines. The error bars are ±1 SE (*n*=3).

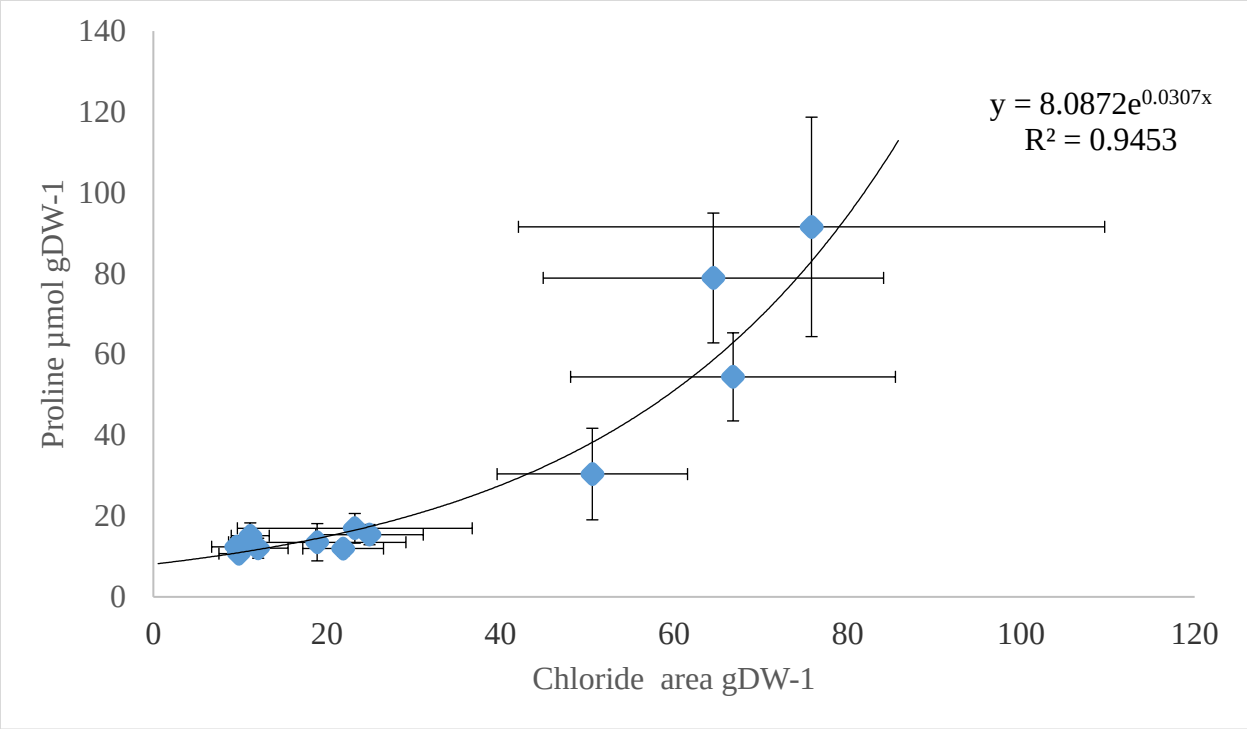

Figure S2.4: Relationships between proline accumulation in µmol gDW^{-1} and peak area change of Cl^{-1} signal per gDW. Values are means of harvesting period (pre-stress, stress, recovery) and treatment (control, drought, heat, heat-drought) with ±1SE. Values represent all samples per group without division in living or dead seedlings. We used Cl^{-1} peak area because we did not quantify this ion with standard rows.

Table S3.1 Shown are daily intervals of environmental control parameters of the glasshouse facility. Values depict Monthly averages ±1SE of half hourly data during the cultivation of the P. halepensis seedlings

Interval			Temperature	Relative humidity	Photos. active radiation
Hour of day	Month	Year	[°C]	[%]	µmol $m^{-2}s^{-1}$
0-6	7	2015	17.8 ± 1.3	74.8 ± 3.6	46.6 ± 122.4
6-9	7	2015	22.5 ± 1.3	60.3 ± 5.2	710.1 ± 359.3
9-12	7	2015	24.4 ± 0.9	50.9 ± 2.3	1044.8 ± 353.1
12-15	7	2015	23.9 ± 1.2	54.5 ± 6.4	834 ± 478.2
15-18	7	2015	21.9 ± 1.2	64.6 ± 6.4	385.3 ± 324.9
18-21	7	2015	19.5 ± 1.4	73.1 ± 5.1	8.1 ± 57.6
21-0	7	2015	17.9 ± 1.4	75.3 ± 4.1	0 ± 0.6
0-6	8	2015	16.3 ± 2.1	74.7 ± 3.9	14.3 ± 77.8
6-9	8	2015	22 ± 2.6	60.9 ± 9.7	658.3 ± 586.9
9-12	8	2015	25.1 ± 1.4	48.3 ± 7.1	975.8 ± 319.7
12-15	8	2015	25.7 ± 1.9	48.9 ± 6.4	925.8 ± 611.2
15-18	8	2015	23 ± 1.8	59.2 ± 5.9	299 ± 208.4
18-21	8	2015	19.5 ± 1.8	72 ± 6	0 ± 19
21-0	8	2015	17.4 ± 1.8	74.1 ± 4.7	0 ± 0.9
0-6	9	2015	14.8 ± 2.6	68.1 ± 5.3	0 ± 37.6
6-9	9	2015	19.9 ± 3.4	58.5 ± 9.9	621.6 ± 546.6
9-12	9	2015	24.6 ± 3.1	45.5 ± 8.2	935 ± 651.5
12-15	9	2015	24.8 ± 2.7	44.3 ± 5.6	910.7 ± 603.8
15-18	9	2015	20.5 ± 2.7	57 ± 7.3	184.5 ± 255.2
18-21	9	2015	16.2 ± 1.3	68.2 ± 5.3	0 ± 0.9
21-0	9	2015	15 ± 1.7	68.6 ± 4.4	0 ± 1.1
0-6	10	2015	16.6 ± 0.5	61.9 ± 4.6	0 ± 11.6
6-9	10	2015	19.8 ± 2.2	55.9 ± 7.6	316.9 ± 238.4
9-12	10	2015	22.9 ± 2.6	47.2 ± 7.3	660.5 ± 245.6
12-15	10	2015	21.7 ± 2	52.4 ± 5	728.1 ± 576.8
15-18	10	2015	18.6 ± 1.2	62.7 ± 4.2	55.9 ± 114.9

Q

18-21	10	2015	16.3	±	0.3	64.1	±	4.7	0	±	0.1
21-0	10	2015	15.8	±	0.1	63.9	±	4.9	0	±	0.3
0-6	11	2015	13.7	±	1.2	58	±	4.5	0	±	2.1
6-9	11	2015	16.3	±	1.8	49.9	±	8.9	140	±	225
9-12	11	2015	19.8	±	2.6	38.8	±	8.1	501.7	±	250.2
12-15	11	2015	20.4	±	2.3	39.3	±	10.3	331.1	±	231.3
15-18	11	2015	18.4	±	1.5	49.2	±	10.8	0	±	27.2
18-21	11	2015	15.2	±	1.4	57.1	±	6.4	0	±	0
21-0	11	2015	13.9	±	1.3	57.9	±	4.9	0	±	0.4
0-6	12	2015	12.5	±	0.6	50.7	±	3	0	±	2.5
6-9	12	2015	15.8	±	1.2	39.5	±	4.3	56.2	±	63.9
9-12	12	2015	18.2	±	1.9	34.9	±	8.6	292.3	±	150.8
12-15	12	2015	19.6	±	1.4	33.5	±	7.8	190.7	±	111.8
15-18	12	2015	18.4	±	1	38.4	±	4.7	0	±	15.7
18-21	12	2015	13.1	±	0.8	46.9	±	6.3	0	±	0
21-0	12	2015	12	±	0.2	47.8	±	6.3	0	±	0.2
0-6	1	2016	9.9	±	1.8	54	±	4.7	0	±	2.1
6-9	1	2016	13.1	±	1.9	48	±	6.8	76	±	111.3
9-12	1	2016	17.3	±	3.1	43.6	±	10.7	443.2	±	274.3
12-15	1	2016	18.1	±	3.8	44.2	±	11.9	332.6	±	246.1
15-18	1	2016	15	±	2.4	50	±	7.7	2.6	±	40.5
18-21	1	2016	11.4	±	1.3	53.1	±	6.9	0	±	1.1
21-0	1	2016	10.2	±	1.4	53	±	6.3	0	±	1.1
0-6	2	2016	8.9	±	1.5	55.2	±	5.1	0	±	1.6
6-9	2	2016	13.4	±	2.8	50.8	±	5.6	158.5	±	160.1
9-12	2	2016	19	±	3.7	40.9	±	11.1	585.2	±	240.5
12-15	2	2016	19.8	±	4.9	37.1	±	12.4	414.7	±	170.7
15-18	2	2016	14.9	±	2.6	47.9	±	8.1	52.2	±	104
18-21	2	2016	10.6	±	1.7	52.2	±	5.8	0	±	0.8
21-0	2	2016	9.1	±	1.3	53.9	±	5.1	0	±	0.8

Table S3.2: List of all TD-GC-MS quantified endogenous terpenoids from biomass samples of only surviving seedlings at the end of the second heatwave (*n*=6 per treatment, Control, Heat). Monoterpenes and Sesquiterpenes were summarized in MT_sum and SQT_sum. Values are averages ± 1SE. These data were used to generate Fig 5 in the main document.

Component	Control			Heat		
Monoterpene [µmol gDW^{-1}]						
Tricyclene	0.87	±	0.04	0.84	±	0.07
a-Pinen	47.26	±	2.50	44.14	±	3.12
Camphene	0.33	±	0.01	0.31	±	0.02
Sabinen	0.94	±	0.21	0.76	±	0.15
b-Pinen	2.42	±	0.54	3.23	±	0.87
Myrcen	2.39	±	0.70	1.98	±	0.70
d-3-carene	26.80	±	5.80	28.62	±	4.50
Limonen	1.88	±	0.21	2.10	±	0.09
b-Phellandren	1.65	±	0.05	1.71	±	0.12
g-Terpinene	0.34	±	0.07	0.33	±	0.06
a-Terpinolene	3.19	±	0.70	2.94	±	0.53
allo-Ocimene	0.07	±	0.01	0.03	±	0.01
Bornylacetate	0.98	±	0.19	0.49	±	0.26
03_Geranylacetate	0.25	±	0.05	0.22	±	0.10
Sesquiterpene [µmol gDW^{-1}]						
02_SQT	0.01	±	0.00	0.02	±	0.01
01_d-Elemene	0.19	±	0.04	0.11	±	0.04
02_b-Elemene	0.76	±	0.20	1.23	±	0.16
03_b-Cubebene	0.88	±	0.19	1.06	±	3.15
Caryophyllene+SQT	40.72	±	5.46	60.77	±	4.56
05+06_b-Cubebene+ trans-b-Farnesene_S	1.03	±	0.19	0.85	±	0.12
03_SQT	0.16	±	0.06	0.59	±	0.13
07_e-Muurolene	0.33	±	0.07	0.26	±	0.05
a-Humulene	7.10	±	0.96	10.96	±	0.87
04_SQT	1.14	±	0.26	0.77	±	0.18
09_a-Muurolene	7.58	±	1.08	7.72	±	0.83
05_SQT	0.36	±	0.06	0.24	±	0.05
11_cis-alpha-Bisabolene	0.18	±	0.02	0.33	±	0.03
01_Elemol	3.09	±	0.74	2.78	±	0.42
MT_sum	95.68	±	6.68	86.76	±	5.88
SQT_sum	71.52	±	5.96	85.59	±	7.67

Table S3.3: Shown are Transpiration E, net photosynthesis A_{net} and stomatal conductance g_s for the different treatments control (C), drought (D), heat (H), heat-drought (HD) and seedlings that died (dead) during the heatwave experiment. Values are experimental phase averages of daily averages per seedling (n_C=4, n_D=4, n_H=3, n_{HD}=1, n_{dead}=4) with ±1SE given.

Experimental Phase	Treatment	Status	E mmol m-2s-1	A_{net} µmol m-2s-1	g_s mmol m-2s-1
Reference		dead	1.03 ± 0.02	8.88 ± 0.18	53.0 ± 1.2
Heatwave 1		dead	0.95 ± 0.08	3.62 ± 0.77	23.2 ± 3.8
Recovery		dead	0.17 ± 0.02	0.91 ± 0.18	6.2 ± 0.9
Heatwave2		dead	0.11 ± 0.02	-0.09 ± 0.09	1.5 ± 0.3
Recovery		dead	0.03 ± 0.01	0.10 ± 0.06	1.1 ± 0.2
Rewetting		dead	0.02 ± 0.00	-0.04 ± 0.01	0.6 ± 0.1
Reference	C	alive	1.50 ± 0.06	10.63 ± 0.34	75.5 ± 3.7
Heatwave 1	C	alive	1.83 ± 0.13	11.32 ± 0.77	80.4 ± 8.0
Recovery	C	alive	1.75 ± 0.12	10.39 ± 0.64	73.8 ± 6.3
Heatwave2	C	alive	2.01 ± 0.19	10.93 ± 1.10	72.3 ± 8.8
Recovery	C	alive	1.41 ± 0.10	8.19 ± 0.55	55.1 ± 5.0
Rewetting	C	alive	1.41 ± 0.08	7.80 ± 0.39	51.7 ± 3.4
Reference	D	alive	1.68 ± 0.08	10.99 ± 0.45	77.2 ± 3.4
Heatwave 1	D	alive	1.25 ± 0.19	8.08 ± 1.05	47.6 ± 6.9
Recovery	D	alive	0.83 ± 0.11	5.70 ± 0.74	30.2 ± 4.5
Heatwave2	D	alive	0.86 ± 0.16	5.18 ± 0.92	25.6 ± 4.8
Recovery	D	alive	0.80 ± 0.10	5.09 ± 0.61	26.1 ± 3.3
Rewetting	D	alive	1.38 ± 0.14	7.36 ± 0.56	45.9 ± 4.3
Reference	H	alive	1.33 ± 0.07	11.31 ± 0.58	70.8 ± 3.0
Heatwave 1	H	alive	2.51 ± 0.35	7.01 ± 1.25	52.0 ± 6.3
Recovery	H	alive	1.08 ± 0.16	7.14 ± 0.87	41.8 ± 5.7
Heatwave2	H	alive	2.05 ± 0.32	4.28 ± 0.65	29.7 ± 4.4
Recovery	H	alive	1.06 ± 0.16	6.42 ± 0.94	38.6 ± 6.1
Rewetting	H	alive	1.30 ± 0.13	7.58 ± 0.74	43.2 ± 4.5
Reference	HD	alive	1.47 ± 0.07	10.61 ± 0.38	80.9 ± 3.7
Heatwave 1	HD	alive	1.56 ± 0.23	5.70 ± 2.14	38.1 ± 13.0
Recovery	HD	alive	0.48 ± 0.03	3.98 ± 0.43	20.6 ± 2.8
Heatwave2	HD	alive	0.50 ± 0.05	1.50 ± 0.21	7.9 ± 0.7
Recovery	HD	alive	0.34 ± 0.05	2.56 ± 0.38	11.4 ± 1.8
Rewetting	HD	alive	0.66 ± 0.04	4.40 ± 0.17	21.6 ± 1.0

Table S3.4: Shown are all continuously analyzed BVOCs for the different treatments control (C), drought (D), heat (H), heat-drought (HD) and seedlings that died (dead) during the heatwave experiment. Values are Experimental Phase averages of daily averages per seedling (n_C=4, n_D=4, n_H=3, n_{HD}=1, n_{dead}=4) with ±1SE given.

Experimental Phase	Treat	Status	m33			m45			m59			m99			m137			m153		
			nmol m-2s-1			nmol m-2s-1			nmol m-2s-1			nmol m-2s-1			nmol m-2s-1			nmol m-2s-1		
Reference		dead	0.25	±	0.02	0.03	±	0.01	1.30	±	0.07	0.010	±	0.001	0.47	±	0.07	0.003	±	0.000
Heatwave 1		dead	0.99	±	0.24	0.06	±	0.01	1.24	±	0.18	0.025	±	0.004	3.71	±	1.13	0.012	±	0.002
Recovery		dead	0.88	±	0.24	0.01	±	0.00	0.98	±	0.17	0.010	±	0.002	1.57	±	0.29	0.003	±	0.001
Heatwave2		dead	4.39	±	1.24	0.38	±	0.15	1.41	±	0.40	0.045	±	0.013	8.32	±	2.93	0.022	±	0.008
Recovery		dead	0.36	±	0.07	0.13	±	0.02	0.39	±	0.06	0.009	±	0.002	0.98	±	0.16	0.003	±	0.001
Rewetting		dead	0.39	±	0.06	0.19	±	0.03	0.36	±	0.04	0.010	±	0.001	0.74	±	0.16	0.002	±	0.001
Reference	C	alive	0.41	±	0.02	0.04	±	0.00	1.41	±	0.11	0.014	±	0.002	0.41	±	0.06	0.003	±	0.000
Heatwave 1	C	alive	0.58	±	0.05	0.05	±	0.01	1.89	±	0.27	0.020	±	0.002	0.38	±	0.06	0.005	±	0.001
Recovery	C	alive	0.58	±	0.05	0.04	±	0.01	1.51	±	0.21	0.017	±	0.002	0.31	±	0.05	0.005	±	0.001
Heatwave2	C	alive	0.81	±	0.07	0.07	±	0.01	1.56	±	0.34	0.025	±	0.003	0.49	±	0.07	0.006	±	0.001
Recovery	C	alive	0.55	±	0.05	0.05	±	0.01	1.27	±	0.17	0.012	±	0.001	0.39	±	0.08	0.005	±	0.001
Rewetting	C	alive	0.56	±	0.04	0.06	±	0.01	1.27	±	0.15	0.017	±	0.001	0.71	±	0.08	0.006	±	0.001
Reference	D	alive	0.48	±	0.03	0.04	±	0.00	1.83	±	0.16	0.019	±	0.002	0.70	±	0.12	0.004	±	0.000
Heatwave 1	D	alive	0.47	±	0.08	0.04	±	0.01	1.47	±	0.22	0.016	±	0.004	0.58	±	0.08	0.003	±	0.000
Recovery	D	alive	0.27	±	0.05	0.03	±	0.01	0.49	±	0.07	0.011	±	0.004	0.27	±	0.04	0.003	±	0.000
Heatwave2	D	alive	0.37	±	0.10	0.05	±	0.02	0.41	±	0.09	0.011	±	0.003	0.32	±	0.06	0.002	±	0.000
Recovery	D	alive	0.27	±	0.04	0.04	±	0.01	0.45	±	0.08	0.007	±	0.002	0.23	±	0.04	0.003	±	0.001
Rewetting	D	alive	0.53	±	0.06	0.03	±	0.00	1.01	±	0.10	0.010	±	0.002	0.42	±	0.04	0.006	±	0.001
Reference	H	alive	0.29	±	0.02	0.03	±	0.01	1.61	±	0.15	0.012	±	0.002	1.28	±	0.17	0.004	±	0.001
Heatwave 1	H	alive	1.56	±	0.41	0.10	±	0.03	2.27	±	0.37	0.028	±	0.009	4.33	±	1.16	0.019	±	0.005
Recovery	H	alive	0.43	±	0.08	0.01	±	0.01	0.87	±	0.18	0.013	±	0.003	1.01	±	0.24	0.002	±	0.000
Heatwave2	H	alive	1.63	±	0.28	0.13	±	0.04	1.50	±	0.28	0.031	±	0.008	2.35	±	0.46	0.013	±	0.003
Recovery	H	alive	0.33	±	0.04	0.03	±	0.01	1.23	±	0.17	0.006	±	0.001	0.31	±	0.04	0.002	±	0.000
Rewetting	H	alive	0.35	±	0.04	0.03	±	0.01	1.65	±	0.17	0.008	±	0.002	0.53	±	0.06	0.002	±	0.000
Reference	HD	alive	0.33	±	0.02	0.01	±	0.01	1.07	±	0.06	0.007	±	0.003	1.03	±	0.12	0.004	±	0.001
Heatwave 1	HD	alive	0.93	±	0.25	0.05	±	0.01	1.62	±	0.34	0.023	±	0.006	4.32	±	1.00	0.013	±	0.003
Recovery	HD	alive	0.15	±	0.06	-0.02	±	0.01	0.27	±	0.03	-0.001	±	0.005	0.39	±	0.06	0.000	±	0.001
Heatwave2	HD	alive	0.93	±	0.57	0.15	±	0.17	0.55	±	0.06	0.031	±	0.025	1.14	±	0.16	0.001	±	0.001
Recovery	HD	alive	0.08	±	0.01	0.01	±	0.01	0.20	±	0.04	0.002	±	0.004	0.07	±	0.01	0.000	±	0.000
Rewetting	HD	alive	0.21	±	0.03	0.01	±	0.01	0.68	±	0.06	0.000	±	0.003	0.20	±	0.04	0.001	±	0.000

Table S3.5 Shoot biomass, leaf area (half-sided) and monoterpene (MT) pools and emissions from the surviving heat-treated (H, HD) and control (C) seedlings measured in the gas exchange chambers. Cumulative MT emissions are shown from the first day of heatwave 1 to the last day of heatwave 2. Endogenous MT pools were scaled to the seedling-level using the median of the MT pool per heat and control treatment multiplied by the biomass per seedlings. Note that seedlings in the cuvettes and seedlings analyzed for MT pools were not the same because whole seedlings where sampled – Biomass of the cuvette seedlings (shoot [g]) was taken at the end of the experiment.

Treatment	Cuvette num.	Shoot [g]	MT pool [mg]	MT Emission [mg]	Emission % from total pool
H	8	16.02	189	34.18	18.1
H	11	9.65	114	25.72	22.5
H	16	17.53	207	35.94	17.4
HD	12	6.51	80	16.67	20.8
C	2	21.79	284	13.78	4.9
C	5	13.58	177	10.01	5.6
C	10	9.05	118	2.13	1.8
C	13	8.61	112	4.72	4.2

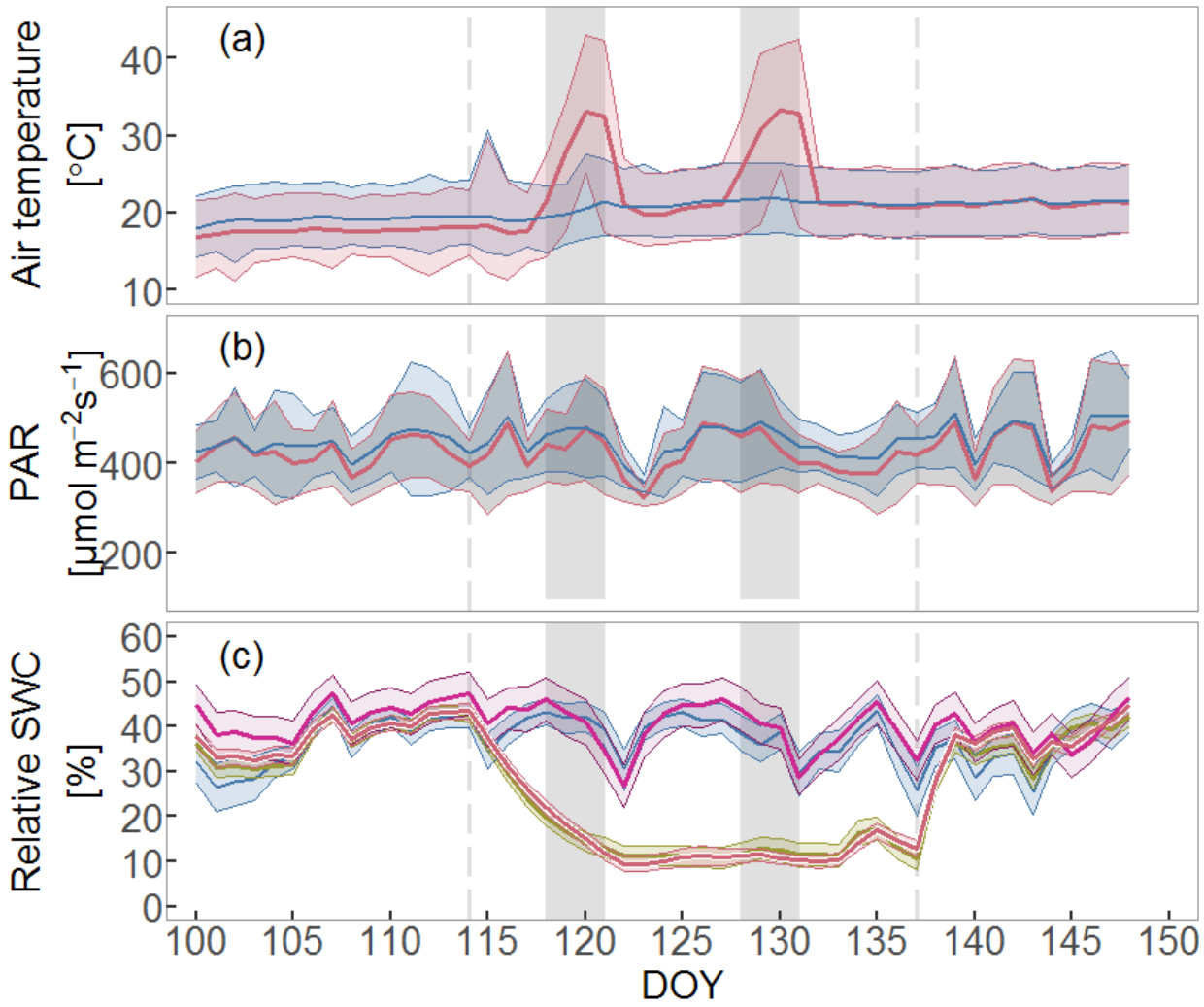

Figure S3.1: Overview of the environmental drivers during the heatwave experiment. Shown are air temperature (a) and photosynthetic active radiation PAR (b) of the heat (red) and non-heat (blue) treatments. Relative substrate water content rSWC (c) is shown for control (blue), drought (green), heat (magenta) and heat-drought (red) with *n*=10 per treatment. Data are shown as daily averages and standard deviation (±1SD) for (a, c) and for the 16 hours light period in (b). This is a modified figure previously published in (Birami et al. 2018).

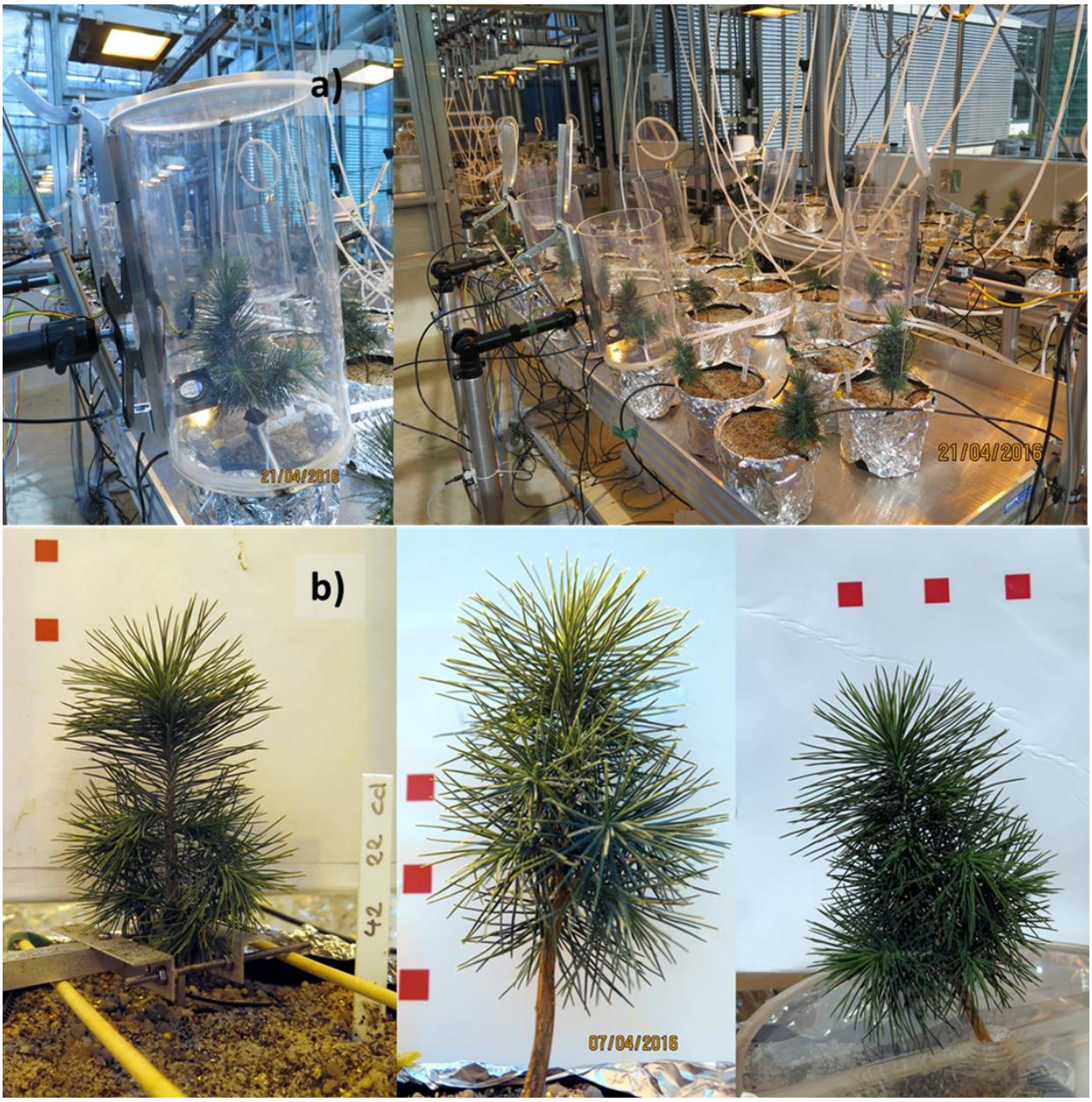

Figure S3.2: Experimental setup together with a gas exchange cuvette placement example (a), and example photographs, which were taken from seedlings to derive their projected leaf area (b). Red squares are 1 cm² each to calibrate for the estimated needle area. Area was estimated using the software ImageJ, color threshold was adjusted with method “RemyiEntropy”, RED, HSB, Hue:60/113, Saturation:40/255, Brightness: 35/130.

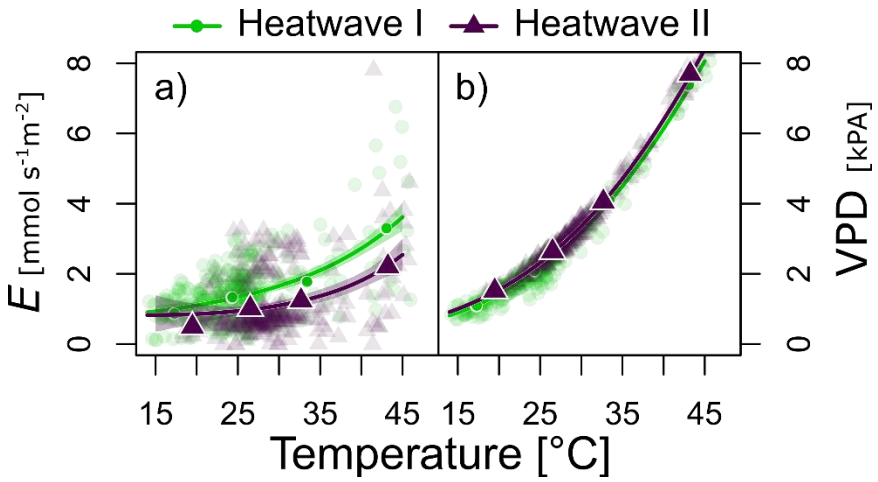

Figure S3.3: Differences in temperature responses of Transpiration (E, a)) and vapor pressure deficit (VPD, b)) between the first (filled circles, light green) and second heatwave (triangles, lilac) of Aleppo pine seedlings is depicted by exponential functions (exp(b(T)+c). Data are measurements of the surviving heat-treated seedlings (*n*=3) for PAR ≥ 100 µmol $m^{-2}s^{-1}$ including several days before each heatwave to investigate a larger temperature range. Shaded areas depict the 95% confidence intervals of the fitted functions. Larger shapes depict bin-averaged data. Note that VPD increased exponentially with temperature: VPD=exp(b(T)+c, with b= 0.066[0.0658-0.0669 CI95%] and c=-0.85[-0.08678 - -0.0829 CI95%], R^2 = 0.94 of log-transformed function.

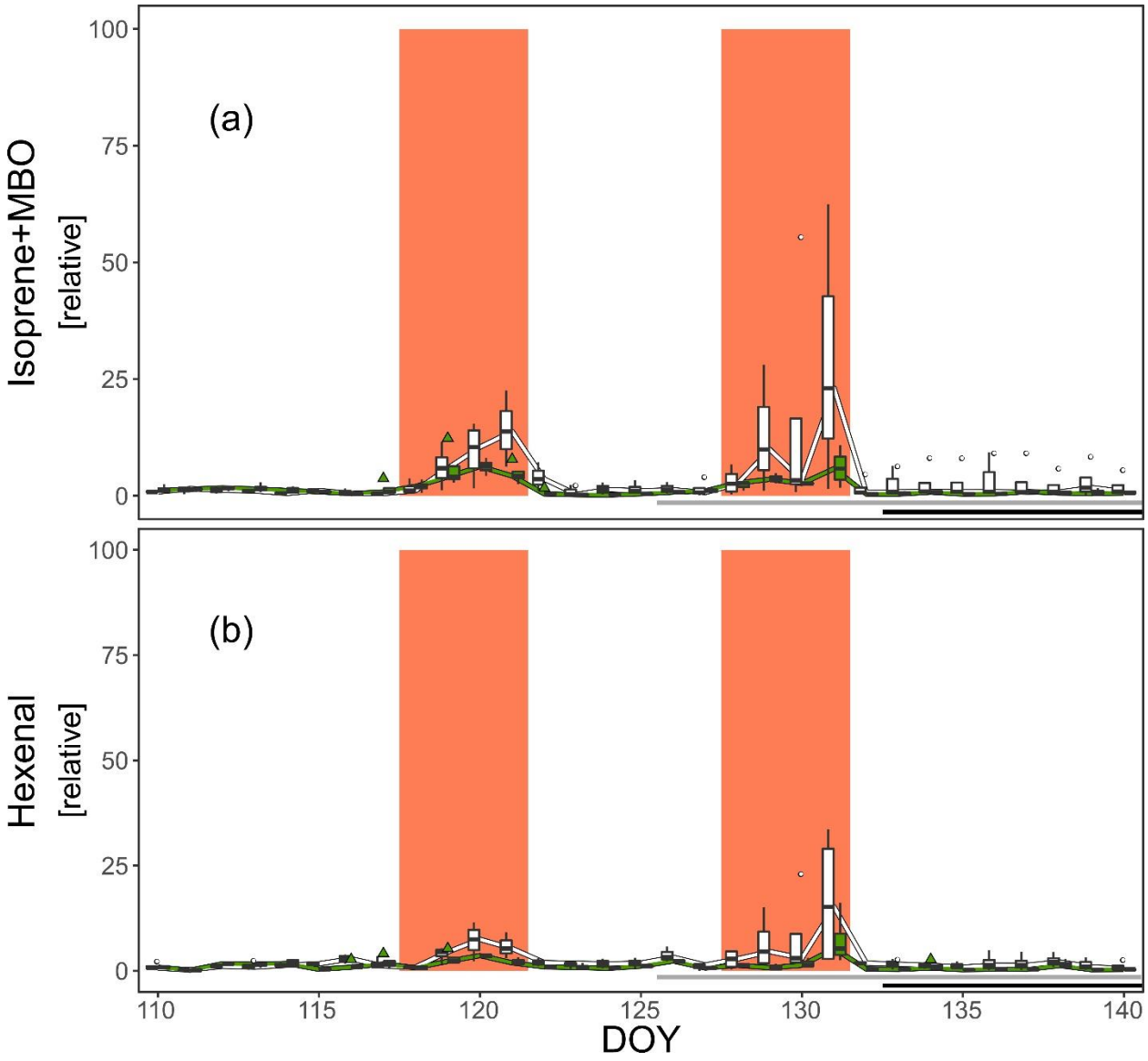

Figure S3.4 Responses of Isoprene + MBO (a) and hexenal (b) emissions during tree mortality. The data is presented as boxplots derived from daily-averages per seedling, separated in surviving (green, *n*=4) and dying (white, *n*=4). The two heatwaves are highlighted by a solid colored background (DOY 118-121; 128-131 Horizontal grey bars mark the time course on when daily-averaged transpiration and net photosynthesis of the dying seedlings reached zero. Dark respiration ceased is indicated by black horizontal bars (asymptotic approximation to 0). Data shown originate from the seedlings of the heat and heat-drought treatment. Daily-averages of emission data is for PAR ≥ 100

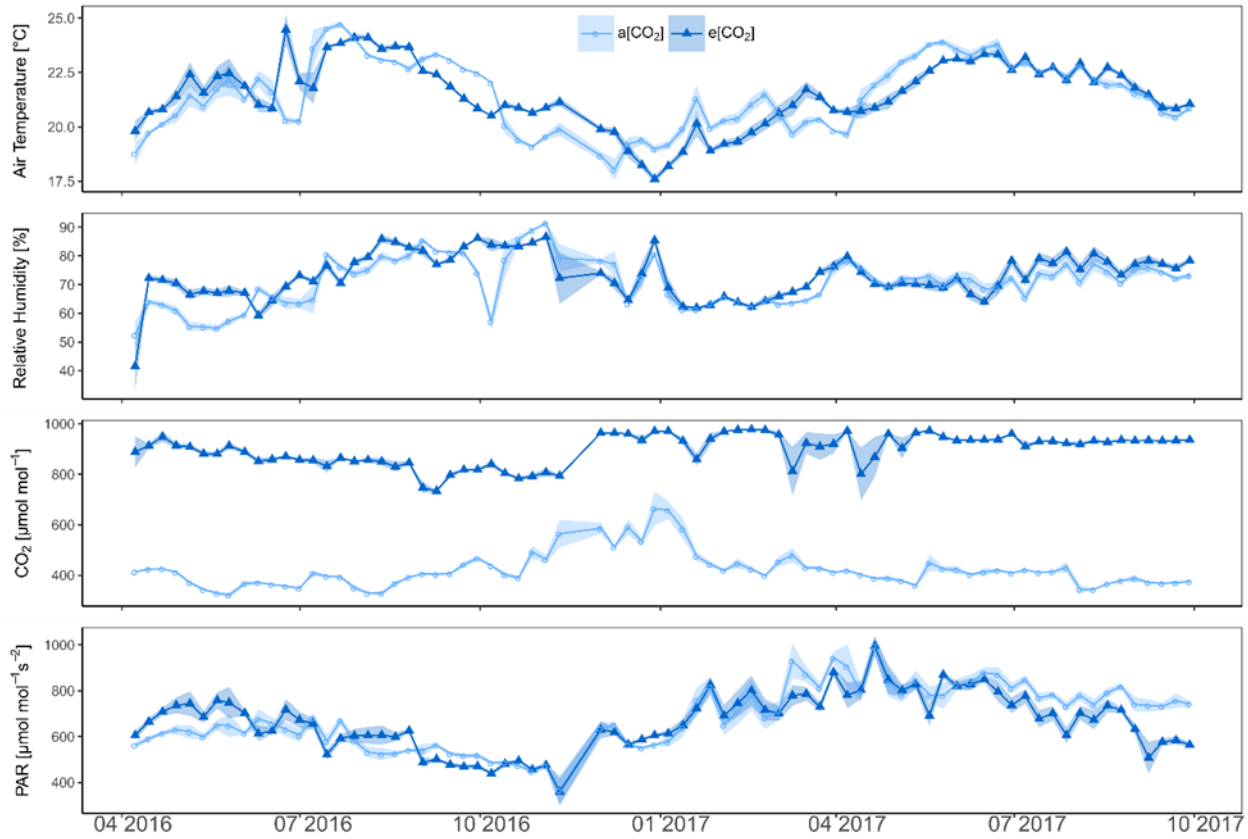

Fig. S4.1 Growth conditions of Aleppo pine seedlings during 30-month are shown separately for the two CO_2 treatments: e[CO_2] (900 ppm, blue triangle) and a[CO_2] (400 ppm, light blue circle). The shaded areas depict standard error of mean (±1 SE). Averages are weekly means of daily average daytime data (PAR>10). Seedlings were grown under average light intensity of 670.8±143 µmol $m^{-2}s^{-1}$ a[CO_2] and 650.1±134 e[CO_2] (supplemented by sodium vapor glasshouse lamps, T-agro 400 W, Philips) and average day-time temperatures were 21.29±1.7°C a[CO_2], 21.23±1.6°C e[CO_2] and humidity 69.9±9% a[CO_2], 70.4±12% e[CO_2]. Average atmospheric CO_2 concentration was 421±71 ppm a[CO_2] and 867±124 ppm e[CO_2].

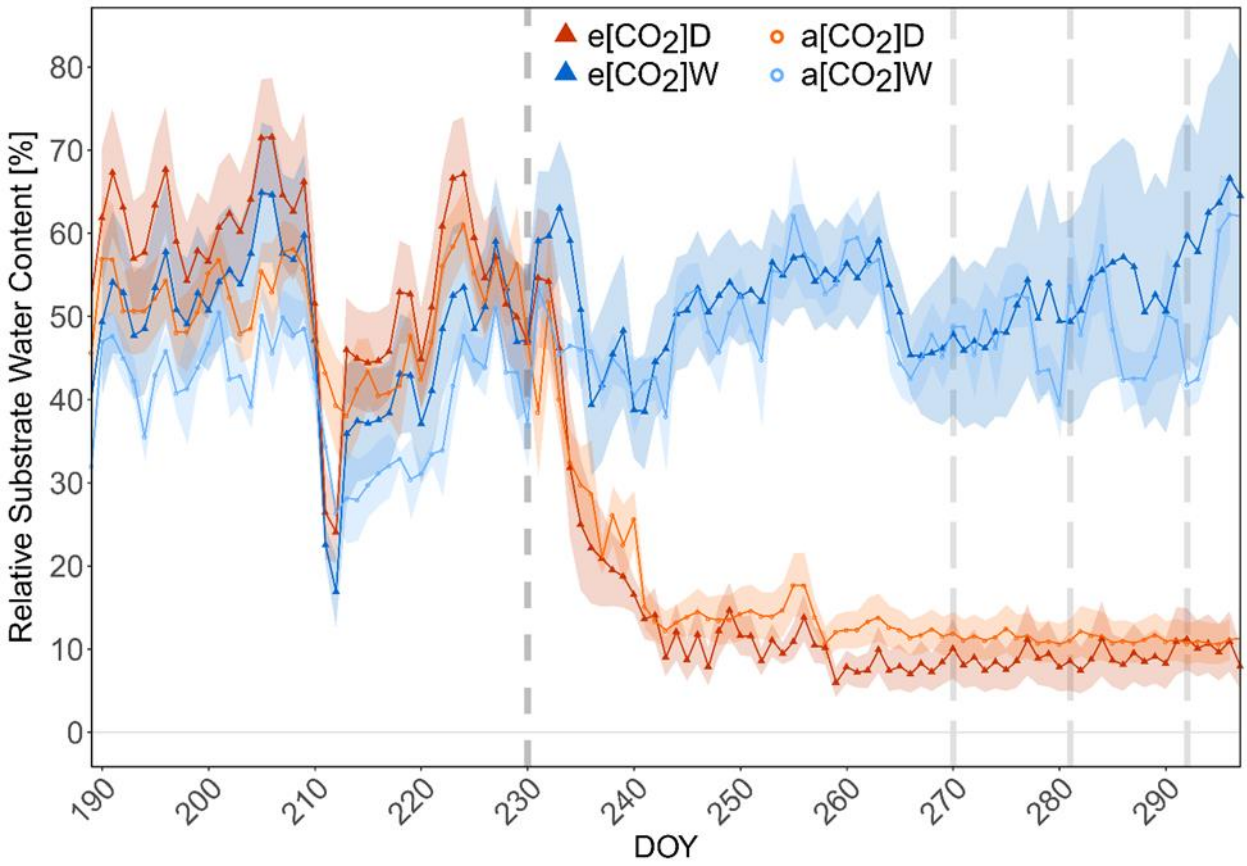

Fig. S4.2 Soil moisture conditions in 2017 when drought was initiated are shown in percent of relative substrate water content (RSWC) averaged per treatment: e[CO_2]D (red triangle), e[CO_2]W (blue triangle), a[CO_2]D(orange circle) a[CO_2]W (light blue circle). The shaded areas depict standard error of mean (±1 SE, n=6). Dotted vertical lines depict beginning of drought (DOY 230) and start and end of the two consecutive heatwave experiments (DOY 270/281/292). The irrigation was adapted to result in a relative substrate water content (RSWC) of 50%. Drought-treated seedlings were acclimated for a minimum of 40 days to drought (drought ambient [CO_2], a[CO_2]D: 15.2±7.9%, drought elevated [CO_2], e[CO_2]D: 12.7±9.7%). RSWC before onset of drought did not differ between the treatments (TukeyHSD, $P \geq 0.1$).

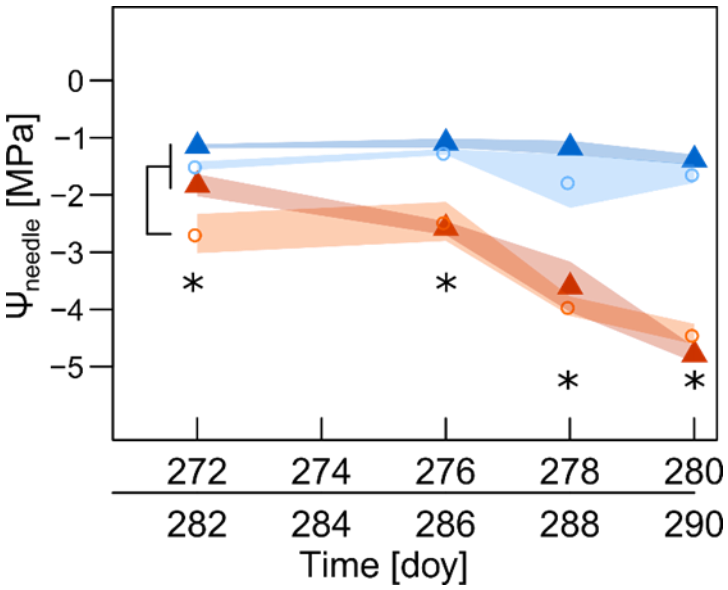

Fig. S4.3 Temperature responses of midday needle water potential (ψ_{needle}, MPa) measured via pressure chamber (Model, 600 PMS Instruments, Albany, OR, USA). The treatments e[CO_2]D (red triangle), e[CO_2]W (blue triangle), a[CO_2]D(orange circle), a[CO_2]W (light blue circle) are given as averages. The shaded areas depict standard error of mean (±1 SE, *n*=8) with asterisk highlighting differences between treatments (TukeyHSD, $P \leq 0.05$, temperature steps calculated separately.

Notes S4.1 Tree gas exchange chamber system

Each of the 20 aboveground compartments were individually temperature-controlled (Fig.4.2). The aboveground and belowground compartments were separated using a polyamide plate (1 cm thick; Sahlberg, Feldkirchen, Germany) containing an opening (1.5 x 15 cm) for the tree stem. After the tree stem was inserted, a double-sealed polyamide spacer and additional plastic putty (Teroson, Düsseldorf, Germany) ensured gas tightness between the above- and belowground compartment. The root compartment consisted of cylinders made from opaque polyvinyl chloride (30 cm inner diameter and 20 cm height) and was equipped with two ventilators (252N, ebm-papst, St. Georgen, Germany). The aboveground chamber material was made from cylinders of highly light transmitting transparent acrylic glass (PMMA XT, Sahlberg, Feldkirchen, Germany) with an inner diameter of 29 cm and a flexible height of 35–55 cm. Temperature conditions inside the chambers were controlled using fast-response thermocouples (5SC-TTTI-36-2M, Newport Electronics GmbH, Deckenpfronn, Germany) and through an individual cooling system. Each cooling system consisted of two radiators (NexXxoS XT45, Alphacool International GmbH, Braunschweig, Germany) equipped with four small fans (Mini Kaze 60 mm, Scythe, Tokyo, Japan). The radiators were connected to an individual pump, which controlled the inflow of coolant. To avoid condensation inside the chambers, the temperature of the coolant was maintained 2-5°C above the pre-determined dew point temperature.

The air supply (Air_{supply}) to the chambers was delivered by an oil-free screw compressor (SLD-S 7.5, Renner Kompressoren GmbH, Güglingen, Germany) coupled with a condensation trap (DFX9, FST GmbH, Essen, Germany) and adsorption columns (DPS 8 MZ, FST GmbH, Essen, Germany). Almost CO_2-free air (dew point -60°C) was constantly adjusted to pre-defined [CO_2] (F-201CV-500, Bronkhorst, Ruurlo, Netherlands) and [H_2O] using an evaporator mixer (CEM W-303B-330-K, Bronkhorst, Ruurlo, Netherlands) combined with two mass flow controllers for mixing water with air (M13-RGD-33-O-S and F-201CZ 10K-RAD-99-K, Bronkhorst, Ruurlo, Netherlands). A static mixer (SVMW-J-19/19-10-C, Schumacher Verfahrenstechnik GmbH, Germany) ensured adequate mixing and two major air streams of 150 l min^{-1} (F-203AV-M50-RGD-99-V and D-6370-HGD-CC-AV-99-D-S-DF, Bronkhorst, Ruurlo, Netherlands) at either 408 ppm or 896 ppm CO_2 were generated and delivered to each aboveground compartment at 10 l min^{-1} and to each belowground compartment at 5 l min^{-1} (GZ-32461-56 and -52, Cole-Parmer GmbH, Wertheim, Germany).

Sample air (Air_{sample}) was drawn by a pump at 500 ml min^{-1} (NMP830KNDC, KNF Neuberger GmbH, Freiburg, Germany). Air_{sample} from the belowground compartments was dried (Nafion® tubing, Gasmet Technologies GmbH, Karlsruhe, Germany) to avoid condensation. Four selector valve units (EUTA-SD16MWE, Vici AG International) and two three-way valves (0330, Bürkert GmbH & Co. KG, Ingelfingen, Germany) were used to switch between chambers and compartments and thus each seedling was measured once every 80 min using differential gas analysis.

Notes S4.2 Primary metabolite and protein analyses

Primary metabolite concentrations were absolutely quantified via gas chromatography coupled to time-of-flight mass spectrometry (GC-ToF-MS) applying a previously published protocol (Fürtauer et al. 2016, Weiszmann et al. 2018). 2–4 mg of powdered freeze-dried samples were extracted twice with a methanol-chloroform-water mixture (MCW, 5:2:1, v:v:v). Subsequently, pellets were extracted in 80% ethanol at 80°C for 30 min. Phase-separation was induced by addition of H_2Odd. Polar phases were combined and dried in a vacuum concentrator (ScanVac, LaboGene, Allerød, Denmark). Derivatization of dried extracts was done via methoximation (90 min at 30°C, Methoxyamine hydrochloride in pyridine) and silylation (30 min at 37°C, N-Methyl-N-(trimethylsilyl)-trifluoroacetamide). GC-ToF-MS analysis was conducted on an Agilent 6890 gas chromatograph (Agilent Technologies®, Santa Clara, USA) and separation of metabolites was achieved on an Agilent column HP5MS (length:30 m, diameter: 0.25 mm, film: 0.25 µm). The system was coupled with a LECO Pegasus® GCxGC-TOF mass spectrometer (LECO Corporation, St. Joseph, USA). For GC analysis, initial oven temperature was 70°C for 1 min, followed by a 9°C min^{-1} ramp with end temperature of 330°C which was held constant for 8 min. Data acquisition rate of the MS method was 20 spectra sec^{-1} and detector voltage was 1550 V. The acquisition delay was 5.5 min and the detected mass range was 40 to 600 m:z. Deconvolution of the total ion chromatogram and peak integration was performed using the software LECO Chromatof® (LECO Corporation, St. Joseph, USA). Absolute quantification of selected metabolites was done by calibration standards (five concentrations for each recorded metabolite). A pooled sample (n=8) of the 25°C step of the temperature response experiment was used as a technical control for each treatment. In each quantification method run (extraction, analysis, peak quantification, n=4), a complete set of samples per seedling (25°C, 35°C, 38°C, 40°C, root and needle samples) was processed.

To detect protein degradation with increasing stress, we analyzed protein amount using a standard protocol ((Fürtauer et al. 2018). Plant powder (freeze-dried, 15–30 mg) was suspended in 600 µl Urea-Extraction buffer (8M, HEPES 50mM, pH 7.8) and extracted on a shaker for 2 h. Ice-cold acetone with 0.5% β-Mercaptoethanol (proteomic grade, VWR International LLC, USA) was added to 300 µl of supernatant (10000 g, 10 min.) in a reaction tube (LoBind 2 ml, Eppendorf GmbH, Germany) and stored for 15 h at -20°C. Protein was sedimented (12000 g 15 min) and washed twice with 1.8 ml ice-cold methanol and once with 1.8 ml ice-cold acetone. Finally, protein was sedimented once more (14800 g, 10 min) and dried in a vacuum concentrator (Concentrator 5301, Eppendorf GmbH, Germany) before suspending in 60 µl of urea buffer (8 M, HEPES 50 mM, pH 7.8). The final quantification of protein [µg g^{-1}] was done with Bradford Assay (Coomassie Protein Assay Kit, Thermo Scientific, USA).

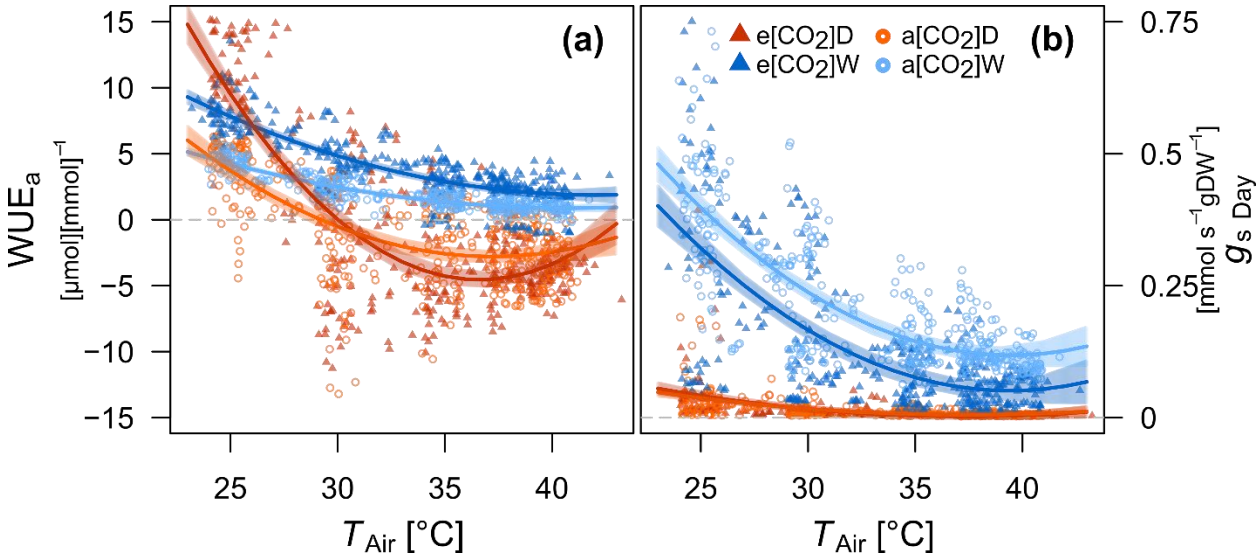

Fig S4.4 Temperature responses of water use efficiency (WUE_a, a) and stomatal conductance (g_s, b) are given per treatment. Data are hourly-averages per seedling during day-time (10 am to 4 pm). The lines were fitted using second-order polynomial functions. The shaded areas depict the 95% confidence intervals of the fitted functions.

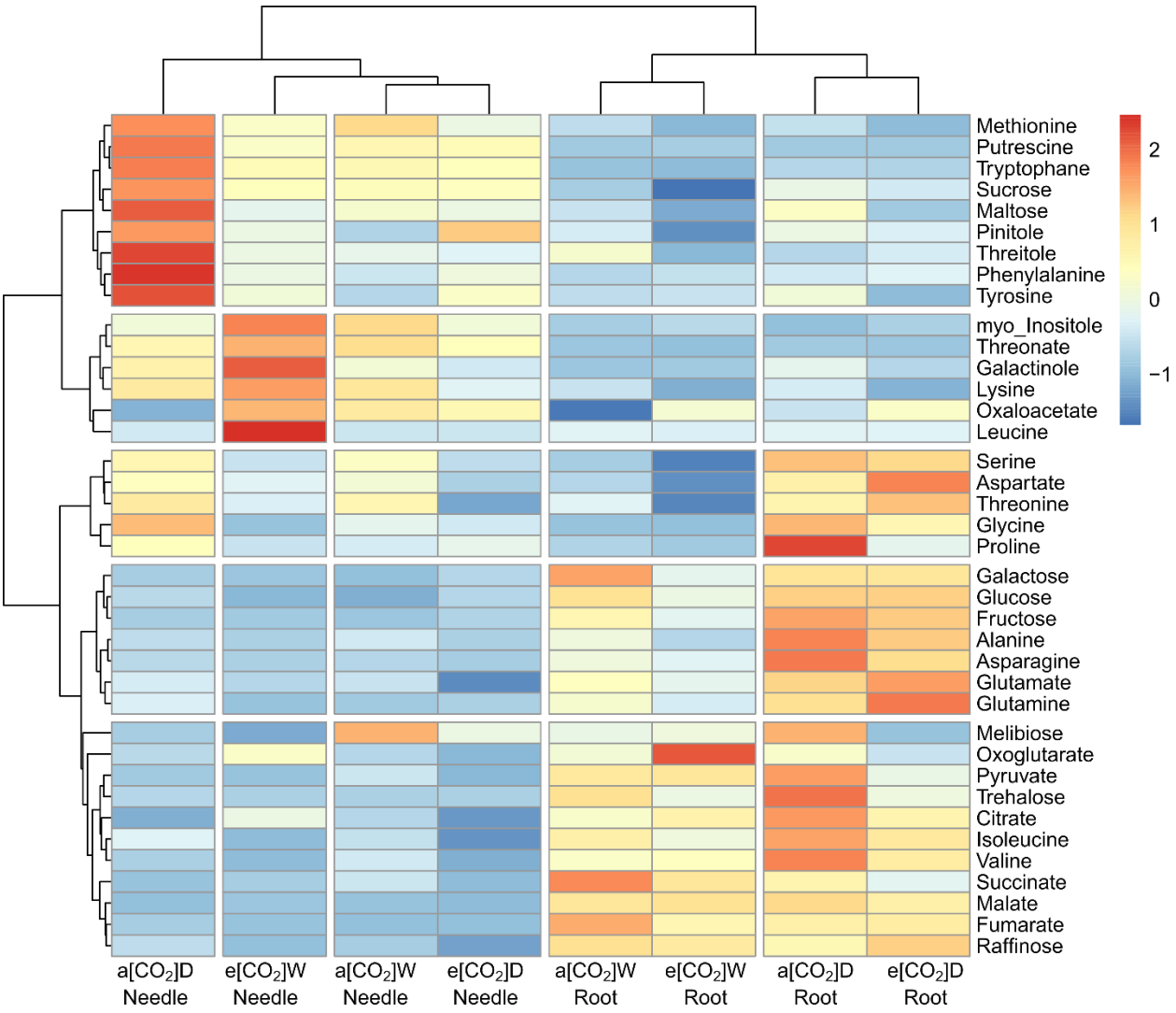

Fig S4.5 Metabolite responses per treatment and tissue are shown by a clustered dendrogram analysis with a scaled heat map of all quantified metabolites during control conditions (25 °C). Data is given as medians (n = 4). Colors depict Euclidian distances between weighted metabolite concentrations (scaled concentrations normalized to SD, see Methods).

Table S4.1 Needle temperatures measured with an infrared camera at the last day of the experiment (15 – 16 pm). Data are treatment averages (±1 SD).

Tair	e[CO2]W	a[CO2]W	e[CO2]D	a[CO2]D
		[°C]		
39.9±0.6	41.1±0.8	40.6±0.4	41.4±0.5	40.8±0.7

Table S4.2 Percentage share in soluble carbon (C) and soluble nitrogen (N) of gram Tissue dry weight. Values are given in Treatment averages ±1SE for 25°C and 40°C. Differences between the means are given via capital letters (TukeyHSD, $P \leq 0.05$).

Treatment	Temperature	Tissue	C		N	
	[°C]		%[gDW]		%[gDW]	
a[CO_2]W	25	Needle	1.62±0.39	A	0.003±0.0006	A
a[CO_2]D	25	Needle	2.67±0.47	A	0.005±0.0008	A
e[CO_2]W	25	Needle	1.92±0.44	A	0.003±0.0004	A
e[CO_2]D	25	Needle	2.23±0.44	A	0.002±0.0002	A
a[CO_2]W	40	Needle	1.51±0.34	A	0.004±0.0005	A
a[CO_2]D	40	Needle	2.49±0.81	A	0.005±0.0008	A
e[CO_2]W	40	Needle	1.78±0.41	A	0.003±0.0007	A
e[CO_2]D	40	Needle	3.78±0.7	A	0.003±0.0003	A
a[CO_2]W	25	Root	2.69±0.41	AC	0.004±0.0009	A
a[CO_2]D	25	Root	3.36±0.6	AD	0.008±0.0015	AB
e[CO_2]W	25	Root	1.78±0.28	AC	0.003±0.0005	A
e[CO_2]D	25	Root	3.07±0.42	AD	0.007±0.0015	AB
a[CO_2]W	40	Root	1.31±0.25	BC	0.011±0.0049	AB
a[CO_2]D	40	Root	3.15±0.54	AC	0.018±0.0051	B
e[CO_2]W	40	Root	1.02±0.09	BC	0.006±0.0012	A
e[CO_2]D	40	Root	3.09±0.54	AD	0.012±0.0017	AB

Table S4.3 Treatment averages of daily tree transpiration given per temperature step.

Tair	e[CO2]W	a[CO2]W	e[CO2]D	a[CO2]D
		[ml d^{-1} $tree^{-1}$]		
25 °C	186	204	53	37
30 °C	184	190	18	19
35° C	185	214	23	25
38 °C	195	262	25	22
40 °C	211	269	24	20

Erklärung:

Eidesstattliche Versicherung

Eidesstattliche Versicherung gemäß § 6 Abs. 1 Ziff. 4 der Promotionsordnung des Karlsruher Instituts für Technologie für die Fakultät für Bauingenieur-, Geo- und Umweltwissenschaften

1. Bei der eingereichten Dissertation zu dem Thema

Carbon and water dynamics during combined heat, drought and elevated atmospheric CO_2 in *Pinus halepensis* seedlings handelt es sich um meine eigenständig erbrachte Leistung.

2. Ich habe nur die angegebenen Quellen und Hilfsmittel benutzt und mich keiner unzulässiger Hilfe Dritter bedient. Insbesondere habe ich wörtlich oder sinngemäß aus anderen Werken übernommene Inhalte als solche kenntlich gemacht.

3. Die Arbeit oder Teile davon habe ich wie folgt/ bislang nicht an einer Hochschule des In- oder Auslands als Bestandteil einer Prüfungs- oder Qualifikationsleistung vorgelegt.

Titel der Arbeit: “Carbon and water dynamics during combined heat, drought and elevated atmospheric CO_2 in *Pinus halepensis* seedlings”

Hochschule und Jahr: *Karlsruher Institute für Technologie, 2021*

Art der Prüfungs- oder Qualifikationsleistung: *Dissertation*

4. Die Richtigkeit der vorstehenden Erklärungen bestätige ich.

5. Die Bedeutung der eidesstattlichen Versicherung und die strafrechtlichen Folgen einer unrichtigen oder unvollständigen eidesstattlichen Versicherung sind mir bekannt. Ich versichere an Eides statt, dass ich nach bestem Wissen die reine Wahrheit erklärt und nichts verschwiegen habe.

Ort und Datum Unterschrift

JJ

Eidesstattliche Versicherung

Belehrung

Die Universitäten in Baden-Württemberg verlangen eine Eidesstattliche Versicherung über die Eigenständigkeit der erbrachten wissenschaftlichen Leistungen, um sich glaubhaft zu versichern, dass der Promovend die wissenschaftlichen Leistungen eigenständig erbracht hat.

Weil der Gesetzgeber der Eidesstattlichen Versicherung eine besondere Bedeutung beimisst und sie erhebliche Folgen haben kann, hat der Gesetzgeber die Abgabe einer falschen eidesstattlichen Versicherung unter Strafe gestellt. Bei vorsätzlicher (also wissentlicher) Abgabe einer falschen Erklärung droht eine Freiheitsstrafe bis zu drei Jahren oder eine Geldstrafe.

Eine fahrlässige Abgabe (also Abgabe, obwohl Sie hätten erkennen müssen, dass die Erklärung nicht den Tatsachen entspricht) kann eine Freiheitsstrafe bis zu einem Jahr oder eine Geldstrafe nach sich ziehen. Die entsprechenden Strafvorschriften sind in § 156 StGB (falsche Versicherung an Eides Statt) und in § 161 StGB (fahrlässiger Falscheid, fahrlässige falsche Versicherung an Eides Statt) wiedergegeben.

§ 156 StGB: Falsche Versicherung an Eides Statt

Wer vor einer zur Abnahme einer Versicherung an Eides Statt zuständigen Behörde eine solche Versicherung falsch abgibt oder unter Berufung auf eine solche Versicherung falsch aussagt, wird mit Freiheitsstrafe bis zu drei Jahren oder mit Geldstrafe bestraft.

§ 161 StGB: Fahrlässiger Falscheid, fahrlässige falsche Versicherung an Eides Statt

Abs. 1: Wenn eine der in den § 154 bis 156 bezeichneten Handlungen aus Fahrlässigkeit begangen worden ist, so tritt Freiheitsstrafe bis zu einem Jahr oder Geldstrafe ein. Abs. 2: Straflosigkeit tritt ein, wenn der Täter die falsche Angabe rechtzeitig berichtigt. Die Vorschriften des § 158 Abs. 2 und 3 gelten entsprechend.

Ort und Datum Unterschrift

KK